Manipulating the p53 pathway for cancer treatment

Patricia Roxburgh

The Beatson Institute for Cancer Research

Supervisor: Professor Karen Vousden

Submitted to College of Medicine, Veterinary and Life Sciences, University of Glasgow towards the degree of Doctor of Philosophy

Abstract

p53 is a tumour suppressor that is dysfunctional in most cancers. In some cancers, mutation of the *TP53* gene results in expression of a mutant protein or loss of p53 expression, while in others wild-type p53 is retained but there is a defect in the mechanisms that allow for the activation of p53, including, but not limited to, upregulation of p53's negative regulators (MDM2 and MDMX). Restoration of wild-type p53 function can lead to tumour regression and is therefore an attractive anti-cancer therapy. Several small molecule compounds that activate wild-type p53 have been described, and in this study the functions of two new compounds that stabilise p53 are described. While these drugs may be useful to activate p53-dependent apoptosis or senescence in wild-type p53 tumours, an alternative approach that depends on the use of transient p53 activation to protect normal cells while leaving p53 null or mutant tumour cells vulnerable to cytotoxic drugs is also explored. Finally, the identification of pharmacodynamic biomarkers for p53 stabilisation is described.

In chapter 3 a new class of MDM2 inhibitor (MPD compounds) is described. The compounds are capable of stabilising and activating p53 in cells by inhibiting the E3 ligase activity of MDM2 in a mechanism that involves compound binding to the RING-tail of MDM2. Although the MPD compounds have limitations in terms of solubility and potency they have demonstrated a new method of achieving MDM2 inhibition and support design of further RING-tail binding compounds with more favourable chemical properties.

In chapter 4 the function of a dual inhibitor of MDM2 and MDMX has been explored (HLI373). This compound is shown to activate p53 in cells and *in vivo* by interfering with ribosomal biogenesis, causing ribosomal stress and inhibiting MDM2. In addition it is capable of reducing MDMX expression at the promoter level by a mechanism that requires intact MDM2-p53 binding. Further work is required to fully define the mechanism of action of this compound and demonstrate its anticancer activity in xenograft and transgenic mouse models.

In chapter 5 a chemoprotective approach for p53 activation, which might be applied to situations where tumours express mutant p53, is explored in cell lines. Low-dose actinomycin D treatment can activate p53 without occult DNA damage via the ribosomal stress pathway, thereby protecting wild-type p53 expressing cells from the cytotoxic effects of paclitaxel. Low-dose actinomycin D may therefore be used to limit chemotherapy-induced toxicity to normal cells while targeting a mutant p53 expressing tumour.

In chapter 6 the potential for developing pharmacodynamic biomarkers for MDM2 inhibition in serum, peripheral blood mononuclear cells and hair follicles taken from patients prior to and following chemotherapy was examined. Measurement of serum MIC-1 level showed most promise, although further evaluation of this marker is needed before it could be used as a pharmacodynamic endpoint in a clinical study.

Table of Contents

List of Figures

List of Tables

List of Accompanying Material

Part of this work contributed to the publication below:

Roxburgh P, Hock AK, Dickens MP, Mezna M, Fischer PM, Vousden KH. (2012) Small molecules that bind the Mdm2 RING stabilize and activate p53. *Carcinogenesis* Apr; 33(4): 791-8.

Acknowledgements

Firstly I would like to thank Karen for giving me the chance to work in her lab where I have benefited from the proactive, learning environment. Most importantly I would like to thank her for her patience and supervision during my PhD. I would also like to thank Jeff Evans for his clinical supervision and for help with sample collection.

I am also grateful to the whole of R15, past and present, who have helped me get to grips with science and been great fun to work with. Especially I would like to thank Patricia and Maren for their guidance and friendship. I have had successful collaborations with Andreas Hock and Mokdad Menza to whom I am grateful. I would also like to thank Professor Allan Weissman for providing HLI373 for testing. I am grateful to patients, nursing staff, trials unit staff and the analytical services unit for assisting in sample collection and preparation for the biomarker work. I am thankful also for all the excellent support in the Beatson Institute especially from Colin Nixon in histology and Margaret O'Prey in Beatson Advanced Imaging Resource.

I would like to thank Cancer Research UK for funding this work.

Above all I need to thank my family who have gone to great lengths to support me. Of course I am grateful most of all to my fantastic husband Campbell and my son Hamish.

Author’s Declaration

This work was performed personally and no part of it has been submitted for consideration as part of any other degree or award.

Abbreviations

5-FU	5-Fluorouracil
act D	Actinomycin D
AFP	Alpha-Fetal Protein
AK	Aurora Kinase
AKT	Protein Kinase B
ALDH4	Aldehyde Dehydrogenase 4
AMPK	AMP-Activated Protein Kinase
ARF	Alternative Reading Frame of p16INK4A
ASU	Analytical Services Unit
ATCC	American Type Culture Collection
ATM	Ataxia Telangectasia Mutated
ATP	Adenosine Triphosphate
ATR	Ataxia Telangectasia and Rad3 related
BAIR	Beatson Advanced Imaging Resource
Bcl	B cell lymphoma
βHCG	β-subunit of Human Chorionic Gonadotropin
BH3	Bcl-2 homology domain
Bp	Base pair
BPDE	Benzo(a)ptrene diolepoxide
B-RAF	B-Rapidly Accelerated Fibrosarcoma
Brn3A	Brain-specific homeobox/POU domain protein 3A
BSA	Bovine Serum Albumin
C/EBPβ-2	CCAAT/Enhancer-Binding Protein β
Ca125	Cancer antigen 125
CBP	CREB1-binding protein
CDK	Cyclin Dependant Kinase
cDNA	DNA complementary to mRNA
CEA	Carcinoembryonic Antigen
CHIP	Carboxyl terminus of Hsc70-Interacting Protein
CHK	Checkpoint Kinase
CK1	Casein Kinase 1
CML	Chronic Myeloid Leukaremia
CRU	Clinical Reseach Unit
CRUK	Cancer Research UK
CTC	Circulating Tumour Cells
CTU	Clinical Trials Unit
DAPI	4', 6-diamidino-2-phenylindole
DBD	DNA Binding Domain
DLT	Dose Limiting Toxicity
DMEM	Dulbecco's Modified Eagle Medium
DMSO	Dimethyl Sulfoxide
DNA	Deoxyribonucleic Acid
DNA-PK	DNA dependent Protein Kinase
DR5	Death Receptor 5
DRAM	Damage Regulate Autophagy Modulator
DTT	Dithiothreitol
DUB	Deubiquitinating enzyme
E1A	Adenovirus early region 1A

ECL	Enhance Chemiluminescence
EDTA	Ethylenediaminetetraacetic Acid
EGFR	Epidermal Growth Factor Receptor
ELISA	Enzyme-Linked Immunosorbent Assay
EORTC	European Organisation for Research and Treatment of Cancer
ER	Estrogen Receptor
FCS	Foetal Calf Serum
FDA	US Food and Drug Administration
Gadd45	Growth arrest and DNA-damage inducible gene no.45
GIST	Gastrointestinal Stromal Tumour
GPX1	Glutathione Peroxidase 1
h	hours
HAUSP	Herpes-virus Associated USP
HCC	Hepatocellular Carcinoma
HDAC	Histone Deacetylases
HECT	Homologous to E6-AP carboxyl terminus
HER2	Human Epidermal growth factor Receptor 2
HPV	Human Papilloma Virus
HRP	Horseradish Peroxidase
HSP 90	Heat Shock Protein 90
HuR	RNA binding protein Human antigen R
hnRNP Q	Heterogenous nuclear ribonucleoprotein Q
HIF1α	Hypoxia Inducible Factor 1 alpha
IARC	International Agency for Research on Cancer
iASPP	inhibitor of Apoptosis-Stimulating Protein of p53
IGF-1R	Insulin-like Growth Factor 1 Receptor
IHC	Immunohistochemistry
IP	Immunoprecipitation
Ip	Intra-peritoneal
kDa	kilo Dalton
KRAS	Kirsten-Rat Sarcoma protein
LB	Lysogeny Broth
LD	Low-Dose
MAP	Mitomycin C, doxorubicin (Adriamycin), cisplatin (Platinum)
MAX	Myc-Associated factor X
MCL	Myeloid Cell Leukemia sequence
MDM2	Mouse Double Minute 2
MIC-1	Macrophage Inhibitory Cytokine-1
Min	Minute
MIRA-1	Mutant p53-dependent Induction of Rapid Apoptosis 1
miRNA	Micro-RNA
Mn-SOD	Mn-Superoxide Dimutase
MPD	Michael Paul Dickens
mRNA	messenger RNA
MTBP	MDM2, Transformed 3T3 cell double minute 2, p53 Binding Protein
MTD	Maximum Tolerated Dose
mTOR	mechanistic Target of Rapamycin
Muc1	Mucin 1 cell surface associated
NES	Nuclear Export Signal
NF-Y	Nuclear transcription Factor Y

NF-κB	Nuclear Factor kappa light chain enhancer of activated B cells
NF1	Neurofibromatosis 1
NLS	Nuclear Localisation Signal
NoLS	Nucleolar Localisation Signal
NP-40	Nonidet P40
NT	Not Tested
OD	Oligomerisation Domain
PAI-1	Plasminogen Activator Inhibitor 1
PAX	Paired box
PCAF	p300/CBP-Associated Factor
PD	Proline rich Domain
PET	Positron Emission Tomography
PIASy	Protein Inhibitor of Activated STAT y
Pidd	p53 induced protein with a death domain
PIN1	Peptidylprolyl cis/trans Isomerase, NIMA-interacting 1
PIRH2	p53-Induced RING H2 protein
PLK	Polo-Like Kinase
PML-RARA	Promyelocytic Leukaemia protein-Retinoic Acid Receptor Alpha
PRIMA	p53 Reactivation and Induction of Massive Apoptosis
PSA	Prostate Specific Antigen
PSD-95	Postsynaptic Density protein 95
PTEN	Phosphatase and Tensin homolog
PUMA	p53 Upregulated Modulator of Apoptosis
Rpm	rotations per minute
Rb	Retinoblastoma protein
RBP-Jκ	Recombination signal Binding Protein Jκ
RD	Regulatory Domain
RECIST	Response Evaluation Criteria in Solid Tumours
RETRA	Reactivation of Transcriptional Reporter Activity
RFA	Radio-Frequency Ablation
RING	Really Interesting New Gene
RITA	Reactivation of p53 and Induction of Tumour cell Apoptosis
RNA	Ribonucleic Acid
ROS	Reactive Oxygen Species
RPE	Retinal Pigment Epithelial cells
RPL26	Ribosomal Protein L26
RT-PCR	Reverse Transcription Polymerase Chain Reaction
SirT1/2	Sirtuin ½
SNP	Single Nucleotide Polymorphism
SREBP	Sterol Regulatory Element Binding Protein
SUMO	Small Ubiquitin-Related Modifier
TAD	Transactivation Domain
TEMED	Tetramethylethylenediamine
TGFβ	Transforming Growth Factor β
TIGAR	*TP53* Induced Glycolysis and Apoptosis Regulator
TRIM	TRIpartite Interaction Motif
TSAP6	Tumour Suppressor Activated Pathway 6
TSC2	Tuberous Sclerosis protein 2
TSP1	Thrombospondin-1
TUNEL	Terminal deoxynucleotidyl transferase dUTP Nick End Labelling

UK	United Kingdom
USP	Ubiquitin-Specific Protease
UTR	Untranslated Region
UV	Ultraviolet
VEGF	Vascular Endothelial Growth Factor
VHL	Von Hippel-Lindau
WWP1	WW domain containing E3 ubiquitin Protein ligase 1
YY1	Yin Yang 1

1 Introduction

1.1 Cancer

Worldwide 10.9 million people are diagnosed with cancer and 7.5 million die from the disease annually[2]. Cancer therefore represents a major global health and economic cost.

In the UK there are approximately 309,500 new diagnoses of cancer per year, of which 54% originate from the four most common cancer sites (breast, lung, colorectal and prostate cancer)[3-6]. Since cancer is primarily a disease of the older population, with 63% of cancer being diagnosed in people of 65 years and older, it is expected that cancer rates will increase as the population ages. This increase in cancer rate will be further exaggerated by improved surveillance and diagnosis methods, resulting in a predicted rise in the number of people living with or after cancer by more that 3% per year[7]. Reassuringly, while cancer incidence rates are increasing, and are expected to continue doing so, deaths from the disease are falling. European age-standardised mortality rates for all cancers taken together fell by 20% between 1979 and 2008, from 219 to 176 deaths per 100 000 people[8-10].

At a molecular level cancer is the result of disordered proliferation of damaged cells. The generally accepted dogma is, that as a result of multiple stresses cells can accumulate damage leading to genetic alterations, allowing these damaged cells to propagate and form a cancer. These genetic alterations result in mutations of genes causing them to become either inappropriately active (oncogenes) or alternatively lose functions that normally prevent cancer (tumour suppressor genes). Additionally epigenetic alterations can cause changes in gene expression that also contribute to tumourigenesis[11]. Exposure to environmental carcinogens such as ultraviolet (UV) light and tobacco increase the frequency of mutations and therefore the risk of cancer. Once a tumour is established, further selective pressure such as the development of hypoxia and the inflammatory response to the tumour enable cancer cells to develop invasive capacity causing malfunction of local organs and metastatic spread to distant sites[12-14]. Many cancer related deaths are due to this metastatic disease[15].

In 2000 Hanahan and Weinberg outlined in a comprehensive review the key molecular characteristics common to cancer cells[16]. This work detailed the multistep evolution of cancer by defining 6 biological abilities that cancer cells acquire to gain advantage over the defences of normal cells. The core capabilities common to all cancers include: “self sufficiency in growth signals, insensitivity to growth inhibitory signals, evasion of programmed cell death, limitless replicative potential, sustained angiogenesis and tissue invasion and metastasis”.

More recently, in recognition of advances in understanding cancer development, two additional hallmarks have been added to the model[17, 18]. These additional hallmarks are: “reprogramming of energy metabolism and evasion of the host’s immune defences”.

The rapid progress in understanding cancer at a molecular level over the last decade is in part due to the success of projects like the Human genome project[19] and the Cancer Genome Atlas[16] which, as well as identifying many of the driver mutations implicated in the neoplastic process have spurred on improvements in technology which allow relatively high throughput, low cost sequencing. In addition, these improvements in high throughput technologies have also facilitated advanced understanding of other levels of regulation such as the study of epigenetic modification of genes, the transcriptome, microRNAome[20], proteome and metabolome[21-23]. Consequently the complexity of the multiple layers of regulation involved in cancer development is now being revealed and the concepts of oncogene addiction[24], non-oncogene addiction[25] and synthetic lethality[26, 27] can be exploited for improved cancer treatment.

Currently the general oncological principles in treatment of solid tumours are that localised disease should be surgically resected then depending on the histological appearance of the tumour and likelihood of recurrence, post-operative (adjuvant) chemotherapy or hormonal therapy is offered in some cases; unresectable disease may be amenable to other local therapies such as radio-frequency ablation (RFA), cryotherapy, and radiotherapy. If disease is too advanced for treatment with local therapies then systemic therapy is required. At present, although the era of targeted therapy has arrived, the vast majority of systemic therapies used in cancer treatment continue to be traditional cytotoxic agents. The

cytotoxic agents in routine clinical use fall broadly into 7 categories (alkylating agents, platinum agents, anti-metabolites, topoisomerase-I inhibitors, intercalating agents, tubulin active agents and cytotoxic antibiotics). These agents work by damaging DNA by a variety of mechanisms (Appendix 1: table 8-1) and cause high levels of damage to normal cells resulting in significant, sometimes life threatening, toxicity. This is due to their lack of specificity for targeting cancer cells.

In contrast, the principle of 'targeted' anti-cancer treatment is that drugs are specifically designed to exploit a feature specific to the cancer cell and can therefore not only be more effective but importantly cause less toxicity to normal tissues. So far examples of targeted agents that have made, or are expected to make, significant clinical impact include Imatinib in treatment of chronic myeloid leukaemia (CML) and gastrointestinal stromal tumours (GIST)[28, 29], Trastuzumab[30] in the treatment of HER2 positive breast cancer and Vemurafenib[31-36] for BRAF mutated melanoma. For these few agents impressive responses and improvements in survival have been demonstrated. However, resistance pathways have emerged resulting in new cancer genotypes against which our therapeutic armoury is limited[35]. This highlights the need for early cell line studies to predict likely resistance mechanisms and to plan strategies for treatment of acquired resistance. Furthermore this raises the question as to whether it may be more advantageous to apply a more broad brush approach by using a combination of biological agents to simultaneously hinder the cancer cells' ability to evade drug induced anti-proliferative effects[37].

Disappointingly many molecularly targeted agents have made less clinical impact than initially hoped for a variety of reasons. Firstly some targeted agents cause significantly more toxicity to normal tissues than predicted, perhaps suggesting the need for more extensive study of the role of a particular target in normal tissues prior to clinical study. Secondly the clinical testing of targeted agents requires a dramatic change in the design of clinical studies, a realisation that is only now being appreciated. New anti-cancer drugs are still mostly being tested in the traditional sequence of phase I, phase II then phase III studies. In phase I a group of heavily pre-treated cancer patients are treated in a dose escalation study,

aimed at establishing the recommended phase II dose, based on reaching a dose where 1/3 of patients experience a dose limiting toxicity (DLT). In the subsequent phase II study a group of patients with a specific primary site are treated to look for evidence of response and then phase III compares the new drug schedule with the current standard of care for a particular patient group. For targeted agents it makes little sense to establish a dose for further study because of its ability to cause toxicity to normal tissues and it would be preferable to establish the dose of maximal target blockade. In phase II it may be more appropriate to select a group of patients who are similar because of the genotype of their malignancy rather than the primary site since there seems to be a lack of correlation between driver mutations even amongst cancers at the same site. On average a tumour has 11 mutated genes which contribute to tumour progression but in a group of cancers of the same primary site there is only a 50% overlap in driver mutations[15]. Initially treating patients based on molecular type rather than disease site would create some problems since the primary site of disease has previously defined the standard of care for comparative study.

Ultimately we are now in the era of personalised medicine with improved response rates being seen by tailoring treatment to molecular type rather than histological type alone in some cases[30]. However our methods of clinical evaluation are not yet fit for evaluation of targeted agents and a dramatic cultural change is required to adopt novel more effective study designs[38].

1.2 Discovery of p53

p53 was originally discovered in 1979, when it was found in complex with the large T-antigen of tumour virus Simian Virus 40 (SV-40)[39-44]. Then, following the first cloning of p53 in 1984[45-50], the oncogenic activities of this cloned p53 were described[50-54].

Subsequent work soon led to a series of important landmark findings including the observation that tumour viruses have the ability to inactivate p53[55-58]. In 1988 murine wild-type p53 was sequenced confirming that the originally cloned p53 was that of a mutated, tumour-associated p53[59, 60]. It was not until 1989 that p53 was

classified as a tumour suppressor after work that confirmed the ability of wild-type p53 to suppress E1A and Ras mediated transformation[61-63].

Consistent with p53's new identity as a tumour suppressor it was confirmed in 1989 that p53 is inactivated or lost in tumours[64] and the cancer predisposition syndrome, Li Fraumeni Syndrome, was first described in 1990. This autosomal dominant syndrome, characterised by neoplasms at multiple sites and occurring at an early age, was found to be due to germ-line mutation in *TP53* and subsequent loss of the wild-type p53 allele in tumour tissues[65, 66].

p53's tumour suppressive function was experimentally confirmed by generation of *TP53* knockout mice. These mice, although appearing essentially normal, develop spontaneous tumours by 6 months of age[67, 68].

Figure 1-1 summarises the landmark findings involved in establishing p53 as a tumour suppressor.

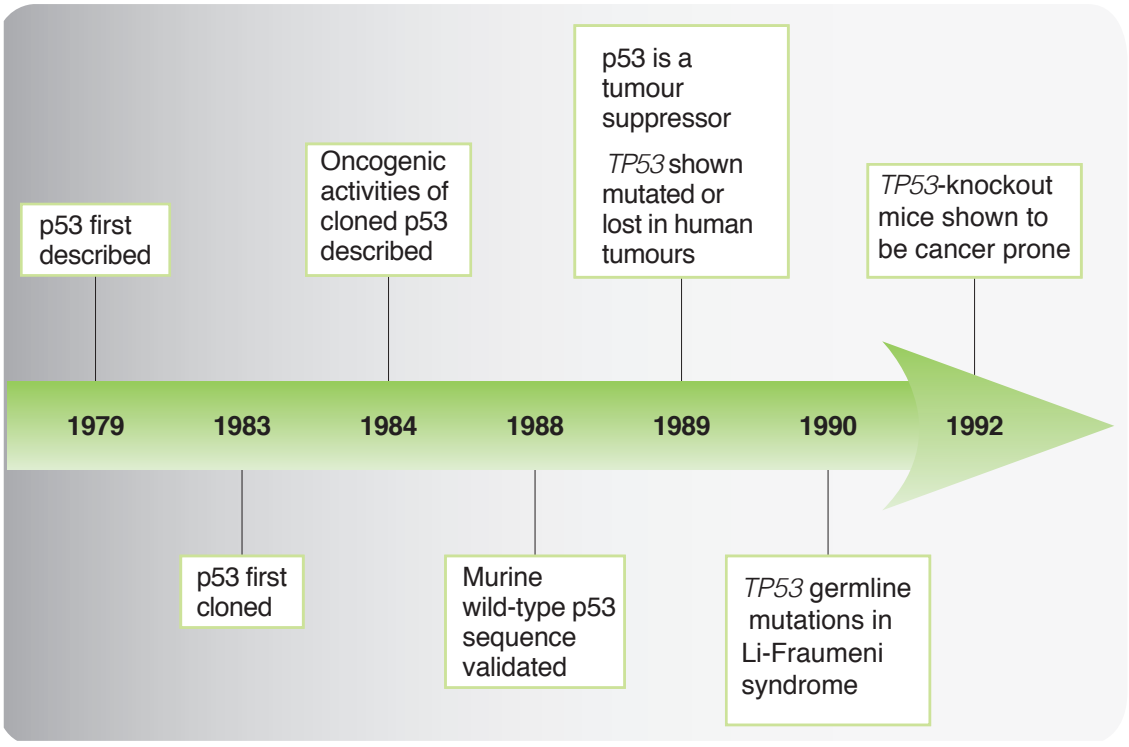

Figure 1-1: p53 timeline.
Adapted from Levine *et al*, 2009 [69].

1.3 Tumour suppressive functions of p53

TP53 functions as a transcription factor. In response to cellular stress (for example: genotoxic damage, oncogene activation, hypoxia, nutrient deprivation and telomere erosion) p53 activates its transcription targets that can mediate a multitude of responses, including cell cycle arrest, DNA repair, altered metabolism, antioxidant effects, anti-angiogenic effects, senescence and apoptosis (Figure 1-2).

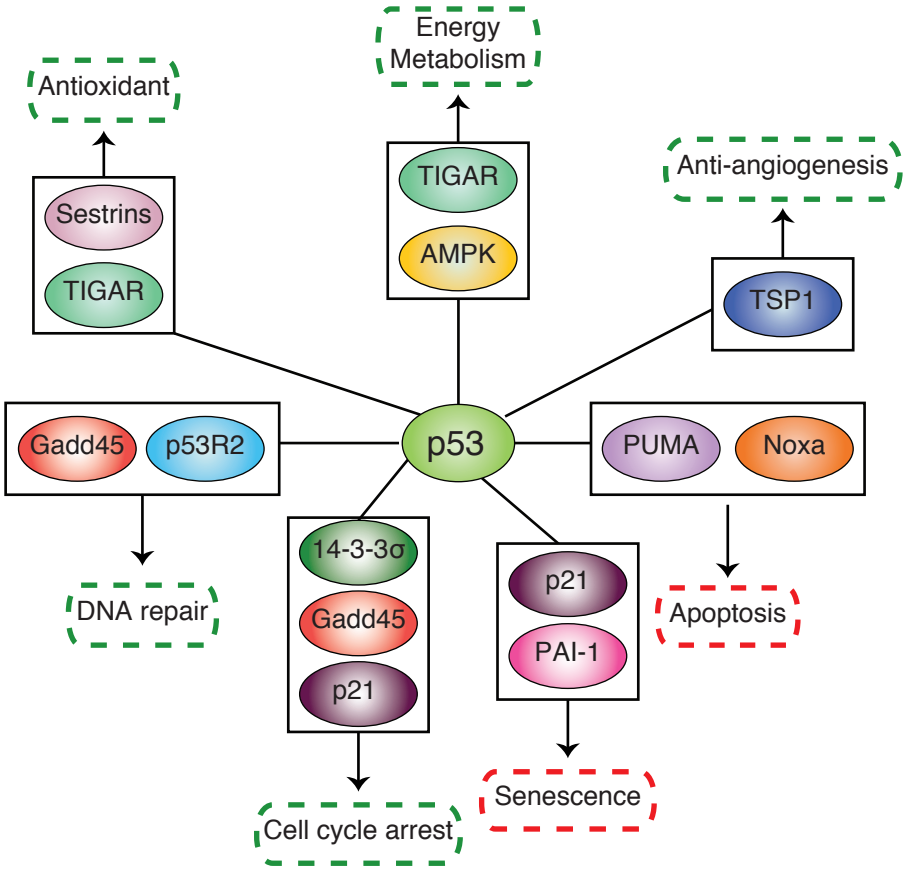

Figure 1-2: p53's tumour suppressive functions.
p53 transcriptional targets are shown in boxes. The outcomes of p53 activation that may play a role in response to repairable damage are highlighted by green boxes and outcomes of p53 activation that would be beneficial in response to irreparable damage are highlighted by red boxes. TIGAR=TP53 Induced Glycolysis and Apoptosis Regulator, AMPK=AMP-Activated Protein Kinase, TSP1=Thrombospondin-1, PUMA=p53 Upregulated Modulator of Apoptosis, PAI-1=Plasminogen Activator Inhibitor 1, Gadd45=Growth arrest and DNA damage 45. Adapted from Vousden *et al*, 2009[70] and Feng *et al*, 2011[71].

When p53 is activated it undergoes extensive post-translational modifications that modulate p53 stability, subcellular localisation and interaction with other proteins. p53 recognises and binds to specific DNA sequences of its target genes and recruits transcriptional co-regulators to control expression. These co-regulators

may be repressors as demonstrated by SLUG, which binds to the p53 upregulated modulator of apoptosis (PUMA) promoter repressing p53's ability to activate PUMA[72], or activators as demonstrated by Muc1, which binds to the p21 promoter increasing p21 transcription[73]. In addition to these co-regulators other proteins influence transcriptional output by binding to p53; for example Brn3A binds to p53 and inhibits its ability to activate Bax and Noxa but activates expression from the p21 promoter[74, 75]. More recently p53 has also been shown to control the expression of various microRNAs[71]. The potential outcomes of p53 activation are variable and are determined by multiple factors including the activating stimulus, the dynamics of p53 induction[76], the amount of p53 protein, p53's modified state and the particular interacting partners and co-regulators present.

Through modulation of p53's transcriptional targets, p53 prevents or responds to the accumulation of cellular damage and therefore prevents the propagation of malignant cells[77]. While transcriptional activity is fundamental for p53's tumour suppressor activity[78, 79], further complexity is introduced through transcriptionally independent functions of p53 (regulating apoptosis, autophagy[80] and metabolism[81]).

It is difficult to predict the transcriptional output of p53 for each given condition. However a simplified model has been suggested where p53 inducible genes can be divided into two categories; those that are induced rapidly by low levels of stress that cause repairable damage and those that are induced by higher levels of p53/stress which cause irreparable damage[82].

1.3.1 p53's response to repairable stress

Under low levels of stress and cellular damage p53's transcriptional activity favours induction of genes causing cell cycle arrest, DNA repair, antioxidant and metabolic modulation and anti-angiogenic effects (Figure 1-2). This is to allow time for repair of damaged DNA prior to re-entry into the cell cycle.

In the cell cycle cells progress through a series of stages including gap phase (G1), DNA synthesis (S), a second gap phase (G2) and then mitosis (M-phase). Progression to each phase is tightly controlled by a series of checkpoints where

cyclins and Cyclin Dependent Kinases (CDK) act in complexes and in concert to allow progression to the next phase. One important regulator of cell cycle is the family of E2F transcription factors, which control the expression of many key proteins required for proliferation. In order to progress to the synthesis phase of the cell cycle the Retinoblastoma protein (Rb) needs to be hyper-phosphorylated. In G1 phase Rb is E2-F bound and hypo-phosphorylated. As cells pass the restriction point in G1 cyclin E-CDK2 begins adding phosphate groups to Rb so that it becomes increasingly phosphorylated (Figure 1-3), causing it to be dissociated from E2F. This allows E2F to initiate its transcriptional program, which contributes to the progress of cells into S phase.

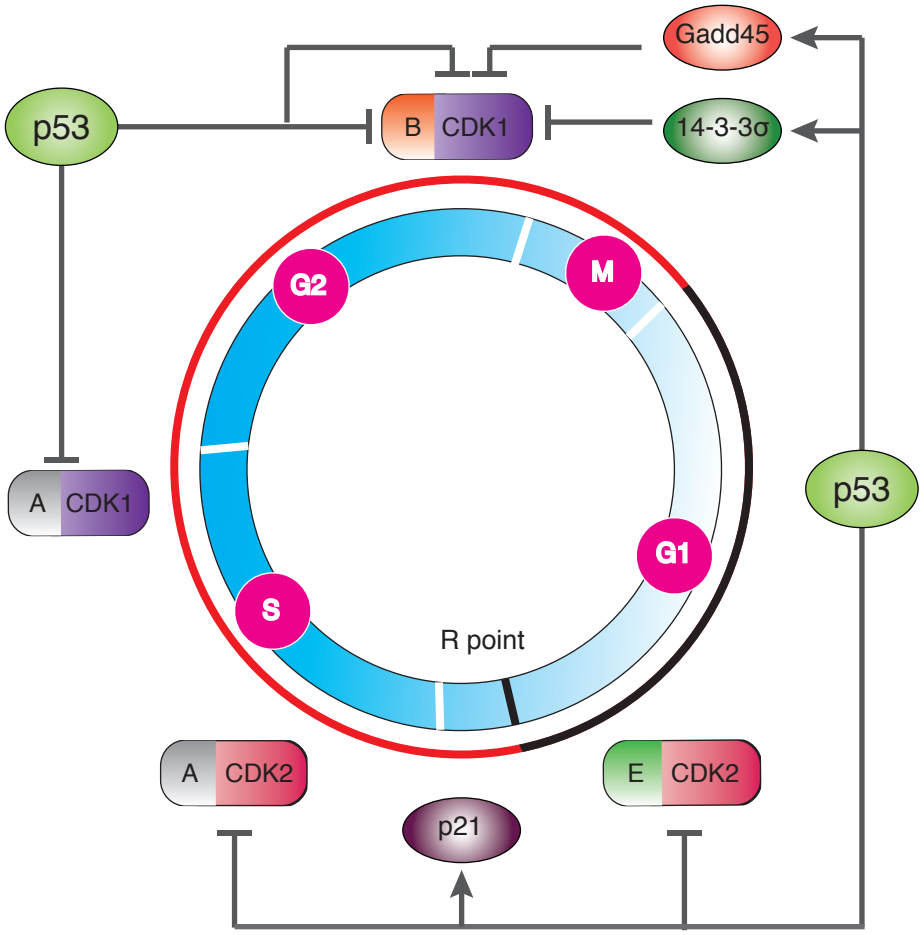

Figure 1-3: p53's control of cell cycle.
R point=restriction point. The black line represents hypophosphorylation of Rb and the red line represents increasing phosphorylation of Rb in a clockwise direction. A, B and E=cyclins and CDK=Cyclin Dependent Kinase. Adapted from 'The Biology of Cancer'[83] and Vogelstein *et al*, 2000[84].

p53 can inhibit cell cycle progression in multiple ways. Cyclin dependent kinase inhibitors including p21, one of the first p53 target genes discovered[85, 86, 87, 88] and p16 can inhibit the cyclin-CDK complexes thereby halting the cell cycle. Upon p53

activation p21 is upregulated and inhibits G1/S specific kinases CDK2, 3, 4 and 6[89] causing Rb to remain hypo-phosphorylated to ensure that cells cannot progress to S phase.

In addition p53 can cause cell cycle arrest at the G2-M checkpoint by transcriptionally regulating Gadd45 and 14-3-3σ expression. Gadd45 interferes with cyclin B-CDK1 complex formation[90] and 14-3-3σ sequesters cyclin B1-CDK1 complex outside the nucleus therefore maintaining G2 blockage[91, 92]. Both proteins act to inhibit CDK1, which is required for the G2-M transition and therefore halt cells in G2.

Furthermore p53 can repress cyclin A, cyclin B1, cyclin B2 and CDK1 via a variety of mechanisms including direct binding to p53 binding elements in the promoters of these genes or by inhibiting binding of other, more potent transcription factors[93-95]. An alternative method by which p53 can repress genes is by directly binding to and recruiting histone deacetylases (HDAC) (via nuclear transcription factor Y (NF-Y)), which can also inhibit genes responsible for cell cycle progression[96, 97].

The genes involved in DNA repair that are activated by p53 in response to low stress conditions include Gadd45[98] and p53R2[99]. Gadd45 has been shown to be required for p53's ability to repair DNA after UV damage and cisplatin treatment and p53R2 encodes a subunit of ribonucleotide reductase that is important for DNA synthesis during cell division[100]. Together they assist in the DNA repair response following stress and therefore contribute to p53's ability to maintain genetic stability.

In response to low/reparable stress p53 also activates antioxidant genes (glutathione peroxidase (GPX1)[101], Mn-superoxide dismutase (Mn-SOD)[102], aldehyde dehydrogenase 4 (ALDH4)[103], sestrins[104]) that contribute to limitation of reactive oxygen species (ROS) induced DNA damage and genetic instability[82].

In contrast with normal cells, which produce energy mostly by oxidative phosphorylation, cancer cells favour glycolysis even in the presence of normoxia - this is referred to as the Warburg effect[105]. For cancer cells glycolysis is advantageous since as well as providing ATP (Adenosine Triphosphate) it also

provides intermediates for anabolic pathways thereby supporting cellular proliferation in conditions of nutrient deprivation. p53 opposes the Warburg effect by promoting oxidative phosphorylation through expression of Synthesis of Cytochrome c Oxidase (SCO2)[106] and glutaminase 2[107] and inhibits glycolysis by downregulation of glucose transporters 1 and 4[108] and upregulation of TP53 induced glycolysis and apoptosis regulator (TIGAR). To inhibit glycolysis TIGAR reduces fructose-2,6-bisphosphate levels. Additionally TIGAR contributes to p53's anti-oxidant function by decreasing ROS[109] in unstressed conditions and therefore TIGAR prevents the accumulation of DNA damage and maintains genetic stability.

As a specific response to stress such as starvation, p53 can regulate AMPK (AMP-Activated Protein Kinase) expression[110] that in turn inhibits mTOR (mammalian target of rapamycin) and therefore limits protein synthesis in times of low nutrient availability[111]. In this way p53 reduces growth signals in line with the interruption in cell cycle progress. Alternatively, p53 targets sestrin 1 and sestrin 2 induce phosphorylation of tuberous sclerosis protein 2 (TSC2) leading to inhibition of mTOR[112] via an additional route.

An increasingly recognised, though complex, tumour suppressive action of p53 is its ability to regulate autophagy (the cells ability to digest the cells own components through the lysosomal pathway). Through p53 mediated activation of AMPK and subsequent inhibition of mTOR and directly by activating the Damage-Regulated Autophagy Modulator (DRAM) p53 increases autophagy. The outcome of this can be either promotion of cellular survival[113] or contribution to apoptosis[114] however how these two conflicting outcomes balance to achieve tumour suppression is unclear. Low levels of cytoplasmic p53 reduce autophagy via induction of mTOR activity[115] adding a further complexity to the system.

As well as controlling cell-autonomous effects p53 can have a more global influence over the cellular microenvironment. For example through p53's activation of a secretory programme[116] and production of exosomes[117] (the cell-membrane derived vesicles that carry proteins, lipid, DNA or microRNA) p53 can have non-cell autonomous effects and mediate cell-cell communication. Formation of secretory exosomes containing several p53 regulated proteins is regulated by p53 target Tumour Suppressor Activated Pathway 6 (TSAP6)[118]. A further example of

p53's ability to influence the microenvironment is through inhibition of angiogenesis. In a multifaceted fashion p53 exerts its effects by interfering with regulators of hypoxia (Hypoxia Inducible Factor 1 alpha (HIF1α))[119], inhibiting proangiogenic agents (Vascular Endothelial Growth Factor (VEGF))[120] and increasing anti-angiogenic factors (Thrombospondin 1 (Tsp1))[121].

Ultimately in low levels of stress p53 causes cell cycle arrest and activates pro-survival pathways to allow cell repair, replenishment of nutrients or resolution of oxidative stress prior to re-entry into the cell cycle.

1.3.2 p53's response to irreparable or oncogenic stress

In response to high stress p53 favours activation of target genes that initiate a terminal cell fate (apoptosis or senescence).

p53 contributes to both the intrinsic and the extrinsic apoptotic pathways by activating p53 target genes Bax, PUMA, Noxa and Fas, Death Receptor 5 (DR5) and p53 induced protein with a death receptor (Pidd) (Figure 1-4).

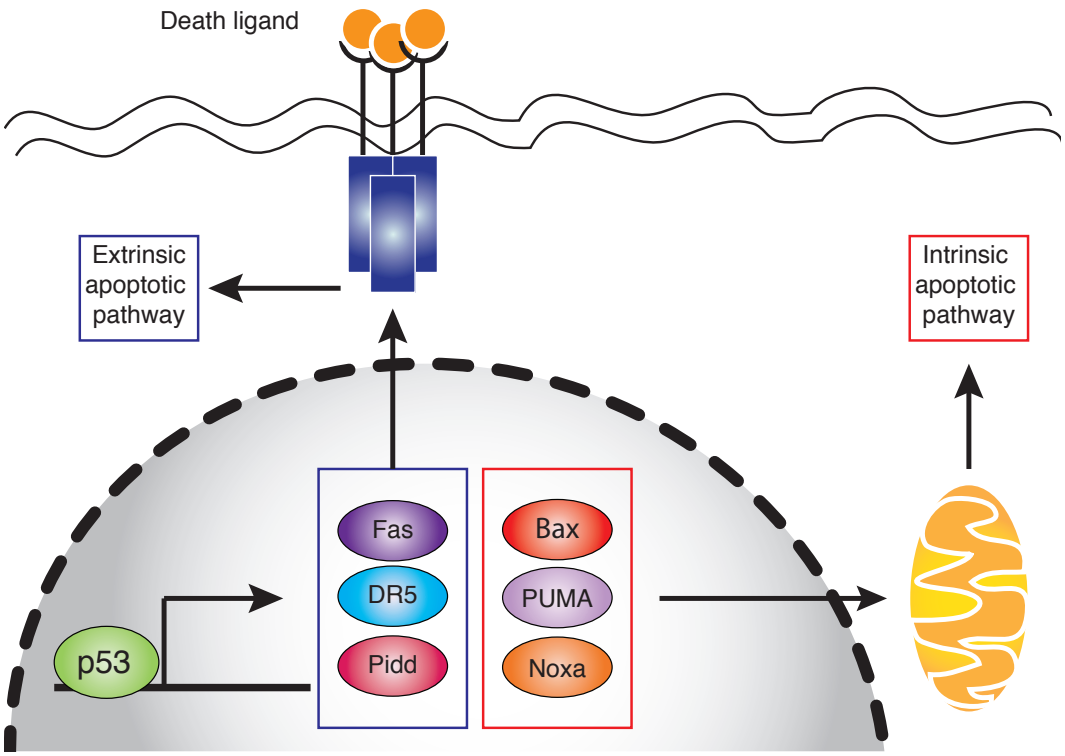

Figure 1-4: p53 and apoptosis.
DR5=Death Receptor 5, Pidd=p53 induced protein with a death domain, PUMA=p53 Upregulated Modulator of Apoptosis. Adapted from Jesenberger *et al*, 2002[122].

In response to high stress p53 activates pro-apoptotic Bcl-2 family members Bax[123], Noxa and PUMA[124]. Noxa and PUMA bind to the anti-apoptotic Bcl-2 preventing it from inhibiting Bax[125, 126]. Bax then localises to the outer mitochondrial membrane, causing opening of mitochondrial channels and subsequent release of cytochrome c[127]. Cytochrome c activates intrinsic apoptosis initiator caspase 9, which in turn activates the executioner caspases 3, 6 and 7. The proteolytic executioner caspases degrade cellular organelles resulting in cell death. In addition p53 can more directly repress the anti-apoptotic Bcl-2 by inhibiting its transcription factor Brn3a[128] resulting in unchecked Bax and Bak activity and ultimately cell death.

The extrinsic apoptotic pathway is so named because it is initiated from outside the cell. p53 activates the expression of a number of transmembrane death receptors (Fas[129], DR5[130] and Pidd[131]). These death receptors are displayed on the cell surface and after binding to their ligands activate the extrinsic initiator caspase cascade (caspase 8 and 10) that eventually joins the common execution caspase cascade causing cell death.

As an alternative to apoptosis, p53 can induce senescence in response to high levels of stress. This is a state of irreversible cell cycle arrest, which is mediated by p53 targets p21 and plasminogen activator inhibitor 1 (PAI-1)[132, 133]. Several mouse models have shown that senescence is important for p53's tumour suppressive functions. In a mouse model of hepatocellular carcinoma, where p53 was modulated using RNA interference, tumour cells became senescent upon p53 reactivation. This provoked an inflammatory response and clearance of tumour cells by macrophages[134]. Furthermore a mouse expressing the apoptosis deficient p53 R172P is able to suppress tumourigenesis through upregulation of p21 and senescence[135]. When this same mutant is expressed in a p21 null mouse there is no senescence and enhanced tumour formation, illustrating the importance of p21 in p53 mediated senescence and tumour suppression[136].

1.4 Regulation of p53

As described above p53 has the ability to supress tumour formation by a wide array of mechanisms and in a vast number of cellular contexts. In order to achieve

this, p53 is subject to regulation at the transcriptional, translational and protein level.

1.4.1 Structure of p53

p53 protein is active as a tetramer of 4 chains of 393 amino acids[137]. Each chain has several domains. At the N-terminal there are two distinct transactivation domains (TADI and TADII), a nuclear export signal (NES) followed by the proline rich domain (PD) and the DNA binding domain (DBD). Then at the C-terminus there is an oligomerisation domain (OD), three nuclear localisation signals (NLS), a second NES and a lysine rich regulatory domain (RD) (Figure 1-5).

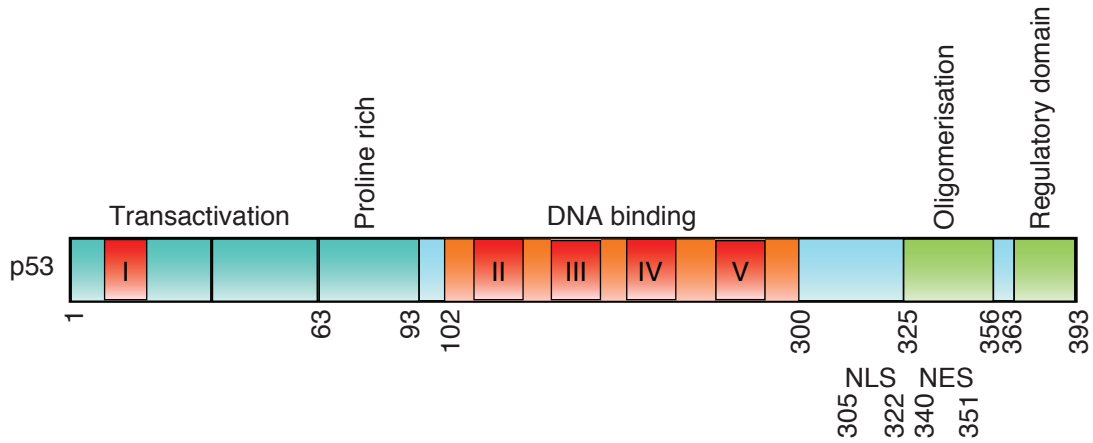

Figure 1-5: Functional domains of p53 protein.
NLS=Nuclear Localisation Signal (only the most active NLS is indicated), NES=Nuclear Export Signal (N-terminal NES is not shown). Red boxes I-IV indicate highly conserved regions of p53.

The TADI (residues 1-40) and TADII (residues 43-63)[138] are critical for p53's regulation since they provide binding sites for the transcriptional machinery and negative regulators MDM2 (mouse double minute 2)/MDMX. The TADs are differentially involved in the activation of a distinct set of p53 target genes[139, 140]. In addition the transactivation domain of p53 contains 1 of the 5 highly conserved regions in p53. This region (box 1) is required for the binding of MDM2 and MDMX[141, 142].

The proline rich domain (residues 63-93) links the TAD and the DNA binding domain. Although the exact function is not well understood, the high proline prevalence is conserved though species. In addition, from work on mouse models it is also known that the length of the proline domain is critical to maintain p53's

tumour suppressive function[143]. Furthermore this domain is the site of a common p53 single nucleotide polymorphism (SNP) at codon 72 indicating *in vivo* importance of this region (implications of this SNP are discussed further in section 1.4.2).

The DNA binding domain (residues 102-300) is pivotal for the transcriptional activity of p53. It contains 4 of the 5 conserved boxes in p53 (boxes II-V as shown in Figure 1-5). Through a series of studies solving the crystal structure of the DNA binding domain of p53 with different target DNAs, signalling proteins and viral oncoproteins it has been established that these conserved boxes are crucial for the p53/DNA interaction[144-149]. Also the DNA binding domain of p53 is only marginally stable with a melting temperature of 44ºC which is thought to allow for rapid cycling between folded and unfolded states and therefore allow more rapid control of p53 response[150].

The oligomerisation domain (residues 325-356) allows p53 to form a tetramer which is organised as a dimers of dimers[151].

The C-terminus of p53 contains a cluster of three NLSs that mediate the nuclear location of the protein[152] (the location of the most active site is indicated in Figure 1-5 however there are 2 further NLS sites between residues 366 and 372 and between residues 377 and 381). These sequences bind to specific receptors and allow selective passage of p53 through the nuclear pore complex[153]. The C-terminal NES, a highly conserved region has been shown to be necessary and sufficient for nuclear export of p53[154]. There has been a further report of an N-terminal NES between residues 11 and 27. This NES was shown to contain 2 sites that are phosphorylated following DNA damage resulting in inhibition of nuclear export of p53 and resultant enhanced p53 activity[155]. Both the NLS and NES regions are required for nuclear-cytosolic shuttling of p53 as a means to regulate p53 transcriptional function.

The regulatory domain is the region where many post-translational modifications including acetylation, ubiquitination, phosphorylation, SUMOylation, methylation and neddylation occur (although these modifications can also occur elsewhere). These modifications coordinate to regulate stability and activity of p53. Studies

using a C-terminally truncated p53 demonstrate that the C-terminus is required for efficient binding and transactivation of target genes[156, 157].

1.4.2 Isoforms of p53 and p53 single nucleotide polymorphisms

The human *TP53* gene spans 11 exons and is located on the short arm of chromosome 17 (17p13.1) (GenBank Accession Number: NC_000017.10). The gene contains two promoters, one upstream of exon 1 and one alternative internal promoter in intron 4[158], resulting in four mRNA variants: full-length p53, Δ40p53, Δ133p53 and Δ160p53 (Figure 1-6).

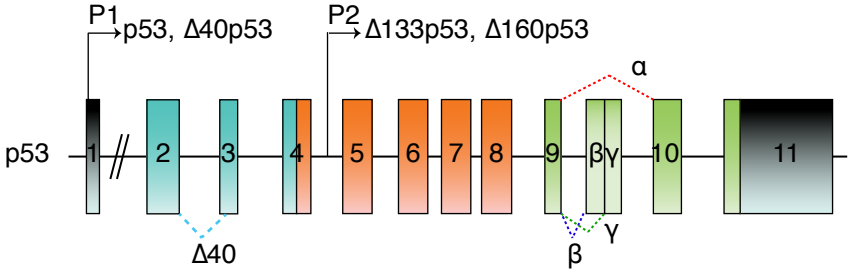

Figure 1-6: Genomic structure of p53.
Noncoding sequence (grey), transactivation domain (turquoise), DNA binding domain (orange), oligomerisation domain (green). Alternative splicing (α, β, γ) and alternative promoters (P1 and P2) are shown. Adapted from Marcel *et al*, 2010 [159].

Full-length p53 is transcribed from the P1 promoter upstream of exon 1[160].

Δ40p53 (p47 or ΔNp53) can be produced by either internal initiation of translation from codon 40 or alternative splicing of intron 2 producing an N-terminally deleted p53 isoform. This isoform does not complex with MDM2 and has impaired transcriptional activity since part of the transactivation domain is lacking. Δ40p53 is able to oligomerise with full-length p53 and negatively regulate its transcriptional activity[161, 162, 163]. In drosophila the p53 gene structure is conserved and expression of a full-length p53 and a ΔNp53 isoform is seen. Recently this drosophila ΔNp53 isoform was shown to induce apoptosis in response to stress by inducing a distinct Inhibitor of Apoptosis (IAP) antagonist in comparison with full-length p53[164]. In humans the clinical relevance of Δ40p53 has been investigated in ovarian cancer where the presence of Δ40p53 is a favourable prognostic marker in the mucinous histological subtype of ovarian cancer[165].

Δ133p53 is transcribed from the alternative promoter in intron 4 and results in an N-terminally truncated p53 protein initiated at codon 133. It is thought to be dominant negative towards full-length p53, inhibiting p53 dependent apoptosis and G1 arrest and instead favouring a G2 arrest[158,166, 167]. Interestingly, clinical data shows that the presence of Δ133p53 predicts improved recurrence free and overall survival in serous ovarian cancer where approaching 100% of patients have a p53 mutation[168, 169]. These data illustrate the biological relevance of p53 isoforms but also indicate the need for further study of these isoforms in the context of both wild-type and mutant p53 background.

Δ160p53 lacks the first 159 residues and is encoded from the Δ133p53 transcript using ATG160 as translation start site[159]. This isoform is expressed in tumour cell lines however its biological significance and role are yet to be established.

As predicted from the lack of a complete N-terminus the p53 isoforms described thus far cannot bind MDM2. Despite this the isoforms are not stabilised in cells since their level is maintained at a low level by one or several, as yet unidentified, ubiquitin E3 enzymes[170]. This could have implications for the treatment of isoform expressing tumours with MDM2 inhibitory therapy (which is discussed later).

In addition to the described p53 isoforms there are C-terminal isoforms that result from alternative splicing of intron 9. This intron 9 splicing can produce p53β (previously named p53i9[171]) and p53γ. These isoforms encode truncated proteins, which lack the oligomerisation domain, fail to bind DNA *in vitro* and are transcriptionally deficient[172].

Through a combination of alternative promoters, alternative splicing and alternative translation start sites the p53 gene can encode at least 11 different p53 protein isoforms (although theoretically there will be a Δ160p53γ, this has yet to be identified). These p53 isoforms are expressed in a tissue-dependent manner and their expression is deregulated in cancers[158,173] suggesting that they are significant *in vivo*. Knowledge of their specific role however is currently lacking with full-length p53 being by far the most studied since several of the antibodies commonly used to detect p53 do not recognise N-terminally truncated p53. Furthermore full-length p53 has been shown to regulate the transcriptional

expression of certain N-terminal isoforms[174]. It is therefore expected that further studies of p53 isoforms will demonstrate that they provide another layer of complexity in modulating p53 response.

To date eighty p53 polymorphisms have been identified of which the majority are in introns, outside splice sites or in non-coding exons. Of the intronic polymorphisms *TP53* PIN3 (polymorphism in intron 3), which consists of a 16 bp duplication, occurs at a site important for the regulation of splicing and therefore modulates splicing[175, 176]. Of the eighteen exonic SNP, five are silent, seven are located after the stop codon in exon 11 and four alter the protein sequence but have only subtle effects on transactivation.

The proline rich domain of p53 is the location of a common SNP (as mentioned earlier). Codon 72 can be either CCC resulting in a proline or CGC encoding an arginine[177, 178]. Its prevalence is related to latitude with the highest rates of P72 in the Southern hemisphere. P72 is less active in induction of apoptosis than R72 since P72 binds the anti-apoptotic iASPP more efficiently[179]. Despite this, studies looking at cancer risk have been inconsistent. A meta-analysis of cohorts of patients with breast cancer[180] and lung cancer[181] showed no significant effect on cancer susceptibility.

V217M is the only non-silent polymorphism in the DBD (DNA binding domain). It increases transactivation of some response elements and may protect from cancer[182]. Another SNP, next to the tetramerisation domain (G360A) slightly reduces transcriptional activity and may increase cancer risk[183].

1.4.3 Transcriptional and translational regulation of p53

Transcription of full-length p53 is influenced by multiple transcription factors (c-myc/max heterodimers[184, 185], NF1 and yin yang 1 (YY1)[186], C/EBPβ-2[187]) that bind to the p53 promoter and increase its transcription. Additionally multiple co-factors can also contribute to transcriptional regulation of p53 by either repressing (PAX2, PAX5 and PAX8[188] and RBP-Jκ[187]) or enhancing transcription (YY1[186]).

p53 is also regulated at a translational level. In response to stress a variety of mechanisms are utilised to increase translation of p53. p53 itself can enhance its translation via the 3' untranslated region (UTR)[189] and HuR also enhances translation via the 3'UTR[190]. RPL26 and nucleolin bind to the 5'UTR and enhance translation[191] as does hnRNP Q[192]. In addition translation efficiency can be influenced by cytoplasmic polyadenylation of p53[193] and MDM2 binding to p53 mRNA[194]. In response to stress an ATM (ataxia telangectasia mutated) dependent phosphorylation of MDM2 on serine 395 leads to p53 mRNA interaction that appears to be required for full p53 activation following stress. Although the primary mechanism of MDM2's regulation of p53 is by control of p53 protein levels though MDM2's E3 ligase activity this demonstrates an additional way in which MDM2 can regulate p53 and highlights the complexity of p53 regulation.

1.4.4 Post-translational modifications of p53

p53's function is influenced primarily by extensive post-translational modifications. This section describes them (ubiquitination, SUMOylation and neddylation and acetylation, phosphorylation and methylation) in more detail.

1.4.4.1 Ubiquitin and Ubiquitin-like modifications of p53

The ubiquitin-proteasome pathway (Figure 1-7) provides a highly regulated pathway, which specifically regulates the turnover of thousands of intracellular proteins including p53. It is primarily via this pathway that p53 levels are controlled.

The degradation of the target protein involves a series of ATP requiring, enzymatic steps that result in degradation of the target protein at the 26S proteasome and subsequent recycling of the produced peptides and ubiquitin[196].

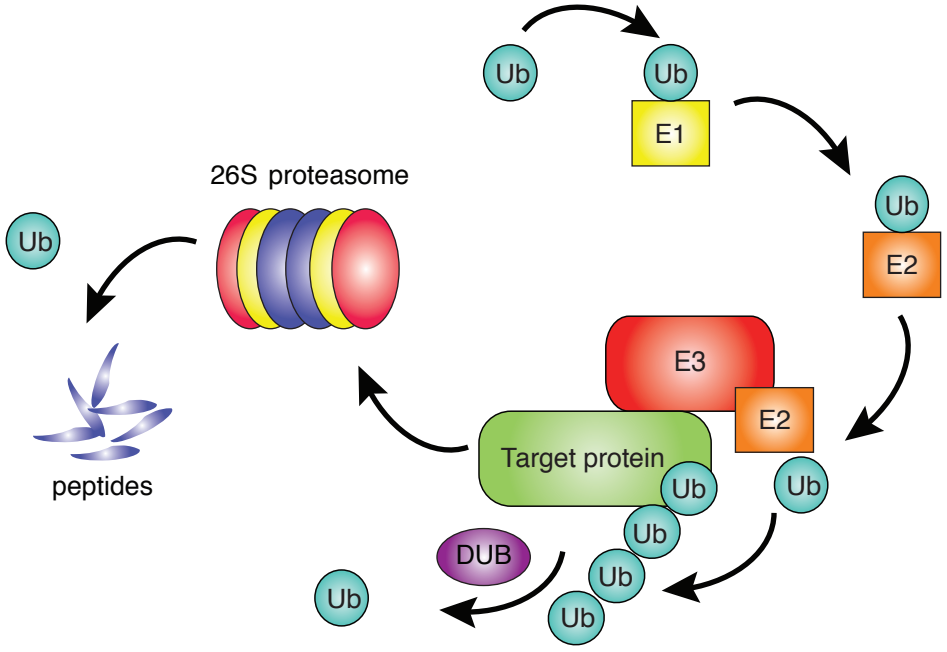

Figure 1-7: Ubiquitin proteasome system.
DUB=Deubiquitinating enzyme, E1=activating enzyme, E2=conjugating enzyme, E3=ubiquitin ligase, Ub=ubiquitin. Adapted from Welchman *et al*, 2005 [195].

The 8.5kDa protein ubiquitin is activated by ubiquitin-activating enzyme (E1) that forms a thiolester bond between its active site cysteine and the C-terminal glycine of ubiquitin. Activated ubiquitin is then transferred to a cysteine on the E2 (ubiquitin conjugating enzyme). The E3 then catalyses the covalent attachment of ubiquitin to an amino-group (mostly from lysines) in the substrate via an isopeptide bond. This sequence of reactions occurs several times to build up a polyubiquitin chain, linking activated ubiquitin to lysine 48 of the previously conjugated ubiquitin. The polyubiquitin chain of at least four ubiquitins provides the mark for 26S proteasomal degradation[197, 198].

Although any of ubiquitin's lysines (K8, K11, K27, K29, K33, K48 and K63) can be used to form chains, linkages via K48 and K63 are the most abundant. Importantly the particular chain linkage determines outcome for example while polyubiquitination via K48 linkages leads to degradation, polyubiquitination via K63 leads to activation of NF-κB, DNA repair and targeting to the lysosome[199]. Furthermore ubiquitin chains may be linear meaning that they link through the amino-terminus again resulting in a different outcome.

In contrast with the outcome seen following polyubiquitination, mono-ubiquitination or multi mono-ubiquitinations of a substrate regulate non-proteolytic processes

including substrate cellular localisation, receptor internalisation, substrate endocytosis and transcriptional regulation[200, 201].

Another important feature of this pathway is that this attachment of ubiquitin to the substrate or other ubiquitins can be reversed by the action of deubiquitinating enzymes (DUBs).

While there are only two E1s[202] in mammalian cells and tens of E2s, there are now thought to be approximately 1000 E3 enzymes[203]. This results in a pathway where E2s are fairly promiscuous being able to act with many different E3s and where the E3 enzyme is primarily responsible for the substrate specificity of each reaction[204-206]. However it is now also recognised that the E2 has more influence on the outcome of ubiquitination than previously thought since the E2 may be able to dictate the type and length of ubiquitin chain formed[199]. Taken together this highlights the importance of efforts to identify E2/E3 pairs[207, 208].

p53 is mono-ubiquitinated and polyubiquitinated at several lysines in the DBD and the C-terminal tail of p53 (Figure 1-8). E3 ubiquitin ligases for p53 are discussed in section 1.4.4.2.

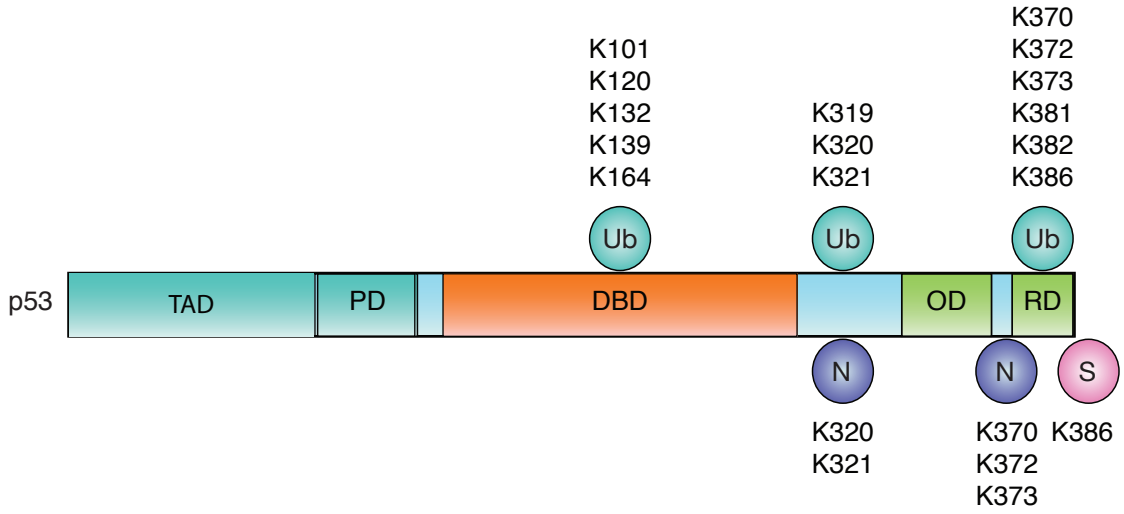

Figure 1-8: Post-translational modifications by ubiquitin-like proteins. Ub=ubiquitinated, N=neddylated, S=SUMOylated, TAD=Transactivation Domain, PD=Proline rich Domain, DBD=DNA-Binding Domain, OD=Oligomerisation Domain, RD=Regulatory Domain. Adapted from Carter *et al*, 2009 [209].

p53 is also modified by two ubiquitin-like proteins, small ubiquitin-like modifier (SUMO) and Nedd8. SUMOylation is the process of covalent conjugation of

SUMO to a substrate. The process involves an enzymatic cascade of events similar to ubiquitination involving a SUMO-activating enzyme (E1), SUMO-conjugating enzyme (E2) and SUMO ligase (E3). SUMO-1 has been more extensively studied than SUMO2/3 and is known to modify lysine 386 of p53 (Figure 1-8). Some studies have reported that SUMOylation enhances transcriptional activity of p53 while others report that SUMOylation drives relocation of p53 from the nucleus to the cytoplasm, two contradictory outcomes[210, 211]. SUMO-2 and SUMO-3, which are 96% identical to each other, have been less widely studied. It is known that they can conjugate to p53 and can modulate p53's transcriptional activity[212]. Several SUMO E3s for p53 have been identified including topors[213], TRIM family proteins[214], MDM2[215] and PIASy[216]. Nedd8 is also a ubiquitin-like protein that can be conjugated to p53 again via an enzymatic cascade involving an E1, E2 and E3. MDM2 is a known Nedd8 ligase with the ability to modify lysines 370, 372 and 373 of p53 while FBXO11, another Nedd8 ligase, modifies lysines 320 and 321[217, 218]. The consequences of Neddylation of p53, although subtle, include inhibition of p53's transcriptional activity and regulation of p53's promoter choice[219].

1.4.4.2E3 ubiquitin ligases for p53

E3 ubiquitin ligases can be divided into three groups based on their functional domain; Homology to E6-associated protein (E6-AP) Carboxy Terminus (HECT)-type E3s, the Really Interesting New Gene (RING) family of E3s and U-box homology proteins.

HECT family E3s have an approximately 350 amino acid C-terminal region homologous to that of E6-AP and an N-terminal region which is highly variable and may be involved in substrate recognition[220]. They are the only E3s, which form thioester intermediates with ubiquitin[221, 222]. The HECT domain binds the E2-ubiquitin and accepts ubiquitin at a cysteine residue.

The largest family of E3s are the RING finger E3 ubiquitin ligases. These consist of a RING finger domain which binds to two zinc atoms via eight conserved cysteines and histidines[223]. This group also includes a sub-family of ubiquitin ligases that contain a plant homeo domain. The RING domain directly binds E2

and functions as an adaptor that positions the substrate lysine in close proximity to E2-ubiquitin complex[224].

U-box E3s contain an approximately seventy amino acid U-box. The U-box is very similar to a RING domain except it lacks the zinc-coordinating cysteine and histidine residues[225, 226]. Like RING E3s U-box E3s bind the E2 and position the substrate aside ubiquitin.

When an E3 polyubiquitinates its substrate (but not when it monoubiquitinates) the substrate can then be delivered to the proteasome for degradation. The functional large 26S proteasome is formed from the ring-shaped 19S and 20S particles. The 20S catalytic core forms a cylindrical stack of 4 rings. The 2 outer rings are composed of 7α subunits and the 2 inner rings 7β subunits[227]. Each of these 28 subunits has distinct peptidase activities. Two 19S complexes cap either side of the 20S core to form the 26S proteasome. The 19S cap is thought to have some control over regulating entry to the 20S core. ATP-dependent unfolding of the polyubiquitinated substrate allows passage of the substrate into the catalytic pore[228].

Ubiquitination and subsequent degradation of p53 is the critical mechanism of p53 regulation. It can occur on any of the six lysines in the C-terminus of p53 as well as other lysines in the DNA-binding domain as shown in Figure 1-8. It is interesting to note that mouse models with p53 lacking the C terminus are still able to control their p53 level therefore it seems likely that in the absence of these C-terminal lysines ubiquitin will use other lysines to target p53 for degradation[229, 230].

Although a number of E3 ubiquitin ligases (table 1-1) are capable of ubiquitinating p53 (Pirh2[231], CHIP[232] & ARF-BP1[233]) MDM2 is crucial for p53 control.

Table 1-1: Known E3 ligases for p53.

E3 (references)	Class	Other known targets
ARF BP1[214, 225, 226]	HECT	Mcl1, Myc
WWP1[231-233]	HECT	KLF2, KLF5, Smad4
Carps[236, 237]	RING	Caspase 8 & 10
Cullin 1/Skip 1[234] Cullin 4a/ DD61/Rac[235] Cullin 5[236] Cullin 7[230]	RING	p21, cyclin D1, BRCA2 p21, c-jun VHL IRS-1
Hades[237]	RING	None identified

MDM2[218-223]	RING	MDM2, MDMX, Histone H2A & Histone H2B, hnRNP K, RB, β-arrestin, MTBP, E2F/DP1, p21, Numb, PSD-95, androgen receptor, PCAF, E-cadherin, G-protein coupled receptor kinase 2, TSG101, Tip60, Insulin-like growth factor 1 receptor, glucocorticoid receptor
MSL2[238, 239]	RING	Histone H2B
Pirh2[212, 224]	RING	HDAC1
Synoviolin[240]	RING	Nicastrin, gp78
Topors[234, 235]	RING	Hairy (Drosophila)
Trim 24[241]/28[242]/39[243]	RING	None identified
CHIP[213, 229]	U-box	Chaperone-bound proteins, HSP70

hnRNP=heterogeneous ribonucleoprotein particle, RB=retinoblastoma, MTBP=MDM2, transformed 3T3 cell double minute 2, p53 binding protein, E2F/DP1=E2F/prostaglandin D2 receptor, PCAF=p300/CBP-associated factor, TSG101=tumour susceptibility gene 101, AIB1=amplified in breast cancer 1, HDAC=histone deacetylase, KLF2=Kruppel-like factor 2, MSL2=male-specific lethal 2. Adapted from Love *et al*[244].

This has been demonstrated by mouse models where a deletion of *MDM2* results in embryonically lethality that can be rescued by simultaneous deletion of *TP53* [245, 246].

In normal tissues, when the tumour suppressive activities of p53 are not required, p53 is kept at very low levels by MDM2. MDM2 binds to p53 at its transactivation domain[141] preventing transcriptional activity. MDM2 then ubiquitinates p53 leading to export of p53 from the nucleus, in the event of monoubiquitinatation[247], and degradation of p53 through the proteasome following polyubiquitination[248-250] (Figure 1-9).

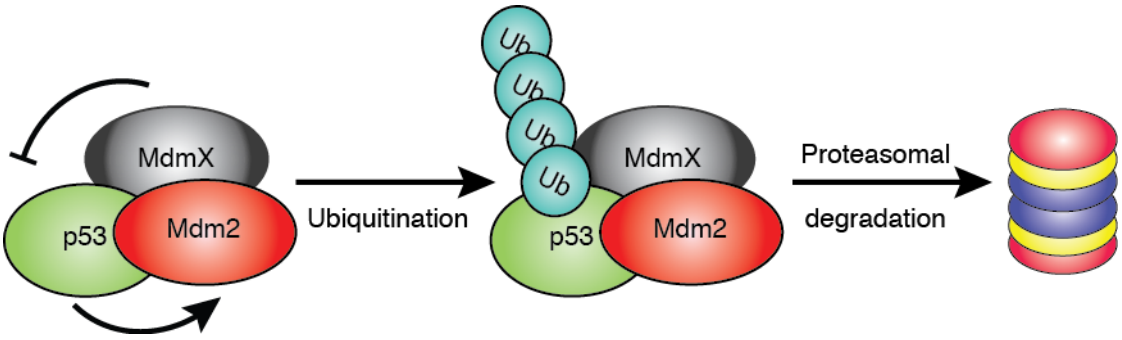

Figure 1-9: p53-MDM2-MDMX pathway.
Ub=ubiquitin.

In the event of cellular stress this inhibition is removed by mechanisms explained below and, in turn, p53 accumulates resulting in tumour suppression activity. Since MDM2 is a transcriptional target of p53, a negative feedback loop is established which is important for recovery of cells following a stress response[251].

Studies of the specific E2 contribution to MDM2 dependent ubiquitination of p53 have shown that E2s, UbcH5B and C can both be involved[252] and as a result of this most mechanistic work on ubiquitination in the p53 pathway have used either of these E2s. Additionally, important advances have been made in mapping the E2-MDM2 interaction surface, which is thought to involve residues Isoleucine 440 (Ile440), Cysteine 441 (Cys441), Glutamine 442 (Gln442), Leucine 468 (Leu468), Lysine 469 (Lys469), Valine 477 (Val477) and Arginine 479 (Arg479), as well as neighbouring residues Valine 439 (Val439), Arginine 471 (Arg471) and Proline 476 (Pro476)[253]. Now that the functional relevance of the specific E2 involved in the E2-MDM2 interaction is beginning to be understood there is growing interest in this area to determine the specific contribution of each E2 to p53 signalling.

Growing evidence suggests that a further group of ubiquitinating enzymes enhance the ubiquitination process. The E4 enzymes or ubiquitin chain assembly factors, enhance the ability of E3 enzymes to form ubiquitin chains. For MDM2 several supporting E4 enzymes have been identified (p300/CBP (CREB1-binding protein)[254], UBE4B[255], Gankyrin[256] and YY1[257]). These enhance MDM2-dependent p53 ubiquitination increasing the degradation of p53.

In opposition with the E4s, deubiquitinating enzymes for p53 (USP10[258], USP29[259] and USP42[260]) respond to various stresses to deubiquitinate and stabilise p53. A further DUB, HAUSP (USP7), is involved in the regulation of p53 levels. HAUSP is a DUB for MDM2 and, p53's other negative regulator, MDMX. In response to stress the interaction between HAUSP and MDM2 and MDMX is inhibited by phosphorylation events allowing p53 to stabilise[261, 262].

MDMX is an MDM2-like protein that is also involved in the regulation of p53. It binds to p53 preventing its transcriptional activity but does not have E3 ligase activity and therefore does not target p53 for degradation[263]. Importantly dimers of MDM2 and MDMX can have E3 activity and these heterodimers seem to be the predominant form in the cell and are more potently active as an E3 ligase than MDM2 homodimers[264-269]. In concordance with the *MDM2* knock-out mice, the *MDMX* knock-out mice also have an embryonic lethal phenotype, which can be rescued by simultaneous p53 deletion[270, 271].

1.4.4.3Stabilisation of p53

Depending upon the particular stress stimuli encountered, p53 is stabilised in response to stress by one of three distinct pathways (Figure 1-10).

In response to oncogenic stimuli the tumour suppressor ARF (alternative reading frame protein expressed from INK4a locus[272, 273]) binds to MDM2 inhibiting its E3 activity and therefore causing accumulation of p53[274, 275].

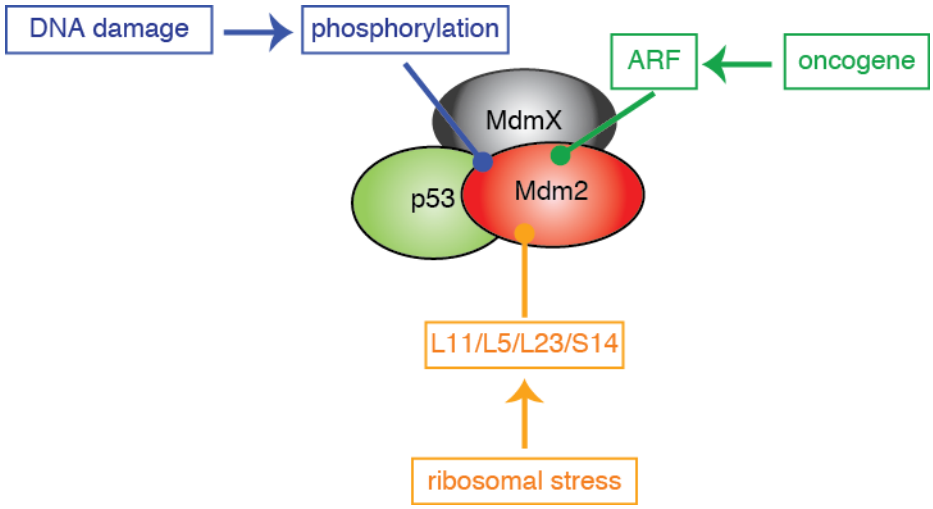

Figure 1-10: p53 stabilisation in response to different stimuli.

In response to ribosomal stress, ribosomal proteins (L11, L5, L23, S14) are able to bind MDM2 blocking the ubiquitination of p53 (without blocking the interaction of MDM2 with p53) while enhancing the ubiquitination and degradation of MDMX[276-279]. Interestingly although MDMX has a similar acidic domain to MDM2 it does not bind ribosomal proteins[280].

In response to DNA damage, ATM and ATR (Ataxia telangectasia and rad3 related) cause phosphorylation of serine and threonine residues at sites in both the N-terminus and C-terminus of p53 reducing its interaction with MDM2[213] (Figure 1-11).

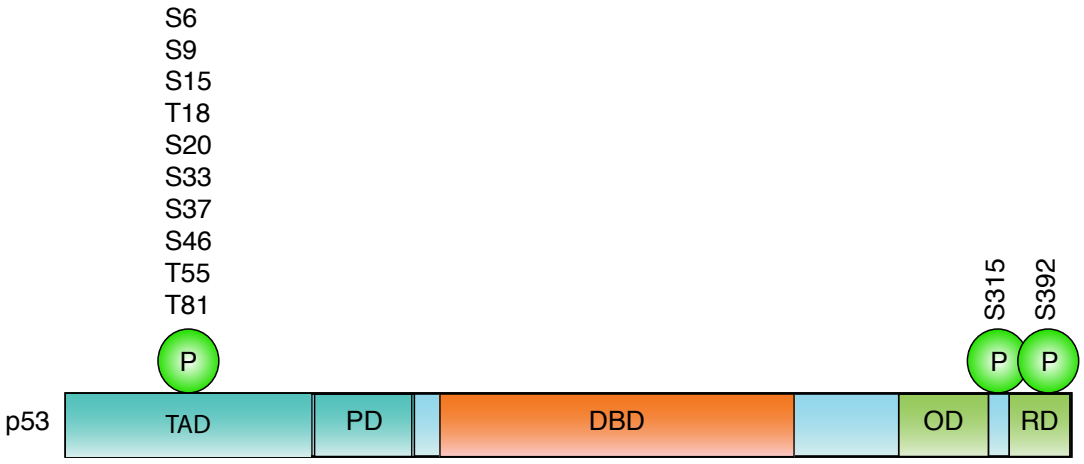

Figure 1-11: Phosphorylation of p53.
P=Phosphorylation, TAD=Transactivation Domain, PD=Proline rich Domain, DBD=DNA-Binding Domain, OD =Oligomerisation Domain, RD=Regulatory Domain. Adapted from Appella *et al*, 2001[281].

Double stranded breaks are recognised by the MRN complex (MRE11-RAD50-NBS1), which leads to activation of ATM. ATM phosphorylates CHK2 (checkpoint kinase 2), which in turn phosphorylates serine 20 of p53[282-285]. CHK2 can however be phosphorylated independent of ATM in response to some types of stress including replication fork stalling and UV irradiation[286]. ATM can also directly phosphorylate p53 on serine 15[210, 211] and 46[287], which regulates the ability of p53 to induce apoptosis[288].

Other forms of DNA damage lead to single stranded regions that become coated with replication protein A. This attracts ATR, which phosphorylates complexes that feed forward and further stimulate ATR. In this situation (when MDM2 is no longer required to keep p53 in check) MDM2 can act as its own E3 ubiquitin ligase and is degraded[289]. As discussed later p53's negative regulators also undergo post-translation modifications in response to stress. These phosphorylation events all contribute to reduced binding between p53 and MDM2 and MDMX and therefore the stabilisation of p53.

A multitude of other kinases phosphorylate p53 in response to various stressful stimuli allowing p53 to integrate multiple stress signals to achieve a variety of functional outcomes. Some further examples include ATR and DNA-PK mediated phosphorylation on serine 37. This results in inhibition of the p53-MDM2 interaction and enhanced apoptosis[284, 290]. p53 is also phosphorylated at serine 392 in response to UV, DNA damage and interferon by kinases FACT-CK2, p38

and PKR (a double-stranded RNA activated protein kinase) respectively[291-295]. This phosphorylation site has been shown to influence cell cycle arrest, DNA binding and transcriptional capabilities of p53[291, 296]. Also in response to DNA damage p53 is phosphorylated at serines 6 and 9 and threonine 18 by casein kinase delta (CK1δ) and casein kinase epsilon (CK1ε)[297] again leading to stabilisation of p53.

Following the N-terminal phosphorylation events described above the prolyl-isomerase, PIN1 has been implicated in integrating the phosphorylation events mediated by different kinases to maximise p53 activity. PIN1 binds to the proline rich domain of p53 following stress induced phosphorylation leading to a change in conformation of p53 which enhances p53 activation by multiple mechanisms including promotion of p300 mediated acetylation (discussed below) and dissociation of anti-apoptotic iASPP[298].

Acetylation of p53 also occurs as a result of a cellular stress and acts as an activating signal for p53. Acetylation can occur at multiple sites in the DBD and C-terminal regulatory domain of p53 (Figure 1-12).

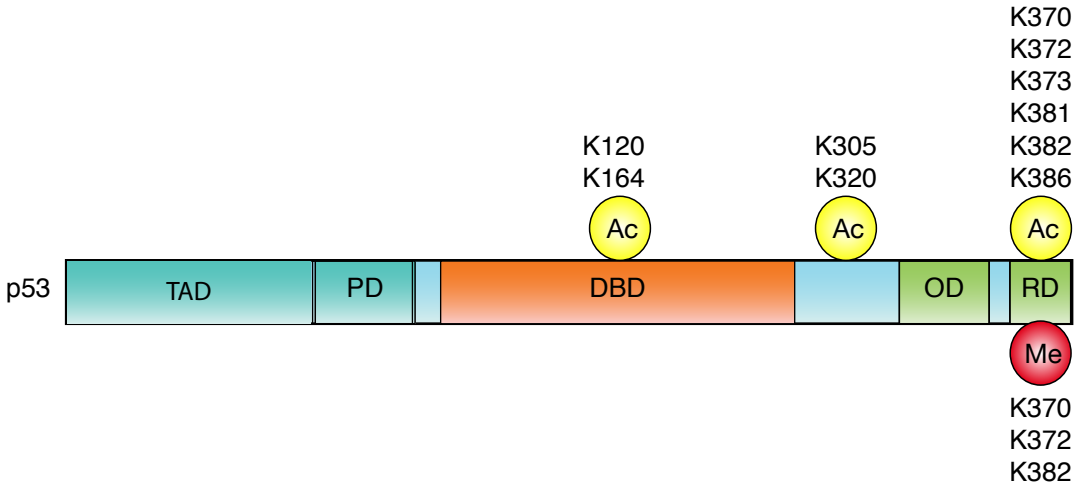

Figure 1-12: Acetylation and methylation of p53.
Ac=acetylated, Me=methylated, TAD=Transactivation Domain, PD=Proline rich Domain, DBD=DNA-Binding Domain, OD=Oligomerisation Domain, RD=Regulatory Domain. Adapted from Carter *et al*, 2009[209].

For example p300/CBP is known to instigate acetylation of p53 on the C-terminal lysines and lysine 164, resulting in enhanced DNA binding and transcriptional activity[299, 300]. Furthermore different acetylations have been shown to have some

influence over which genes are activated, with acetylation of lysine 320 by p300/CBP-associated factor favouring cell cycle arrest genes and Tip60 or hMOF mediated acetylation of lysine 120 favouring apoptotic genes[301-303]. A mouse model, where the eight acetylation sites (in the C-terminus) of p53 were mutated to arginines, has demonstrated the importance of acetylation in the activation of p53. These mutations resulted in a mouse that had lost its ability to cause growth arrest or apoptosis. Despite evidence that p53 was appropriately recruited to the promoter of target genes there was no induction of gene expression. This was thought to be due to the continued binding of MDM2 to p53 since the binding had not been disrupted by acetylation[300]. Intriguingly another acetylation deficient mouse has been shown not to develop tumours despite this inability to activate senescence or apoptosis[304].

To date three methyltransferases have been shown to methylate p53 (Set7/9, Smyd2 and Set8/PR-Set7). Unlike acetylation, methylation at some sites has been shown to activate p53 (Set7/9 mediated methylation of lysine 372) while at others p53 is inactivated by methylation (Smyd2 mediated K370 methylation and Set8/PR-Set7 mediated K382 methylation)[305-307].

Post-translational modifications of p53 are numerous and while individually they may play a small modulatory role in p53 regulation overall they are critical to orchestrate the appropriate p53 response to a variety of stimuli.

1.4.5 Regulation of MDM2

1.4.5.1 Structure of the MDM2 protein

The full-length MDM2 protein has 491 amino acids and consists of several conserved functional domains, including the N-terminal p53 binding domain, a nuclear export signal (NES), nuclear localisation signal (NLS), the central acidic domain, zinc finger domain (ZF), nucleolar localisation domain (NoLS) and the C-terminal RING domain (Figure 1-13).

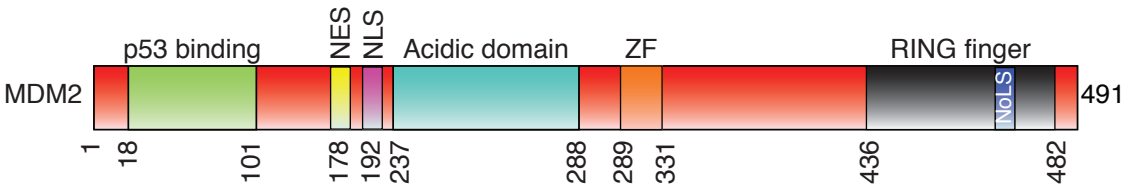

Figure 1-13: Domains of MDM2.
NES=Nuclear Export Signal, NLS=Nuclear Localisation Signal, ZF=Zinc Finger, NoLS=Nucleolar Localisation Signal. Adapted from Wade *et al*, 2010[308].

The p53-binding domain includes the N-terminal 100 amino acids and has been shown to bind to p53 at its transactivation domain and inhibit p53's transcription[141, 309, 310]. Three amino acids of p53's transactivation domain (phenylalanine 19 (Phe19), tryptophan 23 (Trp23) and leucine 26 (Leu26)) insert into a deep hydrophobic cleft in MDM2's p53-binding domain[309].

The NES and NLS of MDM2 both lie between the p53-binding domain and the acidic domain. They are required for the shuttling of MDM2 between the nucleus, where it can bind p53 and inhibit its transcriptional activity, and the cytoplasm[311, 312]. However, mutations of the NES in MDM2 demonstrated that this shuttling is not absolutely required for proteasomal degradation of p53[313]. Located in the C-terminus, MDM2 also has a cryptic NoLS, which is important for the ARF mediated nucleolar localisation of MDM2[314].

The acidic domain of MDM2 is necessary for MDM2's interaction with ribosomal proteins L5, L11, L23 and S14 and ARF[274-276, 279, 315]. In addition this domain is also important for efficient degradation of p53 as demonstrated by a mouse model expressing an MDM2 mutant lacking its central acidic domain which was able to ubiquitinate p53 but not target it for degradation[316, 317]. These findings are consistent with the acidic domain of MDM2 providing a secondary site for interaction with p53[318, 319] and also the site for interaction with p300/CBP, which cooperates with MDM2 to target p53 for degradation[320, 321].

The zinc finger of MDM2 is found between amino acid 289 and 331. Its function is presently undefined although cancer-associated mutations in MDM2's zinc finger disrupt MDM2's interaction with L5 and L11 and impair their ability to stabilise p53[322]. The zinc finger is therefore implicated in p53 response to ribosomal stress.

In the C-terminus, MDM2's RING finger confers vital E3 ligase activity allowing it to monoubiquitinate and polyubiquitinate itself, p53[323] and several other targets (table 1-1). The importance of MDM2's E3 ligase activity has been clearly demonstrated in a mouse model with a C462A mutation (equivalent to C464A in humans) in the MDM2 RING domain, resulting in a catalytically inactive MDM2. Similar to *MDM2* and *MDMX* knock-out mice, mice homozygous for C462A died in the embryonic stage and this phenotype was rescued by concomitant deletion of p53[324]. Also critical for MDM2's E3 ligase activity is the C-terminal tail of MDM2[265, 266]. Although the C-terminal tail is required for dimerisation of MDM2 with itself and MDMX, point mutants of MDM2 C-terminus that retain ability to dimerise are catalytically inactive suggesting that involvement of the C-terminus in catalytic activity is not only because it is required for dimerisation[325].

1.4.5.2The MDM2 gene and isoforms

The human *MDM2* gene is located on the long arm of chromosome 12 (12q14.3-q15) (GenBank Accession Number: NC_000012.11) and spans 12 exons (Figure 1-14).

The *MDM2* gene was identified, along with *MDM1* and *MDM3* in a spontaneously transformed murine cell line, 3T3DM[326, 327]. They were located on small acentromeric extrachromosomal nuclear bodies known as double minutes. The human form of *MDM2* (sometimes referred to as *HDM2* but throughout this thesis MDM2 is used to refer to human MDM2 unless otherwise stated) was cloned from the CaCo-2 colorectal cancer cell line and subsequently MDM2 was found to be amplified in one-third of human sarcomas[328].

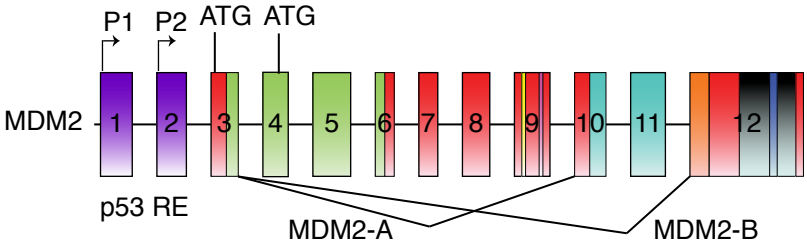

Figure 1-14: Genomic structure of MDM2.
Two promoters are shown (P1 & P2). Full-length MDM2 (p90) is transcribed from the start codon in exon 3 and the short form (p76) from the ATG in codon 4. Two major alternative splice variants are shown (MDM2-A & MDM2-B). Non-coding sequence (purple), p53 binding domain (green), nuclear localisation signal (yellow), nuclear export signal (pink), acidic domain (turquoise), zinc finger (orange), RING domain

(grey), nucleolar localisation signal (navy) and p53 responsive elements (p53 RE). Adapted from Iwakuma *et al*, 2003[329].

MDM2 has two promoters the second of which is p53 responsive[330]. From these promoters both full-length MDM2 and the 14kDa lighter short form, which initiates at an internal ATG, are generated. More than 40 different splice variants of MDM2 have been identified occurring in both tumour and normal tissues[331-333]. The vast majority of these isoforms lack the p53-binding domain. Figure 1-14 shows two of the most commonly occurring *MDM2* splice variants. *MDM2-A* results from deletion of exons 4-9 and *MDM2-B* (*MDM2-ALT1*) from deletion of exons 4-11. The resulting short proteins are unable to bind p53 but bind to full-length MDM2 sequestering it in the cytoplasm and therefore exerting a dominant negative influence on full-length MDM2[334].

1.4.5.3 Post-translational modifications of MDM2

MDM2 is also extensively modified post-translationally (Figure 1-15). Phosphorylation of MDM2 is mediated by both damage-induced kinases (ATM, CHK1, CHK2, DNA-PK and c-Abl) and proliferation/survival kinases (Akt, CK-1/2 and CDK 1/2).

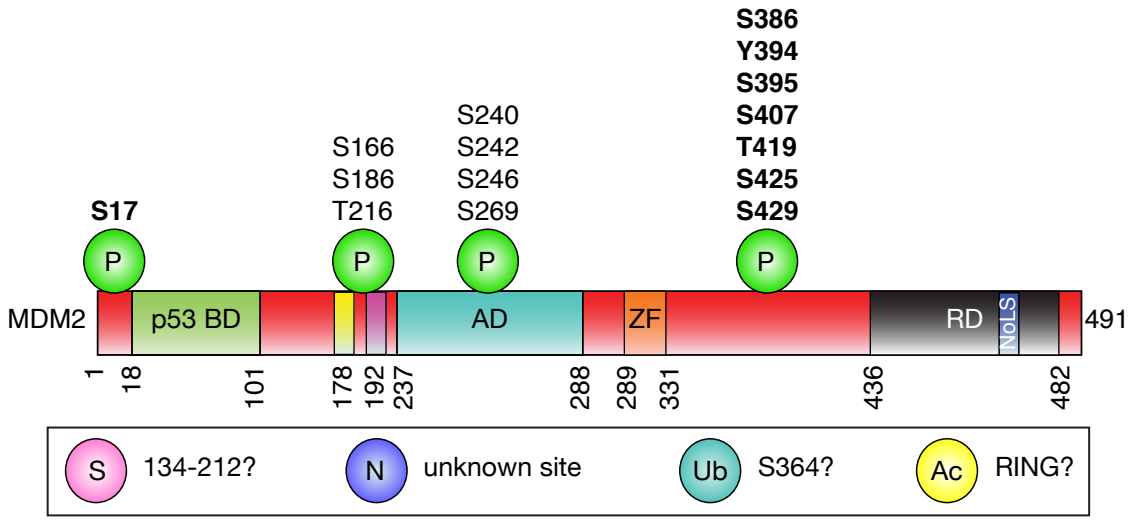

Figure 1-15: Post-translational modifications of MDM2. P=phosphorylation, Ub=ubiquitination, S=SUMOylation, N=Neddylation, Ac=acetylation, p53 BD=p53 Binding Domain, AD=Acidic Domain, ZF=Zinc Finger, RD=RING domain, NoLS=Nucleolar Localisation Signal. Phosphorylation sites regulated by damage-induced kinases are in bold. Adapted from Wade *et al*, 2010[308] and Meek *et al*, 2003[335].

In response to stress ATM phosphorylates the C-terminus of MDM2 (S395 and S407) stimulating rapid degradation of MDM2[336]. DNA-PK mediates damage-induced phosphorylation at N-terminal serine 17, which disrupts p53 binding[337]. ATM also acts via a second kinase c-Abl that phosphorylates MDM2 at tyrosine 394 reducing its ability to inhibit p53[338]. Subsequently, these phosphorylation events result in reduced affinity of deubiqutinating enzyme HAUSP for MDM2 and therefore increased degradation of MDM2[262].

In contrast, phosphorylation events of MDM2 have also been implicated in promoting p53 degradation. In response to oncogenic signals Akt phosphorylates MDM2 at serine 166 and serine 186[331,332]. These modifications enhance MDM2's nuclear localisation. This then promotes interaction of MDM2 with p300 and inhibits MDM2's ARF binding thereby promoting ubiquitination and degradation of p53. This mechanism is one of several that may be responsible for disabling p53 in tumours that retain wild-type p53.

The serines that are phosphorylated in response to stress are dephosphorylated once stress has resolved to allow restoration of p53-MDM2 binding, degradation of p53 and inhibition of MDM2 autoubiquitination. One example of this is the p53 target and dephosphorylase Wip1 that is induced in a delayed manner following stress and is thought to contribute to the stress recovery mechanism[339-341].

While the location of several of the phosphorylation sites on MDM2 have been established, the localisation of acetylation, ubiquitination, Neddylation and SUMOylation that are known to occur on MDM2, remain to be determined.

MDM2 is known to be acetylated somewhere on the RING domain by CBP and p300. This acetylation reduces MDM2's ability to ubiquitinate itself and p53[342].

ARF is known to promote SUMOylation of MDM2 on an N-terminal lysine somewhere between K134 and K212[343]. In addition, TRIM27[214] and SKI[344] enhance SUMOylation of MDM2 causing it to accumulate and degrade p53.

MDM2 is also known to auto-Neddylate resulting in reduced efficiency of MDM2 mediated p53 inhibition[217].

Surprisingly we still have much to learn about the sites on which MDM2 itself is ubiquitinated despite much of the study of MDM2 having focussed on its E3 ubiquitin ligase activity. It has only very recently been suggested, through a mass spectrometry approach, that MDM2 itself is auto-ubiquitinated on lysine 364[345].

1.4.6 Regulation of MDMX

1.4.6.1 Structure of MDMX

MDMX encodes a protein, which is related to MDM2. When it was originally identified, in a screen for p53 interactors, it was shown to inhibit p53 activity, albeit less efficiently than MDM2[346].

As detailed in Figure 1-16 MDMX has a p53-binding domain, acidic domain, zinc finger and RING finger.

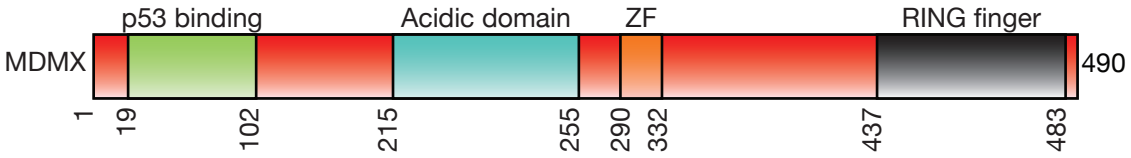

Figure 1-16: Domains of MDMX.
ZF=Zinc finger . Adapted from Wade *et al*, 2010[308].

Like MDM2, MDMX's p53 binding domain binds p53's transactivation domain and blocks its transcriptional activity. This binding prevents p300 interaction with p53 and therefore reduces p53 activation by reducing acetylation[347]. This domain has the highest sequence homology with MDM2. This domain also binds to p53 family member p73[348].

MDMX's zinc finger binds CK1α, which then phosphorylates MDMX at serine 289 enhancing MDMX's inhibition of p53 transcription in unstressed conditions[349].

Despite MDMX having a RING finger domain it does not have intrinsic E3 ligase activity, although as previously mentioned it is important as a heterodimeric partner with MDM2 to form an effective E3 ligase[268].

Unlike MDM2, MDMX has no NLS and is therefore cytoplasmic as a monomer. However, following dimerisation with MDM2 via their respective RING domains,

MDMX becomes nuclear[350]. Several studies studying the importance of MDM2-MDMX heterodimerisation have recently been published[351]. Mice homozygous for a point mutation in MDMX (C462A) that is defective in MDM2 binding have an embryonic lethality phenotype which could be rescued by p53 deletion[352]. However using a conditional mouse model with an MDMX RING deletion revealed that the interaction was dispensable for regulating p53 activity and MDM2 and p53 stability at later stages of development[353]. In general the deletion of MDMX leads to a milder phenotype than loss of MDM2, and although MDMX is required for embryogenesis, it is dispensable in several adult tissues.

1.4.6.2MDMX Isoforms

The human *MDMX* gene (also known as *MDM4*) is located on the long arm of chromosome 1 (1q32) (GenBank Accession Number: NC_000001.10) and spans 11 exons (Figure 1-17).

MDMX is now known to have two promoters. The originally described promoter (P1) is constitutively active and located in exon one while the more recently characterised p53 responsive promoter in located in intron one (P2)[354].

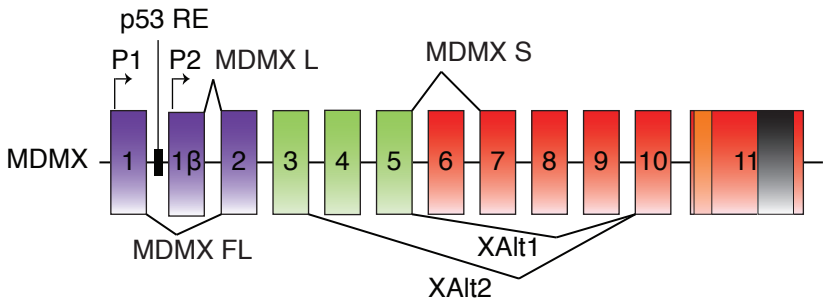

Figure 1-17: Genomic structure of MDMX.
Two promoters are shown (P1 & P2). Four major isoforms are shown. Non-coding sequence (purple), p53 binding domain (green), zinc finger (orange), RING domain (grey) and p53 responsive elements (p53 RE). Adapted from Markey *et al*, 2008[355] and Phillips *et al*, 2010[354].

In addition to the full-length *MDMX* there are 4 major isoforms of *MDMX*. MDMX-L (long-form) is transcribed from P2 and produces a protein that is 18 amino acids longer than the full-length. The other three isoforms result from alternative splicing of *MDMX.* XAlt1 lacks exons 6-9, XAlt2 lacks exons 4-9 and MDMX-S (short form) lacks exons 6[355]. These transcripts are thought to be involved in DNA damage response. In response to stress, full-length *MDMX* transcripts and *XAlt1*

transcripts decrease while *MDMX-L* and *XAlt2* transcripts, which are less efficient at p53 inhibition, increase. It has been proposed that this may help prolong p53 activation following stress[356, 357]. MDMX-S has been associated with decreased patient survival in patients with soft-tissue sarcomas[358] and osteosarcomas[359]. The increase in splicing to form MDMX-S was associated with a reduced protein expression and the presence of another lesion causing inactivation of the p53 pathway (*TP53* mutation or MDM2 overexpression). Furthermore this alternative splicing could predict poor prognosis in a more sensitive manner than the presence of a p53 mutation, suggesting that alternative splicing of MDMX may be a useful biomarker for p53 pathway inactivation[359].

1.4.6.3 Post-translational modifications of MDMX

The known MDMX phosphorylation sites are detailed on Figure 1-18. These phosphorylation sites are also regulated by damage-induced kinases and proliferation/survival kinases.

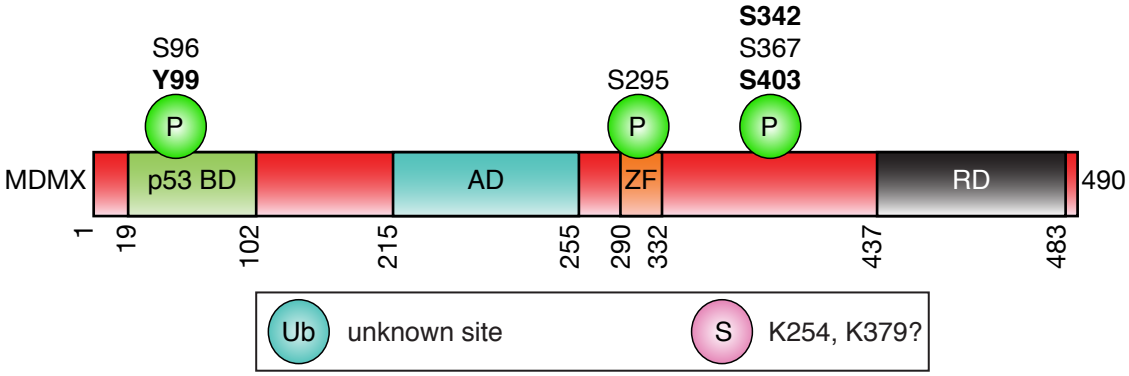

Figure 1-18: Post-translational modifications of MDMX.
P=Phosphorylation, Ub=Ubiquitination, S=SUMOylation, ZF=Zinc Finger, AD=Acidic Domain, RD=RING domain. Phosphorylation sites regulated by damage-induced kinases are in bold. S367 is phosphorylated by damage-induced kinases and proliferation kinases. Adapted from Wade *et al*, 2010[308] and Meek *et al*, 2003[335].

ATM, activated in response to DNA damage, directly phosphorylates MDMX on S403 causing MDMX to be degraded by MDM2 and allowing p53 to be stabilised. Also ATM phosphorylates MDMX via CHK2 at residues S342 and S367[360]. This phosphorylation generates a docking site for 14-3-3σ and stimulates nuclear accumulation and degradation of MDMX by MDM2[360-363]. MDMX is also phosphorylated at Y99 via c-Abl[364] in response to stress. This causes reduced inhibition of p53 by destabilising the MDMX-p53 interaction.

In contrast, in proliferating cells Akt mediates phosphorylation of MDMX at serine 367 leading to the stabilisation of MDMX and MDM2 and consequent degradation of p53[365]. This represents a potential mechanism by which Akt can apply its oncogenic effects.

A mouse model has recently shown the importance of phosphorylation of MDMX in allowing an efficient response to stress. The C-terminal serines, usually phosphorylated by ATM and CHK2 in response to stress, were mutated to alanines. These mice were resistant to ionising radiation displaying reduced p53 dependent transcriptional activity, suggesting that phosphorylation of these residues is required to remove MDMX's inhibition of p53 in the event of stress[366].

As stress resolves, MDMX can also be dephosphorylated by Wip1, causing stabilisation of MDMX and consequent degradation of p53 to maintain low levels in the now unstressed cells[367]. As previously mentioned, in unstressed conditions CK1 alpha can induce MDMX phosphorylation at residue S289[349]. This appears to enhance MDMX's inhibition of p53's transcriptional activity.

In addition to phosphorylation, MDMX is known to be ubiquitinated and degraded by MDM2 but at an unknown site[368]. SUMOylation of MDMX also occurs and requires K254 and K379, but to date the functional relevance of this modification is unknown[369].

1.5 p53 in cancer

Loss of p53 function contributes to the development of most cancers[370]. In approximately 50% of all cancers there are mutations in the *TP53* gene which result in loss of p53 expression or, in most cases, expression of a mutant p53 protein[371]. Recent improvements in sequencing technology have confirmed that p53 is one of the most common genetic abnormalities seen in cancer[372]. In the remainder of cancers where wild-type p53 is retained there is frequently evidence for malfunction of the p53 pathway at some other level[84].

1.5.1 *TP53* mutation

TP53 mutation rates vary significantly depending of the primary cancer site and the histological type[373] (Figure 1-19).

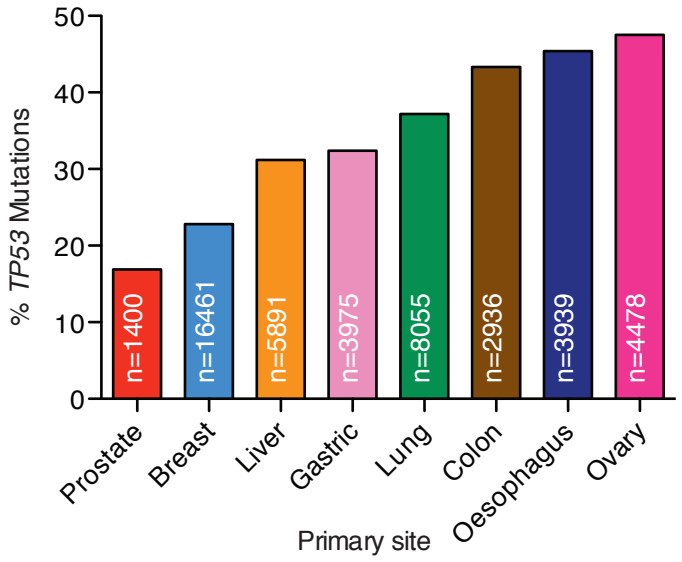

Figure 1-19: *TP53* mutation rate.
n=number of cancers. Generated from IARC database sequencing data. Version R16, Nov 2012[373].

Mutation rates for oesophageal, colorectal, lung, gastric, liver, breast and prostate cancer are 45.4%, 43.3%, 37.2%, 32.4%, 31.2%, 22.8% and 16.9% respectively. Within some cancer sites certain histological subtypes demonstrate an increased *TP53* mutation rate. For example almost 100% of high-grade serous ovarian cancers have a p53 mutation[168] while overall ovarian cancers have a mutation rate of only 47.5%.

In some cases the differences in mutation rates can be explained by environmental exposure to specific carcinogens. In hepatocellular carcinoma (HCC) aflatoxin B1, a food contaminant encountered in the developing world produced by the fungi aspergillus parasiticus, has been implicated in the neoplastic process[374]. Aflatoxin induces G>T substitutions clustering at codon 249 in the DNA binding domain of p53[375]. Benzo[a]pyrene diol epoxide (BPDE), which is one of 3000 mutagens in tobacco, forms adducts on G residues in DNA causing G>T mutations and has been implicated as the cause of p53 mutations in lung cancer, although the importance of this mutant has been called into question by work showing no difference in frequency of G>T mutations in lung cancer from

smokers versus non-smokers[376, 377]. A further example of exposure to environmental mutagens causing mutations of *TP53* is demonstrated by the relationship between UV and squamous cell skin cancer. UV exposure causes CC---TT double-base changes, mutations at dipyrimidine sites and in particular a high frequency of C>T substitutions resulting in a mutation rate in squamous skin cancer of around 58%[378].

In contrast with most other tumour suppressor genes, which are commonly inactivated by frameshift or nonsense mutations, the majority of the mutations in *p53* are missense mutations (~80%).

Figure 1-20 shows the location of the 6 most common somatic mutations which are all in the DNA binding domain in the conserved regions[373, 379]. In this region 88% of mutations are missense while outside this region only 40% are missense[182]. This highlights the importance of the DNA binding domain for p53's tumour suppressive functions.

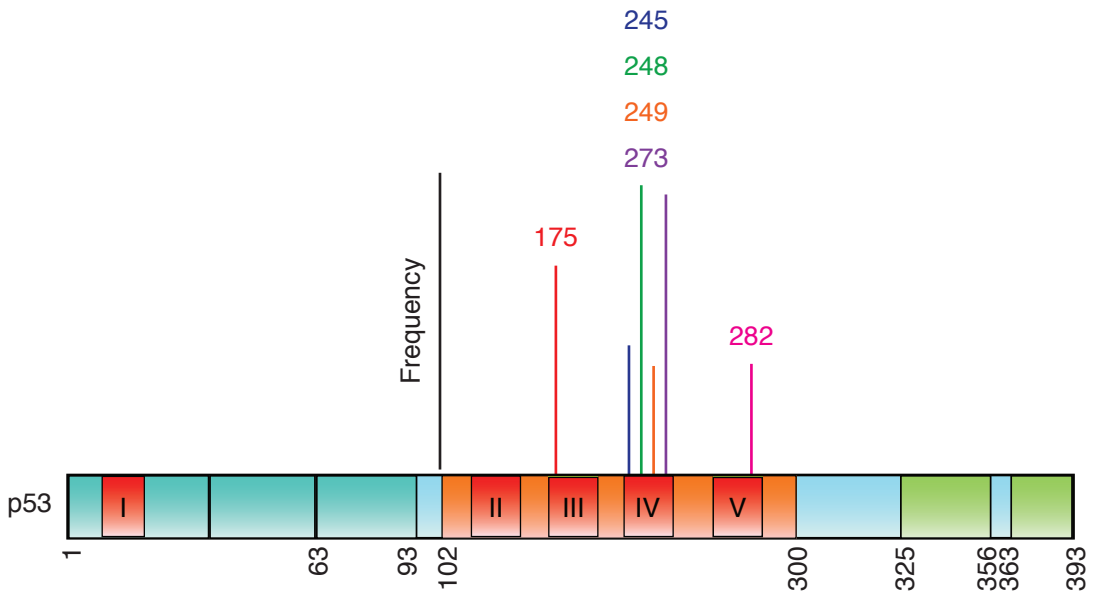

Figure 1-20: p53 hotspot mutations.
The codon number of the 6 most common mutations is given and their location in the p53 DNA-binding domain shown. Adapted from IARC TP53 Database, R15 release, November 2010. n=22356[373].

p53 mutations occurring in the DNA binding domain are classified into one of 2 groups; structural mutants or contact mutants. Structural mutants (R175H) are p53 mutations, which change the conformation of p53, while contact mutants (R248Q) have an alteration of an amino acid critical for DNA binding[144, 380]. It is

worth noting however that even some contact mutants are unfolded to some degree[150].

The consequences of the p53 mutations seen in cancers are dramatic in that expression of mutant p53 has an even greater oncogenic effect than loss of wild-type activity, resulting in the acquisition of a more aggressive phenotype. Many p53 mutants can exert dominant negative regulation of remaining wild-type p53[373]. Moreover mouse models with hotspot *TP53* mutations have demonstrated a 'gain-of-function' phenotype that leads to the development of more invasive tumours[381, 382, 383].

Establishing the mechanism of mutant p53 gain of function is an area of active research where there is still much to learn. Although some mechanisms of gain of function are shared by a group of *TP53* mutations, it is becoming clearer that each individual p53 mutant probably acts in its own specific way, although they may converge to affect the same pathways[384]. So far it has been shown that mutant p53 can regulate a transcriptional programme directly through binding DNA distinct from the canonical p53 binding sites recognised by wild-type p53, or via interactions with other proteins. Various p53 mutants have been shown to interact with numerous transcriptional co-regulators, including the p53 family members p63 and p73, thereby indirectly regulating transcription[385-388]. Numerous consequences of these interactions include the regulation of expression of genes that contribute to invasive and metastatic behaviour, or cell survival. For example in breast cancer cells mutant p53 activates sterol gene promoters via transcription factors SREBPs, driving the mevalonate pathway (that synthesises isoprenoids and cholesterol). This upregulation of the mevalonate pathway is required for the disorganised growth of breast cancer cells in 3D models suggesting its contribution to driving invasion[389]. Mutant p53 has also been shown to form a complex with Smads and p63 leading to pro-metastatic TGFβ activity, in the presence of oncogenic Ras, through inhibition p63[388]. Mutant p53 has also been shown to enhance Rab-coupling protein-dependent recycling of multiple receptors that drive mitogenic signalling pathways (EGFR, MET). In some cellular models this is also dependent on inhibition of p63[385, 390].

The *TP53* status of a tumour can be clinically informative. For example in a study of patients who received neoadjuvant chemotherapy for breast cancer the presence of a p53 mutation conferred a poorer 5-year progression free survival (mutant *TP53* 55.3% versus wild-type *TP53* 64.7%; all patients received FEC (5-Fluorouracil, Epirubicin, Cyclophosphamide) chemotherapy)[391]. Studies exploring whether *TP53* mutation can predict response to chemotherapy have shown conflicting results. This is thought to be due to the heterogeneous populations of breast cancer patients and the heterogeneous chemotherapy regimens included in the studies. Some consistency does seem to have been reached confirming that wild-type p53 predicts a poorer response to anthracycline based chemotherapy[392] and furthermore this have been supported by some mechanistic studies[393]. In colorectal cancer the picture is also complicated with p53 mutations having a different incidence and prognostic impact depending on the specific site of tumour origin in the large bowel[394]. Clinical data on p53 mutation status in previous years has been based on immunohistochemical assessment of tumour p53 expression as mutant p53 is frequently (but not always) stabilised since MDM2 is not a transcription target of mutant p53. This has lead to inconsistent results which will hopefully be addressed in some way now that application of sequencing technologies to clinical samples is much more feasible[182]. It is however likely that the complexities of the p53 pathway will result in on-going inconsistencies which could be further addressed by systems biology approaches.

1.5.2 Other causes of inactivation of the p53 pathway

For those tumours that retain wild-type p53 the p53 pathway is frequently found to be defective at another level[84].

In some cancers mutations in DNA damage signalling (ATM, CHK2) cause inability to activate p53 sufficiently, as demonstrated by the presence of CHK2 mutations in a group of patients with Li-Fraumeni like syndromes[395, 396].

In other cancers there have been reports of methylation of the p53 promoter causing reduced transcription of p53[397] and mutation in 5' UTR reducing translation[398].

Also upstream of p53, epigenetic inactivation, mutation or deletion of ARF (often along with p16 loss), have all been reported[399]. Also mutation of tumour suppressor phosphatase and tensin homolog (*PTEN)* occurs. This allows Akt to increase and causes an increase in nuclear MDM2 and consequent inhibition of p53[400, 401]. Other mechanisms of constitutive activation of Akt activity therefore also inhibit the p53 pathway.

Overexpression of p53's negative regulators, MDM2 or MDMX occur in at least 10% of human tumours[402]. MDM2 is overexpressed in 14% of osteosarcomas[403]. MDMX is overexpressed in 4% of glioblastomas, 5% of breast cancers, 50% of HCCs, 60% of retinoblastomas and 65% of cutaneous melanomas[404-407]. The spectrum of tumours overexpressing MDM2 and MDMX differ suggesting that they may have site specific roles in tumourigenesis[356]. MDM2 can be overexpressed as a result of gene amplification. In addition a single nucleotide polymorphism (SNP) in the MDM2 promoter has been reported which enhances transcription leading to a 2-4 fold increase in MDM2 mRNA and protein[408]. No corresponding SNP in MDMX has been found. MDMX overexpression can result from enhanced translation of its messenger RNA, increased mRNA or increased copy number particularly in retinoblastoma and HCC[406, 409, 410].

For some cancers, tumour associated viruses (HPV in humans, SV40 and adenovirus in other mammals) play a major role in the neoplastic process by inactivating p53. They encode the E6 protein and the E6-associated protein (E6-AP) is capable of binding to wild-type p53 and targeting it for degradation via the proteasome[411]. The most extensively studied of these oncogenic viruses is human papillomavirus (HPV). Approaching 100% of cervical cancers are estimated to be due to infection with oncogenic HPV types 16 and 18[412]. HPV's causative role in cervical cancer has inspired development of an HPV vaccine and a HPV vaccine programme for the prevention of cervical cancer is now underway. This programme is still in its infancy and therefore whether it effectively reduces the incidence of cervical cancer remains to be seen[413].

Another mechanism of inactivation of wild-type p53 seen in cases of some breast cancer is cytoplasmic location of p53 and therefore reduced transcriptional

activity[414-416]. The specific mechanism of cytoplasmic sequestration is not yet known.

1.6 p53 as a target for cancer therapy

Three different mouse models from the groups of Lowe, Jacks and Evan have demonstrated that reactivation of wild-type p53 in mouse models results in tumour regression[134, 417] with no evidence of toxicity in normal tissues[418]. Restoration of wild-type p53 expression has more recently also been evaluated in mice with a mutant p53 background. In this setting the introduction of wild-type p53 suppressed tumour growth but did not cause tumour regression probably due to the dominant negative effect of mutant p53[419]. These models provide strong evidence in support of developing agents that reactivate the p53 pathway.

As described above lesions that inactivate p53 in cancer can occur at several different levels in the p53 pathway. Therefore, although the common goal is restoration of wild-type p53 activity, this will require several different approaches (Figure 1-21).

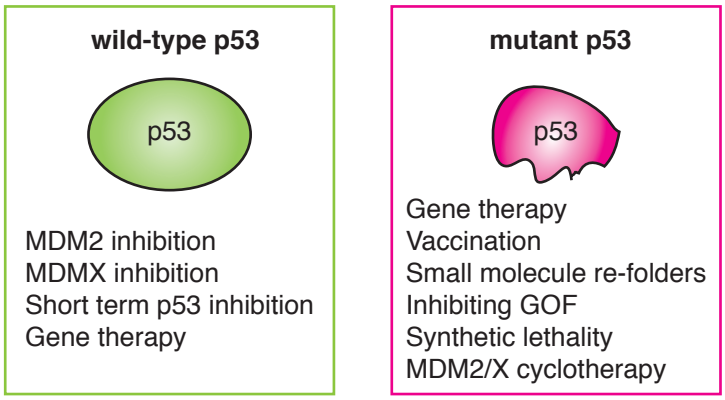

Figure 1-21: p53 activating therapy depends on tumour p53 status. GOF=Gain Of Function.

The approach will, broadly speaking, depend on the tumour p53 status. Where wild-type p53 is present, inhibition of p53's negative regulators would be a reasonable approach. However, in the presence of mutant p53 this would not be desirable since mouse models have shown that *MDM2* deletion in mice expressing mutant p53 leads to more invasive cancers[420].

1.6.1 Treatment of wild-type p53 tumours

The most extensively studied strategy to reactivate wild-type p53 in tumours with a wild-type p53 status has been MDM2 inhibition. Inhibition of MDM2 could restore p53 activity by releasing wild-type p53 from MDM2 mediated proteasomal degradation. Although less studied thus far, inhibition of MDMX is now recognised as another potentially useful method of wild-type p53 restoration. Importantly these strategies will be useful only in cancers that retain wild-type p53.

Mouse models previously described[134, 417, 418] showed that, on restoration of the p53 pathway, toxicity to normal tissues was not a major feature, however, in these mice MDM2 was not altered and seemed to be capable of controlling p53 levels in normal tissues. The issue of potential toxicity to normal tissues on specifically inhibiting MDM2 to achieve p53 activation has been explored using a mouse model with a hypomorphic MDM2 allele that expresses 30% of the normal level of MDM2 and results in increased p53 transcriptional activity. These mice showed no evidence of premature aging and were more resistant to tumour formation[421]. However other models where there is either a hypomorphic MDM2 allele or haploinsufficiency of MDM2 and MDMX have shown that the resultant increased p53 activity causes increased sensitivity to DNA damage, a finding that obviously needs to be taken into consideration when designing therapies which inhibit MDM2 or MDMX[422, 423]. Furthermore in a mouse model with a switchable endogenous *TP53* in a *MDM2* null background the normal mouse tissues underwent apoptosis and arrest[424]. Like germ-line genetic deletion, an MDM2 inhibitory drug should achieve p53 stabilisation in normal and tumour tissues so these genetic studies do raise concerns regarding the potential toxicity of this strategy. To date there has been *in vivo* evaluation of MDM2 inhibitor Nutlin that did not appear to cause significant toxicity to normal tissues in a mouse xenograft model[425]. Furthermore phase I studies of Nutlin have shown the drug to be tolerable[426-428]. Obviously tumour cells are likely to have other genetic abnormalities that make them more sensitive to p53 induced senescence or apoptosis. However, whether there is an adequate therapeutic window remains to be seen.

1.6.1.1 Inhibitors of MDM2 and MDMX

Several different approaches have been taken to inhibit MDM2 (Figure 1-22).

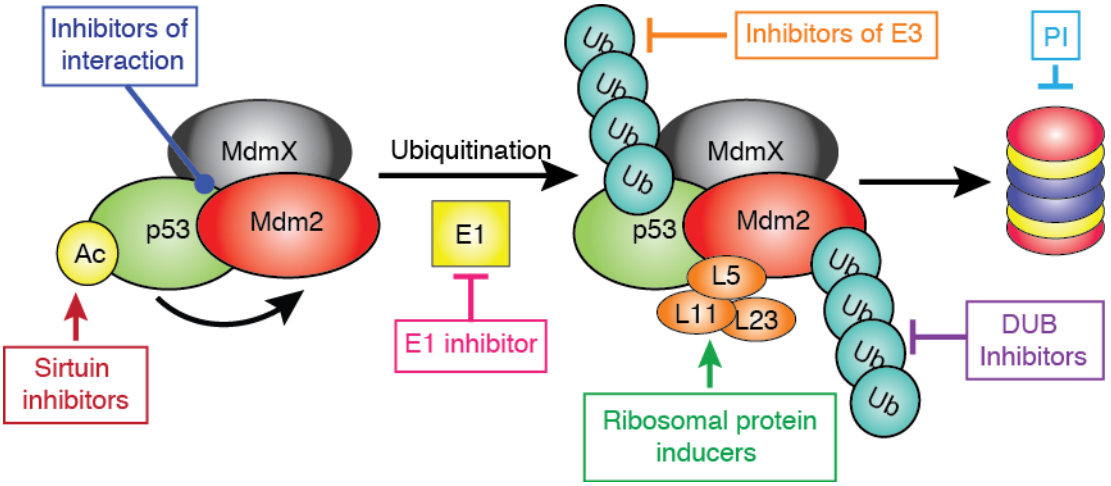

Figure 1-22: Methods of p53 reactivation in wild-type p53 tumours. DUB=Deubiquitinating enzyme, Ub=Ubiquitin, Ac=Acetylation, E1=ubiquitin activating enzyme, PI=Proteasome Inhibitor.

Firstly anti-sense oligonucleotides have been shown to be successful in decreasing MDM2 expression, resulting in xenograft shrinkage in mouse models[429, 430]. Despite these promising results due to the high potential for off target effects with this strategy priority has been given to clinical development of alternative methods of MDM2 inhibition. Secondly agents are in development, which are thought to inhibit the interaction between MDM2 and p53 (Nutlin, spiro-oxinadoles, benzodiazepines and Reactivation of p53 & induction of tumour cell apoptosis (RITA))[309, 425, 431-437]. Thirdly a group of agents designed to inhibit the MDM2 dependent ubiquitination of p53 are in development (HLI98). Finally inhibitors of the MDMX-p53 interaction are in the very early stages of development.

1.6.1.1.1 Inhibitors of p53-MDM2 interaction

Historically it has been presumed that due to the relatively flat interacting surfaces of proteins, structure based design would not be useful in targeting protein-to-protein interaction. However, characterisation of the crystal structure of the MDM2-p53 interaction identified 3 critical amino acids in the interaction between

MDM2 and p53 (Leu26, Trp23 and Phe19)[309]. These amino acids were the focus for a chemical library screen from which Nutlin was identified.

Nutlin is a cis-imidazoline, which binds to the deep hydrophobic p53-binding pocket on MDM2. Nutlin disrupts the interaction between MDM2 and the transactivation domain of p53 resulting in increased p53 expression and functional activity[425]. Despite 50% amino acid sequence identity between the p53-binding domain of MDM2 and MDMX Nutlin does not disrupt the p53-MDMX interaction and fails to activate p53 in cells overexpressing MDMX[438-440].

Other classes of compound have been identified that disrupt the interaction between p53 and MDM2 (table 1-2).

Table 1-2: Compounds that disrupt MDM2-p53 interaction.

Molecule	Strategy	Chemical class	Target	Testing stage
Nutlin/RG7112[425]	Small molecules	Cis-imidazoline	MDM2	Phase 1
RITA[436]		Thiophene	p53	Preclinical
MI-219[432]		Spiro-oxinadole	MDM2	Preclinical
TDP521252/665759[433-435]		Benzodiazepinedione	MDM2	Preclinical
PXN727/PXN822[1]		Isoquinolinone	MDM2	Preclinical
Stabilised alpha-helix of p53 SAH-p53[441]	Stapled peptides		MDM2	Preclinical
SAH-p53-8[442]			MDM2	Preclinical

Adapted from Lehmann *et al*, 2012[443]

Reactivation of p53 & induction of tumour cell apoptosis (**RITA**) was discovered following a cell-based chemical library screen and has been shown to activate p53 and induce p53-dependent cell cycle arrest[436]. It is thought to bind to p53 rather than MDM2, although crystal structures fail to confirm this[437].

Spiro-oxinadoles (**MI compounds**) were developed using structure based design. The oxindole ring mimics the side chain of Trp23. The spiropyrolidine ring mimics the Phe19 and Leu26 side chains. This class of agents has been shown to stabilise p53 in cells expressing wild-type p53 with low toxicity to normal cells[431, 432].

Benzodiazepinediones (**TDP521252/665759**) were also discovered by a high throughput screen for binding of MDM2[433-435]. These were shown to stabilise p53, cause increased transcriptional activity and lead to reduced proliferation of wild-type p53 expressing cancer cells.

Isoquinolinones (**PXN727/PXN822**) are orally bioavailable and have been shown to reverse tumour growth in xenograft models[1, 444].

Finally two stapled peptides have been described that bind to the p53 binding pocket on MDM2[441, 442] thereby preventing interaction of p53 with its negative regulators and activating p53.

1.6.1.1.2 Inhibitors of E3 ligase activity

As discussed above, p53 can be activated by DNA damage via ATM/ATR, by oncogenic stimuli via the ARF pathway or by ribosomal stress via ribosomal proteins (L11, L5, L23 and S14). These pathways cause p53 to be released from the negative regulation of MDM2. Despite retention of the p53/MDM2 interaction, ARF or ribosomal proteins are able to block ubiquitination and degradation of p53, and activate a p53 response. An attempt was therefore made to identify small molecule inhibitors of MDM2s E3 ligase activity based on the observation that preventing degradation of p53 may be equivalent to activation of p53.

The first chemical library screen for inhibitors of MDM2 mediated p53 ubiquitination identified three chemical groups of interest; arylsulfonamides, bisarylureas and acylimidazolones[445]. Surprisingly these compounds did not inhibit MDM2 autoubiquitination and therefore their mechanism of action may involve disrupting the MDM2-p53 interaction.

An alternative approach was taken by Davydov *et al*, who performed a high-throughput screen of small molecule inhibitors of MDM2 autoubiquitination. They identified the HDM2 ligase inhibitor 98 class (HLI98)[446]. Studies have shown that the HLI98 compounds inhibit E3 activity of MDM2, stabilise p53 and cause apoptosis of transformed cells. Their specificity for MDM2 was also investigated, showing some off-target inhibition of HECT domain E3 ubiquitin ligases E3s[447]. The mechanism of action of these 7-nitro-5-deazaflavin (HLI98) compounds is not clear but it is proposed that they may function by blocking E2-MDM2 interaction or by altering RING finger structure. Further study of the mechanism of action of these compounds was limited by the high redox potential of the 5-deazaflavins which have a nitro group which is susceptible to one-electron reduction, leading to

generation of nitro anion radicals. Since p53 can be stabilised by ROS, work was undertaken to synthesise analogues of the original compounds, which lack the nitro group. Reassuringly some of the nitro lacking analogues could stabilise and activate p53 in cellular assays[448].

It has been suggested that these agents, which inhibit MDM2's E3 ligase activity and therefore stabilise both MDM2 and p53, may potentially prevent full activation of p53. Recent mouse models have helped to address this. A model with mutant *MDM2* (lacking E3 ligase activity (MDM2-464)) demonstrated embryonic lethality, which was rescued by deletion of *p53*. These results therefore show that inhibition of MDM2's E3 activity, while retaining the p53 binding activity, is sufficient to inactivate MDM2-mediated control of p53. Interestingly, in this system the mutant *MDM2* expressed in these mice remained at low levels and was targeted for degradation by another, as yet unidentified E3 ligase[324]. Although it is unlikely that drugs inhibiting the E3 ligase activity of MDM2 would provide inhibition equal to deletion of the gene itself, this area does require further study. However, for therapeutic approaches a partial inhibition of MDM2 may be the desired outcome. Mouse studies have shown that complete ablation of MDM2 is highly toxic to normal tissues that retain wild-type p53 activity[424], although *in vivo* treatment with agents that inhibit p53/MDM2 binding (rather than E3 ligase function alone) is well tolerated[425].

Further attempts have been made to identify selective inhibitors of MDM2 mediated p53 ubiquitination by screening a chemical library for p53 ubiquitination followed by a MDM2 autoubiquitination counter screen. From this work the most active chemical identified, inhibited p53 ubiquitination with an IC50 of 8μM while no inhibition of MDM2 ubiquitination was observed at doses up to 100μM[449]. No further update has followed the original publication.

Several other groups have been making efforts to identify inhibitors of MDM2 E3 ubiquitin ligase activity. Further examples are discussed below.

Sempervirine was discovered as an inhibitor of MDM2 E3 ligase activity in a high throughput natural products screen. It inhibits both p53 and MDM2 ubiquitination and stabilises p53 in cancer cells resulting in apoptosis[450].

HLI373 is a water-soluble compound that was originally published as a derivative of the previously described HLI98 compound. HLI373 has shown ability to stabilise MDM2 and p53, activate p53-dependent transcription and it displays selectivity for apoptosis in transformed cells[451].

In addition an E1 inhibitor has been described[452]. Although this strategy has obvious limitations in that it will have p53-independent effects since the E1 enzyme is involved in a multitude of different ubiquitination reactions the clinical success of proteasome inhibitors suggests development of such non-specific strategies may be fruitful. Proteasome inhibitor, bortezomib, has been shown to be tolerable and improve one year survival rates from 66% to 80% when compared to dexamethasone in the treatment of refractory multiple myeloma[453]. An additional method of targeting the ubiquitin proteasome pathway is to design inhibitors of deubiquitinating enzymes. To date a small molecule inhibitor of HAUSP (USP7) has been described to bind to the active site inhibiting its catalytic function. This compound was shown to result in G1 arrest of colorectal cancer cell lines[454].

1.6.1.2Inhibitors of MDMX

As the importance of MDMX in the negative regulation of p53 has become increasingly apparent and study of MDM2 inhibitors has revealed that overexpression of MDMX can serve as a resistance mechanism, efforts have been made to develop inhibitors of MDMX[269, 438, 455].

Table 1-3 shows compounds in development that have been shown to disrupt p53-MDMX binding.

Table 1-3: Compounds that disrupt MDMX-p53 interaction.

Molecule	Target	Testing stage
SJ-172550[456]	MDMX	Preclinical
NSC207895[457]	MDMX	Preclinical

Adapted from Lehmann *et al*, 2012[443]

Reed *et al* developed a high throughput screen to identify small molecules that bind MDMX and prevent its interaction with p53. Using this method they identified the first MDMX inhibitor, SJ-172550. They have shown that SJ-172550 kills

retinoblastoma cells (which overexpress MDMX) and that the addition of Nutlin results in synergistic killing[456].

Another group have used a reporter-based drug screen and identified NSC207895, a benzofuroxan derivative (7-(4-methylpiperazin-1-yl)-4-nitro-1-oxido-2,1,3-benzoxadiazol-1-ium)[457]. NSC207895 could activate p53 in MCF-7 cells resulting in activation of p53 apoptotic transcriptional targets. This compound has also been shown to act additively with Nutlin as a means to both inhibit p53-MDM2 and p53-MDMX interaction.

Table 1-4 shows peptides shown to disrupt MDM2-p53 binding and MDMX-p53 binding.

Table 1-4: Dual MDM2/MDMX-p53 interaction inhibitors.

Molecule	Target	Testing stage
WK298[458]	MDM2/MDMX	Preclinical
Hu *et al*[459]	MDM2/MDMX	Preclinical
LTFEHYWAQLTS[460]	MDM2/MDMX	Preclinical
6-chloro p53 peptidomimetic[461]	MDM2/MDMX	Preclinical
PMI[462, 463]	MDM2/MDMX	Preclinical

Adapted from Lehmann *et al*, 2012[443]

The imidazo-indoles (WK298) have been shown to bind to both MDM2 and MDMX at the three subpockets of the MDM-p53 interface[458]. As yet these compounds, as well as the other dual peptide inhibitors reported, do not appear to have undergone evaluation in cell line studies.

1.6.1.3 Other non-genotoxic p53 stabilising agents

Johnson and Johnson were developing a novel p53 stabilising agent (JnJ-26854165), which was thought to act further down the p53 pathway. It was hypothesised that tryptamine (JnJ-26854165) could prevent binding of the MDM2-p53 complex to the proteasome. Cell line studies showed stabilisation of both wild-type and mutant p53 causing transcriptional activity[464 465 466]. Xenograft studies showed tumour shrinkage in the presence of both wild-type and mutant p53[465-467]. The compound was the first-in-class MDM2 inhibitor in phase I clinical evaluation and preliminary results of this study were presented by Tabernero *et al* at the EORTC annual meeting in 2008[467]. At that time 30 patients had been enrolled and no clinical responses or dose limiting toxicity had been observed. Subsequently

the phase I study was discontinued because of dubiety regarding tryptamine's mode of action, but further details of this are not in the public domain.

Tenovins-1/6 were discovered following a mammalian cell-based screen for activators of p53. Using a yeast genetic screen the target of tenovin was identified as SirT1 & 2 (histone deacetylases). Inhibition of SirT1 & 2 results in increased acetylation at lysine-382 on p53 and therefore activates p53. Tenovin 6 inhibits tumour growth *in vivo* and kills tumour cells by p53-dependent and independent mechanisms[468].

Actinomycin D (act D) is a traditional cytotoxic that has recently been identified as a non-genotoxic p53 activating agent when used at low-dose[469]. A cell based screen was carried out to identify a clinically approved drug that mimicked Nutlin in terms of achieving p53 dependent transcription [468, 470]. Act D was identified as the most effective agent, and shown to be capable of activating p53 without causing DNA damage at low doses.

1.6.1.3.1.1 Limitations of the MDM2/X-inhibition approach

In the clinic, success of MDM2/MDMX inhibitors will depend on the ability to distinguish molecular sub-types of cancer, knowledge of the toxicity risk of p53 activation to normal tissues and the likely mechanisms of resistance to therapy.

Firstly MDM2/MDMX inhibition is expected to only be appropriate and beneficial for patients who have a wild-type p53 containing tumour. Current UK clinical practice does not involve routine analysis of tumour p53 status and although p53 status may be examined in other centres worldwide, at present good evidence that knowledge of p53 status impacts patient care is lacking. Concurrent with the development of MDM2 and MDMX inhibitors sequencing technologies that can feasibly be used to determine p53 mutation status in clinical practice are being developed. Roche are developing one such technology that is designed to detect p53 mutations from DNA isolated from formalin fixed paraffin embedded tissues using an affymetrix amplichip[471]. The use of fixed tissues has obvious practical advantages.

While mice null for *MDM2* displayed significant toxicity to normal tissues upon p53 activation[424], the *in vivo* testing of Nutlin did not appear to demonstrate significant toxicity to normal tissues[425]. Reassuringly phase I evaluation of Nutlin has shown that it was tolerable. The dose limiting toxicity was thrombocytopenia (reduced platelet count) and it was encountered at doses below which there was biomarker evidence of p53 activation[424, 425]. There was also evidence of some promising responses to treatment although clearly the study was not designed to assess efficacy[427, 428].

One further consideration when designing MDM2/MDMX inhibitors is that although they are both negative regulators of p53 there is a growing body of evidence establishing differences in the activities of MDM2 and MDMX. Although both *MDM2* and *MDMX* knock-out mice demonstrate an embryonic lethal phenotype[238, 239, 263, 264] other mouse models have been helping to further dissect the differences between MDM2 and MDMX functions[245, 246, 270, 271]. These differences may be important when designing therapies, which manipulate either MDM2 or MDMX or both. For example embryos deficient in *MDM2* display massive apoptosis, which can be partially rescued by Bax deletion while *MDMX* deficient mice show a mixed growth arrest/apoptosis phenotype that can be partially rescued by p21 deletion[472, 473]. Furthermore differences have been demonstrated in terms of tissue specificity of effects of gene knockout with *MDM2* deletion particularly influencing progenitor neuronal cells and cardiomyocytes but *MDMX* showing milder tissue defects[474, 475]. This information could be useful in determining the likely toxicities from MDM2 and MDMX inhibition and perhaps suggests that MDM2 inhibition has potential to cause cardiotoxicity.

Furthermore other toxicities likely to be associated with MDM2 inhibition could result from modulation of other pathways where MDM2 had been show to act as an E3 ubiquitin ligase. MDM2 acts as an E3 for several other targets including p21, androgen receptor and Tip60 (table 1-1). It is therefore likely that MDM2 inhibitors will also alter signalling via these other pathways to some extent.

MDMX overexpression has been implicated in resistance to MDM2 inhibitors and inhibition of MDMX alone would stabilise p53 leading to increased MDM2 which

could potentially inhibit p53 therefore a dual inhibition strategy may be desirable[264].

MDM2 and MDMX inhibition relies on the pathways downstream of p53 functioning normally. Dysfunction in the mediators of the p53 response could potentially result in resistance to MDMX and MDM2 inhibition. In addition the effects of long-term inhibition of MDM2 are unknown but it is reasonable to hypothesize that this may have impact on homeostasis of the p53 pathway causing emergence of other resistance mechanisms. So far mutations in p53 target genes have not been reproducibly found as a mechanism of resistance to p53 presumably because there are so many mediators of p53 response. Furthermore mouse models with loss of p21, PUMA and Noxa alone do not appear to develop tumours suggesting that there several redundant activities that can provide tumour suppression.

At the outset patients with wild-type p53 expressing tumours should be selected for MDM2 or MDMX inhibitory treatment. However, these same patients may have normal tissues expressing mutant p53[476] and this raises concerns that p53 activating agents could accelerate transformation in these tissues by stabilising mutant p53[477].

One recent study has highlighted some of the concerns of the effects of MDM2 inhibition in the presence of mutant p53. With the specific aim of investigating whether MDM2 regulates the level of mutant p53 in normal cells Terzian *et al* developed a homozygous *TP53* mutant mouse where the *MDM2* gene was deleted (the genetic equivalent of systemic treatment with an MDM2 inhibitor). The absence of MDM2 in this model led to accumulation of p53 protein in normal and tumour cells, the mice died from cancer earlier than mice expressing mutant p53 in a wild-type *MDM2* background. Importantly, 17% of the mice developed metastatic tumours, a feature that was also not apparent in a wild-type *MDM2* background[420]. Since mutant p53 expression is also controlled by MDM2 and mutant p53 results in an increased rate of metastasis in mouse models, MDM2 inhibition may pose a problem in the presence of mutant p53[477, 478]. Consistent with this, a more recent study in zebrafish showed that after morpholino knockdown of zebrafish homologs of MDM2 and MDMX there was dramatic

accumulation of mutant p53[479]. The impact of this accumulation on carcinogenesis was not evaluated.

1.6.1.4 p53 inhibitors for chemoprotection

It is well documented that much of the toxicity caused by cytotoxic chemotherapy is p53-dependent. Consequently it has been hypothesized that p53 inhibitors may protect normal cells from p53-mediated death while allowing delivery of increased doses of chemotherapy and radiotherapy to target cancer cells[480, 481]. Furthermore mouse models have suggested that this need not be at the expense of a reduction in efficacy, since DNA damage induced apoptosis was not required for p53-mediated tumour suppression[482].

1.6.1.5 Gene therapy

Gene therapy to reintroduce *TP53* into tumour cells by means of an adenovirus (Gendicine) has been investigated both as a monotherapy and in combination with chemotherapy and radiotherapy. This approach would be most useful in tumours of wild-type p53 status because due to the dominant negative properties of mutant p53 this therapy may be less effective in mutant p53 tumours. Consistent with this idea mouse studies have shown that restoration of wild-type p53 expression in a mutant p53 background did not cause tumour regression but did stop tumour growth. Nevertheless, some trials in patients of mixed p53 status have demonstrated improved progression free survival in patients with non-small cell lung cancer and squamous cell carcinoma of the head and neck. Gendicine, given by intratumoural injection in combination with chemoradiation, was therefore approved for clinical use in China[483, 484]. It will be interesting to see if the presence of p53 mutation predicts resistance to this strategy.

1.6.2 Treatment of mutant p53 tumours

In tumours where mutant p53 is present, approaches that may stabilise mutant p53 could be detrimental or at least ineffective. Tumours with a mutant p53 status therefore require a different approach.

1.6.2.1 Gene therapy

There has been cell line and clinical studies of an oncolytic adenovirus (Onyx) that was thought to only replicate in *TP53* mutant cells because it was deficient for the E1B gene product that degrades p53[485, 486]. Two non-randomised phase II studies in recurrent squamous cell head and neck cancer patients of intratumoural Onyx showed sustained responses of single agent Onyx[487] and of Onyx in combination with Cisplatin and 5-FU[488]. Onyx has also been evaluated in several other early phase studies including a phase I/II in sarcoma patients in combination with MAP (Mitomycin C, Doxorubicin, Cisplatin) chemotherapy[489] and a study in patients with recurrent colorectal cancer where Onyx was given via hepatic artery infusion[490]. Interpretation of initially promising clinical study results was compromised by difficulties assessing response versus non-specific effects of direct injection of virus intratumourally. Subsequently Onyx was shown to be specific for tumour cells with altered mechanisms for RNA export rather than mutant p53[485].

1.6.2.2Mutant p53 vaccination

Another strategy that has seen some success is vaccination with a p53-modified adenovirus-tranduced dendritic cell vaccine. Mutant p53 may provide an attractive target for immunotherapy when it is highly expressed in tumours. In addition there is evidence that some cancer patients produce p53 reactive T cells in response to p53 mRNA-transfected dendritic cells and some patients have detectable levels of anti-p53 antibodies[491, 492]. There are on-going clinical studies of the p53-modified adenovirus-tranduced dendritic cell vaccine. One phase I/II study in recurrent small cell lung cancer patients showed that 79% of the patients who demonstrated an immune response to the vaccine, responded to subsequent chemotherapy while only 33% of those who did not mount an immune response responded to chemotherapy[493]. The results of on-going clinical studies are awaited with interest.

1.6.2.3Refolding of mutant p53 to wild-type conformation

Each of the following agents aims to restore transcriptional activity to mutant p53 by causing it to fold in a wild-type confirmation (table 1-5). This is an attractive approach, since mutant p53 expression is specific to the cancer cells, and the protein is expressed at high levels in tumours. However, this is technically

extremely challenging and to date only a few tumour derived p53 point mutants have shown themselves to be amenable to this approach.

Table 1-5: Compounds targeting p53 mutants.

Molecule	Target	Testing stage
APR-245 (PRIMA-1)[443]	R273H, R175H	Phase 1
STIMA-1[494]	R273H, R175H	Preclinical
MIRA-1[495]	R273H, R175H	Preclinical
PhiKan083[496]	Y220C	Preclinical
Thiosemicarbazones[497]	R175H	Preclinical
CP-31398[498]	R273H, R249S	Preclinical
SCH529074[499]	R175H, S241F, R248W, R249S, R273H	Preclinical

Adapted from Lehmann *et al*, 2012[443]

p53 Reactivation and Induction of Massive Apoptosis (**PRIMA**) is a low molecular weight compound that can restore transcriptional activity to mutant p53 cells resulting in apoptosis[500]. It is thought to be converted to intermediate compounds that covalently modify mutant p53's DNA binding domain resulting in apoptosis[501]. A derivative of the original PRIMA compound (APR-246 (PRIMA-1MET)) has now been evaluated in a phase I clinical study. APR-246 (PRIMA-1MET) can bind mutant p53 (R273H, R175H) and restore wild-type transcriptional properties to the protein. APR-246 can be safely given to humans at doses that induce p53-dependent transcriptional activity (cell cycle arrest, apoptosis, transcription of Noxa, PUMA and Bax)[416, 468]. We await results of phase II evaluation of anti-cancer activity.

STIMA-1 (SH group Targeting and Induction of Massive Apoptosis) is a low molecular weight compound structurally similar the CP-31398 (described below) and can stimulate mutant p53 DNA binding (R273H, R175H). This leads to an induction of p53 targets and apoptosis in mutant p53 expressing cancer cells[494].

Mutant p53-dependent Induction of Rapid Apoptosis (**MIRA-1**) is a malemide-derived molecule, which like PRIMA-1 can allow mutant p53 to bind DNA and regain wild-type-like transcriptional activity[495]. It has been shown to cause shrinkage of mutant p53 tumour xenografts. The scaffold of this compound is being used to design compounds with more drug-like properties.

PhiKan083, a carbazole derivative, was designed to bind to unfolded p53 mutant Y220C using *in silico* analysis of the crystal structure of Y220C[496]. Study of the crystal structure of the compound bound to Y220C demonstrates key interaction points and informs lead optimisation of a refolding compound.

From the National Cancer Institute's anticancer drug screen data the **thiosemicarbazone** compounds were studied further because they arrested mutant p53 cells (R175H). They were then found to refold p53 R175H into a wild-type conformation and cause p53-dependent cell death in p53 R172H knock in mice[497].

Acridine derivative (**CP-31398**) was originally reported to activate wild-type p53 and also allow mutant p53 to maintain an active conformation, enabling it to be transcriptionally activated[502] by a mechanism that does not disrupt MDM2-p53 binding or result in phosphorylation of the N-terminal of p53[503]. In cellular assays, this compound inhibits p53 ubiquitination, stabilises p53 and activates p53 transcriptional targets inducing cell death. *In vivo* acridine derivatives induced transcriptional activity in tumour xenografts. It is not clear from subsequent mechanistic work how CP-31398 rescues mutant p53 (R273H, R249S).

SCH529074 binds to the DNA binding domain of mutant p53 and restores wild-type function of several mutants (R175H, S241F, R248W, R249S, R273H)[499]. Interestingly binding is displaced by a sequence derived from p53 response element and the compound is also capable of inhibiting ubiquitination of wild-type p53.

In addition to the above-mentioned compounds some p53-derived C-terminal peptides have also been reported[504, 505]. A peptide corresponding to amino acids 361-382 of p53 restored the ability of mutant p53 tumour cells to undergo cell cycle arrest and apoptosis. This peptide could bind the core domain and displace the inhibitory C-terminal domain. A second C-terminal peptide has been described. It can induce p53-dependent Fas mediated cell death in cancer cell lines with mutant p53 or overexpressed wild-type p53[506].

Another strategy to treat mutant p53 expressing tumours is to stimulate degradation of mutant p53. Mutant p53 is known to complex with heat shock protein 90 (HSP90). This inhibits the ability of MDM2 and CHIP to degrade mutant p53. Treatment of mutant p53 expressing cells with a histone deacetylases inhibitor led to inhibition of HSP90 and MDM2 and CHIP mediated mutant p53 degradation[507, 508]. After this treatment tumours would remain null for p53 therefore while tumours may be less invasive tumour regression may not occur. These agents may be useful in early disease as anti-metastatic agents.

1.6.2.4 Targeting mutant p53 gain of function mechanisms

Although it has been known for a considerable time that the presence of mutant p53 results in more aggressive cancer phenotype, the mechanisms underlying this phenomenon are only now beginning to be understood (as mentioned earlier). This improved understanding opens new paths for treatment tumours harbouring p53 mutations.

For example in mutant p53 expressing cells where there is increased recycling of the Epidermal Growth Factor Receptor (EGFR) receptor, treatment with cetuximab may be effective[385]. For tumours where cholesterol synthesis pathways are engaged, statins may prove effective therapeutics[389] and where mutant p53 is inhibiting p53 family proteins inhibitors of p53-p73 or p53-p63 interaction may be useful. RETRA (Reactivation of Transcriptional Reporter Activity) activates a set of p73-dependent genes in mutant p53 cells by preventing interaction with p73[509].

1.6.2.5 MDM2 inhibitors for chemoprotection

An alternative approach to the management of p53 deficient tumours is to use MDM2 inhibition therapy for chemoprotection.

In contrast with p53 inhibition therapy, that may be suitable to protect normal wild-type cells while treating a wild-type tumour, another hypothesis is that MDM2 inhibitors could be used in combination with cytotoxic therapy to more effectively treat tumours expressing mutant p53. This would allow normal tissues expressing wild-type p53 to be held in G1 arrest and therefore be protected from the toxicity

caused by subsequent delivery of cytotoxic therapy (Figure 1-23). Protecting normal cells would allow for a more aggressive treatment of the tumour, since collateral chemotoxicity would be limited.

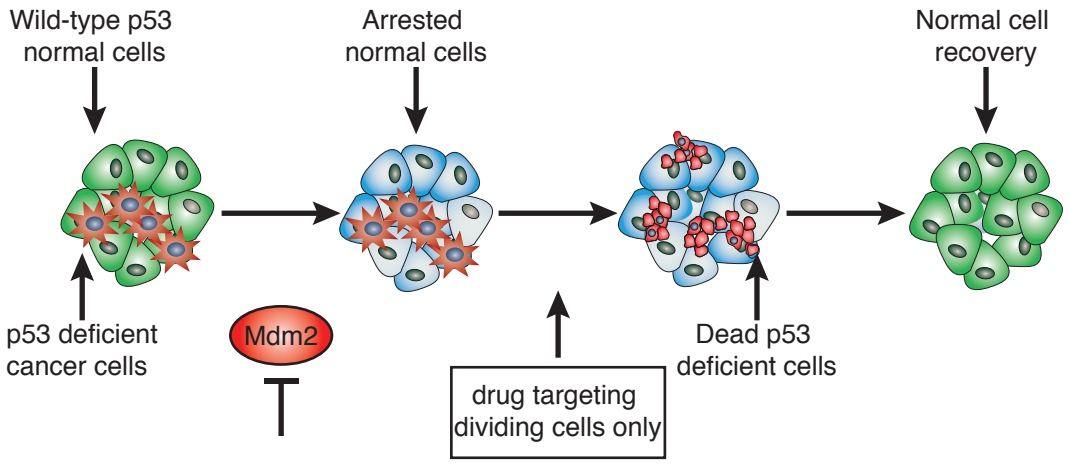

Figure 1-23: Cyclotherapy.
Adapted from Cheok *et al*, Nature Reviews Clinical Oncology 2011[1].

This cyclotherapy principle is aimed at exploiting differences between the cell cycle controls that regulate normal cells (where normal checkpoints are in place) and those that regulate cancer cells (where checkpoint function is frequently lost). The strategy has been studied in cell lines using kinase inhibitors as a protective pre-treatment[510-512] and more recently using MDM2 inhibitors as the protective pre-treatment[513-517].

In mouse models and cell line studies, stabilisation of p53 through MDM2 inhibition demonstrates some specificity for activation of cell death pathways in tumour tissue[425]. When p53 is stabilised in most normal issues it results in cell cycle arrest, which is thought to allow repair of DNA before re-entry into the cell cycle. In contrast stabilisation of p53 in tumour cells is more likely to causes apoptosis or senescence. Therefore pre-treatment of cells with an MDM2 inhibitor should not lead to loss of normal wild-type p53 expressing cells.

Tumours expressing mutant p53 have a deficient p53 pathway and therefore in response to traditional cytotoxic agents G1 arrest and apoptosis are not activated. This loss of G1 arrest leaves the G2/M-phase as the major checkpoint functional in cells with mutant p53. As such, targeting this phase provides a novel opportunity to specifically target mutant p53 expressing cells with anti-metabolic and anti-

mitotic drugs. Therefore p53 stabilising agents may be utilised to arrest normal cells (with wild-type p53) in the G1-phase of the cell cycle protecting them from the effects of subsequent administration of cell cycle specific cytotoxic agents. Ultimately this provides an opportunity to target the most aggressive types of cancer in a more specific way, which allows some sparing of toxicity to normal tissue.

1.6.3 Biomarkers

Biomarkers are "characteristics that are objectively measured and evaluated as indicators of normal biological or pathogenic processes or of pharmacological responses to therapeutic intervention"[518].

They can be classified into three broad groups;

Prognostic biomarkers can be used to predict the natural history of disease. In clinical practice this is useful for giving patients realistic expectations of survival. Prognostic biomarkers also aid clinicians in making treatment decisions of how aggressively to treat and sometimes who to treat. For example those with a poorer prognosis post cancer resection may be more likely to relapse and therefore may benefit more from postoperative adjuvant systemic treatment.

Predictive biomarkers assess the probability of response to treatment so tell us whom to treat with certain drugs.

Pharmacodynamic biomarkers are markers that determine whether a drug modulates its target pathway in the predicted way. These are proof of mechanism biomarkers for a particular dose and schedule.

Traditionally after pre-clinical evaluation, drugs proceed to phase I clinical evaluation which is the first in human study, aimed at establishing the maximum tolerated dose (MTD) of the investigational agent. In general the MTD of drug is defined as the dose of a drug, which causes drug discontinuation due to toxicity in 1/3 of patients. In the case of cancer drugs these studies are carried out in a

population of cancer patients who have progressed through all proven standards of care.

Once MTD is established drugs are then evaluated in phase II clinical studies where the primary aim is to establish if any therapeutic activity is seen with the investigational agent. Traditionally the primary outcome of this type of study, in patients with solid tumours, would be radiological response rate as assessed by Response Evaluation Criteria in Solid Tumours (RECIST)[519]. Response rates would then be compared to those historically recorded for the standard of care for a particular disease (although there is now a trend to perform randomised phase II studies). This remains the most commonly used measure of antitumour activity but this cannot be sole evidence in support for regulatory approval. Phase II studies are proof of concept studies where intermediate endpoint biomarkers of clinical benefit are evaluated.

Once a drug has shown some evidence of anti-cancer activity it is then assessed in phase III where it is compared in terms of progression free, overall survival and quality of life to standard of care. Phase III studies are usually large, costly studies required for regulatory drug approval.

This system of drug evaluation is now recognised as highly flawed. One fundamental problem is that it allows drugs to proceed from phase I to phase III evaluation without any measure of whether the drug actually hits its biological target at a dose below the dose that is tolerable to humans. MTD is a less relevant endpoint for drugs optimised to modulate specific molecular targets. Omission of pharmacodynamic evaluation in the initial phase of drug development is both costly and unethical, since it exposes large numbers of patients to a drug that may not work. In addition some targeted agents are not designed to cause shrinkage of a tumour and can have cytostatic effects or induce necrosis. Both of these outcomes are not easy to evaluate by RECIST criteria and therefore other biomarkers of efficacy, for example functional imaging[520], are required.

The frequency of response assessment is of critical importance in determining progression free survival. This is a particular issue when radiological assessment is being used since due to the risks of accumulating significant exposure to

ionising radiation frequent radiological assessment is not justified. It is however more feasible and cost effective to perform biochemical measures of response at a more frequent interval. Some biochemical measures of response are in clinical use (Ca125 in ovarian cancer, CEA in colorectal cancer, AFP in hepatocellular carcinoma, βHCG in germ cell tumours) however these are infrequently relied upon (with the exception of germ cell tumours) in the presence of radiologically measurable disease since these are organ specific rather than tumour specific and so can be misleading in the presence of benign disease.

For a multitude of reasons, including the above mentioned, the process of clinical evaluation of cancer drugs is being modernised. In an aim to prevent the futile development of drugs that do not hit their particular therapeutic target and to maximise the impact of the vastly improved understanding of the molecular basis of cancer, biomarkers are being developed and adopted in early phase clinical evaluation.

To date some predictive biomarkers have been identified that are clinically useful (table 1-6).

Table 1-6: Predictive biomarkers currently useful in clinical practice.

Primary site	Biomarker	Drug
Breast cancer	HER2 amplification	Response to trastuzumab
	ER expression[521]	Response to tamoxifen
Lung cancer	EGFR kinase domain mutation[522]	Response to erlotinib or gefitinib
	KRAS mutation[523]	Resistance to erlotinib or gefitinib
Colon cancer	KRAS mutation[524]	Resistance to cetuximab
Acute promyelocytic leukaemia	PML-RARA translocation	Response to all-trans retinoic acid
Chronic myelocytic leukaemia	BCR-ABL fusion	Response to imatinib
Gastro Intestinal Stromal Tumours	C-kit mutation[525]	Response to imatinib
Melanoma	BRAF mutation[35, 36]	Response to vemurafenib or dabrafenib

In most of these cases the prevalence of a particular abnormality is high and therefore the drugs efficacy signal was not lost in studies of patients unselected for the predictive molecular abnormality.

Many molecular abnormalities, which may predict efficacy of anti-cancer drugs, are not of such high prevalence and therefore incorporation of development of

predictive biomarkers is needed at an earlier stage in the drug development process.

While tumour diagnostic biopsy specimens or resection specimens are sufficient for study of prognostic biomarkers, predictive and pharmacodynamic biomarkers require multiple tumour biopsies. Analysis of tumour biology in a primary tumour may not reflect biology when metastatic disease has developed therefore it could be argued that patients need re-biopsy at each point of progression of disease. Furthermore high levels of intratumoural heterogeneity[526] support attempts at multiple biopsies at each time point to attain a specimen as representative of active disease as possible. For pharmacodynamic biomarkers tumour biopsies prior to the experimental treatment and then at different time points through the dosing schedule are required.

In reality this is fairly impractical, especially in early phase clinical studies where patients have already been heavily pre-treated and have resistant disease. For some patients the site of their disease is simply too difficult to access even with image guided biopsy techniques. In current UK practice many clinical studies are now requesting access to archival tissues, with all its limitations and in addition an optional re-biopsy is requested (meaning that re-biopsy is not a required entry criteria). Uptake of re-biopsy is generally poor for multiple reasons, including inability of consenting clinicians to justify the need for the biopsy to patients, patient's preference and difficulty in organising biopsy due to poor infrastructure and lack of resource to support the process.

In an attempt to address some of these problems the Stratified Medicine Programme has been initiated in the UK. This is a collaboration between pharmaceutical industry, UK government Technology Strategy Board and Cancer Research UK. The aim of the project is to establish a national service of standardised, high quality, cost-effective genetic testing of tumours for cancer patients. In addition this will have the added benefit of building a National database of genetic information from cancer patients, which will be useful for future research. In France there is a similar project underway by the national cancer institute, INCa (Institut National Du Cancer). Their project is focusing on lung cancer, colorectal cancer and melanoma and like the UK Stratified Medicine

Programme the aim is to develop standardised, cost-effective testing for specific mutational abnormalities. The need for standardisation of molecular testing has been highlighted in the development of trastuzumab where significant problems with inconsistent sensitivity and specificity of HER2 testing has significantly impacted on patient care[527]. In contrast, in the USA many centres have local programmes in place but there is no standardised approach. In some US centres the move towards personalised medicine even stretches to whole exome sequencing in some rare cases[528]. In the UK, where the National Health Service requires convincing evidence of patient benefit and cost-effectiveness, more in-depth genetic testing in unlikely to be adopted as routine practice soon however as evidence of the benefit builds and the cost of sequencing reduces genetic testing will make clinical impact.

One other approach to the re-biopsy problem is to move pharmacodynamics studies forward to the neoadjuvant, pre-surgical, setting. This would allow analysis of molecular abnormalities in the diagnostic specimen then after pre-operative administration of the investigational agent the resection specimen could be analysed to confirm proof of mechanism.

An alternative approach is to invest in development of non-invasive strategies for molecular profiling. Some groups have been investigating circulating tumours cells (CTCs) and circulating DNA as potential non-invasive strategies.

CTCs can be isolated from blood using antibodies against cell-surface proteins restricted to epithelial cells[500]. Though only small numbers of CTCs are isolated from patients with metastatic cancer the CTC number has been shown to be prognostic[501,529]. Several studies to assess the impact of systemic treatment on CTC number are on going. Furthermore, in prostate cancer CTCs it has been shown that tumour specific genetic abnormalities including androgen receptor amplification, IGF-1R (insulin-like growth factor receptor) expression and ERG (Ets Related Genes) expression can be independently detected in the CTCs[530,531-533].

Circulating DNA has also been explored as a potential non-invasive route to molecular profiling. It was shown that cancer patients have a higher detectable level of circulating DNA which appears to be modulated with anti-cancer

treatment[534] and have prognostic value[535]. Additionally mutational analysis of circulating DNA is feasible[536,534, 535]. The detection of oncogenic mutations in the circulating DNA and its association with survival together suggest that the circulating DNA is tumour derived.

Ideally tumour tissue, rather than germ-line DNA from normal tissue, is required for molecular profiling. However, normal tissue samples are much more accessible and may be used as a surrogate for events in tumour tissues. This, although not ideal, is a reasonable approach since from a plethora of experience with cytotoxic agents it is clear that those normal tissues with a high proliferative index (hair follicles and blood cells) are sensitive to drug effects.

Normal tissues used in development of biomarkers include plucked hair follicles[537, 538], peripheral blood mononuclear cells (PBMCs), serum/plasma[539] and tumour specific autoantibodies[540].

Overall a biomarker assay needs to objectively measure a particular pathway of interest with a reasonable specificity and sensitivity. The technique needs to be reproducible so that the biomarker can be used for multi-site clinical studies and analytically validated. We are now beginning to see some phase I studies with biomarker assessment incorporated into their primary outcome, although so far these are still the vast minority probably due to the upfront cost of initial biomarker development[541].

1.6.3.1 p53 as a biomarker

p53 itself has been shown to have some value as both a prognostic and predictive biomarker.

The presence of a *TP53* mutation detected by sequencing has been shown to predict poor outcome (ie be prognostic) in some sub-types of breast cancer, colon cancer, head and neck cancers and leukaemia[373].

As a predictive biomarker *TP53* mutation status has also been shown to predict resistance to adjuvant tamoxifen and radiotherapy in the treatment of breast

cancer[542] and predict response to anthracycline based chemotherapy as discussed earlier[392, 393].

Hundreds of additional studies have investigated the role of *TP53* mutation as a prognostic and predictive biomarker in many different types of cancer but results have been inconsistent due to the assumption that accumulated p53 detected by immunohistochemistry is equivalent to *TP53* mutation. With the current improved access to sequencing technology these inconsistencies should be partly addressed.

1.6.3.2 Biomarkers of MDM2 inhibition

With the emergence of inhibitors of MDM2 and their progress into clinical evaluation, the need for biomarkers predictive of MDM2 inhibition has been recognised.

So far some effort has been made to establish predictive and pharmacodynamic biomarkers of MDM2 inhibition.

The main candidates as predictive biomarkers for MDM2 inhibition would be expected to be wild-type p53 status and overexpression of MDM2. In addition detection of induction of some of the numerous p53 targets (p21, MDM2, PUMA, Bax, MIC-1) following treatment may be useful. In particular measurement of serum macrophage inhibitory complex-1 (MIC-1)[543, 544] may prove useful since this is a secreted protein that has been shown to be highly induced after chemotherapy treatment. Furthermore MIC-1 is easily measured by Enzyme-Linked Immunosorbent Assay (ELISA).

To date there have been 2 biomarker studies of MDM2 inhibitor Nutlin (RG7112)[427, 428] (the results of which were not reported at the outset of this work).

A phase 1 dose escalation study in patients with wild-type p53 tumours was undertaken. MTD was reached with the dose limiting toxicity being thrombocytopenia. The study had an expansion cohort (at MTD) of patients with sarcoma who had pre and post treatment tumour biopsies for assessment of

biomarkers. Analysis included *TP53* mutation testing, MDM2 amplification, MDM2 rtPCR, and immunohistochemistry (IHC) for p53, p21, Ki67, TUNEL (Terminal deoxynucleotidyl transferase dUTP Nick End Labelling) staining, serum MIC-1 measurement and PET scanning. One radiological partial response was seen and one PET response. Evidence of p53 activation was seen in terms of increased p53 and p21 on IHC, increased MDM2 on rtPCR, increased serum MIC-1, reduced Ki67 on IHC and increased TUNEL activity. Activation of the p53 pathway did not correlate with MDM2 gene amplification.

The second study was in liposarcoma patients with MDM2-amplified tumours who were eligible for tumour resection. 20 patients were enrolled in the study and had pre treatment and post treatment biopsy/resection. Analysis of the p53 pathway was as for the prior phase I study. Two patients in this study had a *TP53* mutation. Again p53 activation was demonstrated by increased p53 and p21 on IHC and increased MDM2 on rtPCR as well as reduced Ki-67. Drug exposure and haematological toxicity correlated with MIC-1 level. One patient had a partial response and 14 had stable disease. This study was innovative in terms of evaluating pharmacodynamic biomarkers in the neo-adjuvant setting.

These studies establish that Nutlin is tolerable at doses which activate the p53 pathway. However, a robust predictive biomarker for response to MDM2 inhibition has not yet been identified.

1.7 Aims of thesis

The aim of this thesis was to explore different ways of manipulating the p53 pathway for cancer treatment. This has been addressed in four main sections:

1. Characterisation of a new class of inhibitors of MDM2's E3 ligase activity (MPD compounds) (chapter 3)

2. Characterisation of an MDM2 inhibitory compound HLI373 (chapter 4)

3. Cellular evaluation of act D and 5-Fluorouracil as chemoprotective agents for the treatment of mutant p53 expressing tumours (chapter 5)

4. Development of pharmacodynamics biomarkers of MDM2 inhibition and p53 activation (chapter 6)

2 Materials, patients and methods

2.1 Materials

2.1.1 General reagents

The sources of all chemicals and reagents mentioned in this work are listed in table 2-1.

Table 2-1: Chemicals and reagents.

Reagent	Source
1% Acid Alcohol	Beatson Histology Services
5-Fluorouracil	Beatson Cancer Centre
Acetone	Thermo Fisher Scientific
Acetic acid	Thermo Fisher Scientific
Acrylamide 29:1 (40% w/v)	National diagnostics
Actinomycin D	Beatson Cancer Centre
Agar	Fluka
Agarose	Sigma-Aldrich
Ampicillin	Sigma-Aldrich
APS (Ammonium persulfate)	Sigma-Aldrich
ATP (adenosine-5'-triphosphate)	Roche
Bromophenol blue	Sigma-Aldrich
BSA (bovine serum albumin)	Sigma-Aldrich
Chloroform	Thermo Fisher Scientific
Cisplatin	Beatson Cancer Centre
DAPI (4',6-diamidino-2-phenylindole)	Sigma-Aldrich
DMEM (Dulbecco's modified Eagle medium)	Life Technologies
DMSO (dimethyl sulfoxide)	Sigma-Aldrich
DNase	Roche
Doxycycline	Sigma-Aldrich
DPX Mountant	CellPath
DTT (dithiothreitol)	Sigma-Aldrich
ECL (enhanced chemiluminescence) reagent	Perbio
EDTA	Sigma-Aldrich
Eosin	Beatson Histology Services
Ethanol	Thermo Fisher Scientific
Fetal Calf Serum	GE Healthcare
Gene Juice	Novagen, Merck
Giemsa	Sigma-Aldrich
Glutamine	Life technologies
Glycerol	Sigma-Aldrich
Haem Z	CellPath

HBS buffer	Biacore
Histology wax	Leica (code 3808605E)
HLI373	A Weissman
IPEGAL CA-630 (NP-40 equivalent)	Sigma-Aldrich
Kanamycin	Sigma-Aldrich
KCl	Thermo Fisher Scientific
KH_2PO_4	Thermo Fisher Scientific
Methanol	Thermo Fisher Scientific
MG132	Sigma-Aldrich
$MgCl_2$	Sigma-Aldrich
MTT assay kit	Roche No. 11 465 007 001
Na_2HPO_4	Thermo Fisher Scientific
NaCl	Thermo Fisher Scientific
Nitrocellulose membranes	VWR
NP-40 (nonylphenoxypolyethoxylethanol)	Roche
Nutlin-3A	Cayman chemicals
Opti-MEM	Life technologies
Orange G	Sigma-Aldrich
Penicillin-Streptomycin	Life technologies
Formaldehyde	TAAB labs
Propodium Iodide	Sigma-Aldrich
Protease inhibitor cocktail	Roche
Puromycin	Sigma-Aldrich
RNase	Sigma-Aldrich
RPMI-1640 medium	Sigma-Aldrich
SDS (sodium dodecyl sulphate)	Thermo Fisher Scientific
STWS (Scott's tap water substitute)	Beatson Histology Services
TEMED (tetramethylethylenediamine)	Sigma-Aldrich
Tris-HCL	Sigma-Aldrich
TritonX-100	Sigma-Aldrich
Trypsin 2.5%	Life technologies
Tween-20	Sigma-Aldrich
Vectashield Hard Set mounting media	Vector Laboratories
β-Mercaptoethanol	Sigma-Aldrich

2.1.2 Solutions and buffers

Buffers and solutions used in this study are listed in table 2-2.

Table 2-2: Composition of buffers and solutions.

Solution	Composition
Phosphate Buffered Saline (PBS)	170mM NaCl 3.3mM KCl 1.8mM Na_2HPO_4 10.6mM KH_2PO_4 pH 7.4
Tris-Buffered Saline (TBS)	25mM Tris-HCl pH 7.4 137mM NaCl 5mM KCL
TBS-T (TBS-Tween)	TBS+0.1%Tween-20
Lysogeny broth (LB)	1% Bacto-tryptone 86mM NaCl 0.5% yeast extract 1.5% agar
Tris-EDTA (TE)	10mM Tris-HCl pH 8 1mM EDTA
2x SDS-PAGE (polyacrylamide gel electrophoresis) sample buffer	125mM Tris pH 6.8 4% SDS 10% β-mercaptoethanol 15% glycerol 0.01% bromophenol blue
3x SDS Sample Buffer	188mM Tris pH 6.8 9% SDS 15% β-mercaptoethanol 30% Glycerol 0.1% Orange G
SDS-PAGE running buffer	0.1% SDS 192mM glycine 25mM Tris-HCl pH 8.3
Electroblotting buffer	192mM glycine 25mM Tris 20% methanol
NP-40 buffer	20mM Tris-HCL pH 8 120mM NaCl 1mM EDTA 0.5% NP-40
Lysis buffer (*in vitro* ubiquitination)	50mM Tris-HCL pH 7.5 100mM NaCl 1% Triton 0.8 mg/ml DTT supplemented with PMSF
Reaction buffer (*in vitro* ubiquitination)	50mM Tris-HCl pH 8 2mM DTT 5mM $MgCl_2$

	2mM ATP
Blocking solution (Western blotting)	5% milk powder in TBS-T
Blocking solution (immunostaining)	1% BSA in PBS
Fixing solution (cells)	4% PFA in PBS
Fixing solution (hair follicles)	50% methanol 50% acetone
Resolving gel	8-10% acrylamide 375mM Tris-pH 8.8 0.1% SDS 0.1% APS 50mM TEMED
Stripping buffer	0.2M glycine 1% SDS pH 2.5
HUNT Buffer	20 mM Tris pH 8 120 mM NaCl 1 mM EDTA 0.5% IGEPAL
PBMC freezing medium	RPMI-1640 medium 10% FBS 10% DMSO protease inhibitor

2.2 Patients

All patients and volunteers involved in this study were consented and recruited to the MI45 sample collection study at The Beatson West of Scotland Cancer Centre. The MI45 study was first commenced in 2005 and approved by the Research Ethics Committee (REC ref: 04/S0709/61). The study involved collection of plasma and serum from patients with advanced gastrointestinal malignancy who were due to receive 5-fluorouracil based chemotherapy and collection of samples from a small group of healthy volunteers. An amendment to allow collection of hair follicles and peripheral blood mononuclear cells was made in 2009.

2.3 Methods

2.3.1 Cells

Cell lines used in the work are listed in table 2-3. All cell lines used are of human origin. The tissue type of origin, p53 status and the culturing medium are listed.

HCT116 and RKO cells were gifted from Bert Vogelstein.

U2OS PG13 luciferase cells were made in the laboratory by stably transfecting the PG13 luciferase construct.

U2OS-GFP-MDM2 TetOn cells were made by transfecting a U2OS TetOn cell line with a pTRE2 GFP-MDM2 plasmid and pBabe Eco Puro plasmid. Cells were then selected for 2 weeks using puromycin. Colonies resistant to puromycin were picked and cultured in DMEM supplemented with 10% fetal calf serum, 1% glutamine, 50U/ml penicillin G and 50μg/ml streptomycin sulfate at 37°C and 5% CO_2.

Table 2-3: Cell lines.

Cells	Tissue type	p53 status	Medium*
A2780/8	epithelial ovarian cancer	wild-type p53	DMEM
A431	epidermoid cancer	R273H mutation	DMEM
H1299	non-small cell lung adenocarcinoma	homozygous deletion of p53	DMEM
HCT116 p53-/-	colorectal adenocarcinoma	exon 2 deletion	DMEM
HCT116 p53+/+	colorectal adenocarcinoma	wild-type p53	DMEM
Hek293T	embryonic kidney cells	Inactivated by E6	DMEM/F12
Hela	cervical adenocarcinoma	wild-type p53, HPV-E6/E7	MEM
Hep3B	hepatocellular carcinoma	p53 null	MEM
HT29	colorectal adenocarcinoma	R273H mutation	McCoys medium
MCF-10A	mammary gland	wild-type p53	DMEM/F12
MCF-7	breast cancer cells	wild-type p53	DMEM
MDA-MB231	breast cancer cells	R280K mutation	DMEM
RKO p53-/-	colorectal adenocarcinoma	p53 null	DMEM
RKO p53+/+	colorectal adenocarcinoma	wild-type p53	DMEM
RPE	retinal pigment epithelial cells	wild-type p53	DMEM/F12 HAM**
U2OS	Osteosarcoma	wild-type p53	DMEM
U2OS PG13 luciferase	Osteosarcoma	wild-type p53	DMEM
U2OS GFP-MDM2	Osteosarcoma	wild-type p53	DMEM

TetOn			

* supplemented with 10% fetal calf serum, 1% glutamine and 50 U/ml penicillin G and 50μg/ml streptomycin sulfate; cultured at 37°C 5%CO_2

** medium also supplemented with 1.6% sodium bicarbonate

DMEM=Dulbecco's Modifies Eagle Medium, MEM=Minimum Essential Medium

2.3.2 DNA preparation

DNA preparations were carried out according to standard methods[545]. E. Coli DH5α competent cells (Molecular Biology services, Beatson Institute, Glasgow, UK) were thawed on ice. The 0.5μg of DNA plasmid was added to 50μl bacteria, mixed and incubated on ice for 20min. After a heat shock of 45 seconds at 42°C, the cells were incubated in 0.5 ml LB for 1 hour at 37°C with shaking at 450rpm. Cells were spread on agar plates with ampicillin or kanamycin and grown upside down at 37°C overnight. The next day the colonies were inoculated in LB with ampicillin or kanamycin and grown overnight at 37°C whilst shaking. Small scale plasmid DNA preparations were performed by Beatson Molecular Technology Services with the QIAgen BioRobot 9600 according to the manufacturer's instructions.

2.3.3 Plasmids

The GFP-MDM2 plasmid used to make the U2OS GFP-MDM2 TetOn cell line described above was cloned from pEGFP-C1 MDM2 (wild-type MDM2 cloned into Clontec backbone) into the pTRE2 plasmid (Clontec).

The following plasmids were used in this study:

Table 2-4: Plasmids.

Plasmid	**Source**
pTRE2 GFP-MDM2	Cloned by A. Hock
pBabe Eco Puro	Addgene
pEGFP C1 MDMX	Cloned by R Ludwig
pcDNA3 empty	Life Technologies
pcDNA3 p53 (72R)	published[546]
pCHDM1A MDM2	published[141]
pCHDM1A MDM2 C464A	published[547]
pMT123 HA-Ubiquitin	from R Hay[478]

PG13 Luciferase	published[548]
TK Renilla	published[385]
MDMX Luciferase	published[549]

2.3.4 Transfections

Cells were transfected with GeneJuice (MERCK Biosciences) according to the manufacturer's instructions. 10cm plates were plated with 15 x 10^5 cells and cells were left to attach in 10ml medium overnight at 37°C. GeneJuice (at 3:1 ratio with μgDNA) was added to 500μl Optimem drop-wise. Sample was vortexed briefly and incubated for 5mins. 5-10μg DNA was added and mixed by pipetting. The mixture was incubated at room temperature for 5-15mins. Mixture was added to plates drop-wise. Cells were incubated for 24 hours. Cell number, medium, GeneJuice and Optimem volumes and amount of DNA were scaled depending on plate size.

2.3.5 Luciferase assays

Cells were seeded to 70% confluency in 24 well plates (Fig 4-2, Fig 5-3) or 6 well plates (Fig 4-26).

Fig 4-2 & Fig 5-3: U2OS PG13 luciferase cells were treated with indicated drugs for 16 hours. Cells were then lysed in 100μl Promega lysis buffer for 30 minutes at 4°C. 20μl of lysate was transferred to multi-well plates, Luciferase substrate (Promega) added, and luminescence was measured with the Veritas Microplate luminometer (Turner Biosystems) using the Glomax Software. Data was plotted as fold change over no treatment condition. Luciferase activity in vehicle treated cells was set to 1. Error bars represent the SEM for 3 independent experiments. For Fig 5-3 error bars represent standard deviation.

Fig 4-26: Cells were transfected using GeneJuice (0.5μg MDMX-luciferase and 0.1μg TK Renilla Luciferase). 24 hours after transfection, cells were treated with indicated drugs for 16 hours then lysed in 500μl Promega lysis buffer for 30 minutes at 4°C. 20μl of lysate was transferred to luminometer plates and both Renilla and Luciferase substrates were added (Promega Dual Luciferase Kit), readings were carried out at the Veritas Microplate luminometer (Turner

Biosystems) using the Glomax Software. To correct for cell number and transfection efficiency relative luciferase units were determined by dividing the Luciferase readings by the values obtained for Renilla luciferase. Data was plotted as fold change over no treatment condition. Luciferase activity in vehicle treated cells was set to 1. Mean values of at least three experiments are plotted with error bars showing the SEM.

2.3.6 SDS-PAGE electrophoresis and Western blotting

SDS-Polyacrylamide gel electrophoresis was performed according to standard methods[550]. Lysates in sample buffer were heated to 95ºC for 5 mins. After a short spin, samples were loaded on appropriate SDS-polyacrylamide gels (8%, 10% or 12% acrylamide content). Electrophoresis was performed in SDS-PAGE buffer at 45mA on Hoefer Mighty Small vertical units SE250 (Amersham). By Western blotting[551, 552] protein was transferred to nitrocellulose membrane using the Hoefer TE22 Mini transfer tank (Amersham) at 200 mA for 1-2 hours. Membranes were blocked in 5% milk powder in TBS-T for one hour and incubated with primary antibodies over night at 4ºC. The following antibodies were used for blotting at the indicated dilutions:

Table 2-5: Primary antibodies.

Target	Dilution	Antibody name and supplier
Actin	1:5000	C4 (Chemicon, Merck)
CDK4	1:1000	C-22 sc-260 (Santa Cruz)
Flag tag	1:1000	M2 (Sigma)
GFP	1:1000	7.1/13.1 (Roche)
HA-tag	1:2500	16B12 (Covance, Cambridge Bioscience)
L11	1:1000	Made in laboratory
MDM2	1:2000	Ab-1 (Calbiochem, Merck)
MDM2	1:2000	Ab-2 (Calbiochem, Merck)
MDMX	1:2000	A300-287A (Bethyl Laboratories)
NEDD4	1:1000	2740 (Cell Signaling technology)
p21	1:2000	SC-397 (Santa Cruz)
p21	1:1000	2946 (Cell Signaling technology)
p53	1:10000	DO-1 (aa 20-25) (Beatson Molecular Services)[553]
p53 pS15	1:1000	16G8 (Cell Signaling technology)
p53 pS392	1:1000	9281 (Cell Signaling technology)

Ring1b	1:1000	sc-17265 (Santa Cruz)
Ubiquitin	1:1000	clone 6C1 (Sigma)
XIAP	1:1000	61073 (Becton Dickenson)

Membranes were then washed three times in TBS-T and incubated for 1 hour with appropriate secondary antibodies either horseradish-peroxidase (HRP) conjugated or fluorescently labelled at 1:10 000 dilution (table 2-6).

Proteins were visualised by Pierce ECL reagent, using Fuji X-Ray Film Super RX on an AGFA classic E.O.S film processor. Alternatively, fluorescent signal was detected using an Odyssey infrared scanner (LiCor Biosciences) and quantified with Odyssey software.

Table 2-6: Secondary antibodies.

Antibody	**Supplier**
Donkey anti rabbit HRP-linked	Amersham, GE Healthcare
Sheep anti mouse IgG HRP-linked	Amersham, GE Healthcare
IRDye800CW	LiCor Biosciences
IRDye6980LT	LiCor Biosciences

2.3.7 Immunoprecipitation

(Figure 4-14) U2OS cells at 50% confluency in 10 cm plates were transfected with MDM2 (pCHDM1A) 1.5μg and p53 (pcDNA3) 1.5μg or empty vector (pcDNA3) 1.5μg) using GeneJuice. 24 hours later, cells were treated with the indicated drug treatment. Cells were scraped, washed in PBS and lysed in NP-40 buffer with proteasome inhibitor. The suspension underwent 3 freeze-thaw cycles. After a 5min centrifugation at maximum speed, a 5% aliquot of the supernatant was taken for total protein input. The remainder of the supernatant was taken for immunoprecipitation (IP). Supernatant was rotated at 4°C with 5μl DO-1 antibody and 30μl Protein G Dynabeads (Invitrogen) for 2 hours. Beads were then washed three times with NP-40 buffer and resuspended in 3x sample buffer. Beads were incubated in denaturing sample buffer at 95°C for 5min to release precipitated proteins. Input and IP samples were run on SDS-Page gel, transferred to membrane by Western blotting and immunoblotted for p53 and MDM2.

(Figure 4-16) & (Figure 5-22) U2OS cells were treated with the indicated drug treatment then scraped, washed and lysed as described above. For this experiment, immunoprecipitation was carried out with 5μl L11 antibody and 30μl Protein A sepharose beads for 4 hours rotating at 4°C. Beads were washed three times with NP-40 buffer and resuspended in 2x sample buffer. Input and IP samples were run on SDS-Page gel and immunoblotted for L11 and MDM2.

2.3.8 *In vivo* ubiquitination of p53

(Figure 3-6) 10 cm plates were plated to 50-70% confluence with H1299 cells. 24 hours later cells were transfected with 2.4μg p53, 0.8μg MDM2 and 1μg HA-ubiquitin with GeneJuice. Cells were washed 20 hours later and treated with the indicated drug treatment and MG132 (5μM). Cells were lysed in 200μl 1% SDS in TBS. The lysate was boiled for 5mins, vortexed then boiled for a further 5mins. 400 μl 1.5% Triton-X in TBS was added. Lysates were rotated overnight at 4°C with 5μl DO1 antibody and 30μl Protein G beads. Beads were washed 3 times with HUNT buffer (20mM Tris pH8, 120mM NaCl, 1mM EDTA, 0.5% NP-40) and resuspended in 3x sample buffer. Samples were boiled for 5 minutes at 95°C and supernatant loaded on gel for Western blot analysis.

(Figure 4-11) H1299 cells were plated to 70% confluence in 10 cm plates. 24 hours later cells were transfected with 2.4μg p53, 0.8μg MDM2 or 0.8μg MDM2 C464A and 0.1μg GFP with GeneJuice. Cells were washed 20 hours later and treated with the indicated drug treatment and MG132 (5μM). Cells were lysed in 50μl NP-40 with complete protease inhibitor. Protein concentration was determined using the Pierce BCA (bicinchoninic acid) Protein Assay Kit (Thermo Fischer scientific) as per manufacturers instructions and 30μg protein per sample were diluted in 3x sample buffer. Samples were boiled for 5 minutes at 95°C and supernatant loaded on gel for Western blot analysis.

2.3.9 Immunofluorescence labelling

2.3.9.1 Cells

Cells (RPE, U2OS, HCT116) were plated to 60% confluence then treated with drug as indicated. For experiments using the Operetta system (PerkinElmer) cells

were plated on Borosilicate glass plates (Figure 5-17 & Figure 5-18). For other immunofluorescence experiments cells were plated on coverslips.

Cells were washed with PBS and fixed in 4% paraformaldehyde (PFA) in PBS for 10min at 4ºC. After a further 3 washes cells were permeabilised with 0.02-0.4% Triton X-100 in PBS for 1-10min. Cells were then washed 3 times with PBS and blocked with 1% BSA in PBS for 30min.

Cells were then incubated with indicated primary antibodies in 1% BSA/PBS. Primary antibodies used for immunofluorescence labelling are listed in table 2-7. Cells on coverslips were incubated in 100μl of the antibody solution and cells in glass plates were incubated in 200μl. After overnight incubation at 4ºC, cells were wahed 3 times in PBS and were then incubated with secondary antibody solution (Alexa Fluor 488 (green), Alexa Fluor 594 (red) antibodies in 1% BSA/PBS) and DAPI (1:2000) for 30min at room temperature. After a further 3 PBS washes cells on coverslips were mounted on slides with Vectashield hard set mounting media and confocal images were taken at an Olympus FV100 microscope. For cells not on coverslips, after washing cells were left in PBS and fluorescence was monitored by the high-content screening Operetta system (PerkinElmer). At least 10,000 cells were evaluated.

Table 2-7: Antibodies used in immunofluorescence.

Target	Dilution	Name and supplier
p53	1:250	DO-1 (aa 20-25) (Beatson Molecular Services)[553]
p53	1:100	1801 (aa 46-55) (Beatson Molecular Services)[29]
Ki67	1:500	RM-9106-s, (Lab Vision)
γH2AX ser^{139}	1:200	HCS 201685, (Millipore)
p21	1:100	554262, (BD Pharmingen)
pHH3	1:100	sc-8656-R, (Santa Cruz)
MDM2	1:200	Ab-1 (Calbiochem, Merck)
MDM2	1:200	Ab-2 (Calbiochem, Merck)
Rb	1:100	sc-50, (Santa Cruz)
B23 (nucleophosmin)	1:100	c-19-R, sc-6013 (Santa cruz)

Dilutions listed were used for cell and hair follicle staining.

2.3.9.2 Hair Follicles

Plucked hair follicles, collected as part of the MI45 study previously described, were initially fixed in cold 4% PFA, 100% methanol or 50:50 methanol:acetone for 10mins. Following assay optimisation all subsequent hairs were fixed in 50:50 methanol:acetone. After fixation, hair follicles were stored in microcentrifuge tubes at -70ºC until processing. Hairs were washed 3 times in PBS by rotating at 4ºC for 5mins. Hairs were then rotated in primary antibody solution (1% BSA) at 1:100-1:500 dilutions overnight at 4ºC. After further washes, hairs were incubated in secondary antibody (1:500) and DAPI (1:2000) in 1% BSA for 1 hour, rotating at 4ºC. Hairs were then mounted on coverslips with Vectashield hard set. Cells were visualised on Olympus FV100 Confocal microscope. Percentage positive nuclei was quantified on ImageJ.

2.3.10 Flow cytometry

2.3.10.1 Cell cycle profile

For analysis of cell cycle profile after vehicle or drug treatment floating and adherent cells were harvested with trypsin-EDTA, cells were washed in PBS and fixed in ice cold methanol for at least 30mins at 4°C. Cells were rehydrated with PBS and treated with 50μg/ml RNase for at least 15 mins. DNA was stained with propidium iodide (PI) before flow cytometric analysis (FACScan, Becton Dickinson)[554]. DNA content was analysed in channel FL2 and the percentage of cells in each phase was determined by DNA content and displayed as fold changes versus vehicle treated cells. Experiments were performed in triplicate and means and SEM are plotted.

2.3.10.2 Quantification of MDM2-GFP fluorescence

U2OS GFP-MDM2 TetOn cells were plated in 10cm plates and induced with doxycycline. After 48 hours cells were incubated with doxycycline plus DMSO, MPD compound (5μM) or MG132 (10μM) for 4 hours. Attached cells and floating cells were collected by trypsin-EDTA. Cells were fixed in 0.05% paraformaldehyde for 30 minutes and then rehydrated with PBS. Cells were PI stained and treated with 50μg/ml RNase A or 2 hours. GFP signal was measured (channel FL1) in

each condition by flow cytometric analysis (FACScan, Becton Dickinson). Sub G1 cells were excluded. Experiments were performed in triplicate and means and SEM are plotted.

2.3.10.3 Peripheral Blood Mononuclear Cells

Peripheral blood mononuclear cells, collected as part of the MI45 study previously described, were isolated from blood samples collected in CPT tubes (BD). Samples were mixed by inverting 8-10 times then centrifuged at 4000rpm for 20mins at room temperature. The majority of plasma was removed and resuspended in PBS. Cells were then spun at 2000rpm for 10mins at 20°C. The supernatant was then discarded. PBMCs were stored in freezing medium (RPMI-1640 medium supplemented with 10% FBS and 10% DMSO and protease inhibitor) at -70°C until processing. PBMCs were spun at 2000rpn for 5mins and freezing medium was removed. Cells were then resuspended in 500μl PBS and fixed in ice cold methanol for 10mins. After a spin at 2000rpm for 5mins, methanol was removed and cells were resuspended in 500ml PBS. Cells were incubated in 1% FCS for 15mins. After a further spin at 2000rpm for 5mins cells were resuspended in primary antibody or vehicle for 30mins at room temperature then overnight at 4°C. Primary antibodies used are listed in table 2-8. Cells were washed in PBS then incubated in secondary antibody (Alexa Fluor 488 and Alexa Fluor 647) at 1:50 dilution for 30mins at room temperature and in the dark. Cells were then washed in PBS and flow cytometry performed to quantify mean fluorescence in 2 channels (FL1, FL4). The value for cells incubated with no primary antibody was subtracted from the mean value for each sample. 10 000 cells in the gated population (lymphocytes) were counted for each sample.

Table 2-8: Antibodies used in PBMC staining.

Target	Dilution	Name and supplier
p53	1:100	DO-1 (aa 20-25) (Beatson Molecular Services)[28]
p21	1:50	SC-397 (Santa Cruz)

2.3.11 Colony formation assays

(Figure 5-13) 5000 RPE cells were plated on 10cm plates and incubated with the indicated dose of drug or vehicle for 24 hours. Cells were then washed and drug

free medium was replaced. Cells were maintained in drug free media for 9 days, with fresh media replaced every second day. Cells were then washed, fixed in ice cold methanol and Giemsa stained for 5 minutes. The stain was washed off with water and allowed to dry. Images were taken on Epson scanner and colonies were counted using ImageJ software.

(Figure 5-20) HCT116 cells null for p53 plated on 15cm plates were treated with act D (4nM) or 5-FU (5μg/ml) for 24 hours. Cells were washed, fixed with ice cold methanol and Giemsa stained for 5 minutes. The stain was washed off with water and allowed to dry. Images were taken on Epson scanner and colonies were counted using ImageJ software.

2.3.12 RNA extraction and qRT-PCR

RNA was prepared using an extraction column (Qiagen) according to the manufacturer's instructions. cDNA was synthesized from two micrograms of RNA using a dedicated kit (DyNAmo SYBR Green two-step qRT–PCR kit (Finnzymes)) with Oligo (d)T as mRNA specific primers. For detection of pre-mRNA (Fig 4-17, 4-18, 4-25, 4-32), RNA was subjected to DNase treatment followed by DNase inactivation (65°C for 20 mins) prior to reverse transcription and random hexamers were used instead of Oligo(d)T primers. Primers for pre-mRNA detection were designed to span intron-exon junctions. Quantitative PCR (qPCR) analysis was performed with 5μl of a 1:20 dilution of the cDNAs using DyNAmo SYBR Green two-step qRT–PCR kit (Finnzymes).

Accumulation of fluorescent products was monitored by real-time PCR using a Chromo4reader (Bio-Rad) and was analysed with the Opticon Monitor 3 software. qPCR cycling parameters were 15 min at 95°C hot start; 40 cycles of 20 sec denaturing at 94°C, 30 sec annealing at 60°C, and 30 sec elongation at 72°C followed by 10 min final elongation at 72°C. Examination of the melting curves verified that each primer pair used for the PCR amplified only one product. The relative quantification of gene expression was performed using the comparative ΔΔCt method, with normalization of the target gene to the control genes β2-microglobulin and RPLP0 (ribosomal protein, large, P0). Results are presented

relative to target gene induction after treatment of cells with vehicle only. Error bars represent the SEM of three independent experiments.

The following primers were used:

Table 2-9: qRT-PCR primers.

Target	Sequence
RPLP0 fw	gcaatgttgccagtgtctg
RPLP0 re	gccttgacctttcagcaa
B2M fw	gtgctcgcgctactctctc
B2M re	gtcaacttcaatgtcggat
MIC-1 fw	gttgcactccgaagactcca
MIC-1 re	gagagatacgcaggtgcagg
MDMX fw	ctccgtgaaagacccaagccctct
MDMX re	tcagactctcgctctcgcacagg
Pre-MDMX fw	agactctcgctctcgcacagg
Pre-MDMX re	tgtccctggtctgtgaactcccaa
Pri-miR-34a fw	cctccaagccagctcagttg
Pri-miR-34a re	tgactttggtccaattcctgttg
Pre-45S rRNA fw	gtccgggttcctccctcgg
Pre-45S rRNA re	ctcctcccccaccaccacac

2.3.13 Viability: Tetrazolium dye (MTT) colorimetric assay

Cells (HCT116 and RPE) were plated in a 96 well plate (2000 per well). Following an overnight incubation to allow the cells to attach, cells were treated with indicated drugs or vehicle. Cells were subjected to chemo-protective treatment for 24 hours, medium was then removed and cells were treated with the cytotoxic agent for 24 hours. After treatment cells were incubated with 10μl of MTT solution (Roche) for 3-4 hours at 37°C followed by an overnight incubation with 100μl of solvent to dissolve formazan crystals The plate was then read on a microplate reader at 550-600nM. Only viable, metabolically active cells convert tetrazolium salt MTT to formazan crystals. Percentage viable cells was calculated by dividing average absorbance values of 4-8 replicates for vehicle-cisplatin/paclitaxel, 5-FU-cisplatin/paclitaxel or Nutlin-cisplatin/paclitaxel by values for vehicle or corresponding protective agent then multiplying by 100. Values plotted are

therefore relative to the vehicle or protective agent treatment. Mean values of three independent experiments are shown and error bars represent SEM.

2.3.14 MIC-1 ELISA

The MIC-1 ELISA assay was performed on serum samples collected as part of the MI45 study previously described. The human GDF-15 Quanitkine ELISA Kit (R&D Systems) was used. 100μl of assay diluent RD1-9 was added to each well of a microplate. 50μl of serum from each patient (in duplicate) as well as standards were then added. The microplate was incubated for 2 hours at room temperature. Wells were washed four times using a squirt bottle with wash buffer. To dry wells the plate was blotted on paper towels. 200μl GDF-15 conjugate was added to each well and incubated for one hour. Wells were again washed four times with wash buffer. 200μl of substrate solution A and B were added to each well and then incubated in the dark for 30 minutes. 50μl of stop solution was added to each well. The optical density of each well was measured at 450nm on a microplate reader. Measurements were also taken at 540nm and subtracted from the values at 450nm to correct for plate irregularities. A standard curve was plotted and serum MIC-1 levels were calculated.

2.3.15 Mice/Xenografts

(Fig 4-33) C57Bl/6 mice weighing at least 20g were treated with vehicle or HLI373 50mg/kg by intraperitoneal (IP) injection. Mice were also injected with 0.25mL of BrdU (Amersham) 1hour prior to cull. Mice were culled at 2 and 8 hours after treatment. The small intestine was removed and flushed with water. It was then opened ‘en face’ and fixed for at least 3 hours in methacarn (4 parts methanol, 2 parts chloroform, 1 part acetic acid). Samples where then rolled into ‘swiss rolls’ and stored in formalin prior to embedding in paraffin.

(Figure 4-34) Mice were treated at National Cancer Institute at Frederick USA (NCI) as part of a collaboration with Professor A Weissman. The experimental set up was as follows: Athymic mice were injected subcutaneously with HCT116 cells into the flank. Tumours were staged to 200mg. Mice were then treated by an IP injection of vehicle or HLI373 and culled after 2 hours. Xenografts were removed

and formalin-fixed and paraffin-embedded. Blocks were sent to BICR for immunohistochemistry.

2.3.16 Immunohistochemistry

2.3.16.1 Mouse Tissue

Immunohistochemistry was performed by the Beatson Histology services using the following protocol:

Formalin-fixed paraffin-embedded sections were deparaffinized and rehydrated by passage through xylene and a graded alcohol series. Endogenous peroxidase activity was inactivated by treatment with 3% hydrogen peroxide, after which antigen retrieval was performed using microwave-heated citrate buffer (Labvision) or by incubation in citrate buffer in a pressure cooker. Sections were blocked in 5% serum for 1h and then incubated with primary antibody for 1h at room temperature or overnight at 4°C. Sections were incubated with secondary antibody for 1h (Dako Envision+ Kit, or Vectastain ABC system) and the staining was visualized with DAB (3, 3'-Diaminobenzidine).

Table 2-10: Antibodies used in immunohistochemistry.

Target	Dilution	Supplier
p53	1:100	CM-5 (Vector Labs)
p53	1:1000	DO-7 (Dako M7001) for xenograft
p21	1:500	Santa Cruz
BrdU	1:5000	BD Biosciences

IHC imaging was performed using a Zeiss AxioImager A1 microscope and Axiovision Rel 4.7 (Zeiss) acquisition software.

2.3.16.2 Hair follicles

Plucked hair follicles from healthy volunteers were fixed as above (section 2.2.9.2) then embedded in paraffin blocks and sectioned (6μm) by the Beatson Institute Histology services. For hematoxylin and eosin staining the following protocol was used:

Table 2-11: H&E staining of hair follicles.

Reagents	Time
Xylene	4 mins
Xylene	2 mins
100% Ethanol	1 min
100% Ethanol	1 min
70% Ethanol	1 min
Wash Tap Water	1 min
Haem Z	13 mins
Wash Tap Water	1 min
1% Acid Alcohol	2 secs
Wash Tap Water	30 secs
STWS	2 mins
Wash Tap Water	30 secs
Eosin	3 mins 15 secs
Wash Tap Water	30 secs
70% Ethanol	30 secs
100% Ethanol	30 secs
100% Xylene	30 secs
Xylene	30 secs
Xylene	1 min
Xylene	1 min

Mount sections with DPX mountant

IHC imaging was performed using a Zeiss AxioImager A1 microscope and Axiovision Rel 4.7 (Zeiss) acquisition software.

2.3.17 *In vitro* ubiquitination assays

The expression of recombinant GST-tagged MDM2 (GST-MDM2) was induced in 25ml culture of exponentially growing Escherichia coli BL21 cells (OD600 0.6) by 1mM IPTG for 3h. GST-MDM2 was purified on glutathione-sepharose beads (Amersham). Prior to the assay, GST-MDM2 bound beads were washed with 50mM Tris (pH7.5). Fluorescent-ubiquitin (5μg, Invitrogen), 50ng mammalian E1 (Enzo), 200ng human recombinant UbcH5B E2 (Enzo) and 200ng His-p53 (Enzo) were mixed with reaction buffer (50mM Tris pH8, 2mM DTT, 5mM $MgCl_2$, 2mM ATP). Indicated drugs or vehicle were added to the reaction mixture and the mixture was pipetted onto GST-MDM2 beads. The reaction was incubated at 37°C, shaking at 1200rpm for 1h and then stopped by the addition of 3xSDS

sample buffer. Free fluorescent-ubiquitin was washed off and total fluorescent-ubiquitin signal was measured on a monochromator plate reader (Safire).

For non-fluorescent *in vitro* ubiquitination assays the procedure was as above except 5μg unlabelled ubiquitin (Enzo) was used. Drugs or vehicle were added to the mixture and the mixture was pipetted onto GST-MDM2 beads. Incubation was as described above and reaction products were resolved by SDS–PAGE and analysed by Western blotting with anti-p53 DO-1 antibody.

For the MDM2 RING ubiquitination assay GST-MDM2 RING beads were prepared as above and used in place of the full-length MDM2.

For the MDM2 auto-ubiquitination assay the procedure was performed as detailed above except that no His-p53 was added to the reaction and Western blotting was with Ab1 and Ab2 antibodies.

For the Cbl auto-ubiquitination assay, bacterially expressed full-length Cbl was used in a reaction with the previously described quantities of E1, E2 and ubiquitin. Ubiquitinated Cbl was detected by Western blotting using anti-ubiquitin antibody (Sigma clone 6C1).

2.3.18 Surface plasmon resonance

Sensor chip surfaces were prepared on a Biacore T100 instrument (Biacore Inc.), using reagents obtained from the manufacturer. FLAG antibodies where cross-linked on a CM5 chip via amine coupling and individual flowcells where injected with FLAG-MDM2 RING where appropriate, or GST as a control protein. Measurements were performed at 25°C, 30µL per min, and a collection rate of 10Hz. A range of compounds concentrations were prepared in 100mM HBS buffer with a final DMSO concentration of 5%. The experimental data were corrected for instrumental and bulk artefacts by comparison to a control sensor chip surface and buffer injections using Biacore software package V 2.0.1.

2.3.19 Statistical analysis

Statistical analysis was carried out using GraphPad Prism 5 software.

To generate IC50s for inhibition of ubiquitination Prism's built-in standard curve fitting equation for non-normalised values was used.

For parametric data p-values were determined using Student's t-test (paired or unpaired). For non-parametric data Mann Whitney U test or Wilcoxon matched-pairs signed rank test was used when there were two variables. Kruskal-Wallis test was used for comparisons of non-parametric data where more than two variables were involved. P-values of less than 0.05 were deemed statistically significant.

To test correlation between variables Spearmann correlation Fisher's exact correlation were used.

Co-efficient of variation was calculated by diving the standard deviation of the samples by the mean. This was then multiplied by 100 to express it as a percentage.

3 MPD compounds

3.1 History of MPD compounds

The MPD compounds are analogues of a group of compounds originally named the HDM2 Ligase Inhibitor 98 (HLI98) class that were identified in a high-throughput screen for inhibitors of MDM2 autoubiquitination[446,447]. 100,000 compounds from a chemical library were screened. Of those, 40 were found to inhibit ubiquitination of MDM2 and further testing for dose-dependent inhibitory activity of MDM2 in cells validated 4 compounds as inhibitors of MDM2 autoubiquitination. Of these remaining 4 compounds, 3 were 7-nitro-5-deazaflavins (Figure 3-1). These compounds were shown to increase MDM2 and p53 levels by specifically inhibiting MDM2, without interfering with the p53-MDM2 interaction, resulting in activation of p53's transcriptional program and induction of apoptosis particularly in transformed cells. Due to the presence of the nitro group that can react with oxygen to form superoxide radicals, the HLI98 compounds could potentially stabilise p53 via production of reactive oxygen species (ROS). In an attempt to eliminate the contribution of ROS to p53 stabilisation, analogues of the HLI98s, lacking the nitro group, were synthesised[448]. Reassuringly these initial analogues could also stabilise p53, increase expression of p53 targets and cause cell cycle arrest/apoptosis without evidence of DNA damage (as determined by a lack of phosphorylation of p53 on serine 15). This work therefore supported the mechanism of function of these compounds as direct inhibitors of MDM2.

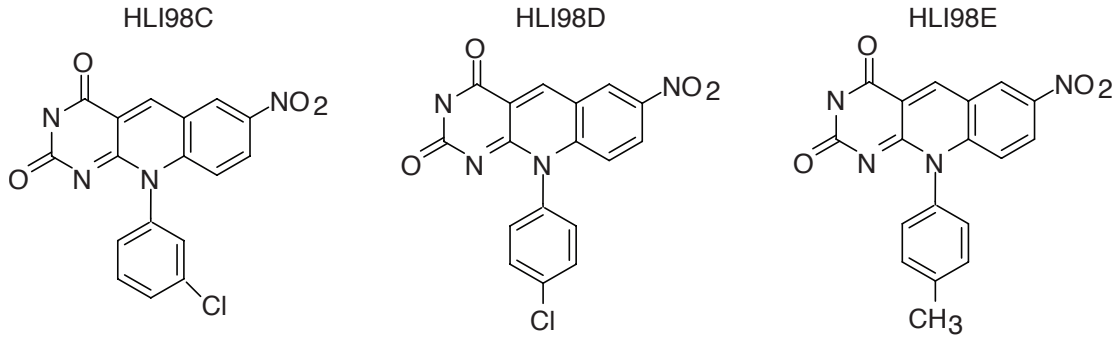

Figure 3-1: Chemical structures of HLI98C, D & E[447].

Despite the promise of the HLI98 compounds in *in* vitro experiments, the compounds were not suitable for further development as MDM2 inhibitors since they were not soluble in water and had relatively low activity in MDM2 inhibition. The group of Professor Peter Fischer, Professor of medicinal chemistry at Nottingham University, developed further derivatives of the HLI98 class,

rearranging or replacing the active groups of the molecule with more soluble groups (Figure 3-2). These compounds, now referred to as the MPD compounds (after the chemist Michael P Dickens), were developed in an attempt to study the structure-activity relationship and produce more potent inhibitors of MDM2's E3 ligase activity. The aim of this work was to test the biological and biochemical activities the MPD compounds and establish their mode of action.

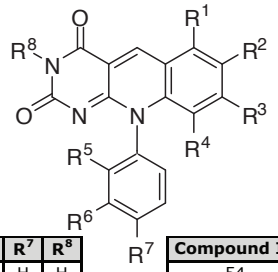

active compounds

Compound ID	R^1	R^2	R^3	R^4	R^5	R^6	R^7	R^8
3	H	H	H	H	H	H	H	H
6	H	H	H	H	H	H	**Cl**	H
7	H	H	H	H	**F**	H	H	H
9	**CF_3**	H	H	H	H	H	H	H
10	**CF_3**	H	H	H	H	H	**Cl**	H
11	**CF_3**	H	H	H	**F**	H	H	H
12	H	**CF_3**	H	H	H	H	H	H
13	H	**CF_3**	H	H	**F**	H	H	H
14	H	**CF_3**	H	H	H	H	**Cl**	H
15	**Me**	H	H	H	H	H	H	H
16	**Me**	H	H	H	**F**	H	H	H
17	H	H	**CF_3**	H	H	H	H	H
18	H	H	**CF_3**	H	**F**	H	H	H
19	H	H	H	**CF_3**	H	H	H	H
20	H	H	H	**CF_3**	**F**	H	H	H
21	H	**NO_2**	H	H	H	H	H	H
22	H	**NO_2**	H	H	**F**	H	H	H
24	H	**Cl**	H	H	H	H	H	H
25	H	**Cl**	H	H	**F**	H	H	H
26	H	**Cl**	H	H	H	H	**Cl**	H
27	H	H	**Cl**	H	H	H	H	H
28	H	H	**Cl**	H	**F**	H	H	H
29	H	H	**Cl**	H	H	H	**Cl**	H
30	H	H	H	**Cl**	H	H	H	H
31	H	H	H	**Cl**	**F**	H	H	H
32	H	H	H	**Cl**	H	H	**Cl**	H
33	**Cl**	H	H	H	H	H	H	H
34	**Cl**	H	H	H	**F**	H	H	H
35	**Cl**	H	H	H	H	H	**Cl**	H
36	H	H	**CF_3**	H	H	H	**Cl**	H
37	H	H	H	**CF_3**	H	H	**Cl**	H
38	H	**Me**	H	H	H	H	H	H
39	H	**Me**	H	H	**F**	H	H	H
40	H	**Me**	H	H	H	H	**Cl**	H
42	**Me**	H	H	H	H	H	**Cl**	H
46	H	H	H	**Me**	H	H	H	H
47	H	H	H	**Me**	**F**	H	H	H
48	H	H	H	**Me**	H	H	**Cl**	H
49	H	H	**Me**	H	H	H	H	H
50	H	H	**Me**	H	**F**	H	H	H
51	H	H	**Me**	H	H	H	**Cl**	H
53	H	H	H	**NO_2**	**F**	H	H	H

Compound ID	R^1	R^2	R^3	R^4	R^5	R^6	R^7	R^8
54	H	H	H	**NO_2**	H	H	**Cl**	H
55	**NO_2**	H	H	H	H	H	H	H
56	**NO_2**	H	H	H	**F**	H	H	H
57	**NO_2**	H	H	H	H	H	**Cl**	H
67	H	H	**NO_2**	H	H	H	H	H
68	H	H	**NO_2**	H	**F**	H	H	H
69	H	H	**NO_2**	H	H	H	Cl	H
83	H	H	H	H	H	H	H	**Me**
87	H	H	H	H	H	H	H	**Et**
126	H	H	H	H	**Cl**	H	H	H
127	H	H	H	**Cl**	**Cl**	H	H	H
128	H	H	H	**CF_3**	**Cl**	H	H	H
129	H	H	H	H	H	**Cl**	H	H
131	H	H	H	**CF_3**	H	**Cl**	H	H
132	H	H	H	H	H	**F**	H	H
133	H	H	H	**Cl**	H	**F**	H	H
134	H	H	H	**CF_3**	H	**F**	H	H
135	H	H	H	H	H	H	**F**	H
136	H	H	H	**Cl**	H	H	**F**	H
137	H	H	H	**CF_3**	H	H	**F**	H
138	H	H	H	H	**Me**	H	H	H
139	H	H	H	**Cl**	**Me**	H	H	H
140	H	H	H	**CF_3**	H	**Me**	H	H
141	H	H	H	H	H	**Me**	H	H
142	H	H	H	**Cl**	H	**Me**	H	H
143	H	H	H	**CF_3**	**Me**	H	H	H
144	H	H	H	H	H	H	**Me**	H
145	H	H	H	**Cl**	H	H	**Me**	H
146	H	H	H	**CF_3**	H	H	**Me**	H
147	H	H	H	**F**	H	H	H	H
148	H	H	H	**F**	H	H	**Cl**	H
149	H	H	H	**OH**	H	H	H	H
150	H	H	H	**OH**	H	H	**Cl**	H
151	H	H	H	H	**F**	H	**Cl**	H
152	H	H	H	**Cl**	**F**	H	**Cl**	H
158	H	H	H	**Br**	H	H	H	H
159	H	H	H	**Br**	H	H	**Cl**	H
162	H	H	H	**CF_3**	H	**Cl**	**Cl**	H
165	H	H	H	**CF_3**	H	H	**Cl**	**Me**
166	H	H	H	**CF_3**	H	H	**Cl**	**Et**
199	H	H	H	**CN**	H	**Cl**	H	H
200	H	H	H	**CN**	H	H	**Cl**	H

Figure 3-2: Chemical structures of MPD compounds.

3.2 Active MPD compounds inhibit ubiquitination of MDM2 and p53

First, the new derivatives were tested in an *in vitro* ubiquitination assay in which fluorescent ubiquitin was used to quantify ubiquitination of both p53 and MDM2 simultaneously (Figure 3-3).

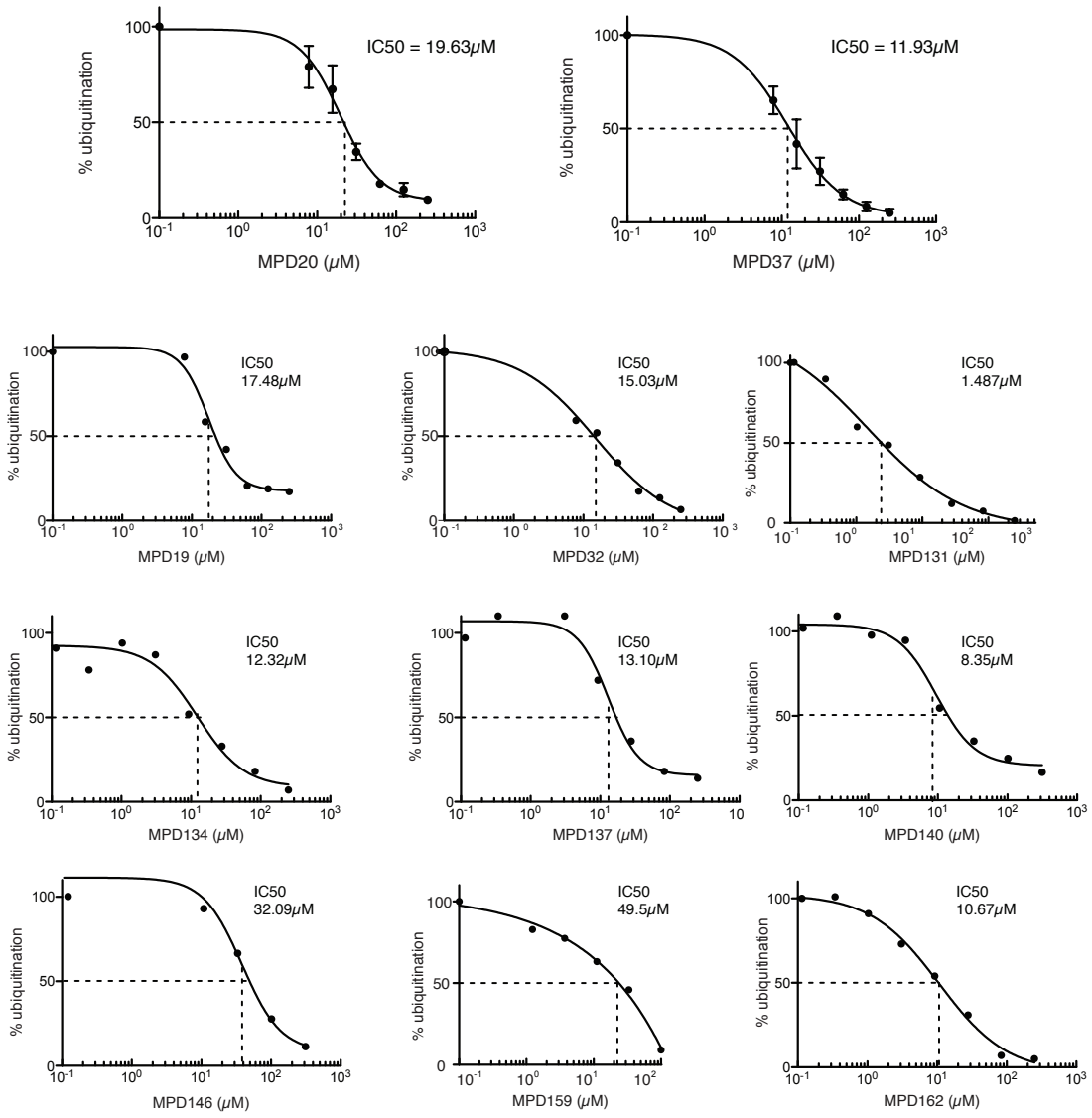

Figure 3-3: IC50s for inhibition of ubiquitination of MDM2 and p53.
IC50s were calculated with PRISM 5. For core compounds (20 and 37), the assay was performed in triplicate. Error bars represent SEM of 3 independent experiments.

Ubiquitination reactions were set up using glutathione S-transferase (GST)-tagged MDM2, fluorescein isothiocyanate (FITC)-ubiquitin, E1, E2 (UbcH5b) and His-p53. A dose titration of each MPD compound was added to the mixture and the mixture was pipetted on glutathione sepharose beads to capture GST-MDM2 complexes. Free ubiquitin was washed off and fluorescence was measured on a fluorescence

plate reader set for 340nm excitation wavelength and 490nm emission wavelength.

From this assay, IC50s for the inhibition of p53 and MDM2 ubiquitination were generated. Of the 84 new analogues tested, 73 were inactive (Figure 3-2). Of note, 10 of the MPD compounds possessed a nitro group and all of these were inactive.

11 compounds showed inhibition in the ubiquitination of MDM2 and p53 with IC50s ranging from 1.5 to 50μM (Figure 3-3). Subsequent experiments were designed to include an inactive compound, a moderately active compound and a highly active compound. For most experiments these core compounds were MPD39 (inactive), MPD20 (moderately active, IC50 19.6μM) and MPD37 (highly active, IC50 11.9 μM).

Next the compounds were tested in gel-based *in vitro* ubiquitination assays to assess the relative contributions of inhibition of MDM2 autoubiquitination and inhibition of p53 ubiquitination to the previously generated IC50. Ubiquitination reactions were set up using GST-purified MDM2, E1, E2 (UbcH5b), non-tagged ubiquitin and reaction buffer containing ATP. A reaction lacking the E1 and E2 was used as a negative control. Reactions were incubated with a randomly selected panel of MPD compounds and core MPD compounds at 10μM. MDM2 was able to polyubiquitinate itself in the presence of the E1 and E2 enzymes as shown by the presence of a smear of higher molecular weight forms of MDM2 due to the addition of multiple or polyubiquitin molecules. In the absence of the E1 and E2 enzymes no smear was detected, as expected. The compounds previously categorised as inactive failed to inhibit this autoubiquitination of MDM2 while the active compounds inhibited MDM2 autoubiquitination (Figure 3-4). Compound MPD26 appeared to cause a minor reduction in MDM2 autoubiquitination despite being an inactive compound in the mixed *in vitro* ubiquitination assay.

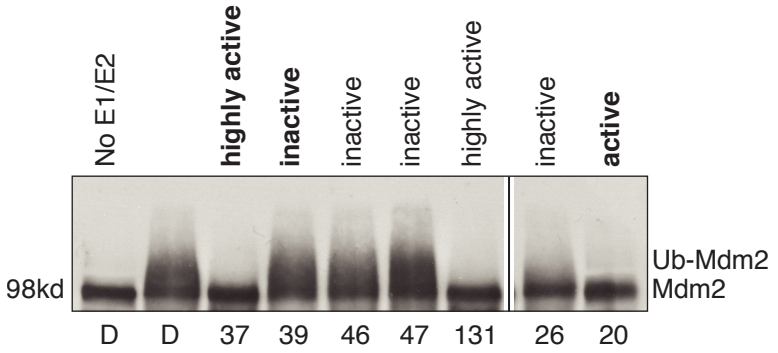

Figure 3-4: Active MPD compounds inhibit *in vitro* autoubiquitination of MDM2. MDM2 was detected by Western blotting using AB1 and AB2 antibodies. Activity according to mixed ubiquitination assay is indicated. For core compounds, the activity status is indicated in bold. D=DMSO.

To test if the compounds could also inhibit ubiquitination of p53, they were tested in an *in vitro* assay of p53 ubiquitination. Ubiquitination reactions were set up as before for MDM2 autoubiquitination but His-p53 was also added to the reaction mixture. Similar to the observed inhibition of MDM2 autoubiquitination, most compounds also inhibited p53 ubiquitination in a pattern that reflected the previously generated IC50s with compounds MPD20, MPD37 and MPD131 being active and MPD39, MPD46 and MPD47 being inactive (Figure 3-5). Compound MPD26 again showed a modest reduction in polyubiquitinated p53 despite being negative in the mixed ubiquitination assay.

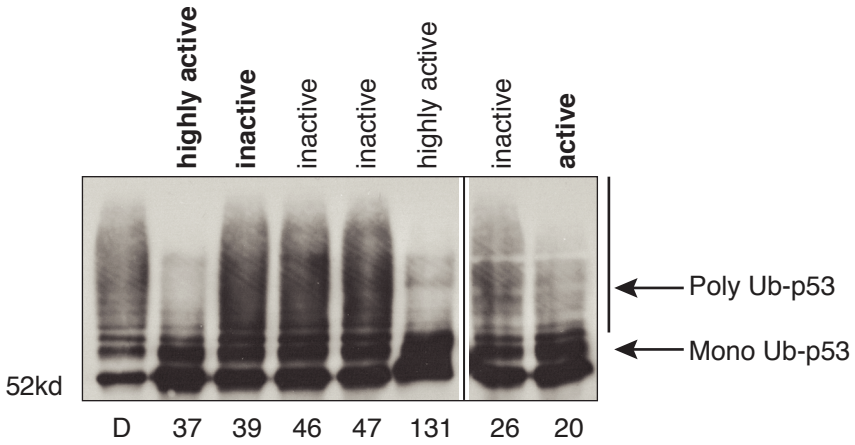

Figure 3-5: Active MPD compounds inhibit *in vitro* ubiquitination of p53. p53 was detected by Western blotting using DO1 antibody. Activity according to mixed ubiquitination assay is indicated. For core compounds this is in bold. D=DMSO.

In this *in vitro* assay the active compounds do not appear to inhibit the monoubiquitination of p53. Although the higher molecular weight forms of ubiquitinated p53, which represent multiple and polyubiquitination of p53, are

reduced by active compounds, none of the compounds diminished the appearance of the first, monoubiquitinated p53 band.

To establish the efficacy of the compounds in a more biologically relevant system, they were tested for their ability to inhibit ubiquitination of p53 in cells (Figure 3-6). p53 negative H1299 cells were transfected with MDM2, p53 and HA-ubiquitin. HA-ubiquitin was used to ensure detection of ubiquitinated p53 rather than other posttranslational modifications such as acetylation, methylation, neddylation and SUMOylation, which are known to occur on p53[209]. Cells were then treated with 10μM of each MPD compound and 10μM of proteasome inhibitor MG132, to prevent degradation of ubiquitinated p53. Compounds MPD37, MPD148 and MPD159 were used to represent a compound of high activity, no activity and moderate activity respectively as defined by the previous *in vitro* studies. Cells were lysed in denaturing conditions to disrupt binding to any covalently bound interactors (ie MDM2) while not disrupting the non-covalent p53-ubiquitin binding. p53 was then immunoprecipitated using DO1 antibody and lysates were subjected to immunoblot analysis in which an HA antibody was used to detect ubiquitinated forms of p53. Active compound MPD37 abolished all ubiquitination of p53, inactive compound MPD148 had no effect, while moderately active compound MPD159 caused a small reduction in ubiquitination of p53 (Figure 3-6). Nutlin, a small molecule that prevents p53-MDM2 interaction[555], reduced but did not abolish ubiquitination of p53, in contrast with MPD37. The apparent lack of inhibition of monoubiquitination seen *in vitro* was not seen when the compounds were tested in cells since active compound MPD37 appeared to reduce all higher molecular weight forms of p53.

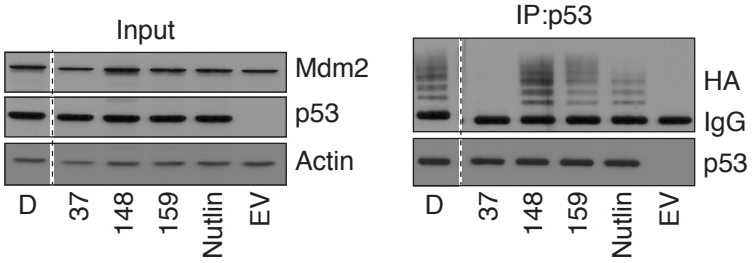

Figure 3-6: Active MPD compounds inhibit ubiquitination of p53 in cells.
H1299 cells were transfected with p53/empty vector (EV), MDM2 and HA-ubiquitin. Cells were incubated with MPD compound (10μM) and MG132 (10μM) for 2 hours. Denaturing p53 immunoprecipitation (IP) was performed with DO1 antibody. Input and IP were blotted with the indicated antibodies. Actin was loading control. D=DMSO.

The data presented here confirms that the active MPD compounds can inhibit ubiquitination of both p53 and MDM2 *in vitro* and in cells.

3.3 Active MPD compounds inhibit the RING of MDM2 specifically

Next, efforts were made to examine the potential mechanisms by which the MPD compounds could inhibit the E3 ligase function of MDM2. Clearly a ubiquitination reaction depends on the presence of a functional E1, E2, E3 and substrate, which in the case of MDM2, may be MDM2 itself.

The RING finger E3 ubiquitin ligases are the largest family of E3 ligases and are responsible for regulation of a vast number of different functions in the cell through regulation of multiple substrates. It is therefore important to establish whether the MPD compounds are specific for inhibition of MDM2 or capable of inhibiting any RING E3 ubiquitin ligase protein. For this the previously described *in vitro* ubiquitination assay was performed using Cbl (Casitas B-lineage Lymphoma). Cbl is structurally similar to MDM2 and also capable of autoubiquitination[556], making it a suitable comparator for testing specificity of the MPD compounds (Figure 3-7). Furthermore since Cbl is capable of ubiquitination in this assay using the same E1 and E2 as used to test MDM2's E3 ligase activity, conclusions could be drawn regarding any possible non-specific activity of the MPD compound against the E1 or E2.

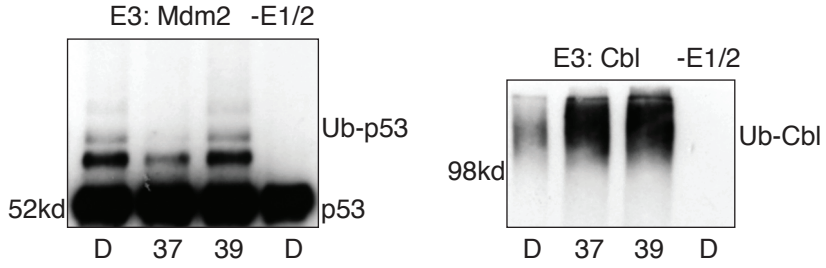

Figure 3-7: Active MPD compounds do not inhibit Cbl mediated ubiquitination.
Full-length Cbl, E1, E2 and reaction buffer were incubated with MPD compound (10μM). Ubiquitinated Cbl was detected by Western blotting using anti-ubiquitin antibody (right panel). Bacterially expressed GST-MDM2 RING, His-p53, E1, E2 and reaction buffer were incubated with MPD compound (10μM). p53 was detected by Western blotting using DO1 antibody (left panel). D-DMSO.

The Cbl ubiquitination assay showed that the active compound MPD37 was unable to inhibit Cbl ubiquitination at doses that could inhibit MDM2's ability to

ubiquitinate p53, while inactive compound MPD39 was unable to inhibit either Cbl or MDM2 activity (Figure 3-7).

These results therefore indicate that the MPD compounds are not capable of inhibiting E3 ligase activity of all RING E3s, and also that they are not general inhibitors of E1 and or E2.

Multiple domains of MDM2 have been shown to contribute to MDM2's ability to ubiquitinate p53, including the C-terminal RING and tail, the N-terminal p53-binding site and the central acidic domain[265, 266, 316-318, 445]. However in *in vitro* ubiquitination assays the MDM2 RING domain alone is sufficient to (poly) ubiquitinate p53[289, 557]. To analyse if the MPD compounds inhibit MDM2's RING domain directly, the ability of the MPD compounds to inhibit MDM2 RING (a construct comprising residues 417-491 of MDM2)-mediated ubiquitination of p53 was tested in an *in vitro* assay. Indeed, the active MPD compounds (MPD20, MPD37 and MPD159) also inhibited MDM2 RING ubiquitination of p53 (Figure 3-8). This is consistent with previous results published for the original HLI98 compounds and confirms that the N-terminal p53-binding site of MDM2 is not required for the compounds' function[557].

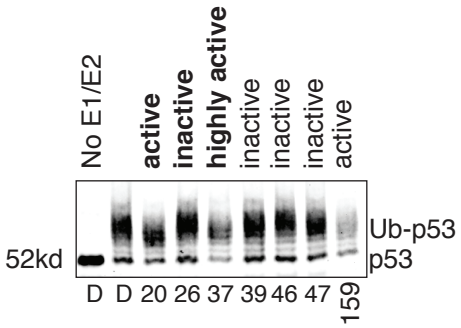

Figure 3-8: Active MPD compounds inhibit MDM2 RING dependent p53 ubiquitination. MDM2 RING, His-p53, E1, E2 and reaction buffer were incubated with 10μM MPD compound. p53 was detected by Western blotting using DO1 antibody. Activity in mixed ubiquitination assay is indicated. For core compounds activity is bold. D=DMSO.

More importantly, the site of action of the MPD compounds must be the RING-tail domain of MDM2 (since the MDM2 construct used here contained only the RING-tail region).

To test directly whether the active MPD compounds bind to the MDM2 RING-tail, in collaboration with Dr Andreas Hock, compounds were assessed for their ability

to bind to the MDM2 RING-tail using Biacore Surface Plasmon Resonance (SPR). SPR can be used to examine protein-compound interactions in real time. The experiment involved coupling purified FLAG-tagged MDM2 RING-tail on a sensor chip using FLAG antibody then injecting a series of concentrations of each compound across the surface. Single wavelength fixed angle light was directed onto the sensor surface and the surface plasmon resonance angle was measured. Compound binding to MDM2 caused changes in the surface plasmon resonance angle, which reversed relative to compound dissociation therefore provided a measure of the interaction and affinity of the inhibitors to the RING-tail of MDM2.

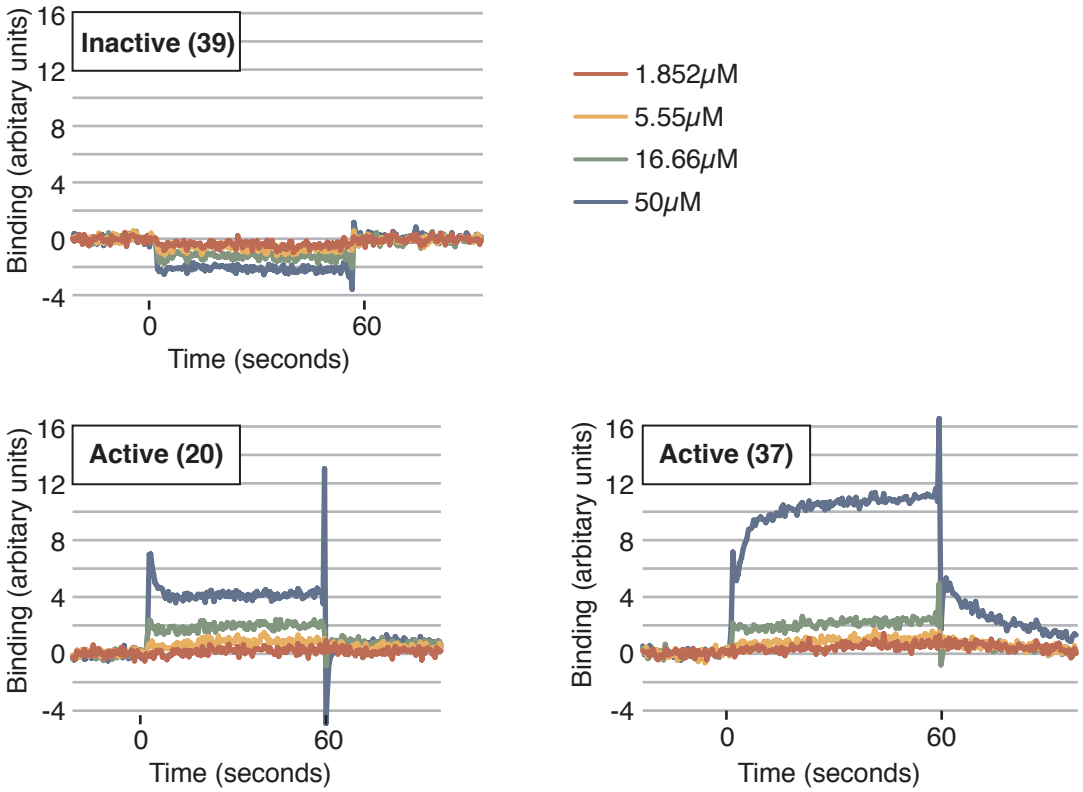

Figure 3-9: Active MPD compounds bind the MDM2 RING.
FLAG antibody was amine coupled to a Biacore CM5 series sensor chip and subsequently loaded with FLAG-tagged RING domains of MDM2. Relative units were measured with various doses of compounds. Data are normalised to an antibody only surface to exclude MDM2-independent effects.

Some of the MPD compounds presented technical difficulties when being tested using SPR technology due to their poor solubility, especially at higher concentrations. Since the Biacore does not allow use of high DSMO concentrations to alleviate this problem, we were unable to obtain reliable data for the full panel of MPD compounds. For example MPD159 displayed high levels of non-specific binding. Fortunately we were able to test the more soluble compounds, obtaining data for a representative compound from the inactive,

moderately active and highly active groups. As shown in Figure 3-9, the active MPD compound (MPD37) did bind to the MDM2 RING-tail in a dose dependent manner while inactive compound MPD39 did not. Furthermore, information about the binding rate suggests that compound MPD37 had a relatively slower off rate than the less active compounds. Moderately active MPD compound MPD20 showed some evidence of binding at higher dose levels.

Taken together these data provide evidence that compounds bind to the MDM2 RING-tail and so inhibit MDM2's E3 ligase function. By analogy with other RING E3 ligases, it seems the RING domain of MDM2 forms the E2 binding domain, and it is possible that the interaction with the compounds inhibits the E3/E2 interaction. However, the MDM2 RING is also necessary for homodimerisation or heterodimerisation with the RING domain of MDMX[351]. Any compound that binds the MDM2 RING could therefore disrupt dimerisation, which is important for MDM2's E3 ligase function. Inhibition of dimerisation is therefore another possible mechanism by which MPD compounds inhibit ubiquitination. Interestingly, *in silico* docking of the original HLI98 compound shows that the HLI98 compound fits into the hydrophobic cleft of MDM2 RING, consistent with the compounds ability to bind (Figure 3-10).

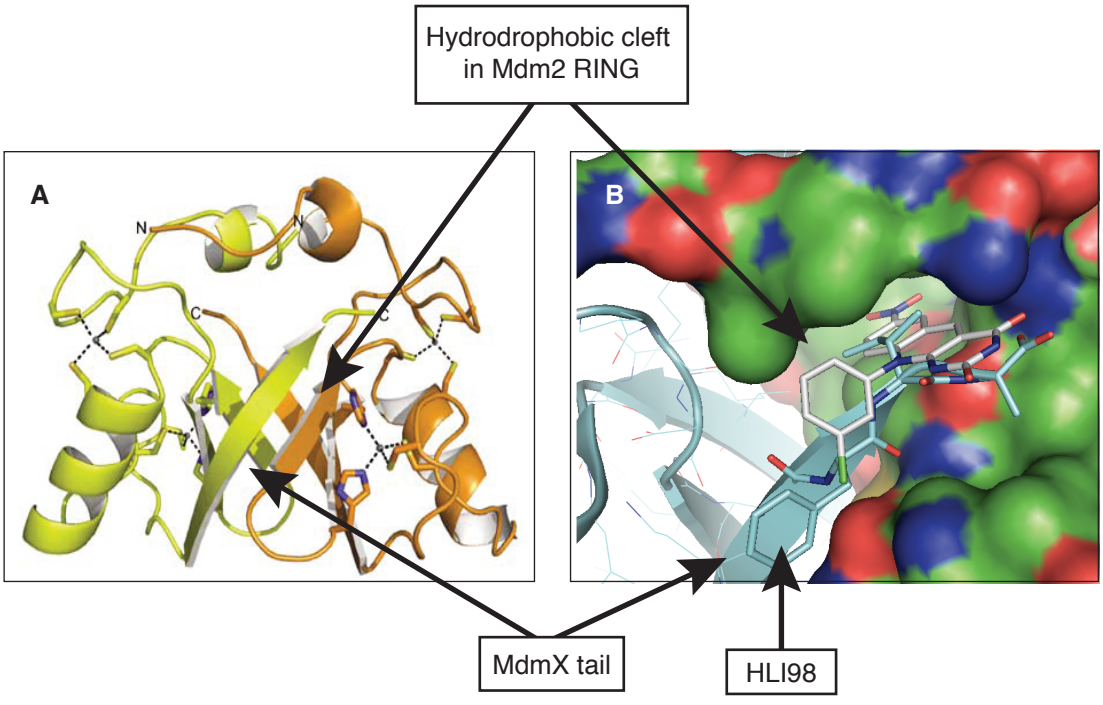

Figure 3-10: The structure of MDM2/MDMX interaction & *in silico* docking of HLI198. (A) MDMX is shown in yellow and MDM2 in orange[351] (B) *In silico* docking model from

Peter Fischer University of Nottingham.

In addition the docking model illustrates that binding to the RING region could potentially disrupt heterodimerisation.

3.4 Active MPD compounds activate p53

Previous studies have shown that the HLI98 class of compounds can stabilise and activate p53 in cells[447]. While the MPD compounds had been shown to inhibit the ubiquitination of ectopically expressed p53, it was important to establish the effect of the MPD compounds on the stability and activity of endogenous p53. Wild-type p53 expressing retinal pigment epithelial (RPE) cells were treated with inactive compounds MPD39, MPD47 and MPD165 and active compounds MPD20, MPD37 and MPD159 at 2.5, 5 and 10μM for 16 hours. DMSO and Nutlin at 10μM were used for the negative and positive controls respectively.

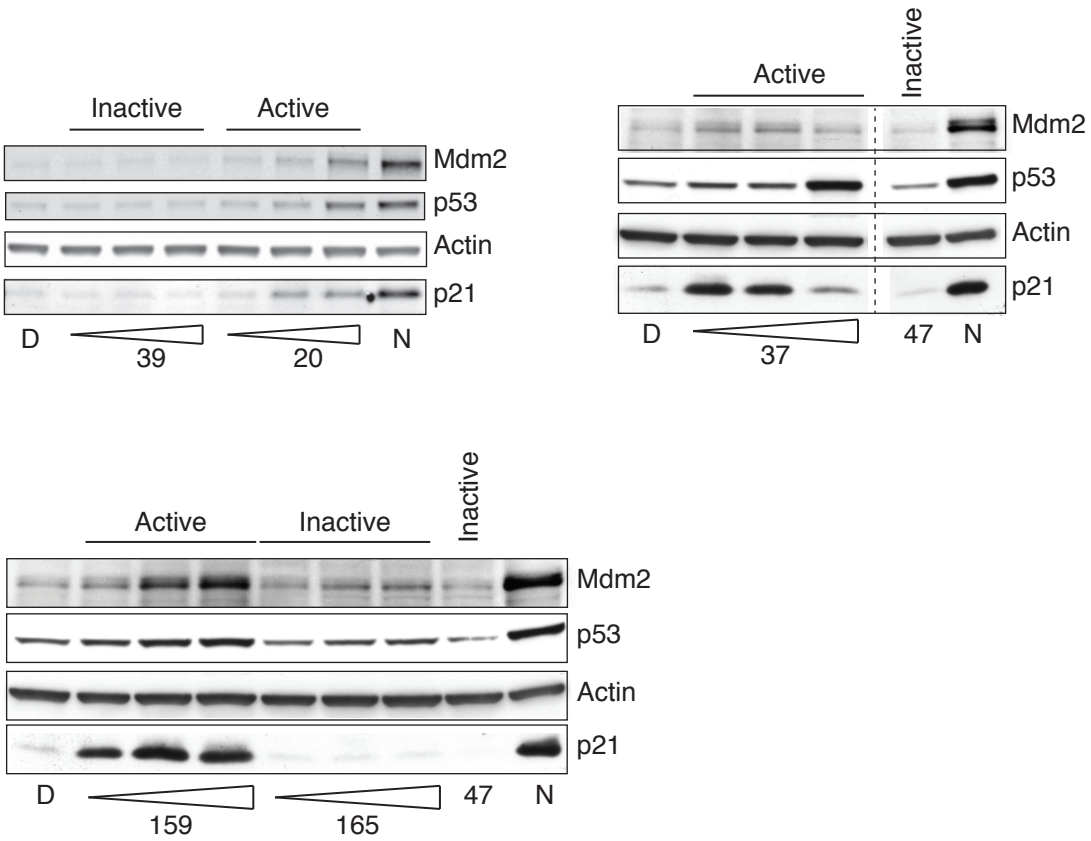

Figure 3-11: MPD compounds stabilise p53 and increase expression of p53 targets. MDM2, p53 and p21 were detected by Western blotting using AB1, AB2, DO1 and p21 antibodies. Actin was used as loading control. D=DMSO, N=Nutlin. n≥3.

Figure 3-11 shows that all 3 active compounds stabilised p53 and increased expression of p53 targets MDM2 and p21 to a similar degree as Nutlin. MDM2

was detected as a doublet around 80kD. This is thought to represent the full-length MDM2 protein. The double band suggests the presence of a modified form of MDM2 however the specific modification remains unknown[408, 558]. When used at the highest dose level, compound MPD37 appeared to stabilise p53 but did not result in increased target expression. This was a reproducible effect which is most likely a reflection of the toxicity of this compound at high concentrations, as demonstrated by an increase in sub G1 fraction on cell cycle analysis (Figure 3-15). The 3 inactive compounds failed to stabilise p53 or induce p53 target genes.

Clearly activation of p53 would increase MDM2 levels by causing increased transcription of MDM2. However, since the active MPD compounds also inhibit ubiquitination of MDM2 we would predict that MPD compounds additionally increase the level of MDM2 by causing an accumulation of the MDM2 protein. To investigate this we used U2OS cells engineered to express a doxycycline-inducible GFP-MDM2. Using this construct allowed us to measure the accumulation of MDM2, as measured by an increased GFP signal, driven by a different promoter and therefore uncoupled from the increase in p53 transcriptional activity. Following induction of the GFP-MDM2, cells were treated with MPD compounds.

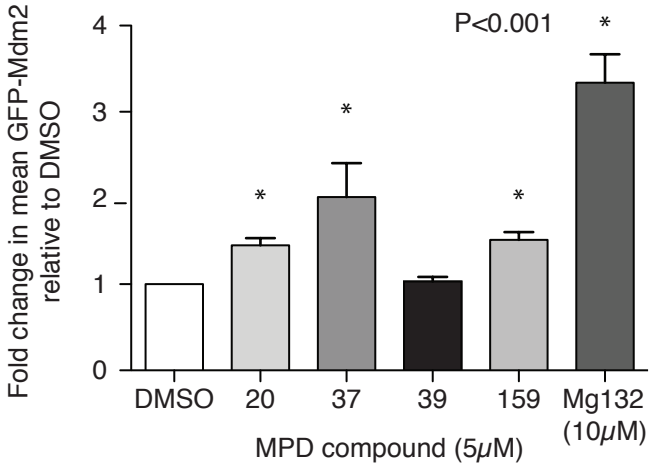

Figure 3-12: Active MPD compounds cause accumulation of MDM2.
U2OS GFP-MDM2 TetOn cells were induced with doxycycline for 48h. Cells were then treated with DMSO, indicated MPD compound or MG132 for 4h. Cells were next harvested, fixed with 0.05% paraformaldehyde, rehydrated and stained with propidium iodine (PI) for flow cytometric analysis. Sub G_1 cells were excluded from analysis and mean GFP signal was quantified for each condition. Error bars represent SEM of 3- to 9-independent experiments.

The active MPD compounds (MPD20, 37 and 159) induced an increase in GFP signal as measured by fluorescence activated cell sorting (FACS) while inactive

compound MPD39 did not, indicating that the active MPD compounds can stabilise MDM2 directly (Figure 3-12). Proteasome inhibitor MG132 was used as a positive control.

As p53 accumulation can lead to cell cycle arrest or apoptosis, the biological effects of the active MPD compounds on the cell cycle profile and apoptosis were next examined.

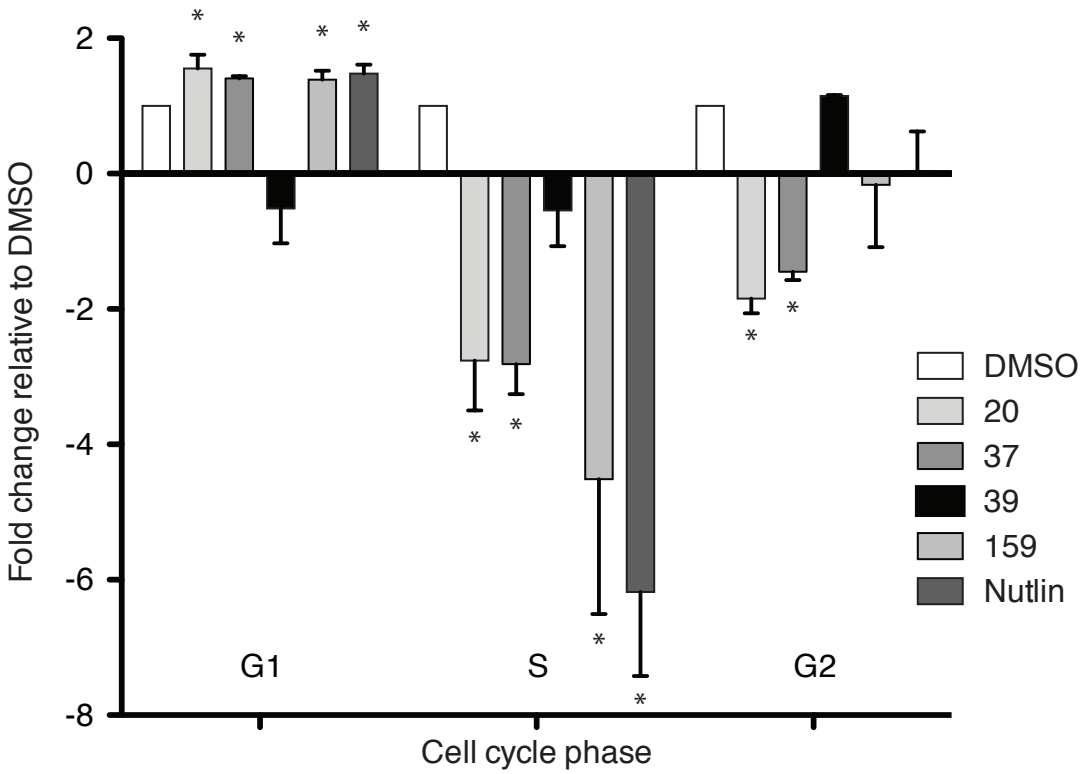

Figure 3-13: Active MPD compounds cause G1 cell cycle arrest.
RPE cells treated with DMSO, 5μM MPD39, 20, 37, 159 or 10μM Nutlin for 16h. Cells were harvested & PI stained for cell cycle analysis by FACS. The mean fold change, relative to DMSO, calculated from at least three independent experiments is shown. Error bars show SEM.

RPE cells were treated with MPD compounds (20, 37, 39 and 159), Nutlin or DMSO followed by cell cycle profile analysis. Figure 3-13 shows that active MPD compounds (20, 37 and 159) cause a G1 arrest similar to Nutlin incubation while MPD39 does not cause cell cycle arrest. The active compounds appear to be effective regardless of their predicted potency based on *in vitro* data. This could be because of differences in the cellular uptake, metabolism or efflux of these compounds. In contrast with Nutlin, some active MPD compounds (20 and 37) also cause a slight decrease in G2.

To investigate whether these cell cycle effects were p53 dependent isogenic matched p53+/+ and p53-/- colorectal cancer RKO cell lines were used to examine the effects of MPD compounds on the cell cycle profile (Figure 3-14).

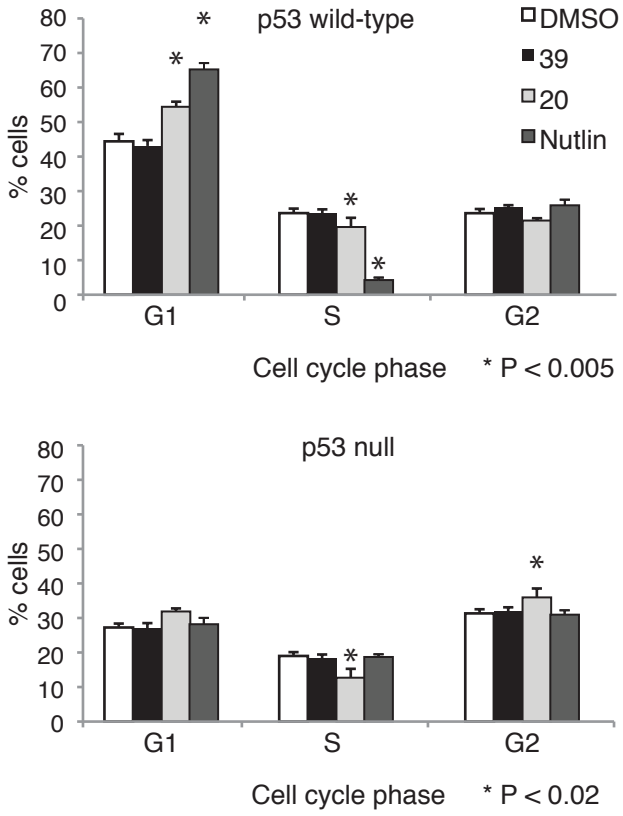

Figure 3-14: Active MPD compounds cause a p53 independent G2 cell cycle arrest. RKO cells either wild-type or null for p53 were treated with DMSO, 5μM of MPD 39 or 20 or 10μM Nutlin for 16h. Cells were harvested & PI stained for cell cycle analysis by FACS. 4 independent experiments were performed. Error bars show SEM.

As seen in RPE cells the active MPD compound 20 caused a G1 arrest in the p53+/+ cells. However on loss of p53, MPD20 causes a modest increase in cells in G2 which although statistically significant is unlikely to be biologically meaningful. Further investigation of the p53 dependence of the effects of MPD compounds demonstrated that the highly active MPD37 also had some p53 independent effects since when tested in the p53 RKO null cells, MPD37 caused significant apoptosis (Figure 3-15).

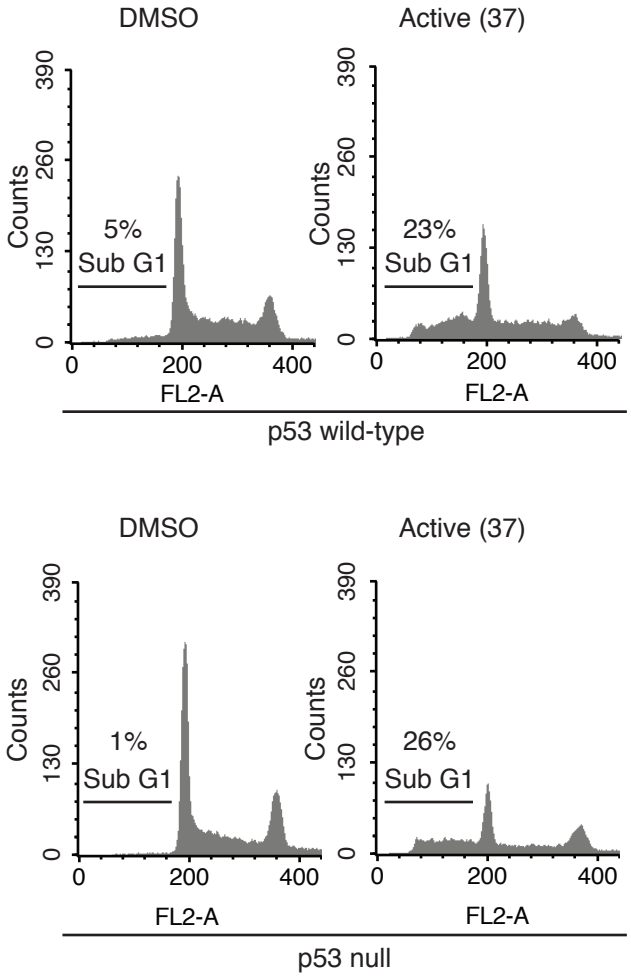

Figure 3-15: Highly active MPD compounds cause p53 independent apoptosis.
RKO cells either wild-type or null for p53 were treated with DMSO or 5μM of compound 37 for 16h. Cells were then harvested and PI stained for cell cycle analysis by FACS. Experiments were performed at least in triplicate. Representative histograms are shown. The % of FACS event with sub G1 DNA content is indicated.

3.5 Summary and discussion

In this chapter the biological and biochemical activities of the MPD compounds were analysed and their mode of action explored.

The results show that, like their parent compounds (HLI98), the active MPD compounds inhibit the ubiquitination of MDM2 and p53 *in vitro* and in cells. However, in comparison with the original HLI98 class of compounds many of these new compounds are more potent inhibitors of MDM2 and p53 ubiquitination (IC50 1.5-50μM versus 75μM). Direct evidence has been described to show that the MPD compounds bind directly to the MDM2 RING-tail and that they are specific for MDM2, being unable to inhibit E1 and E2-dependent and Cbl-mediated ubiquitination. This is the first description of direct binding and inhibition of MDM2

via the RING-tail domain. Importantly the resultant inhibition of MDM2's E3 ligase activity by the MPD compounds results in stabilisation and activation of p53.

In the present study a major challenge was presented by the availability, stability and poor solubility of the MPD compounds. For these reasons, following initial testing, a core set of compounds was selected for further evaluation. This set included a representative compound from each of the three groups: inactive, moderately active and highly active (as based on their IC50 in the mixed ubiquitination assay). This allowed discontinuation of use of compounds that required high levels of DMSO for suspension since high levels of DMSO are not compatible with cell line testing or evaluation by SPR. Furthermore, focus was given to those compounds less active *in vitro* but less detrimental to cell growth because it was more feasible to assess them in cellular assays. Initial analysis showed that all of the compounds that were highly active *in vitro* were toxic to cells, and so their testing was limited.

For cellular assays a dose of 10μM was selected as a reasonable dose level because the active compounds were able to stabilise p53 at this dose. Since *in vitro* experiments do not account for differences in compound uptake into cells and differing cellular metabolism or efflux it was difficult to extrapolate a suitable dose for cell line testing from *in vitro* data. In line with this the compounds most active *in vitro* did not necessarily retain this relative activity in cells.

Here the active MPD compounds were shown to inhibit ubiquitination of p53 resulting in stabilisation of p53 in cells. This increased p53 level caused increased expression of p53 targets and cell cycle arrest. It is generally accepted that the outcome of p53 activation depends on multiple factors including the level of p53, the dynamics of the increased p53, the modified state of p53 and the particular co-factors recruited[76, 82]. It has therefore been suggested that activating p53 by inhibiting MDM2's E3 ligase activity may not fully activate p53 for several reasons including the induction of an elevated MDM2 level, the lack of disruption to MDM2-p53 binding, the absence of a DNA damage signal and the differing post-translational modification profile.

In opposition to the suggestion that the increased MDM2 level induced by E3 ligase inhibitors could act in some way to inhibit p53 activation, mouse models with ligase inactive MDM2 display the ability for full p53 induction. By substituting a zinc-coordinating cysteine 462 (464 in humans) with alanine, a mutant *MDM2* that lacks E3 ligase activity but retains p53 binding capabilities was created. The mouse model expressing this MDM2-C462A mutant had elevated levels of both p53 and MDM2 and was embryonic lethal. The phenotype was rescued by deletion of p53 demonstrating that p53 was active despite accumulation of MDM2[324]. Drug induced inhibition of MDM2's E3 ligase function would be expected not to be as catastrophic as demonstrated in this mouse models since drugs will cause only reversible inhibition in the E3 ligase activity of MDM2 and are unlikely to provide inhibition equal to genetic abolition of MDM2's E3 ligase function.

Although it has been proposed that persistent p53-MDM2 binding following MDM2 E3 ligase inhibition may prevent maximal transcriptional activity of p53 there is evidence to the contrary. Bortezomib, a proteasome inhibitor in clinical use in treatment of multiple myeloma, activates p53 without disrupting p53-MDM2. On a physiological level p14ARF, L11, L5 and L23 all activate p53 without causing disruption of the p53-MDM2 interaction and shown here MPD compounds activate p53[276, 278, 559-561]. Previous data suggest that HLI98 does not affect p53-MDM2 binding[447]. It will therefore be interesting to study whether MPD compound mediated-p53 activation would be enhanced further following additional disruption of p53-MDM2 binding. This could be explored by examining the p53 activating capabilities of the MPD compounds in combination with Nutlin, which could act to disrupt p53-MDM2 binding and also inactivate the excess of MDM2 caused by E3 ligase inhibition.

Currently the vast majority of anti-cancer drugs work by causing irreparable DNA damage to cancer cells. It has been proposed that the lack of a DNA damage signal seen following treatment with MDM2 inhibiting, non-cytotoxic, drugs may result in inadequate p53 activation. In contrast however a mouse model where p53 status was reversibly switched showed adequate suppression of radiation-induced lymphoma despite abrogation of the acute radiation response by temporarily turning off p53[482]. Therefore acute DNA damage response is not

required for p53-mediated tumour suppression. Although from this model it can be concluded that the acute damage response is not necessary for tumour suppression it does not rule out a requirement for intact DNA damage signalling for tumour suppression. This has however been addressed by other mouse models where the DNA-damage dependent phosphorylation sites on p53 were mutated to alanines. The S18A[562, 563](equivalent to human S15A) and S23A[564, 565](equivalent to S20A) mice have only subtle defects in p53-induced apoptosis but maintained intact tumour suppressor function, supporting a model where at least some DNA damage induced post-translational modifications are not required for tumour suppression. The non-genotoxic activation of p53 achieved by inhibition of MDM2's E3 ligase activity should therefore lead to adequate tumour suppression.

In contrast with the modest effects demonstrated by mouse models with deficient phosphorylation of p53, recent work examining the importance of acetylation of p53 has shown that acetylation is required for cell cycle arrest, apoptosis and senescence. However, despite absence of all of these responses this acetylation deficient mouse also maintained tumour suppression capabilities[300, 304]. Importantly this emphasises the contribution of p53's regulation of metabolism and antioxidant function to tumour suppression. Acetylation sites seem to be common to both DNA damage and ARF-mediated pathways and since the MPD compounds function through a mechanism with similarity to ARF-mediated p53 induction, in that they cause p53 activation by binding to MDM2 and inhibiting its E3 ligase function without breaking the p53-MDM2 interaction, they may cause acetylation in a similar pattern[566, 567]. An important difference between MPD mediated p53 induction and ARF mediated induction is that MPD compounds and ARF bind at different locations on MDM2 (the RING-tail and acidic domain respectively). It would be of particular interest to examine whether the post-translational modifications seen, if any, following MPD treatment mirror those induced by ARF or if the binding in a different area of MDM2 causes a unique post-translational modification profile resulting in a different spectrum of p53 activity. Furthermore since p53's lysines are subject to several other types of modifications including methylation, NEDDylation and SUMOylation perhaps by inhibiting one modification (ubiquitination) you drive the other modifications and therefore again affect the spectrum of p53 activity[209]. Alternatively the modification

pattern of p53 could be altered via changes in MDM2 function caused by MPD-MDM2 RING-tail binding. Since MDM2 promotes ubiquitination, NEDD8 modifications and SUMO modifications of p53's lysines inhibiting ubiquitination could cause MDM2 itself to drive the other modifications of p53. In particular MDM2 driven SUMOylation of p53 is known to require intact p53-MDM2 binding but not be dependent on the MDM2 RING function[212]. It could be predicted therefore that the MPD compounds could drive SUMOylation of p53 with consequent impact on the transcriptional output of p53.

Work on the original HLI98 compounds showing that, in addition to being able to inhibit MDM2, they were able to inhibit *in vitro* autoubiquitination of the HECT E3, Nedd4, when used at high doses. This led to the hypothesis that the compounds may work by binding to E2, preventing transfer of ubiquitin from E1 to E2[447]. The present study has shown that the MPD compounds are unable to inhibit Cbl mediated ubiquitination in a reaction utilising the same E1 and E2 as used in the MDM2 ubiquitination assay. The site of action is therefore not on the E2 and is specific to MDM2.

Despite attempts to map the MDM2-E2 interaction site, poor solubility of the MDM2 RING under NMR conditions and weak E2-E3 interaction have made attempts unsuccessful[568]. It is therefore not possible to directly test for inhibition of MDM2-E2 binding although this remains a potential mechanism of action. Recent work by Dou *et al,* which may be relevant to many E3s, has shown an additional level of regulation of Cbl ubiquitination[556]. In the inactive state Cbl has an auto-inhibited conformation where the tail shields the E2 binding site on the Cbl RING. Upon activation, a phosphorylation event at the linker region, leads to a conformational change of Cbl where the E2 binding site is exposed and the E2 binding site and RING domain are moved closer to the substrate. In the study presented here the MDM2 RING-tail was used and therefore the MPD compounds may function through either the MDM2 RING or tail. If MDM2 autoubiquitination is similar to Cbl ubiquitination perhaps binding of the MPD compounds to the MDM2 RING-tail maintains an inhibited conformation that shields the E2 binding site and therefore inhibits ubiquitination. Alternatively MPD binding could block a phosphorylation event required for E3 ligase activation. To examine this further

the crystal structures of MDM2-MPD complex and MDM2-E2 complex would be helpful.

Another possible mechanism of function of the MPD compounds is to inhibit MDM2 homodimerisation or heterodimerisation with MDMX. The MDM2-MDMX heterodimer is thought to be a more abundant and potent E3 dimer therefore the MPD compounds could work by binding to the MDM2 RING and impeding heterodimerisation[264-269]. A recent publication by Wade *et al* demonstrated inhibition of MDM2's ubiquitin ligase activity by expression of an MDMX C-terminal tail point mutant F488A or an MDM2 C-terminal tail point mutant Y489A both of which are unable to form dimers[569]. Surprisingly this model of E3 ligase inhibition by inhibition of dimerisation seemed to not be adequate for full p53 activation and the authors suggested that inhibition of both MDMX and MDM2 together might be required for p53 activation. It would therefore be interesting to explore the effect the MPD compounds have on dimerisation of MDM2 and MDMX. This could be investigated by immunoprecipitation experiments firstly with overexpressed proteins where MDM2 C464A could be used as a control to show reduced MDM2/MDMX binding and then with endogenous MDM2 and MDMX. Furthermore it would be interesting to examine whether the MPD compounds are capable of binding to MDMX since as suggested by Wade *et al* dual inhibition of MDM2 and MDMX may be an attractive strategy for p53 activation and due to the structural homology between the 2 proteins it may be anticipated that compounds binding the MDM2 RING-tail could also bind MDMX RING-tail.

Small molecules that prevent the MDM2/MDMX interaction would also inhibit the MDM2 mediated degradation of MDMX, which contributes to full activation of p53 and this could perhaps explain the findings of Wade *et al*[360, 361, 366]. In contrast, cell line studies have shown that the high level of MDM2 seen following Nutlin treatment can actually enhance Nutlin induced cell death due to an increase in MDM2 mediated degradation of MDMX[570]. The MDM2 present after Nutlin treatment is Nutlin-bound but maintains E3 ligase activity and therefore is capable of mediating MDMX degradation. This is in contrast with the abundance of E3 ligase dead MDM2 induced by MPD treatment. A full analysis of the stability of MDMX following MPD treatment may be informative.

This work provides proof of the principle that compounds that bind the MDM2 RING-tail can inhibit MDM2's E3 ligase activity. Ultimately solving a co-crystal structure of the compounds bound to the MDM2 RING-tail would provide the information required to design other MDM2 inhibitors, which bind the MDM2 RING-tail and display more desirable chemical characteristics and improved potency. In addition the co-crystal structure would allow informed predictions to be made regarding likelihood of influence on dimerisation and potential to also bind the similarly structured MDMX RING-tail.

4 HLI373

4.1 History of HLI373

HLI373 was first described by Kitagaki *et al* in 2008[451]. Following identification of the 7-nitro-5-deazaflavins (HLI98 compounds) described in chapter 3, which displayed poor solubility and potency[447], a chemical database was searched for soluble compounds with a structure bearing some similarity to HLI98. From this HLI373 (5-[3-(dimethylamino)propylamino]-3,10-dimethylpyrimido[4,5-b]quinoline-2,4-dione) was identified (Figure 4-1). This compound was reported to be soluble and stabilise p53 and MDM2 in cells.

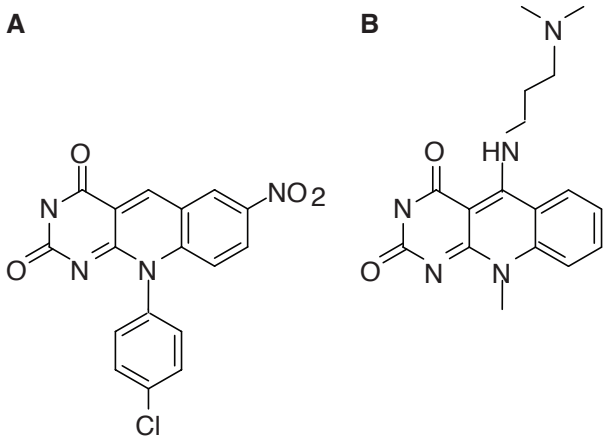

Figure 4-1: The structure of HLI373 in comparison with HLI98.
(A) HLI98 (B) HLI373

The previous report showed that treatment of cells with 1μM HLI373 inhibited ubiquitination of p53 and MDM2, increased p53 transcriptional activity and had a p53 dependent mode of action. Further mechanistic details were not provided, apart from an *in vitro* MDM2 autoubiquitination assay using 32 P-labeled ubiquitin, where HLI373 was shown to inhibit ubiquitination at a dose of 3μM.

In collaboration with Professor Allan Weissman from The National Cancer Institute, Maryland, USA, the *in vivo* activity and mode of action of HLI373 was further analysed.

4.2 HLI373 stabilises and activates p53 in cells

To confirm HLI373 induced activation of p53's transcriptional activity, a wild-type p53 expressing osteosarcoma cell line (U2OS) stably expressing PG13-luciferase, a p53 reporter with a firefly luciferase gene under the control of 13 p53 consensus

response elements[548], was treated with vehicle or a dose titration of HLI373 for 16 hours. From 1μM a significant increase in luciferase signal was seen indicating activation of the response elements (Figure 4-2).

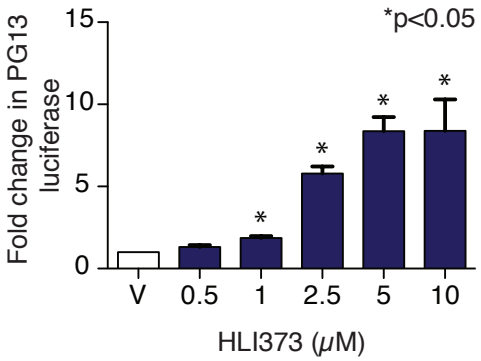

Figure 4-2: HLI373 increases transcriptional activity of p53.
U2OS cells stably expressing a PG13 luciferase reporter were treated for 16 hours with vehicle (V) or the indicated doses of HLI373. After addition of luciferin substrate, luciferase activity was determined using a luminometer. Error bars represent SEM of 6 replicates.

A further p53 target, Macrophage Inhibitory Cytokine-1 (MIC-1), was assessed using quantitative real time-PCR (qRT-PCR). As discussed more fully in chapter 6, MIC-1 is dramatically induced by p53 activation[571] and as such may be a potentially useful marker of efficacy of p53 activating therapies[544]. p53 wild-type expressing colorectal cancer cell line, HCT116 was treated with vehicle, HLI373 or Nutlin (the non-genotoxic p53 activating agent). Quantitative RT-PCR detection showed that HLI373 induced transcription of MIC-1 mRNA to a similar magnitude as achieved by Nutlin treatment in HCT116 cells (Figure 4-3).

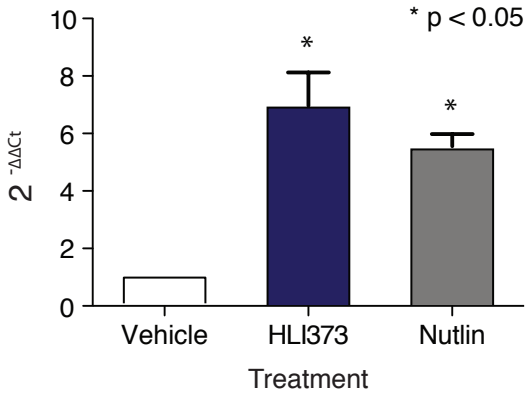

Figure 4-3: HLI373 increases MIC-1 mRNA expression.
HCT116 cells were treated with vehicle (V), HLI373 (H) 5μM or Nutlin (N) 10μM for 22 h. MIC-1 mRNA levels measured by qRT-PCR. Expression is quantified relative to control genes according to the comparative $\Delta\Delta C_t$ method. Values from three independent experiments are displayed as mean of $2^{-\Delta\Delta Ct}$. Student's two-tailed T-test indicated a significant change for H and N compared to V. Error bars represent SEM.*p<0.05.

To confirm that HLI373 stabilises and activates p53, retinal pigment epithelial cells (RPE) were treated with vehicle or a dose titration of HLI373 for 16 hours. In agreement with Kitagaki *et al*, HLI373 stabilised p53 and caused increased expression of p53 targets p21 and MDM2, although this effect required a slightly higher dose than previously published (2.5μM versus 1μM). Furthermore when tested in the wild-type p53 expressing, ovarian cancer cell line, A2780, HLI373 similarly stabilised p53 and increased expression of p53 targets (Figure 4-4 A & B).

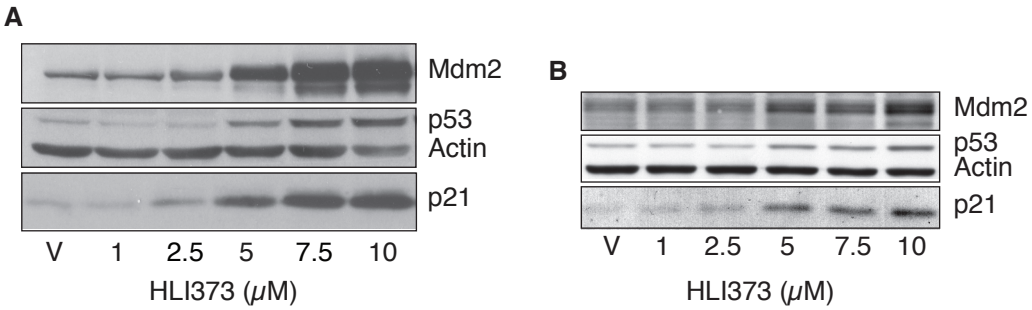

Figure 4-4: HLI373 stabilises p53 & increases expression of p53 targets.
(A) RPE cells or (B) A2780 cells were treated for 16 hours with vehicle or concentrations of HLI373 as indicated. Expression of p53, p21, MDM2 and Actin (loading control) determined by immunoblot analysis.

To establish the dynamics of this increase in p53 and its targets, RPE cells were treated with 5μM of HLI373 over a time course from 1 hour to just over 7 hours. HLI373 stabilised p53 after only 1 hour of treatment while MDM2 expression increased at 4 hours consistent with at least some of the increase in MDM2 expression being due to an increase in p53's transcriptional activity (Figure 4-5).

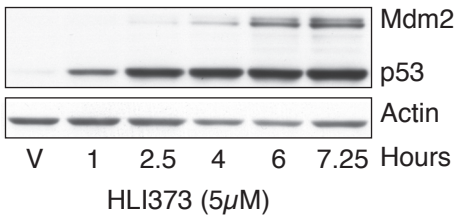

Figure 4-5: HLI373 stabilises p53 after 1 hour of treatment.
RPE cells were treated with 5μM of HLI373 for indicated time. Expression of p53, MDM2 and Actin (loading control) determined by immunoblot analysis.

To confirm that the increase in p21 seen following HLI373 treatment resulted in a cell cycle arrest, RPE cells were treated with vehicle, HLI373 or Nutlin for 24 hours. As seen following treatment with Nutlin, HLI373 treatment caused a cell cycle arrest in G1 with a concomitant loss of cells in S-phase (Figure 4-6). No sub-

G1 population of cells was seen, suggesting that the activation of p53 does not lead to apoptosis in this untransformed cell line.

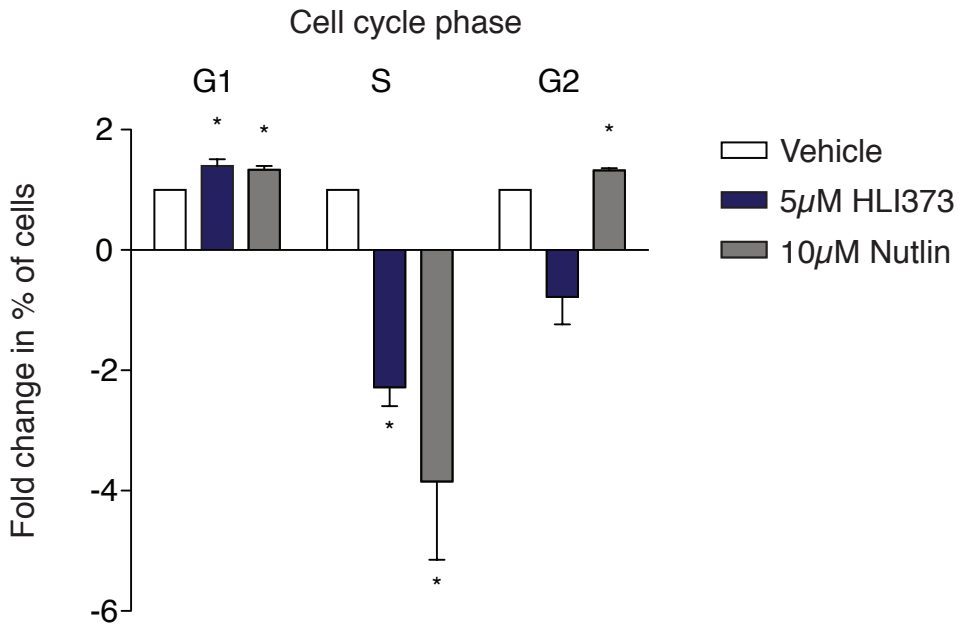

Figure 4-6: HLI373 causes cell cycle arrest as measured by FACS analysis.
RPE cells were treated with vehicle, 5μM HLI373 or 10μM Nutlin for 24 h. Cells were harvested, PI stained & analysed by FACS. The percentage of cells in G1, S and G2-phase was determined and displayed as fold changes versus vehicle treated cells. Experiments were performed in triplicate, means & SEM are plotted. * p<0.05 using an unpaired, two-tailed T-test.

To determine whether the effects of HLI373 are dependent on p53, isogenic HCT116 p53 wild-type and HCT116 p53 null cells were treated with vehicle, HLI373 or Nutlin as a positive control, and the cell cycle profile was quantified by flow cytometry. In this case, HLI373 treatment caused cell death (as measured by an accumulation of cells with a subG1 DNA content) in p53 expressing, but not p53 null cells (Figure 4-7A).

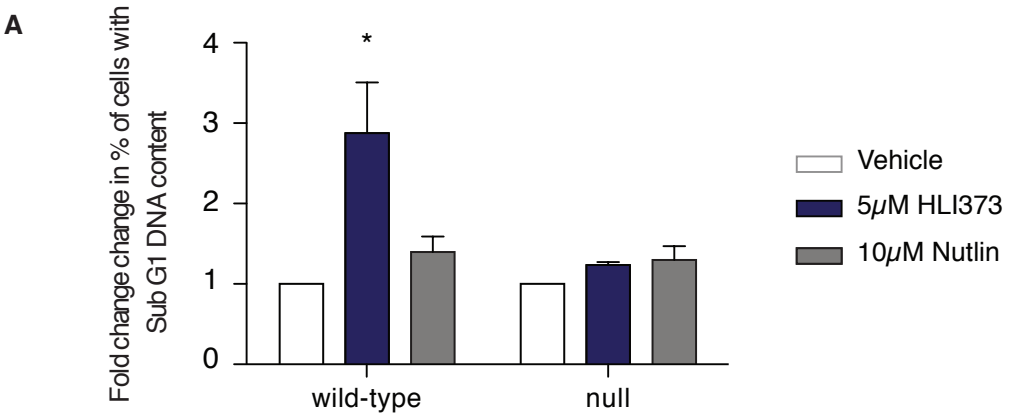

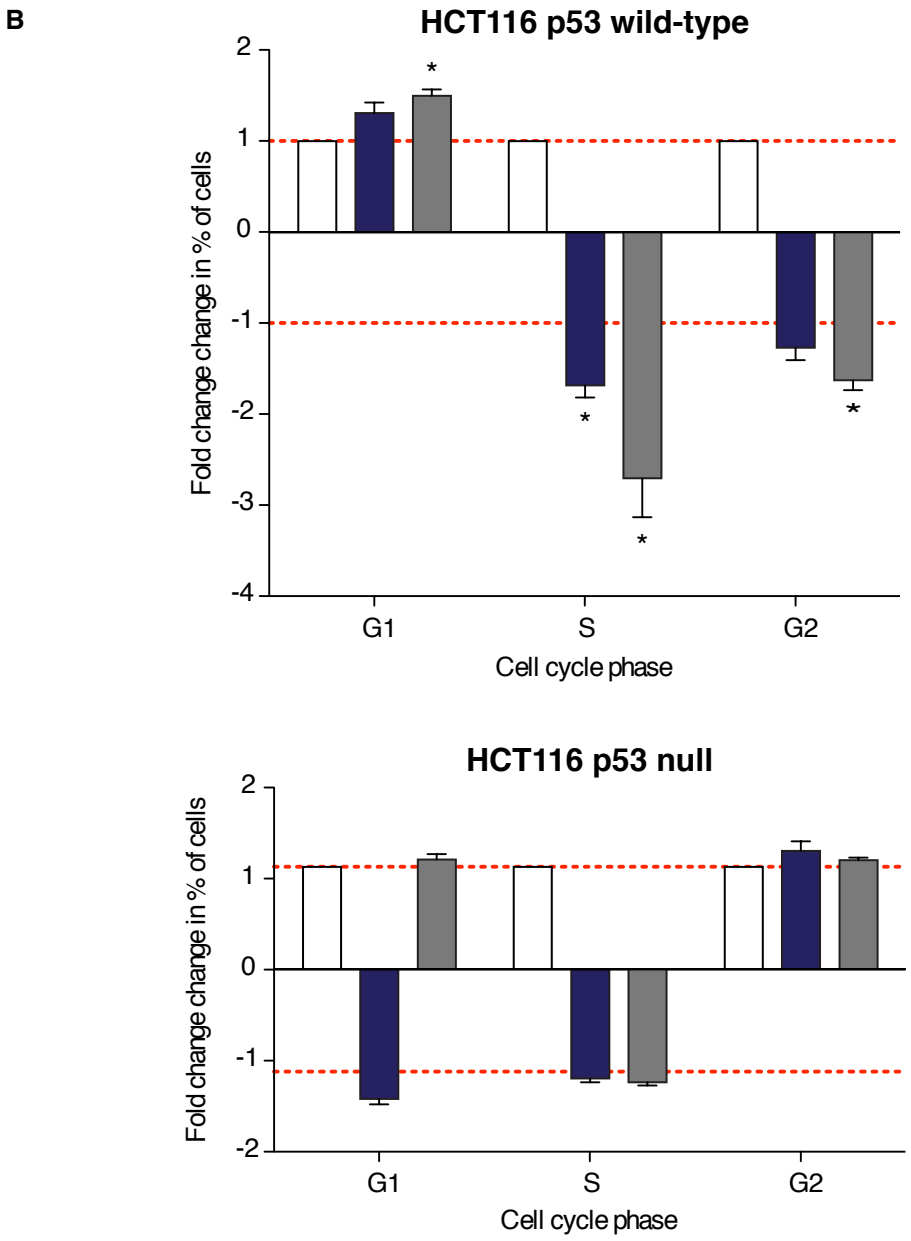

Figure 4-7: HLI373 causes a p53 dependent S phase reduction and sub G1 increase. HCT116 p53 wild-type or null were treated for 16 hours with indicated treatment then after PI staining cell cycle profile was analysed by FACS. The cell number in each cell cycle phase was determined using cell quest software. Experiments were performed in triplicate. Fold change in percentage of cells in each cell cycle phase was calculated for each experiment and vehicle treated cells were set to 1 in each cell cycle phase. Averages values are plotted with SEM. * p<0.05 as calculated by T-test.

HLI373 also caused a significant and p53 dependent decrease in S-phase (Figure 4-7B). By contrast, Nutlin caused a p53-dependent G1 cell cycle arrest in HCT116 cells without a significant induction of apoptosis.

In conclusion, both HLI373 and Nutlin caused p53 dependent responses. In untransformed cells (RPE), both drugs led to a p53-dependent cell cycle arrest. In HCT116 cells (a tumour cell line) the responses were different, with Nutlin inducing

a cell cycle arrest and HLI373 promoting p53-dependent apoptosis. Previous studies have shown that the presence of additional oncogenic insults or DNA damaging signals (E2F-1, Ras, 53BP1) in cancer cells can sensitise cells to cell death following MDM2 inhibition treatment[572-574]. While Nutlin treatment does not provoke this response, HLI373 can induce cell death in the cancer cell lines tested.

4.3 HLI373 inhibits p53 ubiquitination in cells

HLI373 causes an increase in expression of MDM2 (Figure 4-4) and on the basis of previous data suggesting HLI373 stabilises MDM2 via its inhibition of E3 ligase function it was assumed that this increase in expression represented both an increase in p53's transcriptional activity to contribute to enhanced MDM2 transcription and an increase in MDM2 stability. There are several hundred RING E3 ligases, many of which function as dimers like MDM2. To test whether HLI373 is specific for inhibition of MDM2's E3 ligase activity, or capable of inhibiting other E3 RING ubiquitin ligases, the effect of HLI373 on the stability of two related E3 ubiquitin ligases, XIAP and Ring1b, was examined[575, 576]. HLI373, at doses sufficient to stabilise p53 and increase expression of MDM2, was unable to stabilise RING E3 ligases XIAP or Ring1b (Figure 4-8A). There was also no clear effect on the expression levels of a HECT domain E3 ligase, NEDD4 (Figure 4-8B).

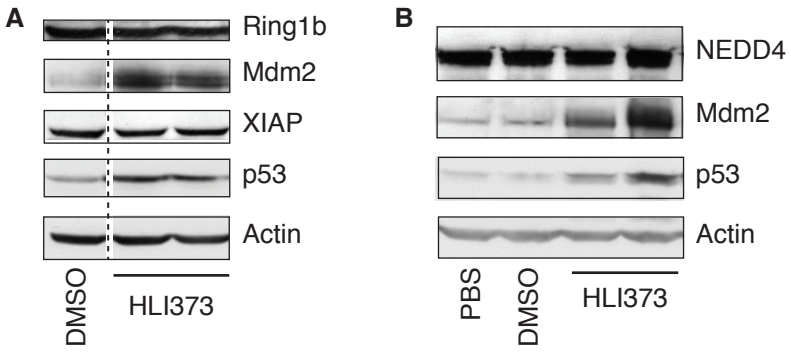

Figure 4-8: HLI373 does not inhibit XIAP or Ring 1b degradation.
(A) U2OS cells were treated with DMSO or two dose levels of HLI373, 2.5μM and 5μM. Lysates were run on Western and blotted for Ring1b, MDM2, XIAP, p53 and Actin (loading control). (B) U2OS cells were treated with PBS, DMSO or two dose levels of HLI373, 2.5μM and 5μM. Lysates were run on Western and blotted for NEDD4, MDM2, p53 and Actin (loading control).

To confirm that HLI373 is a direct inhibitor of MDM2's E3 ligase activity its ability to inhibit MDM2 autoubiquitination was assessed in an *in vitro* ubiquitination assay. However, even high doses of HLI373 were not able to inhibit the *in vitro* MDM2 autoubiquitination reaction (Figure 4-9).

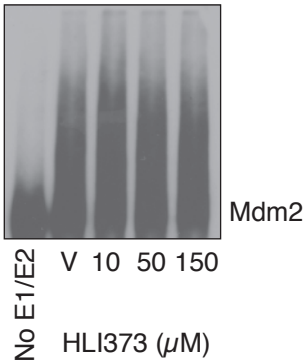

Figure 4-9: HLI373 does not inhibit MDM2 autoubiquitination.
Bacterially expressed full-length MDM2, E1, E2 and reaction buffer (including $MgCl_2$ and adenosine triphosphate (ATP)) were incubated with vehicle (V) or a dose titration of HLI373. MDM2 was detected by Western blotting using AB1 and AB2 antibodies.

To further investigate the mechanism of HLI373's reported ability to inhibit p53 ubiquitination, *in vitro* p53 ubiquitination assays were carried out. Both full-length MDM2 and the MDM2 RING promoted efficient ubiquitination of p53 (although the full-length MDM2 functioned more efficiently to polyubiquitinate p53), an activity that was dependent on the presence of E1 and E2. Surprisingly, HLI373 failed to inhibit ubiquitination by the MDM2 RING and only weakly impeded full-length MDM2 driven ubiquitination at very high doses (Figure 4-10).

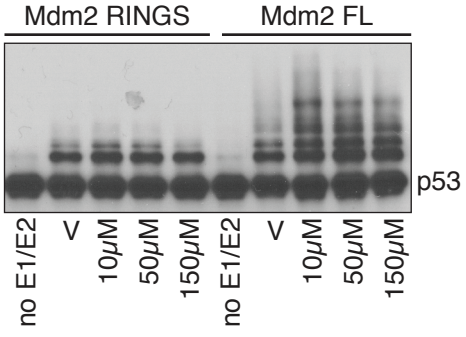

Figure 4-10: HLI373 does not inhibit the *in vitro* ubiquitination of p53.
Bacterially expressed MDM2 RING or full-length MDM2, His-p53, E1, E2 and reaction buffer (including $MgCl_2$ and adenosine triphosphate (ATP)) were incubated with vehicle (V) or a dose titration of HLI373. The reaction was incubated at 37ºC shaking at 1200 rpm for 1 h. p53 was detected by Western blotting using DO1 antibody.

This is in contrast with previous work by Kitagaki *et al* showing inhibition of p53 ubiquitination at doses of 3μM in an alternative assay.

Previous studies had identified HLI373 on the basis of its structural relationship to the HLI98 compounds, although this similarity was not profound. However, HLI373 clearly induced a p53-dependent response in cells, so I sought to confirm the reported activity of HLI373 in the inhibition of ubiquitination of p53 in cells. Non-small cell lung cancer, p53 null H1299 cells, overexpressing p53, GFP, MDM2 or MDM2-C464A (an E3 ligase deficient mutant) were treated with proteasome inhibitor MG132 to allow accumulation of ubiquitinated p53, and Nutlin or HLI373. Wild-type MDM2, but not MDM2-C464A promoted the ubiquitination of p53 that was inhibited by Nutlin. In agreement with Kitagaki *et al*, HLI373 also inhibited ubiquitination of p53 from 1μM (Figure 4-11).

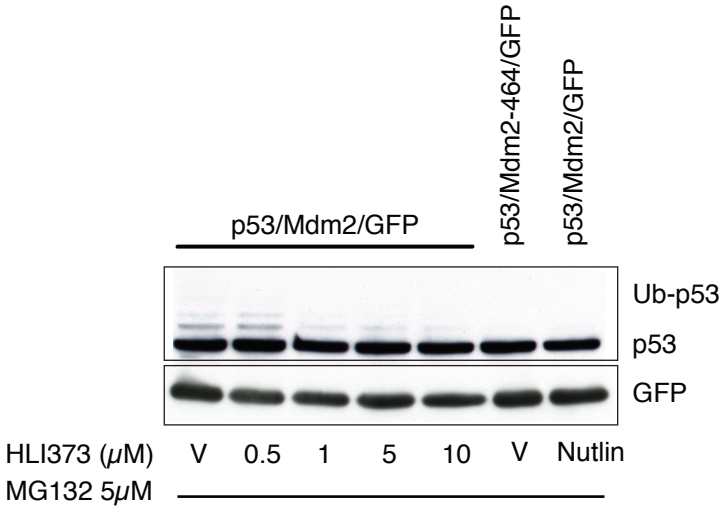

Figure 4-11: HLI373 inhibits ubiquitination of p53 in cells.
H1299 cells transfected with p53, MDM2 or MDM2-C464A and GFP were treated with MG132 and vehicle, HLI373 or Nutlin (10μM) for 5 hours. Lysates were run on Western and blotted for p53 and GFP.

These results show that although HLI373 inhibited ubiquitination of p53 and stabilised and activated p53 in cells, this was not the result of the direct inhibition of MDM2's E3 activity.

4.4 HLI373 does not cause DNA damage or disrupt p53-MDM2 binding

The results so far indicated that HLI373 was not able to inhibit MDM2's E3 ligase activity. However, HLI373 was found to inhibit ubiquitination of p53 in cells, activating p53's transcriptional programme and resulting in cell cycle arrest and apoptosis. These results suggested that the effect of HLI373 on p53 might be

indirect, so further studies were carried out to identify the mechanism of function of HLI373.

p53 can be activated via at least three distinct pathways; the DNA damage pathway, the oncogene activation pathway or the ribosomal stress pathway. To test whether HLI373 functions through the induction of DNA damage, RPE cells were treated with vehicle, HLI373 at 5μM or a DNA damaging dose of act D. The presence of γH2AX foci, which can be induced by double-strand DNA breaks, replication stalling or single stranded breaks, was detected by immunofluorescence[577-580]. After treatment with 5μM of HLI373, a dose capable of p53 induction, there was no evidence of γH2AX foci (Figure 4-12). However following high dose act D treatment multiple γH2AX foci were seen in each cell since act D treatment at high dose causes DNA damage. Thus, HLI373 does not appear to enhance p53 expression by inducing DNA breaks.

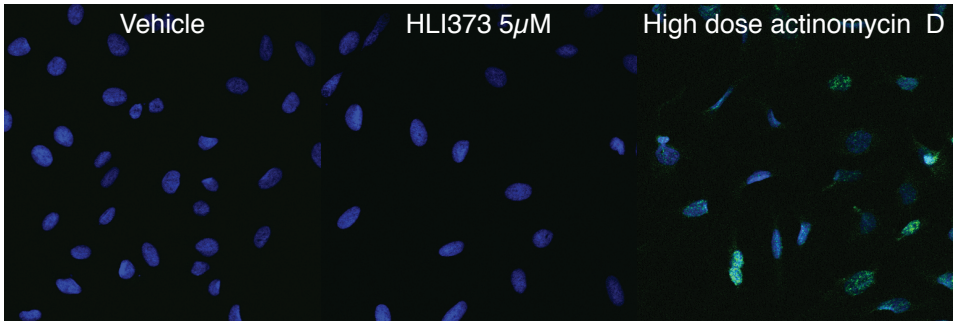

Figure 4-12: HLI373 does not cause formation of γH2AX foci.
RPE cells were plated then treated for 20 hours with vehicle, 5μM HLI373 or 500nM act D. Cells were then fixed, permeabilised, blocked and stained with anti-γH2AX antibody (green). DAPI (blue) indicates the nuclei.

In response to a multitude of stresses including replication stress, stalled replication forks, hypoxia, DNA strand breaks and glucose starvation p53 is phosphorylated on serine 15 by activation of kinases ATR, DNA-PK, ATM and AMPK [110, 290, 581-583]. This phosphorylation serves to disrupt the binding of p53 and MDM2, thereby allowing p53 to accumulate and become active. HLI373's ability to induce phosphorylation of p53 on serine 15 was tested[284]. U2OS cells were treated with vehicle, a dose titration of HLI373 or Nutlin, the non-genotoxic p53 stabiliser. HLI373 stabilised p53 and increased expression of p21 from 2μM. However, despite the increase in overall p53 levels, there was no increase in the detection of p53 phosphorylation on serine 15, which remained at levels very

similar to those seen in untreated or Nutlin treated cells (Figure 4-13). HLI373 therefore does not induce strong phosphorylation of serine 15 in p53.

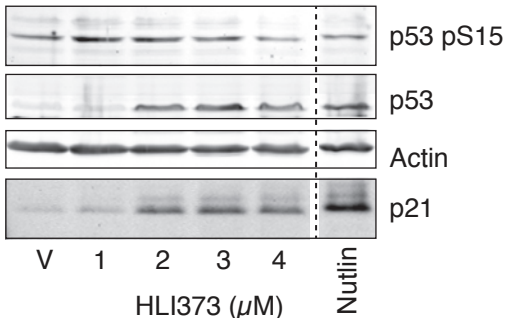

Figure 4-13: HLI373 does not cause phosphorylation of p53 serine 15.
U2OS cells treated with vehicle (V), a dose titration of HLI373 or Nutlin 10μM for 22h. Lysates were run on Western and blotted for p53, pS15 p53, p21 and Actin (control).

HLI373 displays a similar effect on p53 activity in cells as Nutlin. Furthermore Nutlin also does not inhibit MDM2 in an in vitro p53 ubiquitination assay, since Nutlin binds to the N-terminus of MDM2 in a region that is not required for E3 activity (which is carried out by the RING)[319]. This similarity led me to consider whether HLI373 could inhibit p53-MDM2 binding. To test this, the effect of HLI373 and Nutlin on the p53-MDM2 interaction was tested in cells. This interaction could be detected in control conditions, and was clearly reduced by Nutlin (Figure 4-14). However, HLI373 treatment led to only a small reduction in the immunoprecipitation of MDM2 with p53, but this correlated with slightly lower levels of MDM2 input. Lane 4, where no p53 was transfected demonstrated that the immunoprecipitation was specific for pull down of p53 (Figure 4-14). Taken together, there is no evidence that HLI373 interferes with the ability of MDM2 to bind p53.

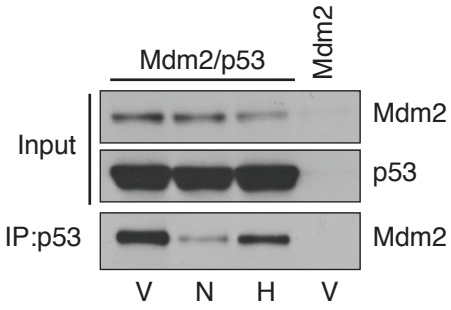

Figure 4-14: HLI373 does not disrupt p53-MDM2 binding.
U2OS cells were transfected with MDM2 and p53 or empty vector. Cells were treated with vehicle (V), Nutlin (N, 10μM) or HLI373 (H, 5μM). Cells were lysed and 5% taken for input. p53 was immunoprecipitated using DO1 antibody. Input and IP samples were

run on Western and blotted for p53 and MDM2.

4.5 HLI373 causes ribosomal stress

As detailed in chapter 1 p53 can also be activated via pathways that do not require disruption of p53-MDM2 binding. Oncogene activation causes ARF to bind to MDM2 and inhibit MDM2-mediated p53 ubiquitination without breaking the interaction between p53 and MDM2. Similarly ribosomal stress causes ribosomal proteins to bind MDM2 inhibiting it without preventing the p53-MDM2 interaction[276, 278, 279, 559, 561, 584-587]. Since HLI373 is capable of stabilising p53 in U2OS cells, which have lost ARF[588], it is unlikely that HLI373 works via ARF. HLI373's ability to cause ribosomal stress was therefore investigated.

U2OS cells were treated for 20 hours with vehicle, HLI373 or low doses of act D, which causes ribosomal stress and perturbs ribosome biogenesis by inhibiting RNA polymerase I (as discussed further in chapter 5)[469, 589]. This is in contrast with act D's use at high doses where it inhibits RNA polymerase II[590, 591]. After drug treatment cells were fixed and nucleolar protein nucleophosmin/B23 was detected by immunofluorescence. Both act D, and HLI373 - used at a dose sufficient to activate p53 - caused loss of nucleolar integrity as determined by translocation of nucleophosmin staining from the nucleoli to the nucleoplasm[592] (Figure 4-15).

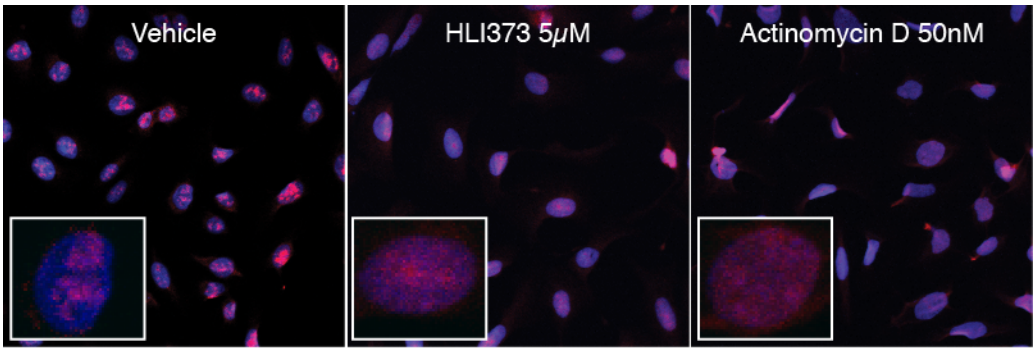

Figure 4-15: HLI373 causes translocation of nucleophosmin.
Equal numbers of U2OS cells were plated & treated with vehicle, HLI373 5μM or act D 50nM for 12 hours. Cells were fixed & permeablised then probed with anti-B23 antibody (red). DAPI indicated the nuclei (blue). A higher magnification of a single cell image is shown in the white box.

To establish further evidence that the activation of p53 seen following HLI373 treatment is via the ribosomal stress pathway, ribosomal protein binding to MDM2 was investigated. U2OS cells were treated with vehicle, HLI373 or act D for 16

hours, after which ribosomal protein L11 was immunoprecipitated and MDM2 binding assessed. Like act D, HLI373 appears to enhance MDM2-L11 binding (Figure 4-16). This is consistent with HLI373 inducing ribosomal stress dependent MDM2 inhibition.

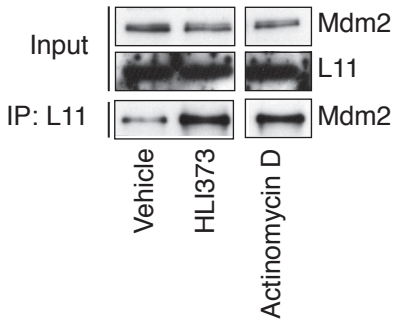

Figure 4-16: HLI373 enhances MDM2-L11 binding.
U2OS cells were treated with vehicle, HLI373 5μM or act D 5nM for 16h. Cells were treated with MG132 for 4h pre-harvest. Cells were lysed and 5% taken for input. L11 was immunoprecipitated. Input & IP samples were run on Western & blotted for L11 & MDM2. Act D was run on the same blot but irrelevant bands have been removed.

As ribosomal stress is caused by perturbations in the biogenesis of ribosomes, the effect of HLI373 treatment on production of ribosomal RNA was explored. U2OS cells were treated with vehicle, HLI373 or act D. Pre-RNA was harvested and after reverse transcription, 45S pre-rRNA and the control genes, ribosomal protein large P0 (RPLP0) and beta-2-microglobulin (B2MG), were measured by qRT-PCR. HLI373 clearly reduced transcription of 45S pre-rRNA relative to the control genes consistent with HLI373 having effects similar to act D on ribosomal biogenesis (Figure 4-17).

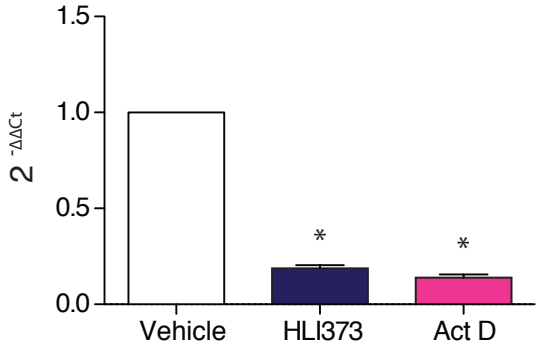

Figure 4-17: HLI373 reduced 45S pre-ribosomal RNA expression.
45S Pre-rRNA expression determined by qRT-PCR in cells treated with 5μM HLI373 or act D (Act D) 5nM as compared to vehicle alone. Expression is quantified relative to control genes according to the comparative $\Delta\Delta C_t$ method. Values from three independent experiments are displayed as mean of $2^{-\Delta\Delta Ct}$. Student's two-tailed T-test for all comparisons indicated a significant change for both HLI373 and act D compared to vehicle treated cells (*). Error bars represent SEM.

Like act D, HLI373 appears to activate p53 via the ribosomal stress pathway by interfering with ribosome biogenesis. As both HLI373 and act D are able to activate p53 while retaining p53-MDM2 binding the role of p53-MDM2 binding in inhibition of 45S pre-rRNA was investigated by examining the effect of Nutlin treatment on 45S pre-rRNA expression following HLI373 and act D treatment. Since Nutlin would interfere with p53-MDM2 binding, it would be expected to prevent an HLI373 induced reduction in 45S pre-rRNA, if p53-MDM2 binding is required for this effect. Indeed, there was significant although modest rescue of the inhibition of 45S pre-rRNA expression by HLI373 treatment by the addition of Nutlin, consistent with a role for the p53-MDM2 interaction in this response. However, Nutlin treatment failed to rescue the act D induced decrease in 45S pre-rRNA production (Figure 4-18), suggesting that this was achieved through a different mechanism. Importantly, Nutlin treatment alone did not affect 45S pre-rRNA expression.

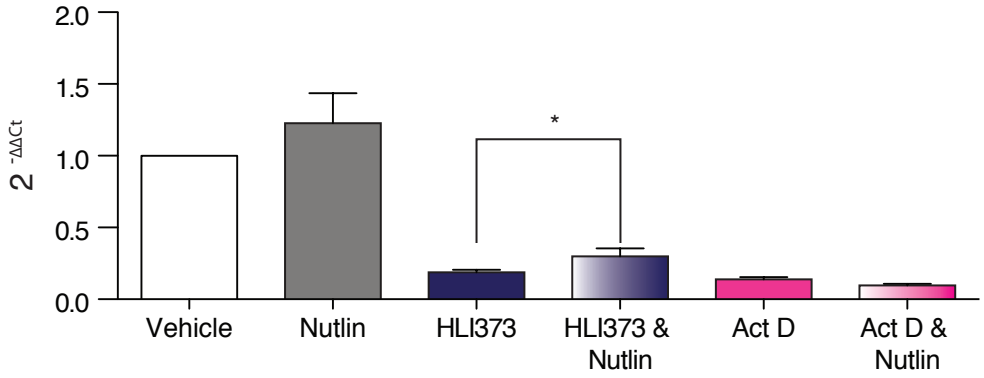

Figure 4-18: Intact p53-MDM2 binding contributes to HLI373 induced reduction in 45S pre-mRNA.
45S Pre-rRNA expression determined by qRT-PCR in cells treated with Nutlin 10μM, 5μM HLI373, Nutlin 10μM, act D 5nM, HLI373 & Nutlin or act D & Nutlin as compared to vehicle alone. Expression is quantified relative to control genes according to the comparative $\Delta\Delta C_t$ method. Values from three independent experiments are displayed as mean of $2^{-\Delta\Delta Ct}$. Error bars represent SEM.*p=0.0082 using Student's two-tailed T-test compared to HLI373 treatment alone.

HLI373 interferes with ribosomal biogenesis causing ribosomal stress and p53 activation via a mechanism that at least partly dependent on p53-MDM2 binding.

4.6 HLI373 reduces MDMX expression

It has previously been shown that MDMX modulates p53's response to ribosomal stress. Gilkes *et al* proposed that the decrease in MDMX seen following ribosomal stress is due to an increase in MDM2 dependent degradation of MDMX[280]. The

MDMX levels following HLI373 treatment were therefore examined in U2OS cells. HLI373 clearly reduced the level of MDMX at doses where it stabilised p53 and increased levels of MDM2, By contrast, Nutlin had no effect on MDMX levels (Figure 4-19A). Furthermore, the HLI373 induced reduction in MDMX expression after 4 hours of HLI373 treatment was concomitant with the increase in MDM2 levels. MDMX was no longer detectable after 8 hours of treatment (Figure 4-19B).

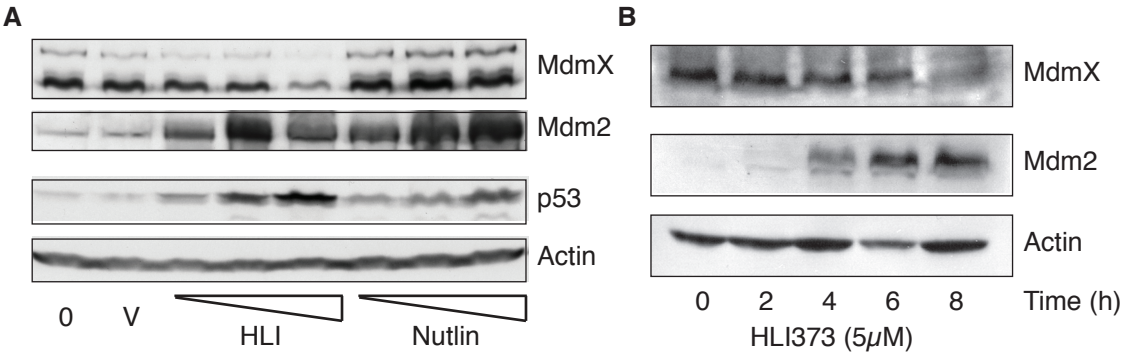

Figure 4-19: HLI373 causes a reduction in MDMX expression.
(A) U2OS cells were treated with vehicle, HLI373 (2.5μM, 5μM, 10μM) or Nutlin (2.5μM, 5μM, 10μM) for 16 hours. Expression of MDMX, MDM2, p53 and Actin (loading control) was detected by immunoblot analysis. (B) RPE cells were treated with 5μM of HLI373 for varying times as indicated. Expression of MDMX, MDM2 and Actin (loading control) was detected by immunoblot analysis.

To examine whether the reduction in MDMX is due to increased degradation of the protein, cells were treated with HLI373 and MG132 to inhibit the proteasome, to rescue the MDMX expression levels. MG132 treatment resulted in the stabilisation of p53, indicating that proteasomal inhibition has been successfully achieved. However, MG132 treatment was unable to restore MDMX levels after HLI373 treatment (Figure 4-20).

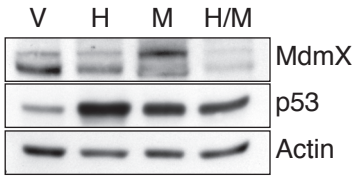

Figure 4-20: MG132 treatment does not rescue HLI373 induced MDMX reduction.
HCT116 cells were treated as indicated. Expression of MDMX, p53 & Actin (loading control) was detected by immunoblot analysis. V=Vehicle, H=HL1373, M=MG132.

To further confirm that HLI373 treatment does not cause MDMX degradation, U2OS cells were transfected with MDM2 and GFP-MDMX then treated with HLI373. Consistent with the HLI373 induced reduction in MDMX expression not

being due to an increase in degradation of MDMX via the proteasome, HLI373 was not able to reduce the level of MDMX when driven by an exogenous promoter (Figure 4-21).

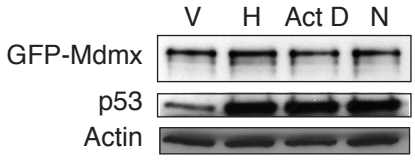

Figure 4-21: MDMX expressed from an alternative promoter is not reduced by HLI373. U2OS cells were transfected with MDM2 and GFP-MDMX. 24 hours later cells were treated with vehicle (V), HLI373 (H,5μM) or Nutlin (N,10μM) for 16 hours. Expression of MDMX, p53 and Actin (loading control) was detected by immunoblot analysis.

Since HLI373 does not affect MDMX protein stability, other mechanisms to regulate expression were examined. The extent of protein expression reflects a series of regulatory steps that include transcription, the modification of the primary transcript to become mature messenger RNA, and translation (Figure 4-22). As such some of these steps were explored to establish at which point HLI373 influences MDMX expression.

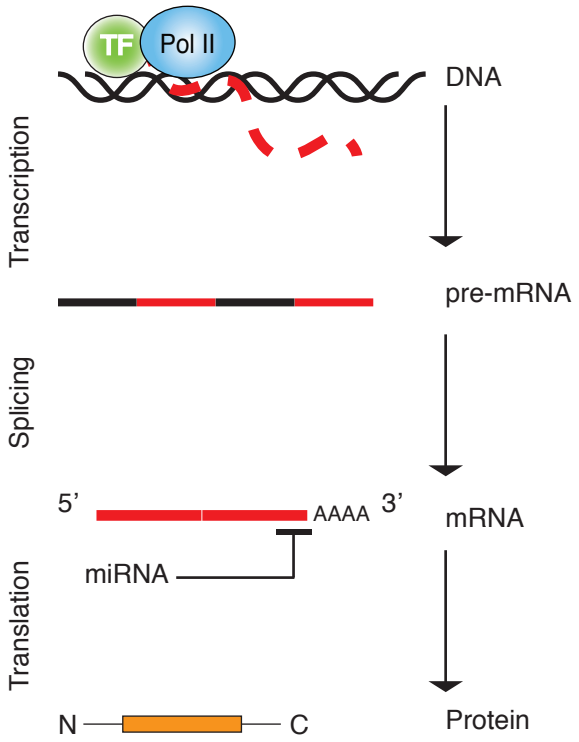

Figure 4-22: RNA processing.
TF=transcription factor.

Firstly, MDMX mRNA was examined to explore whether the reduction in MDMX protein seen following HLI373 treatment could be the reflection of a decrease in

transcription. MDMX mRNA levels were measured following vehicle, HLI373 or Nutlin treatment of RPE, HCT116 and U2OS cells. A significant reduction in MDMX mRNA expression was seen following HLI373 treatment of each cell line tested (Figure 4-23).

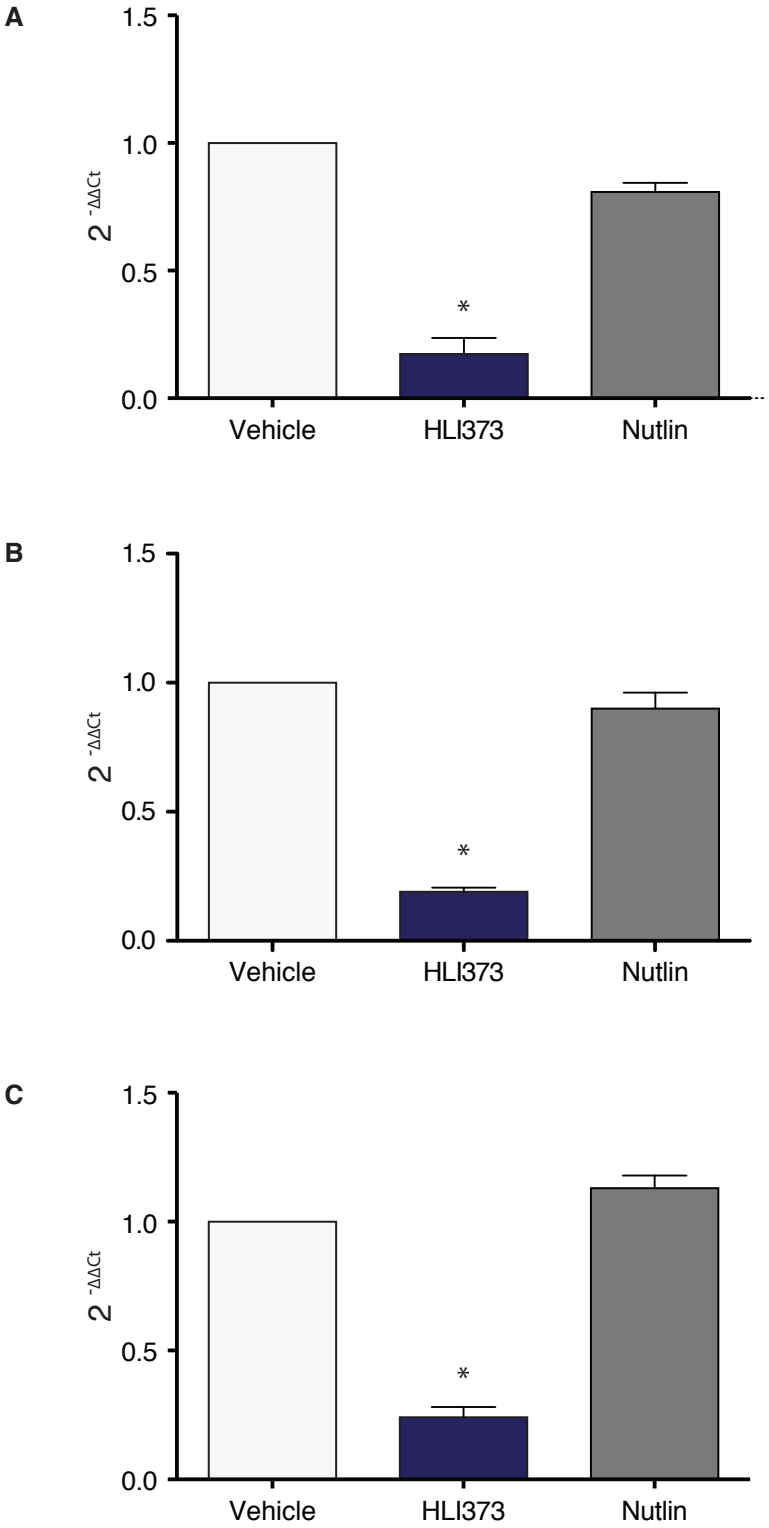

Figure 4-23: HLI373 reduces MDMX expression at a transcriptional level.
RPE (A), HCT116 p53 wild-type (B) and U2OS (C) cells were treated with vehicle, HLI373 (5μM) or Nutlin (10μM) for 20 hours. Levels of MDMX mRNA were measured on real-time PCR. Expression is quantified relative to control genes according to the

comparative $\Delta\Delta C_t$ method. Values from three independent experiments are displayed as mean of $2^{-\Delta\Delta Ct}$. Error bars represent SEM.

The most profound reduction was seen in RPE cells, although the largest variation between experiments was also seen in this cell line. The reduction in MDMX mRNA levels occurred under conditions where transcription of Pol II-dependent gene beta 2 microglobulin was not affected, demonstrating the selectivity of HLI373 for MDMX. As expected there was no change in transcription of MDMX following Nutlin treatment.

Both HLI373 and Nutlin induce p53, increase expression of p53 targets (to a similar degree) and cause cell cycle arrest. However, only HLI373 induced a reduction in MDMX, suggesting that this effect is likely to be p53 independent. To assess this directly, MDMX mRNA was measured following 17 hours of vehicle, HLI373 or Nutlin treatment in isogenic HCT116 cells either wild-type or null for p53. HLI373 clearly reduced MDMX mRNA regardless of p53 status, therefore HLI373 reduces MDMX via a p53 independent mechanism (Figure 4-24).

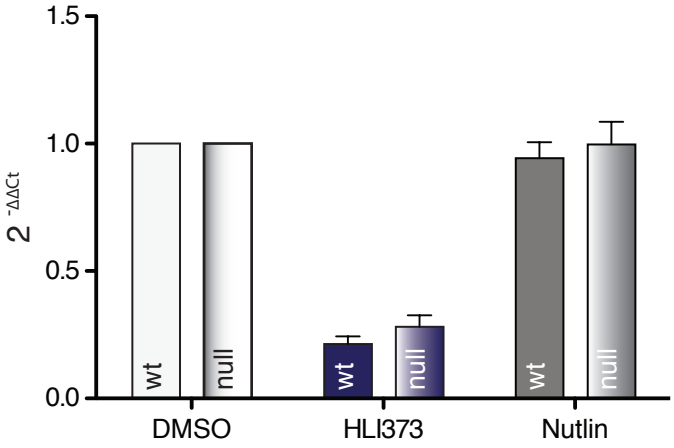

Figure 4-24: The effect of HLI373 on levels of MDMX mRNA expression is p53 independent.
HCT116 cells wild-type (wt) or null for p53 were treated with vehicle, HLI373 (5μM) or Nutlin (10μM) for 17h. MDMX mRNA measured by real-time PCR. Expression is quantified relative to control genes according to the comparative $\Delta\Delta C_t$ method. Values from three independent experiments are displayed as mean of $2^{-\Delta\Delta Ct}$. Error bars show SEM.

Changes in mRNA expression can result from changes in transcription or mRNA stability. In order to address whether MDMX transcription or mRNA stability were affected by HLI373, MDMX pre-mRNA was measured after vehicle, HLI373 or Nutlin treatment of RPE cells, revealing a clear ability of HLI373 treatment to reduce MDMX pre-mRNA levels, although no change was seen following vehicle

or Nutlin treatment (Figure 4-25). These data support a model where HLI373 inhibits the MDMX promoter activity.

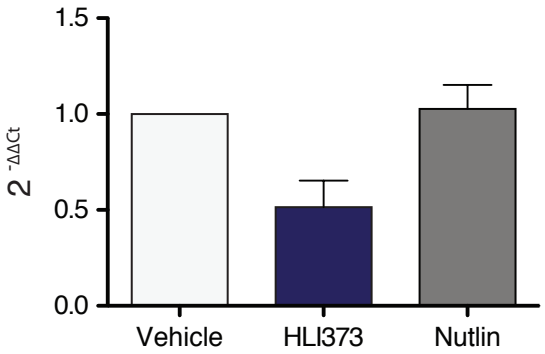

Figure 4-25: HLI373 reduces MDMX pre-mRNA.
RPE cells were treated with vehicle, HLI373 (5μM) or Nutlin (10μM) for 20 hours. Levels of MDMX pre-mRNA were measured on real-time PCR. Expression is quantified relative to control genes according to the comparative $\Delta\Delta C_t$ method. Values from three independent experiments are displayed as mean of $2^{-\Delta\Delta Ct}$. Error bars represent SEM.

To further establish whether the reduction in MDMX mRNA is through promoter regulation, an MDMX-luciferase construct was used. This construct was previously constructed by cloning the 5' upstream region of MDMX of 1100bp into a luciferase reporter plasmid pGL2-Basic (Figure 4-26A) [549]. The MDMX-luciferase construct and TK-renilla construct (transfection control) were transfected into U2OS cells, which were then treated with vehicle, a dose titration of HLI373 or Nutlin. HLI373 induced a dose dependent reduction in MDMX promoter activity relative to TK promoter activity (Figure 4-26B), supporting the hypothesis that HLI373 represses the MDMX promoter.

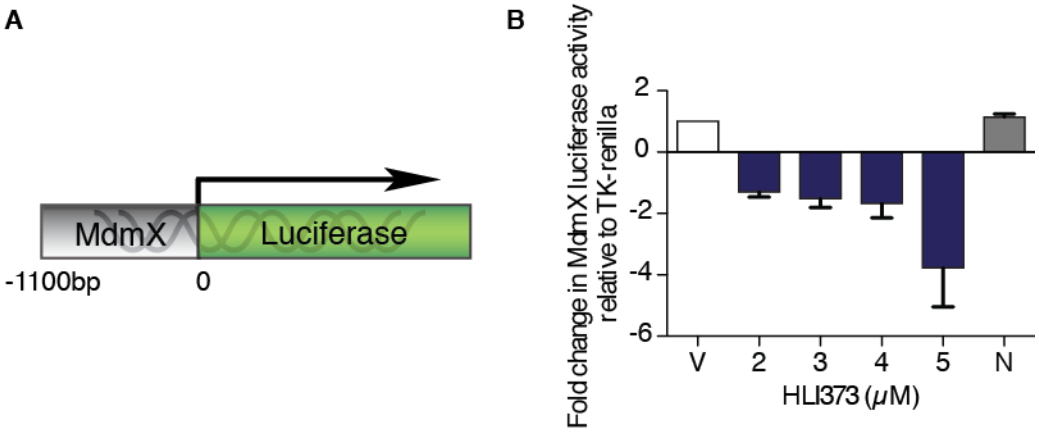

Figure 4-26: HLI373 reduces activity of the MDMX promoter as measured in a luciferase reporter assay.
(A) Schematic model of the MDMX luciferase reporter construct. (B) U2OS cells were transfected with MDMX-luciferase and TK renilla. After 24 hours cells were treated with vehicle, a titration of HLI373 as indicated or Nutlin (10μM) for 16 hours. After lysis and substrate addition luminescence was quantified on a luminometer. Luciferase activity in vehicle treated cells was set to 1. Mean

values of at least three experiments are plotted with error bars showing the SEM.

Since HLI373 causes reduced MDMX mRNA expression at the promoter level a search for potential transcription factors that the regulate MDMX promoter was undertaken. Using Genomatix on-line software, the MDMX promoter was therefore screened for potential transcription factor binding sites. From this, 38 sites (Figure 4-27) for 30 different transcription factors (table 4-1) were predicted. Of the predicted transcription factors two (ETS-1 and Elk) have previously been reported to be involved in the transcription of MDMX[549].

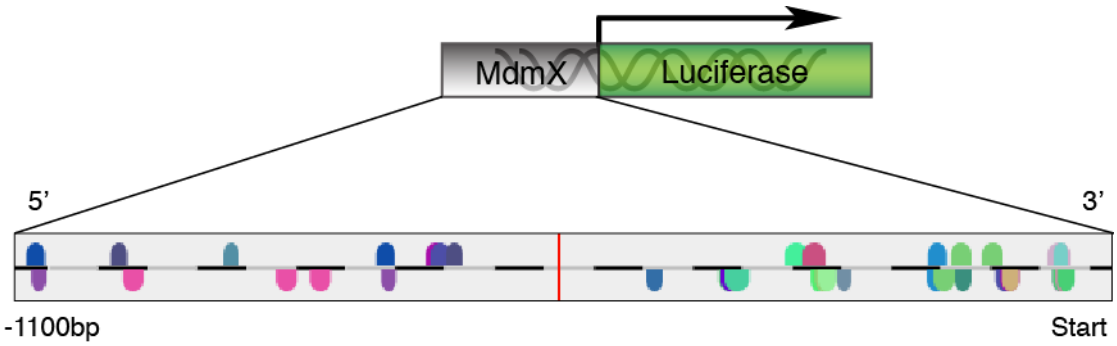

Figure 4-27: Predicted transcription factor binding sites on MDMX promoter.
38 sites for 30 transcription factors identified using genomatix on-line software. Different colours are indicative for different transcription binding sites and upward or downward orientation of the colours indicates the orientation of the transcription binding site. The grey and black divisions indicate 50bp intervals.

Each of these transcription factors may play a role in mediating the effect of HLI373 on MDMX expression.

Table 4-1: Transcription factors predicted to bind the MDMX promoter.

Rank	Transcription factor	Frequency
1	EVI1 encoded factor, amino-terminal zinc finger domain	1
2	Hmx2/Nkx5-2 homeodomain transcription factor	2
3	Pdx1 pancreatic and intestinal homeodomain transcription factor	1
4	Homeobox transcription factor Gsh-1	2
5	Carbohydrate response element binding protein & Max-like protein X bind as heterodimers to glucose responsive promoters	1
6	Collagen krox protein	1
7	Interferon regulatory factor 4	2
8	Interferon regulatory factor 3	1
9	GATA binding factor 3	1
10	Hox-1.3, vertebrate homeobox protein	2
11	**Elk-1**	**2**
12	Homeobox and leucine zipper encoding transcription factor	2
13	**ETS**	**1**
14	Zinc finger transcription factor ZBP-89	1
15	Metal induced transcription factor 1, MRE	1
16	POZ/ zinc finger protein transcriptional repressor	2
17	E2F-1/DP-2 heterodimeric complex	1

18	Wilms tumour suppressor	1
19	Estrogen-related receptor beta	1
20	Nuclear hormone receptor TR2, DR5 binding sites	1
21	POU class 6 homeobox 1	1
22	Zinc finger protein 263, ZKSCAN12	1
23	Monomers of nur subfamily of nuclear receptors	1
24	Serum response factor	2
25	Tumour suppressor p53	1
26	Erythroid krueppel like factor	1
27	PAX-3 paired domain protein, expressed in embryogenesis	1
28	V-myb, variant of AML v-myb	1
29	Myc associated zinc finger protein	1
30	Myeloid zinc finger protein	1

All predicted sites have 100% core similarity & listed ranked by highest matrix similarity. Transcription factors already known to regulate MDMX expression are shown in bold.

In addition to the control of transcription, mRNA levels can be affected by several mechanisms that control mRNA stability (5' capping, 3' polyadenylation, alteration of regulatory elements and nuclease activity, miRNA). To examine this, U2OS cells were treated with act D at doses capable of blocking all pol II activity. Cells were then treated with HLI373 or vehicle and MDMX mRNA levels determined at different time points. No significant difference was seen between the half-life of MDMX mRNA measured in cells treated with vehicle versus those treated with HLI373 (Figure 4-28).

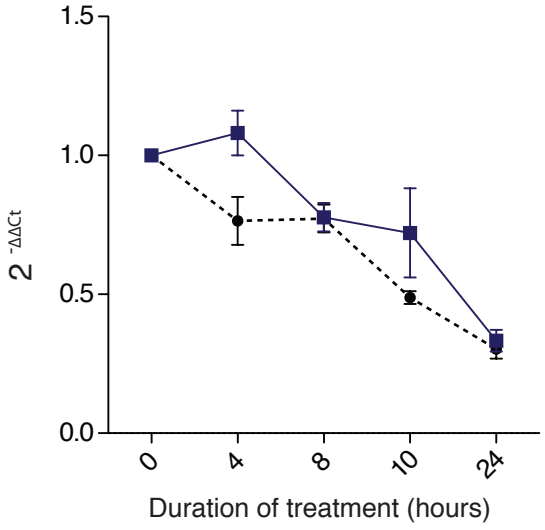

Figure 4-28: HLI373 does not alter the half-life of MDMX mRNA.
U2OS cells were treated with act D (400nM) and vehicle or HLI373 (5μM). Cells were harvest at the times indicated and MDMX mRNA was measured by quantitative real time PCR. Expression is quantified relative to control genes according to the comparative $\Delta\Delta C_t$ method. Values from three independent experiments are displayed as mean of $2^{-\Delta\Delta Ct}$. Error bars indicate the SEM.

Splicing of pre-mRNA provides another level of regulation of gene expression. Furthermore previous publications have reported alternative splicing of MDMX in response to stress that can also occur in cancer cells[355, 357, 358]. Eight splice forms of MDMX are reported in literature however these cannot all be detected with the antibodies used here (Figure 4-29A). Furthermore the quantitative RT-PCR data used primers which detect MDMX FL and MDMX L. (Figure 4-29B).

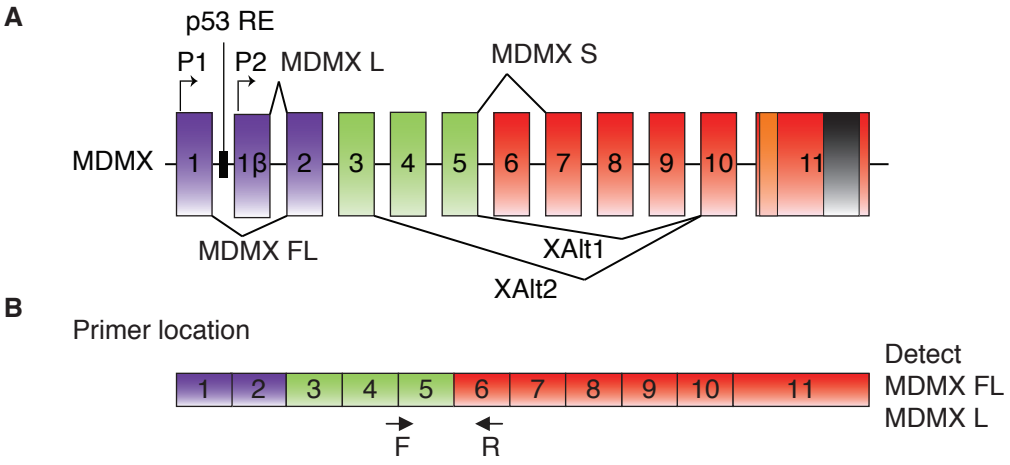

Figure 4-29: MDMX splicing map and qRT-PCR primer location.
(A) Schematic of the known alternative splice forms of MDMX. (B) Location of primers. RE=response element, P=promoter, F=forward, R=reverse.

To investigate a potential effect of HLI373 on mRNA splicing, a panel of normal and cancer cells was examined, to determine whether more than one MDMX isoform was detectable. Several of the cell lines used here display evidence of alternatively spliced forms of MDMX, with most cells expressing two forms of MDMX protein at around 76 and 60kD, while HCT116 has a further form at around 40kD (Figure 4-30). As shown previously, MDMX level correlated with p53 status[593]. p53 null and mutant tumour cell lines (H1299, Hep3B, MDA-MB231, A431, HT29) have a low MDMX levels, as do HPV18 E6 expressing HeLa cells. p53 wild-type tumour cell lines (MCF-7, U2OS, A2780/8, Hek293T, HCT116) show higher levels of MDMX, while the two untransformed cell lines (RPE and MCF-10a) also express low MDMX levels (Figure 4-30). This suggests that the high level of MDMX expression is important for inactivating p53 in these tumour cell lines.

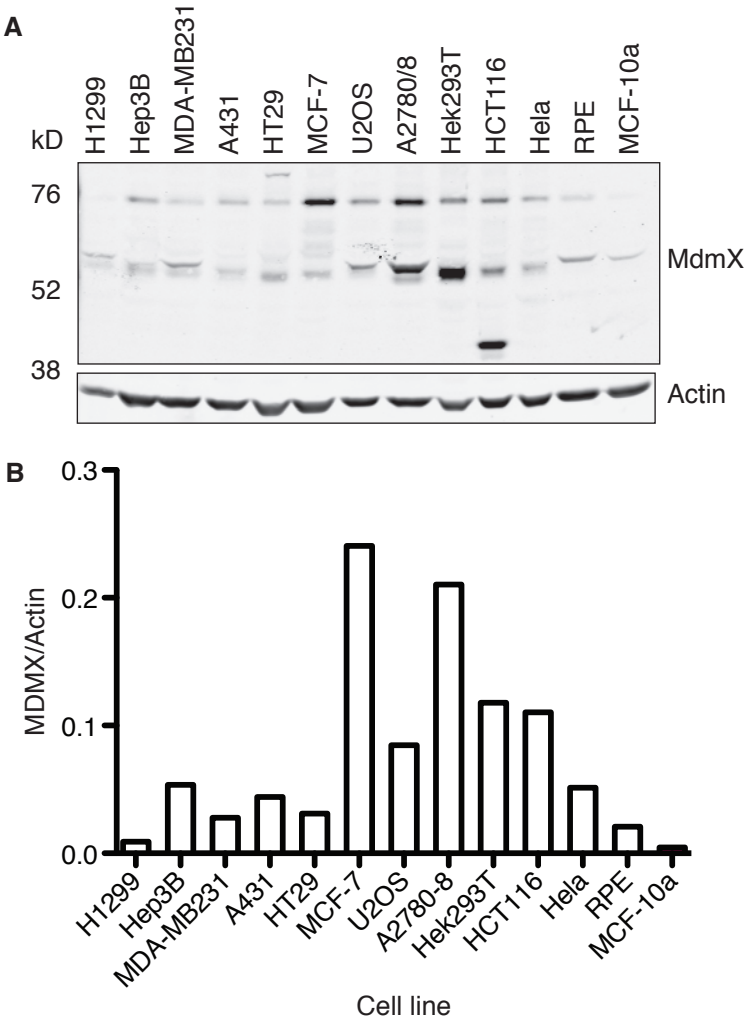

Figure 4-30: Several different isoforms of MDMX are expressed in tissue culture cells. 40µg lysates of each cell line were run on Western and Actin (loading control) and MDMX (polyclonal antibody) level was measured by immunoblot analysis. (B) Quantification of MDMX forms relative to Actin.

To investigate whether HLI373 differentially influences the level of each MDMX form, HCT116 cells (where three isoforms of MDMX can be assessed) were treated with vehicle or a dose titration of HLI373. All three forms of MDMX seem to be reduced to a similar degree, therefore there is no evidence that HLI373 treatment alters the splicing of MDMX (Figure 4-31).

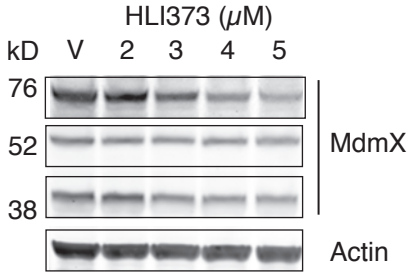

Figure 4-31: Expression of MDMX isoforms in response to HLI373 treatment. HCT116 cells were treated with vehicle (V) or HLI373 as indicated for 16h. Expression of MDMX and Actin (loading control) was assessed by immunoblot analysis.

Finally, micro-RNAs may also contribute to the levels of MDMX expression, miRNAs are small nucleotide sequences that bind the 3' untranslated region of their target mRNA to regulate gene expression through various mechanisms, including the promotion of degradation of mRNA and repression of translation[594]. It is therefore possible that, in addition to the regulation of transcription, HLI373 functions through the control of miRNAs that target MDMX, although the observation that HLI373 does not affect MDMX mRNA stability (Fig 4-28) makes this less likely. Nevertheless, MDMX levels are regulated by miR-34a (a p53 target)[595, 596] which has a miR-34a binding site the its 3' untranslated region[597]. Real-time PCR revealed only a modest increase in pri-miR-34a following both HLI373 and Nutlin treatment in HCT116 cells (Figure 4-32). Since Nutlin treatment induced pri-miR-34a to a similar degree as HLI373, but Nutlin did not induce changes in MDMX mRNA levels, it is unlikely that miR-34a is a major factor contributing to the HLI373 induced reduction in MDMX. However, it remains possible that other miRNAs are involved in mediating the effect of HLI373 on MDMX.

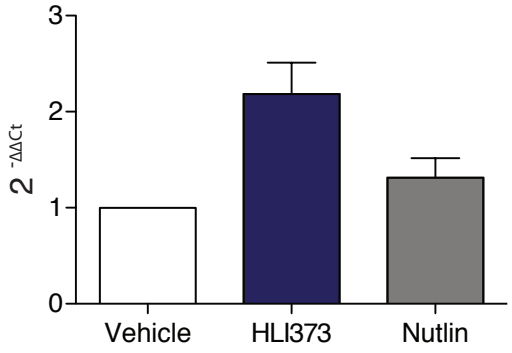

Figure 4-32: HLI373 has a modest effect on miR-34a.
HCT116 cells, p53 wild-type, were treated with vehicle, HLI373 (5μM) or Nutlin (10μM) for 16 hours. pri-miR-34a was measured by quantitative real-time PCR. Expression is quantified relative to control genes according to the comparative $\Delta\Delta C_t$ method. Values from three independent experiments are displayed as mean of $2^{-\Delta\Delta Ct}$. Error bars represent SEM.

4.7 HLI373 *in vivo*

As described earlier, HLI373 was selected for further study in part due to its favourable solubility, which would allow *in vivo* evaluation of its potential as an anti-cancer p53 stabilising agent. In addition, work presented here suggests that HLI373 may be an inhibitor of both MDM2 (via its ability to cause ribosomal stress) and MDMX (by inducing a reduction in activity of the MDMX promoter). As one of

the earliest dual inhibitors of MDM2 and MDMX, HLI373's ability to stabilise p53 *in vivo* was examined. Vehicle or HLI373 50mg/kg was administered intraperitoneally (IP) to C57BL/6 mice. Mice were culled after 2 and 8 hours. No mice were sacrificed earlier than the experimental plan dictated. Immunohistochemistry was performed to look for evidence of p53 pathway activation. At 2 hours after treatment mice treated with HLI373 had an increased expression of p53 in gastrointestinal crypts (Figure 4-33). By 8 hours after treatment the level of p53 was restored to normal levels but p21 activation could be seen, consistent with increased transcriptional activity of p53.

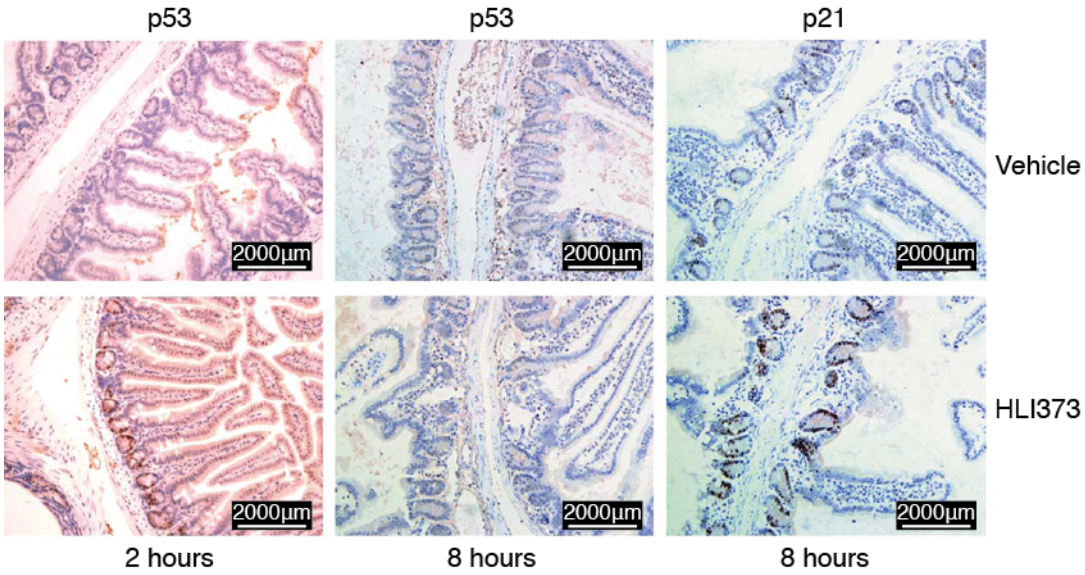

Figure 4-33: HLI373 activates p53 in normal mouse tissues.
C57BL/6 mice were treated with vehicle or HLI373 50mg/kg IP. Mice were taken at 2 and 8 hours. Intestinal tissue was harvested and fixed. Gut rolls were then formed and paraffin embedded. Sections were taken and mounted onto slides for p53 and p21 IHC.

HLI373 was next evaluated in a tumour model to look for evidence of anti-cancer activity as a result of the p53 activation. Nude mice were injected with HCT116 cells to form subcutaneous xenografts. Xenografts were allowed to reach approximately 200mg then mice were treated with vehicle or HLI373 50mg/kg. Mice were also treated with Bromodeoxyuridine (BrdU) IP 1 hour prior to mice being taken. Mice treated with HLI373 had increased levels of p53 in their tumour xenograft at 2 hours post treatment. There was a corresponding reduction in proliferation as shown by a reduction in BrdU staining (Figure 4-34).

HLI373 appears to have the ability to stabilise p53 and reduce xenograft proliferation in the short-term experiments described here. This is encouraging,

and supports further *in vivo* study to look for evidence of anti-cancer activity in terms of xenograft shrinkage. Further evaluation of HLI373 induced MDMX modulation in normal and xenograft tissue will be interesting.

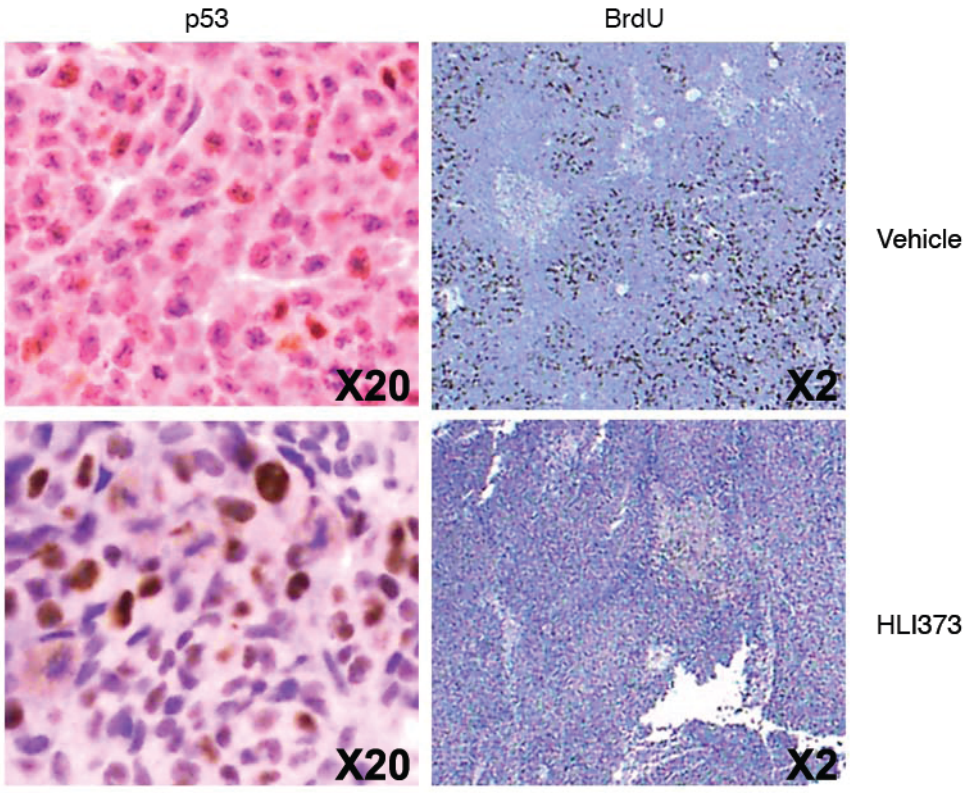

Figure 4-34: HLI373 stabilises p53 and reduces proliferation in xenografts.
Athymic nude mice were injected with HCT116 cells subcutaneously to form a xenograft. Tumours were staged to 200mg then treated with IP vehicle, IP HLI373 50mg/kg Three mice were treated for each condition. Tumour samples from mice taken at 2 hours post treatment are shown. After fixation and paraffin embedding sections were cut to perform IHC for BrdU and p53. Representative images are shown. Magnification is indicated.

4.8 Summary and discussion

These studies show that HLI373 interferes with ribosomal biogenesis at the level of rRNA transcription by a mechanism that is enhanced by intact p53-MDM2 binding. This inhibition of ribosomal production leads to a consequent release of ribosomal proteins, which bind to MDM2 and inhibit it.

Additionally via a p53 independent mechanism HLI373 inhibits MDMX transcription at the promoter level. The specific mechanism of this inhibition of MDMX transcription remains to be determined but one could speculate that HLI373 is

likely to act via one or several of the transcription factors predicted to bind the MDMX promoter.

HLI373 is therefore a dual inhibitor of MDM2 and MDMX and the stabilisation and activation of p53 demonstrated in cells and *in vivo* following HLI373 treatment is therefore likely to be through activation of the ribosomal pathway and inhibition of MDMX expression.

While the importance of MDM2 as a negative regulator of p53 has been appreciated for some time it is only in recent years that MDMX's importance has also been appreciated. Mouse models have shown that MDM2 and MDMX play a non-redundant role in keeping p53 under control during embryogenesis and development[246, 270]. Neither can compensate for the other and both have tissue specific roles. While MDM2 has E3 ligase activity alone, by cooperating with MDMX to form a heterodimer a more effective E3 ligase is created. Mouse models expressing the MDMX C462A mutant, which is unable to heterodimerise with MDM2 and is embryonic lethal have demonstrated that this MDM2-MDMX complex formation is essential for the negative regulation of p53[352] as MDM2 knockout mice are similarly embryonically lethal. Since MDMX is vital in the negative regulation of p53 it makes sense to design drugs to inhibit this negative regulation and therefore reactivate p53 in MDMX overexpressing tumours. Furthermore in a mouse model of c-myc induced lymphomagenesis deletion of one allele of either MDM2 or MDMX suppressed lymphomagenesis suggesting that therapeutic inhibition of MDMX should be effective in reactivating p53s tumour suppressive activities[423, 598]. Moreover pre-clinical experience of MDM2 inhibition therapy thus far has shown that increased expression of MDMX is one of the mechanisms of primary resistance to MDM2 inhibition suggesting that concurrent MDMX inhibition could improve the effectiveness of MDM2 inhibition therapy[434, 438-440]. Taken together this makes dual inhibition of MDM2 and MDMX an attractive anti-cancer strategy[264, 599].

The most well established method of MDMX inhibition to date is through administration of DNA damaging chemotherapeutic agents, which activate DNA damage signalling causing phosphorylation of MDMX and MDM2 leading to dissociation of HAUSP and MDM2-mediated autoubiquitination and ubiquitination

of MDMX[262, 600-602]. Furthermore both cell line studies and animal models have investigated the effectiveness of MDM2 inhibitors in combination with genotoxic chemotherapeutic agents and have shown this to be a particularly effective strategy in treatment of tumours overexpressing MDMX[406, 439, 570, 603, 604].

Despite MDM2 and MDMX having fairly similar structures neither Nutlin nor MI-219 (another low nanomolar inhibitor of the MDM2-p53 interaction) are able to bind to MDMX with high affinity[406, 432]. Attempts at structural based design of specific inhibitors of p53-MDMX inhibitors have proved difficult due to the shallower and less accessible p53 binding pocket of MDMX[605-607]. So far one MDMX inhibitor has been described, however the compound displayed only very poor potency[456]. Bernal *et al* reported a stapled peptide that could inhibit the p53-MDMX, but not the p53-MDM2 interaction[608]. A few MDM2/MDMX dual peptide inhibitors have now also been reported, but these have not yet undergone testing in cells[459-463 458].

More recently Graves *et al* reported a small molecule inhibitor of both MDM2 and MDMX which works by binding the N-terminal p53 binding site of MDM2 and the N-terminal p53 binding site of MDMX causing MDMX and MDM2 to heterodimerise via their N-termini and therefore be unable to negatively regulate p53[609]. This compound has been shown to be able to stabilise and activate p53 in cells.

HLI373 may therefore be the second dual inhibitor of MDM2 and MDMX, which has been tested in cells. However at present there are outstanding questions regarding the specific mechanism of action of HLI373 and in particular regarding its ability to inhibit activity of the MDMX promoter.

Firstly since ELK1 and ETS have previously been shown to be involved in transcription of MDMX HLI373's effect on mitogenic signalling should be explored by cell line studies looking for HLI373 induced alteration in mitogen-activated protein kinase (MAPK) pathway activity[549].

The next step would be to create deletion constructs from the full-length 1100bp MDMX-luciferase construct and then perform luciferase assays with a dose titration of HLI373. This would help identify which area of the MDMX promoter HLI373 is inhibiting. Subsequently predicted transcription factor binding sites in the

region of interest could be mutated to establish which transcription factor the HLI373-induced reduction in MDMX is dependent on. Following this the transcription factor of interest could be chromatin immunoprecipitated to the MDMX promoter after a dose titration of HLI373.

Regardless of the outcome of the work suggested above it would also be of interest to establish the contribution that the HLI373 induced down-regulation of MDMX makes to the p53 activating ability of HLI373 perhaps by testing HLI373's p53 activating ability in a panel of cells with a range of basal levels of MDMX and examining the response of cells to HLI373 treatment with and without MDMX knock down.

Ultimately after cell line studies gaining insight into HLI373's mechanism of action further *in vivo* evaluation of HLI373 would be beneficial. Firstly a larger cohort of mice should be treated to confirm the p53 activating ability of HLI373 in mouse tissue and xenografts. Secondly the ability of HLI373 to inhibit MDMX *in vivo* remains to be explored. Thirdly experiments over a longer time course are required to look for evidence of anti-cancer activity of HLI373. This could include xenograft studies as well as study in genetically engineered mice that express a tumour specific MDMX/MDM2 overexpression.

In conclusion much remains to be studied regarding HLI373's mechanism of action however early indications are that it stabilises p53 by activating the ribosomal stress pathway and inhibits MDMX at the promoter level. This makes HLI373 the first dual inhibitor of MDM2 and MDMX described to work in this way.

5 MDM2 inhibitors for chemoprotection

5.1 History of chemoprotection strategy

In clinical practice, the use of MDM2 inhibition treatment, with consequent p53 activation, may be useful in two broad settings.

Firstly MDM2 inhibitors are being developed as therapeutics for the treatment of wild-type p53 expressing cancers, in particular where p53 has been inactivated via upregulation of MDM2 or MDMX[1]. These tumours would be predicted to be highly sensitive to the stabilisation and activation of p53, and various mouse models have suggested that the activation of p53 can promote tumour regression[134, 417, 418]. A general prediction from mouse models and clinical data[426-428] is that transient activation of p53 in normal tissue is not extensively toxic, and the differential sensitivity of transformed cells to p53-mediated death has been described in a number of systems[572, 573, 610].

The second application for an MDM2 inhibitor is as a chemoprotective agent for use in the treatment of p53 deficient tumours (mutant or null for p53). The principle here is to induce a transient cell cycle arrest in normal cells while allowing tumour cells (that have deregulated proliferative signals) to continue cycling. In this setting, some cytotoxic drugs should be effective only on the proliferating, tumour cells – sparing normal tissue (Figure 5-1). The chemoprotective agent would therefore reduce the toxicity, widen the therapeutic window and allow maintenance of high dose intensity and potentially escalation of the cytotoxic treatment.

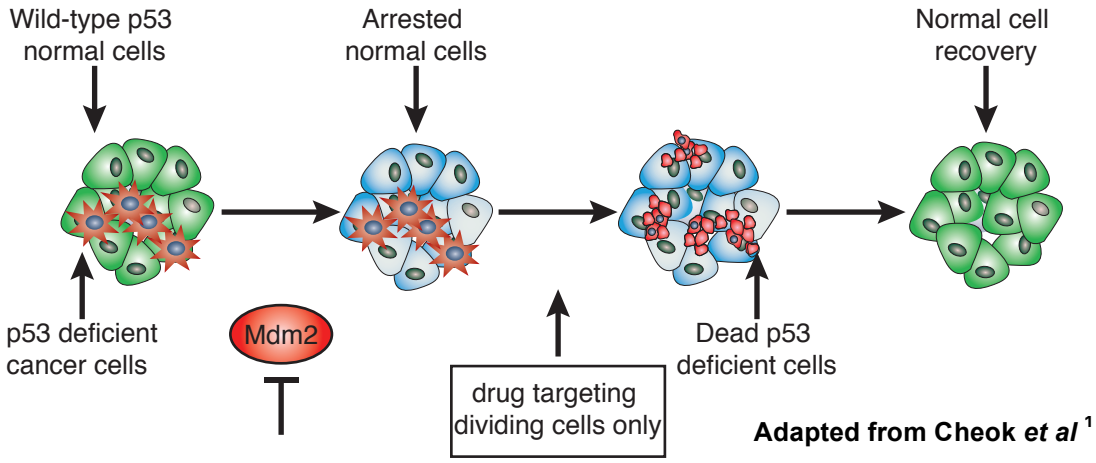

Figure 5-1: Schematic of chemoprotective strategy.

To date there are 2 low-dose traditional chemotherapy agents (low-dose doxorubicin and low-dose act D) that have been investigated in this chemoprotective setting, however as yet none of the studied chemoprotectant/therapeutic combinations are in clinical practice[510-512, 611-613] (table 5-1). MDM2 inhibitors, including the p53-MDM2 interaction inhibitor Nutlin, should also be capable of arresting the cell cycle of normal wild-type p53 expressing tissues prior to administration of cytotoxic agents to target the cycling p53 deficient tumour cells. The cell line studies investigating the potential of a variety of chemoprotectant/therapeutic combinations are listed in table 5-1.

Table 5-1: Cell line studies investigating chemoprotective strategy.

Author	Protective	Therapeutic agent		Protection	
				p53 wild-type	p53 deficient
Blagosklonny *et al*[612]	LD doxorubicin	Anti-mitotic agents	**Epitholones A and B**	**Yes**	**No**
Blagosklonny[511]			Paclitaxel	Yes	Yes
Blagosklonny *et al*[612]			**Vinblastine**	**Yes**	**No**
Rao *et al*[613]	LD act D		AK inhibitor VX680	Yes	Yes
Cheok *et al*[517]	Nutlin		**AK inhibitor VX680**	**Yes**	**No**
Sur *et al*[515]			**PLK inhibitor BI-2536**	**Yes**	**No**
Apontes *et al*[614]			**Nocodazole**	**Yes**	**No**
Apontes *et al*[614] Carvajal *et al*[514] Tokalov and Abolmaali[516]			**Paclitaxel**	**Yes**	**No**
Kranz and Dobbelstein[615]		Anti-metabolite	**Ara-C**	**Yes**	**No**
Kranz and Dobbelstein[615]			**Gemcitabine**	**Yes**	**No**
Kranz and Dobbelstein[615]		Non-specific	Cisplatin	No	NT
Kranz and Dobbelstein[615]			Doxorubicin	No	NT

(NT)=Not Tested (AK)=Aurora Kinase (LD)=Low-Dose (Act D)=Actinomycin D (PLK)=Polo-Like Kinase. Grey shaded boxes indicate combinations where wild-type p53 expressing cells are protected from cytotoxic effects while p53 deficient cells are not. Adapted from van Leeuwen 2012[616].

These studies suggested that several drug combinations may allow specific protection of wild-type, but not p53 deficient cells (grey shaded combinations). Of these, the combinations of particular interest fall into 2 groups:

1. Chemoprotective agent with anti-metabolite.

- Nutlin with Ara-C (cytosine arabinoside).

Ara-C is a pyrimidine analogue, which is administered intravenously and then undergoes intracellular phosphorylation to become active (ara-CTP). This conversion is catalysed by multiple kinases including deoxycytidine kinase, which has its highest activity in S-phase. The active ara-CTP then directly inhibits DNA polymerase, is incorporated into DNA causing chain termination and inhibiting DNA synthesis. Ara-C also inhibits ribonucleotide reductase therefore inhibits synthesis of deoxynucleoside triphosphates. Deaminating reactions catalysed by cytidine deaminase cause degradation of active metabolites of ara-C. In clinical practice ara-C is the cornerstone of treatment for AML (acute myeloid leukaemia) however it has only minor activity in solid tumours. This may be due to the high deaminase levels of solid tissues or differences in the intracellular activation of ara-C[617]. Ara-C's S-phase specific activity makes it an attractive candidate for the chemoprotective/therapeutic combination however since its main use is in AML where the vast majority of tumours express wild-type p53[618] the clinical impact of this combination would be low.

- Nutlin then gemcitabine.

Gemcitabine (2,2-difluorodeoxycytidine) is also a pyrimidine analogue but in contrast this does have activity in solid tumours. Its mechanism of action is very similar to ara-C except that gemcitabine has a far greater affinity for deoxycytidine kinase and its active form (dFdCTP) inhibits cytidine deaminase resulting in more activity and less degradation than ara-C[617]. Although gemcitabine is an S-phase specific agent which is used commonly in treatment of bladder cancer, pancreatic cancer and non-small cell lung cancer[619] clinical studies have demonstrated that maintaining a dose intensity greater than standard dose does not improve outcomes[620]. There is therefore little to be gained by the chemoprotective strategy with this combination.

2. Chemoprotective agent with drugs targeting mitosis.

- Nutlin with the Aurora kinase (AK) inhibitor VX680.

AKs are required for localisation of centromeres, spindle assembly and chromosome segregation. AK inhibitors therefore cause disruption of spindle assembly checkpoint, failure of chromosome segregation, endoreduplication, cytokinesis failure and cell death[621]. From several early phase clinical studies evaluating AK inhibitors the dose limiting toxicity has been established as neutropenia and they appear to be cytostatic[622,623]. Their clinical development is in progress.

- Nutlin then nocodazole.

Nocodazole also targets mitosis but via a different mechanism. It binds to tubulin and inhibits microtubule tubule assembly. It has not undergone clinical evaluation.

- Nutlin then Polo-like kinase (PLK) inhibitor BI-2536.

PLK1 has essential roles in mitosis via control of activation of CDK1. In cellular models inhibition of PLK1 leads to effects in mitosis, loss of cell proliferation, and increased cell death[624]. PLK inhibitors are currently under early phase clinical evaluation. In phase I only minor responses (one partial response and one stable response, n=40 patients) have been achieved and neutropenia is the dose limiting toxicity[625]. PLK inhibitors continue to be in clinical development.

- Nutlin then paclitaxel.

Paclitaxel is a tubulin stabilising agent that causes formation of tubules resistant to depolymerisation therefore it blocks progress to anaphase (discussed further below, Figure 5-18). It is used widely in clinical practice for the treatment of ovarian cancer, breast cancer and lung cancer[619].

With the exception of paclitaxel, all of these drugs targeting mitosis are in pre-clinical or early phase development and therefore it will be considerable time before they are approved for clinical use. Similarly Nutlin, the direct, non-genotoxic activator of p53, which is ideally suited as the chemoprotective agent to induce p53 is in the drug development pipeline and is yet to be approved for clinical use. It is therefore of interest that some more traditional chemotherapeutic

agents have been shown to stabilise p53 through mechanisms that do not require DNA damage[469, 626, 627]. Indeed previous cell line data has shown some potential of a combination of low-dose doxorubicin with epitholones A and B or vinblastine. Ixabepilone, an epitholone B analog is approved by the U.S. Food and Drug Administration (FDA) for treatment resistant advanced breast cancer but failed to achieve approval by the European Medicines Agency (EMEA) due to concerns over the rates of neurotoxicity and relatively small benefit. Although vinblastine is used in the treatment of solid tumours it is only used infrequently.

The aim of this part of the project was firstly to examine the potential of traditional anti-cancer drugs at low-dose as non-genotoxic p53 activators and secondly to explore their potential as chemoprotective agents prior to administration of clinically relevant chemotherapeutics. By focussing on agents currently in clinical use clinical evaluation of the schedule could be streamlined and this would therefore allow for a more immediate realisation of any potential benefit for patients.

5.1.1 Mechanism of action of actinomycin D

Act D is a cytotoxic antibiotic currently used in clinical practice for the treatment of Wilm's tumours, rhabdomyosarcomas, Ewings sarcoma and testicular cancer[628]. As with other traditional cytotoxic agents in clinical use, early phase clinical studies previously established the DLT of act D. The dose required for 1/3 of patients to experience a DLT was used to determine the MTD. In the case of act D neutropenia was established as the DLT[629].

In the early 1960s cell line studies of act D established that it works by binding to the minor grove of DNA specifically where two consecutive guanine-cytosine base pairs are present[630]. By intercalating with the DNA at these points act D blocks the passage of RNA polymerase. Since ribosomal DNA is more guanine-cytosine rich there is a dose-dependent inhibition of first RNA pol I then RNA pol II at higher doses (Figure 5-2)[591, 631]. The ability of act D to intercalate where there are 2 consecutive guanine-cytosine (G-C) base pairs is specific for binding to DNA. Act D is not able to bind consecutive guanine-cytosine base pairs in RNA due to the steric requirement to bind to the most common structured DNA; B-DNA [632-634].

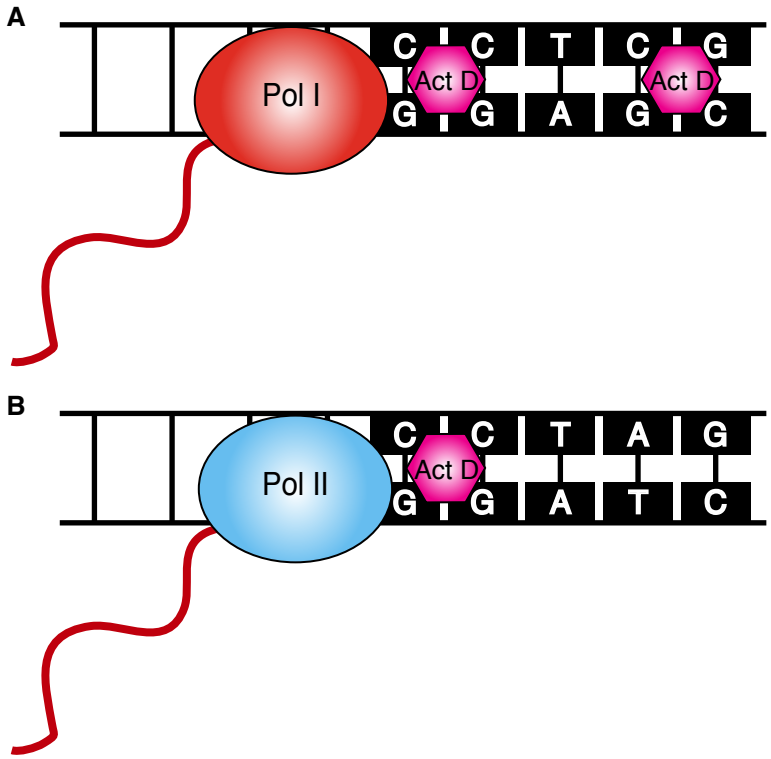

Figure 5-2: Mechanism of action of act D.
(A) RNA polymerase I controls transcription of ribosomal RNA (rRNA). Act D binds to the G-C rich DNA. (B) RNA polymerase II controls transcription of mRNA. Act D binds to the G-C pairs which occur less frequently than in rRNA.

There is strong evidence showing that low-dose act D (which at higher concentrations inhibits transcription) activates p53 via the ribosomal stress pathway due to its impact on ribosome biogenesis[469]. Act D has previously been evaluated in one cell line study as a chemoprotective agent prior to the administration of the AK inhibitor VX680[613]. In this study it appeared to protect both wild-type and p53 deficient cells (table 5-1). Despite this it warrants further examination as a chemoprotective agent with alternative and more clinically pertinent cytotoxic combinations.

5.1.2 Mechanism of action of 5-FU

In current clinical practice the anti-metabolite 5-FU is the backbone for treatment of upper and lower gastrointestinal cancers and is also used in the treatment of breast cancer and head and neck cancers[635]. It is a pyrimidine analog that is 80% catabolised in the liver to dihydrofluorouracil by the enzyme dihydropyrimidine dehydrogenase. The remaining 5-FU in converted intracellularly to three main active metabolites (Figure 5-3).

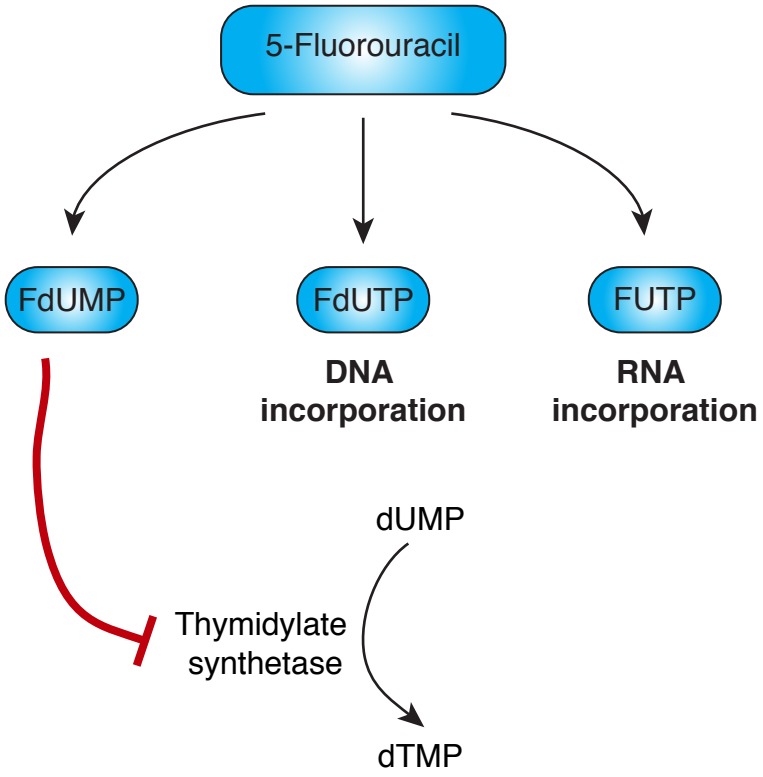

Figure 5-3: Mechanism of action of 5-FU.
5-Fluorodeoxyuridine Monophosphate (FdUMP), Fluorodeoxyuridine triphosphate (FdUTP), Fluorouridine triphosphate (FUTP), deoxyuridine monophosphate (dUMP), thymidine monophosphate (dTMP) Adapted from Longley *et al*[636].

1. 5-FU is converted to **5-fluorodeoxyuridine monophosphate**, which inhibits thymidylate synthetase (TS) preventing the conversion of deoxyuridine monophosphate to thymidine monophosphate. Subsequently the resultant imbalance in the deoxynucleotide pool disrupts DNA synthesis and repair resulting in DNA damage[637, 638].

2. Secondly 5-FU is converted to **fluorodeoxyuridine triphosphate**, which is incorporated into DNA, resulting in uracil DNA glycosylase mediated base excision and subsequent DNA fragmentation and cell death[639].

3. Thirdly 5-FU is converted to **fluorouridine triphosphate**, which is incorporated in all forms of RNA and leads to inhibition of ribosomal RNA processing and ultimately to cell death[640].

Modulation strategies using co-administration of leucovorin, which enhances binding of FdUMP to TS, have been shown to increase anticancer activity of 5-FU

and therefore in clinical practice 5-FU is given in combination with leucovorin[641, 642].

Cell line data suggests that low doses of 5-fluorouracil (5-FU) may be efficient in activating p53 via the ribosomal pathway. Consistent with this, gene expression analysis of cell lines shows that the effects of 5-FU treatment clusters with RNA synthesis inhibitors[276, 469, 643, 644]. 5-FU is therefore suitable for investigation as a potential non-genotoxic p53 activator to be used as a chemoprotective agent.

5.2 Low-dose actinomycin D and 5-FU stabilise p53.

To examine the consequences of low-dose act D treatment on the p53 pathway, untransformed retinal pigment epithelial cells (RPE) were treated with a range of doses of act D for 16 hours. Cell lysates were run on Western blot and probed for p53, MDM2, p21 and Actin, as a loading control. In RPE cells, act D stabilised p53 from doses as low as 1nM and increased expression of both p53 targets MDM2 and p21 (Figure 5-4A). At a dose of 100nM a reduction in MDM2 level was seen consistent with act D induced RNA polymerase II inhibition[591]. Similarly p21 expression was reduced at a dose of 500nM. p53 levels continued to increase in a dose-dependent manner even after high dose act D treatment. This would be consistent with act D causing p53 accumulation by increasing its stability to levels sufficient to compensate for an act D induced inhibition of transcription of p53. Actin levels appear equal demonstrating similar loading of lysates in each lane.

To confirm this effect of act D, wild-type p53 expressing osteosarcoma cell line U2OS cells were treated with a dose range of act D for 16 hours. Consistently, doses of act D as low as 1nM led to a dose-dependent stabilisation of p53 and increased expression of MDM2 levels, with a reduction in MDM2 levels at doses higher than 10nM (Figure 5-4B).

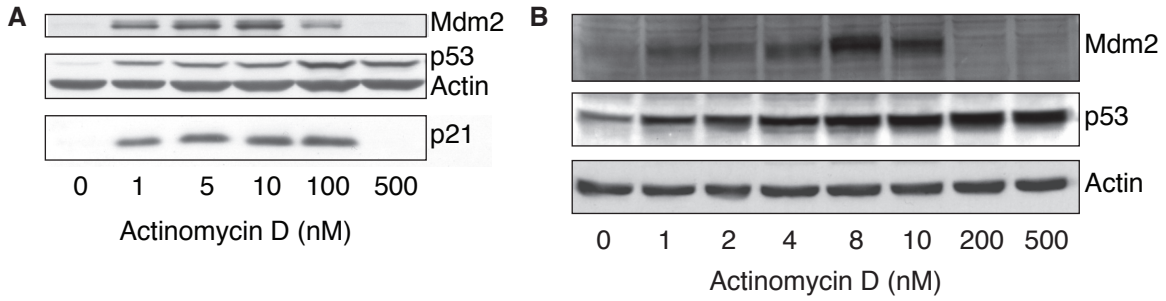

Figure 5-4: Low-dose act D stabilises p53.
(A) RPE cells (B) U2OS cells treated with indicated doses of act D for 16 hours. Lysates were run on Western blot and the expression of MDM2, p53 and p21 was examined. Actin was used as loading control.

Next the p53 stabilising effects of 5-FU were investigated by treating RPE cells and U2OS cells with a dose range of 5-FU. In RPE cells, 5μg/ml 5-FU resulted in a clear stabilisation of p53, with increased expression of MDM2 and p21 (Figure 5-5A). U2OS cells appeared to be more sensitive with an increase in p53 and MDM2 levels in response to 1μg/ml 5-FU (Figure 5-5B).

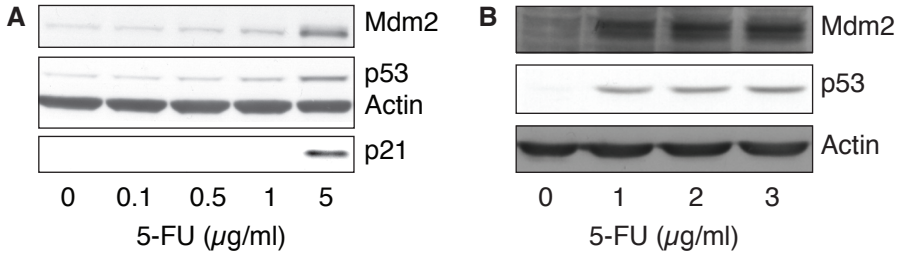

Figure 5-5: Low-dose 5-FU stabilises p53.
(A) RPE (B) U2OS cells were treated with indicated doses of 5-FU. Lysates were run on Western blot and the expression of MDM2, p53 and p21 was examined. Actin was used as loading control.

To confirm that the increase in MDM2 and p21 levels seen following low-dose treatment with either act D or 5-FU resulted from increased transcriptional activity of p53, luciferase reporter assays were performed. U2OS cells stably expressing the PG13 luciferase reporter[86] construct in which a promoter consisting of a series of optimised p53 binding sites is cloned upstream of a luciferase reporter gene, were treated with a dose range of either act D or 5-FU for 16 hours. Luciferase assays, plotted as fold change of relative luciferase units, show a modest but significant increase in p53's transcriptional activity after 1nM of act D treatment and a further increase after 4nM treatment (Figure 5-6A). Treatment of cells with 1μg/ml of 5-FU similarly revealed a modest but significant increase in luciferase activity, which further increased in a dose dependent manner (Figure 5-6B).

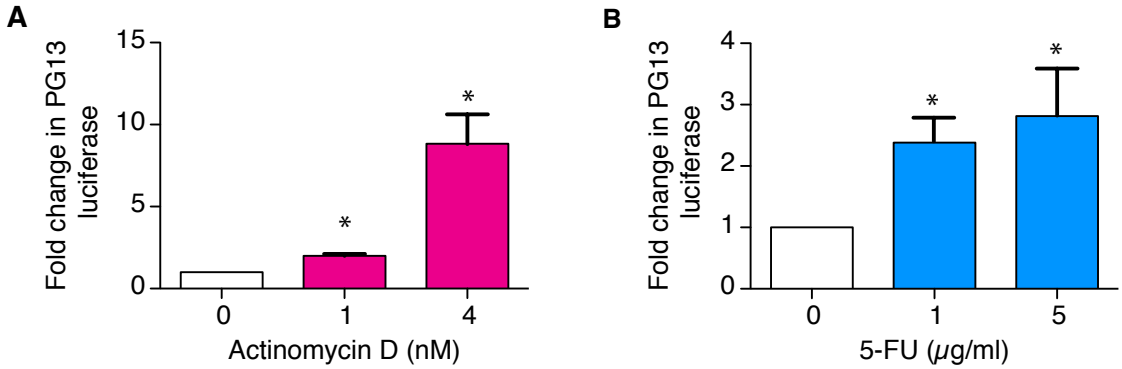

Figure 5-6: Low-dose act D and 5-FU significantly increase p53's transcriptional activity.
U2OS PG13 cells were treated with indicated doses of (A) act D or (B) 5-FU for 16 hours. Cells were lysed and luminescence was measured on a microplate luminometer. Values were plotted as fold change relative to the vehicle (0) treated condition which was set to 1. The mean of triplicates was plotted and error bars display the SD. *p<0.05, Students T-test.

To confirm that p53's increased transcriptional activity following low-dose act D and 5-FU treatment led to functional effects, cell cycle analysis was performed. RPE cells were treated with PBS, act D (4nM) or Nutlin (10μM) for 16 hours. Cells were harvested, fixed and PI (propidium Iodine) stained for FACS analysis. As with Nutlin treatment, act D led to a cell cycle arrest in G1 and a corresponding reduction in S-phase (Figure 5-7A). Similarly treatment of cells with 5μg/ml of 5-FU caused a cell cycle arrest in G1 and a reduction in the cells in S-phase (Figure 5-7B).

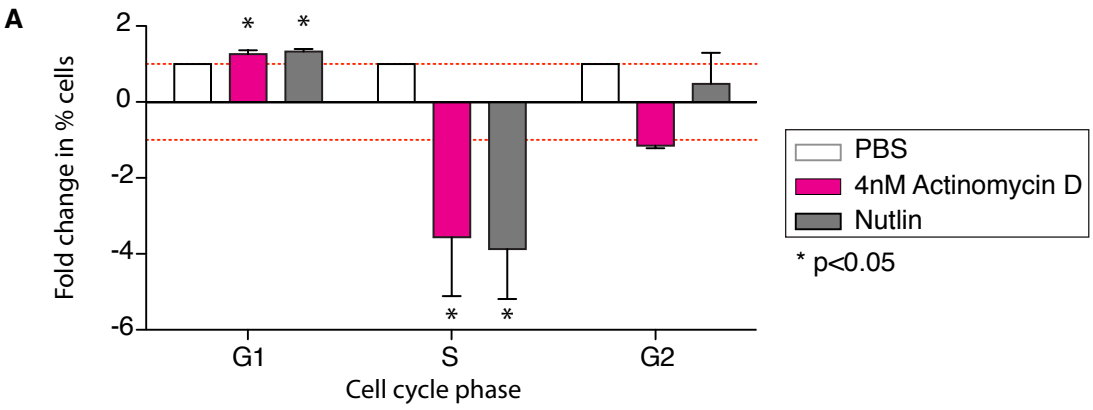

Figure 5-7: Low-dose act D and 5-FU cause cell cycle arrest.
(A) RPE cells were treated with indicted doses of act D. Cells were also treated with PBS (negative control) and Nutlin 10μM (positive control). After 16 hours treatment cells were harvest for PI staining and FACS analysis. Values were plotted as fold change relative to the PBS treated condition which was set to 1. The mean of three independent experiments was plotted and error bars display the SEM. *p<0.05, Students T-test.

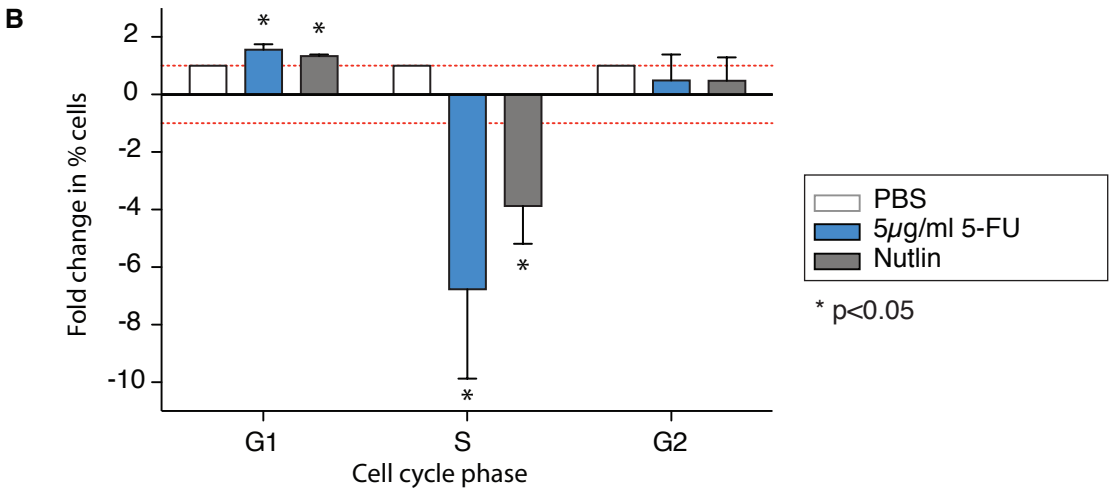

(B) RPE cells were treated with indicted doses of 5-FU. Cells were also treated with PBS (negative control) and Nutlin 10μM (positive control). After 16 hours treatment cells were harvest for PI staining and FACS analysis. Values were plotted as fold change relative to the PBS treated condition which was set to 1. The mean of three independent experiments was plotted and error bars display the SEM. *p<0.05, Students T-test.

5.2.1 Does low-dose actinomycin D cause DNA damage?

The aim of this study was initially to determine the lowest dose of act D that reliably stabilises and activates p53 (the MDM2 inhibitory dose). Furthermore the hypothesis that p53 activation occurred in the absence of DNA damage was tested. DNA damaging agents effectively stabilise p53 as a result of multiple phosphorylations on both p53 and MDM2, which result in an inhibition of degradation. Key phosphorylation sites on p53 are serine 15 and 392, and the modification of these residues can be used as a marker of DNA damage. DNA strand breaks lead to activation of damage activated kinase, ATM which then phosphorylates p53 on serine15[210, 211.] Phospho-serine 392 has been shown to be phosphorylated in response to UV, DNA damage and interferon via kinases FACT (facilitates chromatin transcription)-CK2, p38 and protein kinase R respectively[293-295]. To investigate the relationship between stabilisation of p53 and the induction of genotoxicity by act D, overall p53 levels and phospho-serine p53 was measured in RPE cells after treatment with a dose range of act D. As shown previously, act D stabilised p53 at 1nM – however under these conditions there was no evidence of phosphorylation at serine 15 (Figure 5-8). As a positive control, much higher act D concentrations (100 and 500nM) did induce this phosphorylation event. By contrast, a clear increase in serine 392 phosphorylation could be detected at 1nM act D (Figure 5-8). Taken together, these results suggest that low levels of act D do not stimulate a DNA damage response, but can activate kinases capable of

phosphorylating p53 on serine 392. Importantly, previous studies have shown that Nutlin treatment also results in the phosphorylation of p53 serine 392, but not serine 15, although the exact mechanism of 392 phosphorylation was not defined[469].

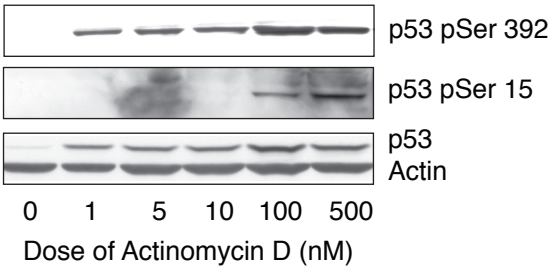

Figure 5-8: Low-dose of act D does not cause phosphorylation of p53 at serine 15. RPE cells were treated with indicated doses of act D for 16 hours. Lysates were blotted for total p53, phosphorylated p53 (pSer15 and pSer 392) and Actin was used as loading control.

To further confirm a lack of DNA damage signalling following low-dose act D treatment, the presence of phosphorylation of H2AX histone, an early sign of DNA double strand breaks, was examined by immunofluorescence[645]. RPE cells were plated and treated with vehicle and Nutlin as negative controls and a titration of act D. In line with previous work showing DNA damage signalling occurring from 200nM-500nM of act D, γH2AX foci were clearly detected at the time point examined. By contrast, only a very small increase in γH2AX positive cells was detected after treatment with 1nM act D, although this did appear to be slightly enhanced over background levels (Figure 5-9 A and B).

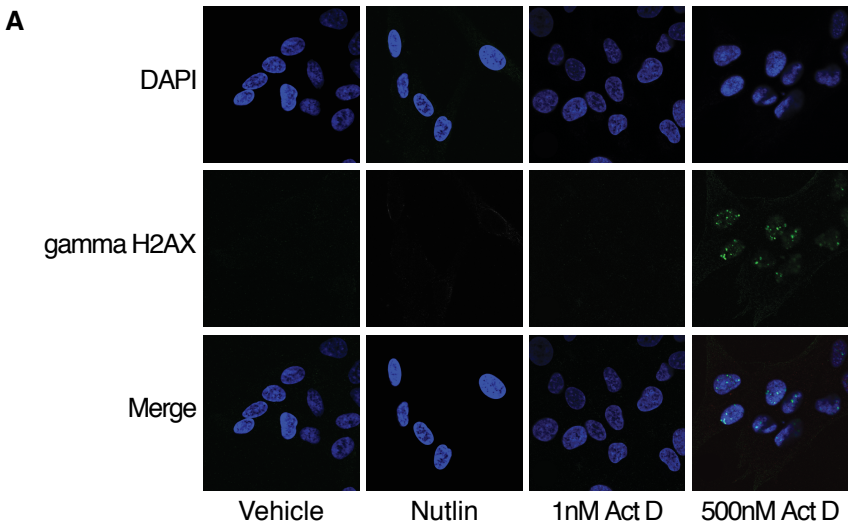

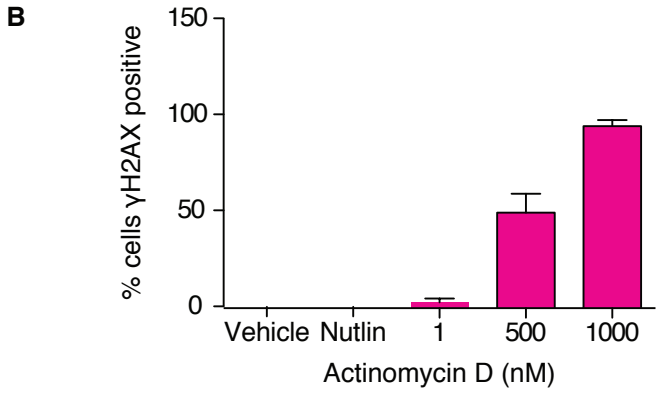

Figure 5-9: Act D causes only low levels γH2AX foci formation at low-dose.
(A) RPE cells were plated on cover slips then treated with 1nM, 500nM and 1000nM of act D for 16 hours. Cells were then fixed, permeabilised and incubated with anti- γH2AX antibody followed by AlexaFluor 466 anti-mouse antibody. Cover slips were mounted on slides and images taken on Olympus FV1000 microscope. (B) Cells with γH2AX foci were counted and the percentage of positive cells plotted. DAPI staining was used to visualize cell nuclei and to count the number of cells with or without positive gamma H2AX staining. Error bars represent SEM of three independent experiments. 50 cells were counted per condition.

Further studies were therefore carried out using doses of act D in the range 1-4nM, since phosphorylation of serine 15 did not occur until doses greater than 10nM and FACS data examining the cell cycle showed a robust G1 arrest at 4nM. Previous pharmacokinetic studies of act D established a Cmax (maximum concentration) in the region of 25.1ng/ml (2M) and a median Area Under the Curve (AUC) at six hours of 2.67mg/l/minute (2.13μM per minute)[646, 647]. A dose of 4nM is therefore around 500,000,000 fold less than the DNA damaging, myelosuppressive dose range used in clinical practice. It has been shown in cell lines that evidence of DNA strand breaks begins to occur at doses above 200nM, albeit by a different assay[590].

5.2.2 Does low-dose 5-FU cause DNA damage?

The minimum dose range of 5-FU that induces p53 is 1μg/ml-5μg/ml (Figure 5-2). To determine whether DNA damage also occurs with these low-dose 5-FU treatments, cells were treated with a dose titration of 5-FU for 16 hours and γH2AX foci were visualised by immunofluorescence. Almost all cells were γH2AX positive after a 50μg/ml 5-FU treatment (Figure 5-10 A & B). This is consistent with previous work which has shown phosphorylation of p53 at serine 15 and induction of γH2AX foci in 50% of cells from 5-FU doses of around 13μg/ml 5-FU[648]. As seen with act D, lower levels of 5-FU treatment (0.05-5ug/ml) induced a low level of DNA damage (above background seen following vehicle and Nutlin treatment),

at the time point examined. The extent of damage was much less profound than the extent of γH2AX staining seen at a known genotoxic dose.

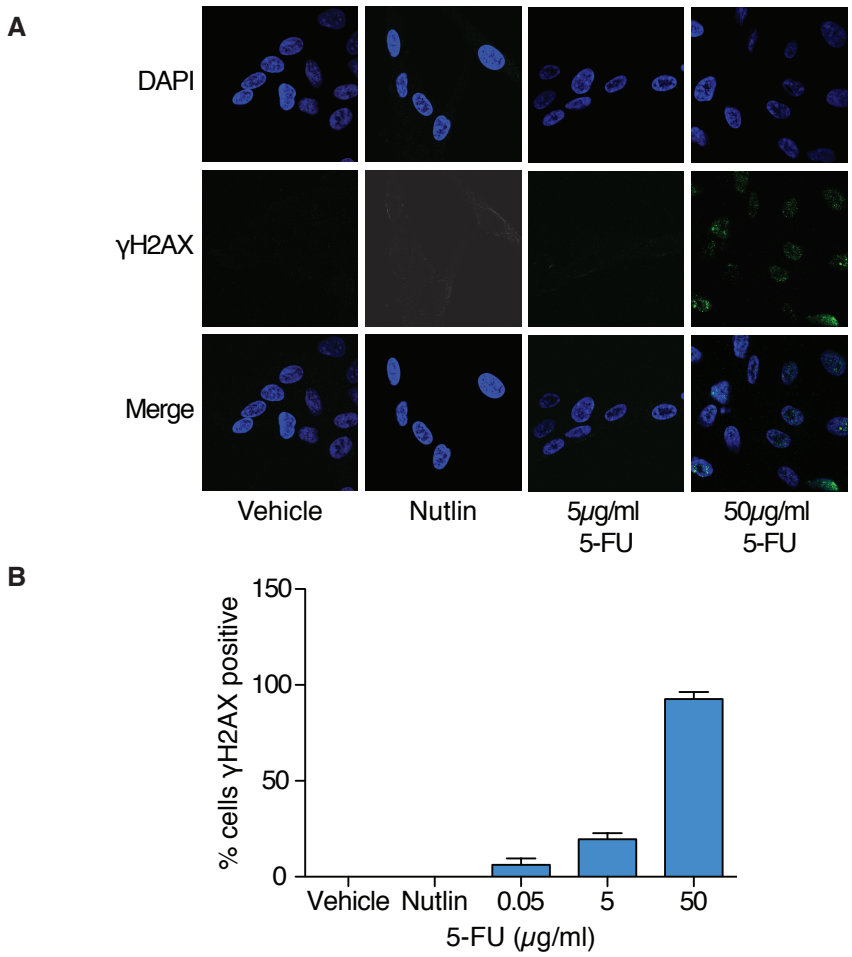

Figure 5-10: 5-FU causes only low levels of γH2AX foci formation at low-dose.
(A) RPE cells were plated on cover slips then treated with indicated doses of 5-FU for 16 hours. Cells were then fixed, permeabilised and incubated with anti- γH2AX antibody followed by AlexaFluoro 466 anti-mouse antibody incubation. Cover slips were mounted on slides and images taken on Olympus FV1000 microscope. (B) Cells with γH2AX foci were counted and the percentage of positive cells plotted using DAPI that stained for nuclei in all cells.

It is difficult to be sure how doses in this low-dose range in cell line studies compare to maximum drug concentration (Cmax) and AUC (Area under the curve) seen in patients when 5-FU is used in its conventional DNA damaging role not least because pharmacokinetic (PK) data demonstrates a large inter-individual PK variability affected by genotype, age, gender, disease state, drug-drug interactions and organ function. Importantly the PK has a direct impact on efficacy and toxicity[649]. In addition the level of dihydropyrimidine dehydrogenase activity in a particular cell line will have a significant impact on the dose of active metabolites that cells are exposed to. In patients this is a clinically significant issue with heterogeneity of dihydropyrimidine dehydrogenase contributing to the PK

variability in a small number of cases and more importantly causing some patients to have severe 5-FU induced toxicity when given conventional 5-FU doses. Studies examining pharmacokinetically guided management, aiming for an optimum AUC of 20-24mg/h/l with an infusional 5-FU/leucovorin schedule resulted in more objective responses, higher survival rates and fewer grade 3/4 toxicities[650, 651]. Despite this pharmacokinetically guided dosing, 5-FU has not been adopted as standard since standard of care is now a chemotherapy doublet. More recently a phase II study has shown that pharmacokinetically guided dosing of 5-FU when given as part of the FOLFOX regimen is also beneficial[651, 652]. Taken overall, however, it is clear that doses of 5-FU that have been used clinically exceed the exposure that would be necessary to induce p53 as a chemoprotective agent.

For further study, a 5-FU dose range of 5-10μg/ml was selected since p53 stabilisation and consequent cell cycle arrest can be seen while there is only very low levels of DNA damage based on the γH2AX foci assays.

5.3 Actinomycin D and 5-FU cause reversible cell cycle arrest.

For the pre-treatment strategy to be feasible it is vital that normal cells arrested by low-dose drug treatment are able to resume normal cycling once the treatment is discontinued. This was examined by studying the cell cycle profile and the longer-term clonogenic capacities of cells upon drug treatment and drug removal.

For cell cycle studies, RPE cells were treated with vehicle or act D 1nM. After 12 hours treatment cells were washed and harvest for FACS to assess the cell cycle profile. Two act D treated plates were incubated in drug free medium then harvested after 12 and 36 hours recovery time. It appeared that 36 hours after removal of act D from cells the proportion of cells in S-phase started to return towards pre-treatment levels (Figure 5-11). This was consistent with the decrease in G1 fraction seen after 36 hours recovery. This suggests that low-dose act D-induced cell cycle arrest is reversible.

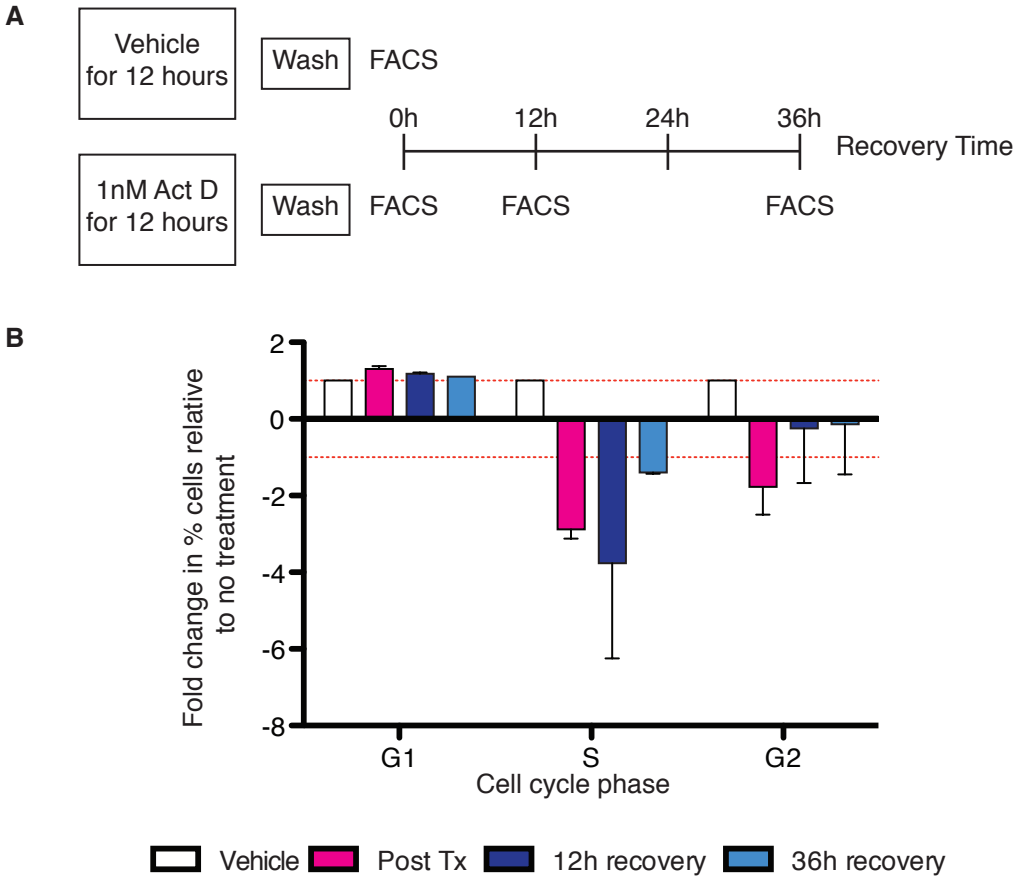

Figure 5-11: Low-dose act D causes a reversible cell cycle arrest.
(A) Schematic of experimental design. (B) RPE cells treated with vehicle or 1nM act D for 12 hours. Medium was removed and cells were washed before incubation in drug free medium for the indicated times. Cells were harvest for PI staining and FACS analysis. Values were plotted as fold change relative to the vehicle treated condition which was set to 1. The mean of two independent experiments is plotted and error bars represent SD.

The reversibility of 5-FU-induced cell cycle arrest was also investigated. RPE cells were treated with vehicle or 10μg/ml of 5-FU for 12 hours followed by drug removal and incubation in drug free medium. Cells were harvested after 24 and 36 hours recovery. p53-induced cell cycle arrest appeared to have resolved by 36 hours as indicated by an increase in S-phase fraction from 2% 24 hours after treatment to 27% after 36 hours recovery (Figure 5-12).

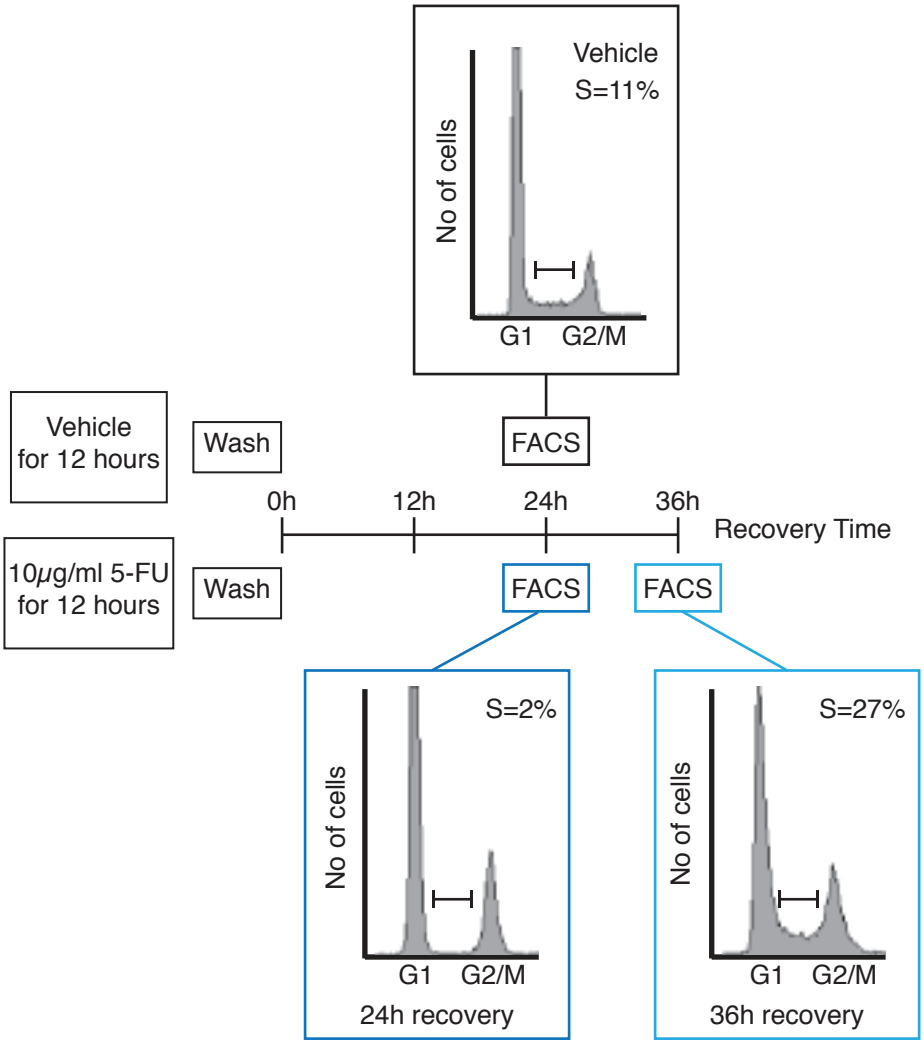

Figure 5-12: Low-dose 5-FU causes a reversible cell cycle arrest.
RPE cells treated with vehicle or 10μg/ml 5-FU for 12 hours. Medium was removed and cells were washed before incubation in drug free medium for the indicated times. Cells were harvest for PI staining and FACS analysis. The bar marks S-phase (S).

Accordingly following 36 hours recovery from 5-FU treatment, levels of p53 returned to pre-treatment levels, as did p21 and MDM2 levels. CDK4 levels show equal protein loading (Figure 5-13).

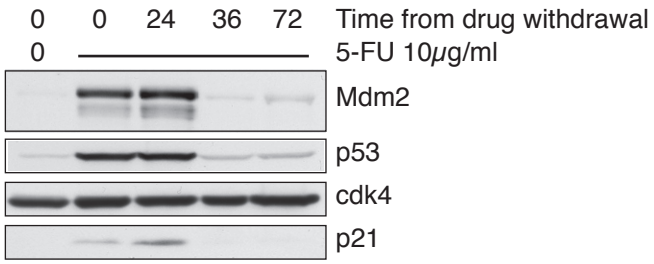

Figure 5-13: After low-dose 5-FU p53 levels normalise after 36 hours recovery.
RPE cells were treated with low-dose 5-FU then allowed to recover. They were then harvested for Western blotting and expression of MDM2, p53, CDK4 (loading control) and p21 was examined.

To examine whether long-term recovery after low-dose drug treatment coincided with a maintenance of clonogenicity, RPE cells were sparsely plated and then treated for 24 hours with vehicle, act D 1nM, act D 10nM, 5-FU 1μg/ml or 5-FU 10mg/ml. Cells were washed and incubated in drug free medium for 9 days. After fixation and Giemsa staining a similar number of colonies could be seen after recovery from the low-dose act D (131 colonies with no treatment and 138 colonies after recovery from 1nM act D) although the colonies were smaller. On recovery from 5-FU, the majority of the colonies were maintained but again smaller (113 colonies with no treatment and 80 on recovery from 1μg/ml). At the higher dose levels of both drugs there is a reduction in the number of colonies – 10nM act D treatment resulted in a drop in colony number from 131 to 73 and for 5-FU the colony number dropped from 113 to 0 after a 10μg/ml treatment (Figure 5-14).

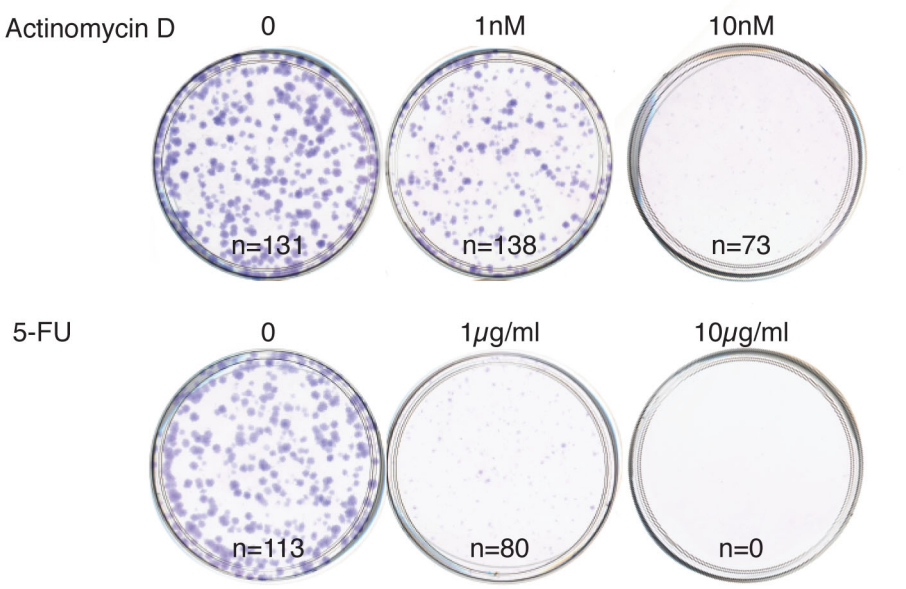

Figure 5-14: After low-dose act D and low-dose 5-FU cells still have clonogenic potential.
RPE cells were plated on 10cm plates (5000 cells per plate). Cells were treated with vehicle, act D or 5-FU at indicated doses for 24 hours. Cells were then incubated in drug free medium for 9 days before Giemsa staining.

5.4 Effects of low-dose actinomycin D are p53 dependent.

To exclude p53 independent off-target effects of low-dose of act D or 5-FU p53 null HCT116 cells were used. To verify that low-dose act D caused similar effects in HCT116 cells as in the cell lines previously studied, HCT116 wild-type or null were treated with vehicle, low-dose act D or Nutlin for 16hrs after which the cell

cycle profile was studied. After both low-dose act D and Nutlin treatment p53 wild-type cells underwent a significant G1 arrest which was not seen in cells null for p53 (Figure 5-15).

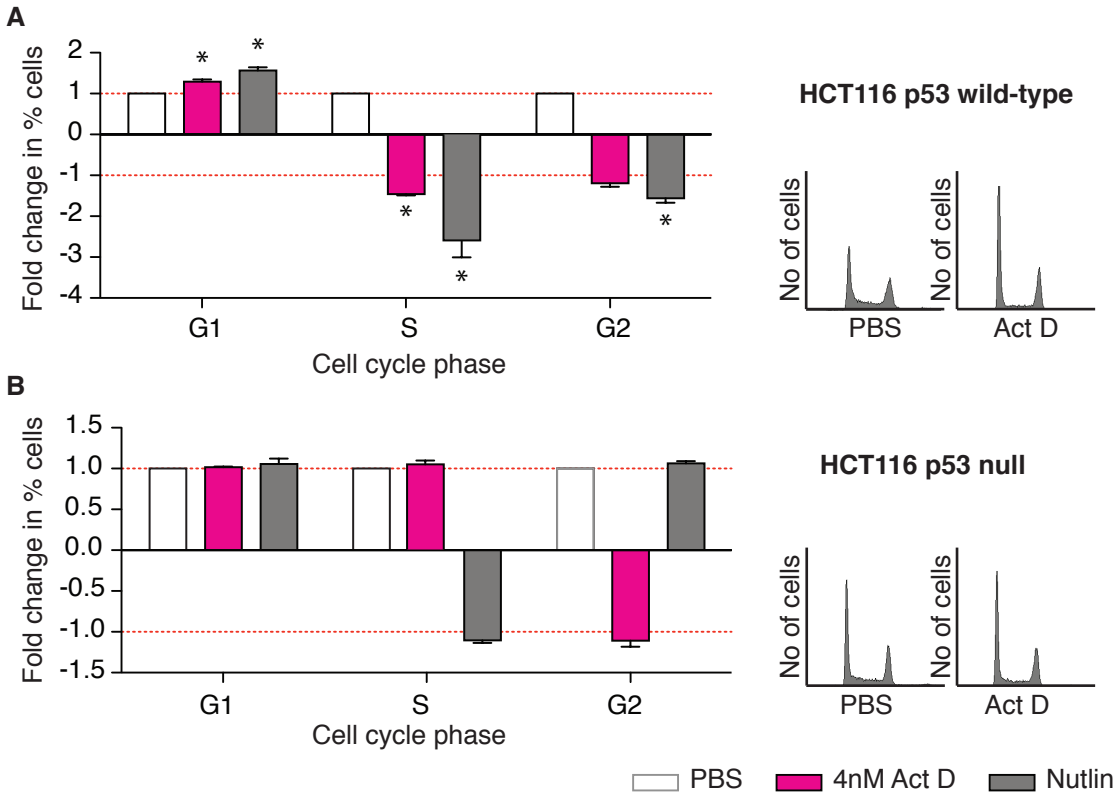

Figure 5-15: Act D has p53 dependent effects on cell cycle.
HCT116 cells wild-type (A) or null (B) for p53 were treated with the indicated doses of vehicle, act D or Nutlin for 16 hours. Cells were harvest for PI staining and FACS analysis. Values were plotted as fold change relative to the PBS treated condition which was set to 1. Error bars *p<0.05 as calculated by Student's T-test.

Next, a colony formation assay was performed in which p53 null HCT116 cells were treated with vehicle, low-dose act D or low-dose 5-FU for 24 hours (Figure 5-15). Cells were then Giemsa stained. Act D treatment had no effect on p53 null cells indicating that the effects of low-dose act D observed in Figures 5-4, 5-6 and 5-7 are p53 dependent. In contrast low-dose 5-FU treatment caused a dramatic reduction in colony formation indicating p53 independent effects. 5-FU at this dosage is therefore unlikely to be a suitable chemoprotective agent.

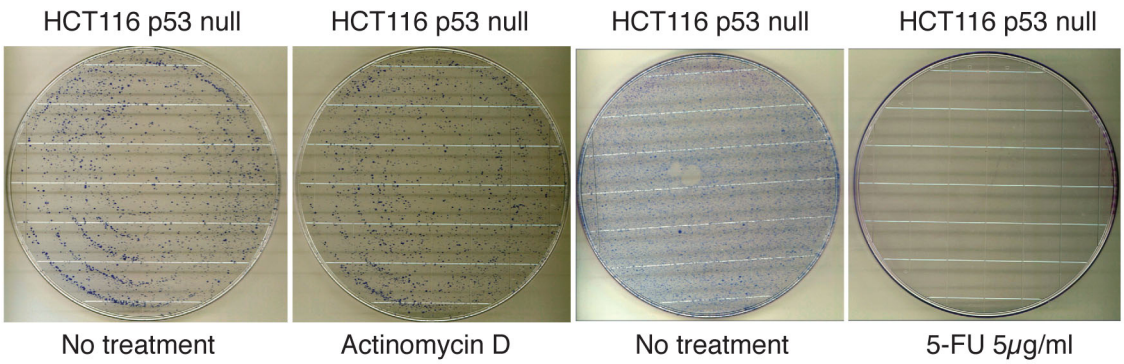

Figure 5-16: Low-dose 5-FU treatment has p53 independent off-target effects on clonogenic survival.
Hct116 cells null for p53 were plated on 15cm plates. Cells were treated with act D (4nM) or 5-FU (5μg/ml) for 24 hours. Cells were washed, fixed and Giemsa stained.

5.4.1 Does low-dose actinomycin D cause ribosomal stress?

Act D's effects on ribosomal RNA biogenesis are thought to lead to ribosomal stress and subsequent translocation of ribosomal proteins such as L11, L5 and L23 to the nucleoplasm where they can bind and inhibit MDM2[653 276, 561]. To confirm that act D-induced p53 activity is initiated via the ribosomal stress pathway, cells treated with act D were examined for evidence of nucleolar disruption. B23, sometimes named nucleophosmin, is a protein normally associated with the nucleolus that can be translocated to the nucleoplasm after ribosomal stress. It has previously been published that act D is capable of disrupting the nucleoli in a dose and duration dependent manner[654], although it has also been shown that disruption of the nucleoli is not necessary for L11-induced p53 activation[655]. Cells were therefore examined for evidence of B23 translocation under treatment conditions used in the present study since its presence confirms nucleolar disruption its absence does not preclude L11-induced p53 activation. U2OS cells were treated with vehicle or act D (5nM) for 16 hours, thereafter B23 localisation was determined by immunofluorescence. Figure 5-17A shows that B23 is located to the nucleolus in untreated cells while after low-dose act D treatment staining is more defuse and not localised to the discreet nucleolar compartments, suggesting that act D indeed caused ribosomal stress under these treatment conditions.

To confirm a corresponding act D induced enhancement in the proportion of MDM2 in complex with L11, MDM2-L11 binding was examined. Consistent with this model, after treatment of cells with act D, MDM2-L11 association was

enhanced (Figure 5-17B). While an increase in MDM2 co-precipitating with L11 was also seen following Nutlin treatment, this resulted from an overall increase in MDM2 levels.

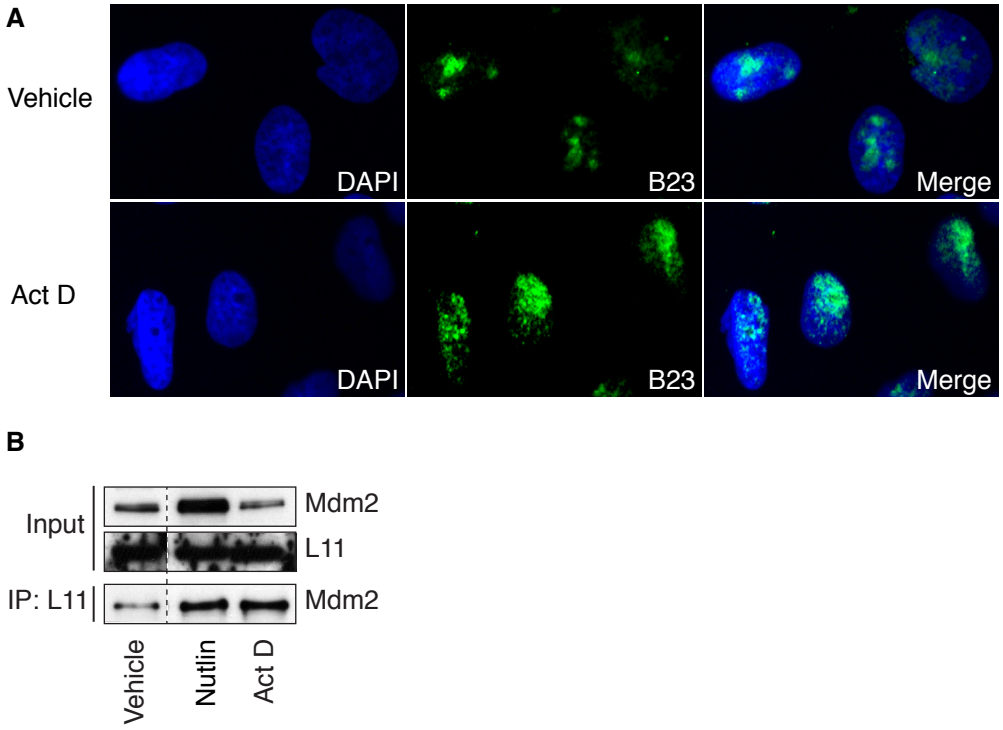

Figure 5-17: Low-dose act D causes ribosomal stress.
(A) U2OS cells were plated on coverslips and treated with vehicle or low-dose act D (5nM) for 16h. The localization of B23 was detected using immunofluorescence with B23 specific antibodies. (B) U2OS cells were treated with vehicle, Nutlin (10μM) or act D (5nM) for 16h. immunoprecipitation (IP) for L11 was then performed, followed by Western blot analysis Expression of MDM2 and L11 in Input and IP samples examined.

Taken together these data show that low-dose act D is clearly capable of inducing ribosomal stress, increasing L11-MDM2 binding and subsequently causing a p53 dependent cell cycle arrest without causing DNA damage.

5.5 Choice of subsequent cytotoxic?

As previous studies have shown the success of the chemoprotection strategy is also dependent on choice of an appropriate chemotherapeutic agent (table 5-1). Furthermore as discussed earlier most success appears to have been demonstrated with chemoprotection/chemotherapeutic combinations where the second agent was an S-phase or M-phase specific drug- that is a drug whose mode of action depends on cells proliferating or dividing. You could however also propose that pre-treatment with a chemoprotective agent prior to other less phase-

specific agents that effect proliferating cells more than resting cells, could still be beneficial.

As also mentioned earlier the objective here is to test the chemoprotection strategy using a combination of agents in current clinical practice since for these agents the DLT will be established and clinical evaluation of the strategy could therefore be more efficiently executed. Other requirements of the appropriate chemotherapeutic agent for combination would be that there is a proven benefit in maintaining dose intensity and that it is currently used for treatment of a tumour site where a reasonable number of tumours would be expected to be p53 deficient (mutant or null).

5.5.1 Mechanism of action of paclitaxel

Paclitaxel meets many of the criteria outlined above. It is the most commonly used mitosis inhibitor, which functions by binding to tubulin causing stabilisation of the mictrotubules and resistance to depolymerisation. This leads to blockade of the transition to anaphase and activation of the mitotic spindle checkpoint and cell death (Figure 5-18).

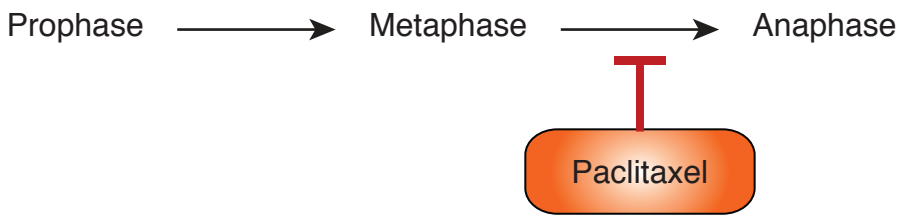

Figure 5-18: Mechanism of action of paclitaxel.
Paclitaxel targets tubulin causing stabilisation of the microtubules and prevents disassembly. This then blocks progression from metaphase to anaphase of mitosis and activates the mitotic spindle checkpoint.

Furthermore paclitaxel is used in the treatment of several tumour sites where there are significant numbers of cancers with a p53 mutation including high-grade serous ovarian cancer, breast cancer and non-small cell lung cancer cancers with p53 mutation rates of 97%[168], 31% and 37% respectively[373]. There have been several clinical studies investigating whether dose-dense paclitaxel leads to clinical benefit and indeed escalated doses did result in improved progression free and overall survival but at the expense of increased treatment related toxicity[656,

[657]. Taken together the combination of a chemoprotective agent with paclitaxel could lead to meaningful increases in dose intensity and therefore patient benefit.

5.5.1.1 Low-dose act D & 5-FU protect wild-type p53 expressing cells from paclitaxel

To test if low-dose act D and low-dose 5-FU are capable of protecting wild-type p53 expressing cells from sequential treatment with paclitaxel, wild-type p53 expressing colorectal cancer cell line, HCT116, were treated with vehicle, act D (2nM) or Nutlin (10μM), as a positive control, for 24 hours. After 24 hours pre-treatment, cells were treated with paclitaxel 3.5nM for 48 hours and then incubated in drug free medium for 5 days. Cell viability was then assessed using a tetrazolium dye (MTT) colorimetric assay. This assay measures activity of mitochondrial reductase enzymes which inactivate shortly after cell death. Both act D and Nutlin pre-treatment resulted in a higher percentage of viable cells following paclitaxel treatment (Figure 5-19).

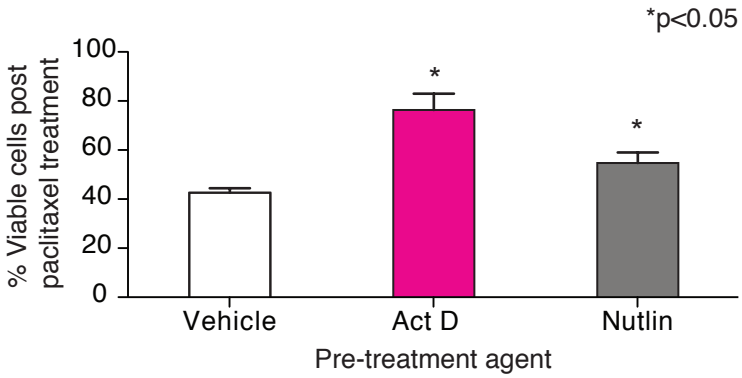

Figure 5-19: Low-dose act D protects wild-type p53 expressing cells from paclitaxel. HCT116 cells expressing wild-type p53 were treated with vehicle/Nutlin/act D then paclitaxel. Viability was measured using an MTT assay. % Viable cells was calculated by dividing average absorbance values for each of vehicle-paclitaxel, act-D-paclitaxel or Nutlin-paclitaxel by values for respectively vehicle, act D or Nutlin treated cells without post-treatment and multiplied by 100. Plotted are the mean values of 4-8 replicates and SEM of three independent experiments. P-values were calculated using a Student's T-test. * indicates significant difference relative to vehicle pre-treatment.

Similarly, the protective effects of 5-FU were demonstrated in wild-type p53 expressing RPE cells that were treated with vehicle, 5-FU (3μg/ml) or Nutlin (10μM) prior to paclitaxel treatment. 5-FU pre-treatment also caused a significant increase in the remaining viable cells (Figure 5-20).

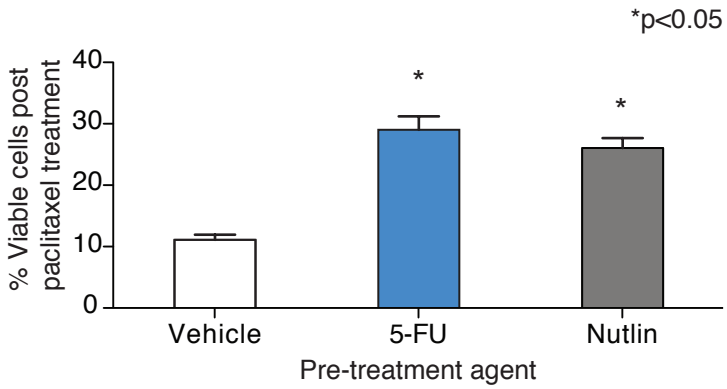

Figure 5-20: Low-dose 5-FU protects wild-type p53 expressing cells from paclitaxel. RPE cells were treated with vehicle/Nutlin/5-FU then paclitaxel. Viability was measured using an MTT assay. % Viable cells was calculated by dividing average absorbance values for each of vehicle-paclitaxel, 5-FU-paclitaxel or Nutlin-paclitaxel by values for respectively vehicle, act D or Nutlin treated cells without post-treatment and multiplied by 100. Plotted are the mean values of 4-8 replicates and SEM of three independent experiments. P-values were calculated using a Student's T-test.

Histone H3 is phosphorylated during mitosis and therefore after paclitaxel treatment high levels of pHH3 would be expected since cells can not progress beyond metaphase. As a proof of principle, 5-FU's potential to protect cells from subsequent paclitaxel-induced histone 3 phosphorylation was also examined. HCT116 cells were treated with vehicle, 5-FU (3μg/ml) or Nutlin (5mM) for 24 hours then paclitaxel (7nM) for a further 24 hours. Phosphorylation of histone H3 was measured by immunostaining. DNA was also stained with DAPI. Staining was quantified with an Operetta automated microscope and, the percentage of cells positive for phosphohistone H3 was calculated. Using this assay 5-FU pre-treatment clearly prevented histone H3 phosphorylation similar to Nutlin pre-treatment (Figure 5-21).

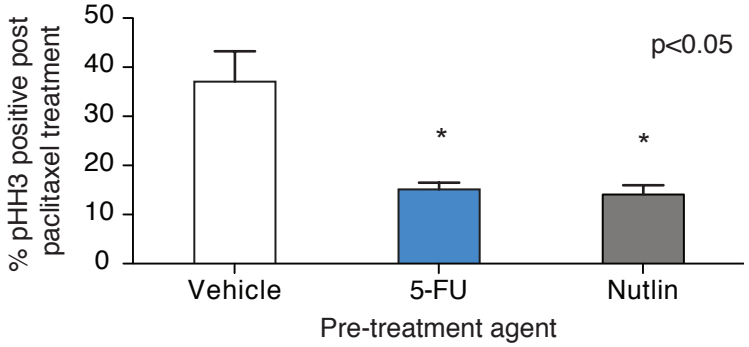

Figure 5-21: 5-FU pre-treatment protects wild-type p53 expressing cells from paclitaxel. HCT116 cells were treated with pre-treatment agent indicated then paclitaxel. Cells were then fixed, permeabilised, and stained for pHH3. % pHH3 positive cells was quantified using the Operetta system. Mean values are plotted and error bars represent SD. 10 000 cells were evaluated.

In addition to the chemoprotective effects of Nutlin and LD doxorubicin on paclitaxel treatment (table 5-1), these results now demonstrate that also pre-treatment with a low-dose of 5-FU or act D can both have protective effects.

5.5.2 Mechanism of action of cisplatin

Cisplatin is another widely used chemotherapeutic[658]. It is used in the treatment of several solid tumours most of which have significant p53 mutation rates[373]; testicular cancer (5%), bladder cancer (26%), squamous head and neck cancer (41%), oesophageal cancer (45%) and ovarian cancer (97%)[168]. It is an organic heavy metal complex. After diffusing into the cell it loses its chloride ions allowing it to bind to DNA causing intrastrand cross-linking lesions and other less abundant lesions (interstrand cross-linking) (Figure 5-22).

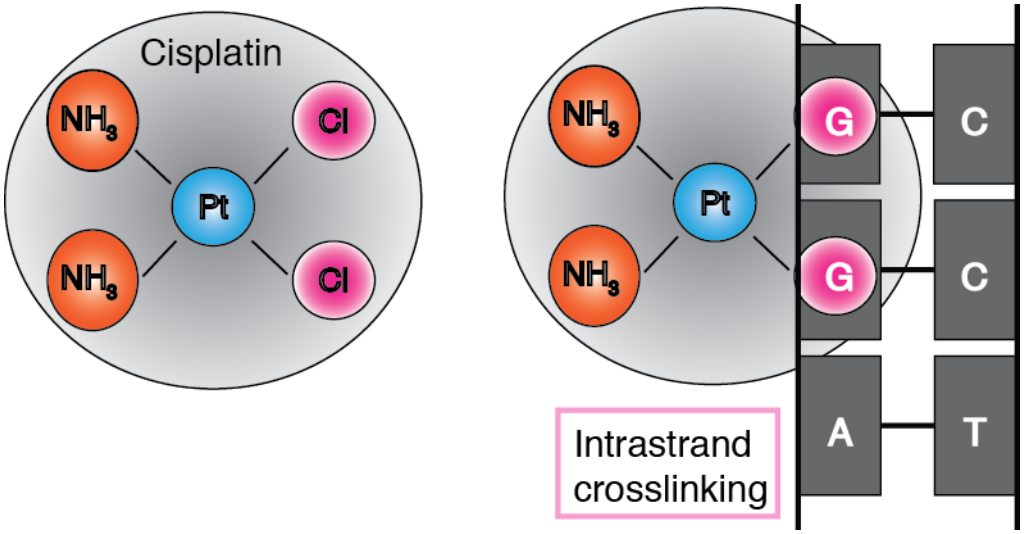

Figure 5-22: Mechanism of action of cisplatin.
Cisplatin causes G-G intrastrand DNA crosslinking as well as C-G intrastrand DNA crosslinking (not shown here) which is much less frequent. Cisplatin also causes interstrand bridging (again not detailed here). Pt=platinum.

These intrastrand lesions are repaired by nucleotide excision repair mechanisms while double strand breaks are repaired by recombinational repair. Together this leads to inhibition of RNA transcription, DNA replication, chain elongation of DNA polymerisation and cell death[659]. Cisplatin can cause DNA lesions regardless of the cells' cell cycle phase and is therefore a cell cycle non-specific agent[660]. Cells that are undergoing proliferation are however more sensitive to cisplatin-induced cytotoxicity than those in a resting phase. In addition it has been shown that achieving a high dose-intensity of cisplatin can have a significant beneficial impact

on clinical outcome for some cancers[661, 662]. Reducing the proliferation of normal, wild-type p53 expressing cells prior to cisplatin treatment may allow increased dose delivery and therefore lead to increased cell death of a p53 deficient tumour.

5.5.2.1 5-FU but not actinomycin D protects wild-type p53 expressing cells from cisplatin toxicity

To assess chemoprotection from cisplatin toxicity in wild-type p53 expressing cells, U2OS cells were treated with vehicle, act D, 5-FU or Nutlin prior to treatment with cisplatin. Act D significantly reduced the viability of cells following cisplatin treatment while Nutlin pre-treatment had no effect on the viability of cells following cisplatin treatment (Figure 5-23 A).

Notably, 5-FU pre-treatment appeared to result in an increase in the remaining viable cells following cisplatin treatment (Figure 5-23 B).

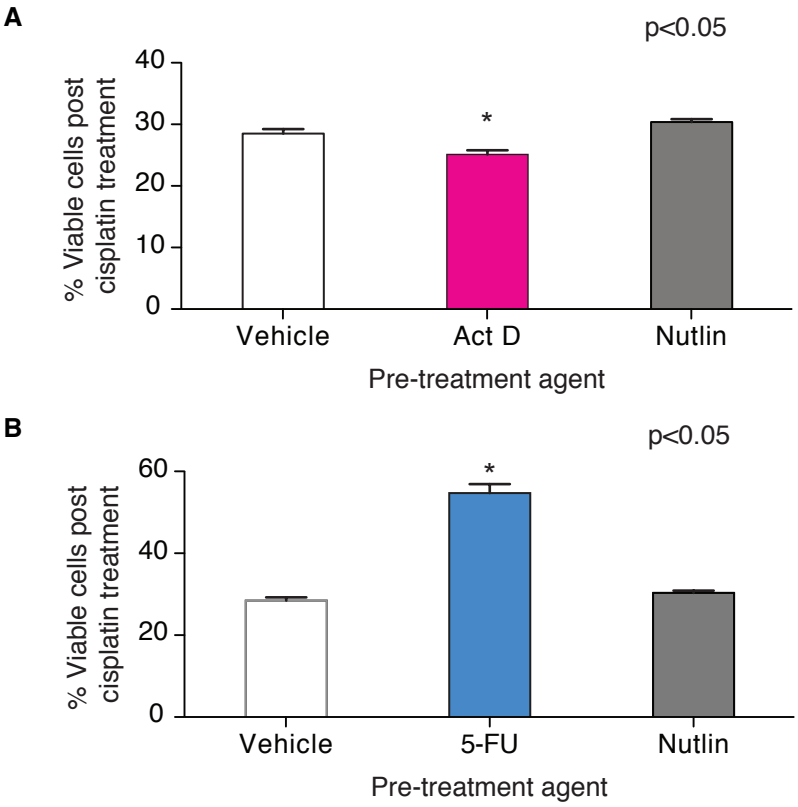

Figure 5-23: Act D or 5-FU prior to cisplatin treatment of wild-type p53 expressing cells.

% Viable cells was calculated by dividing average absorbance values for of 4-8 replicates of vehicle-cisplatin, act D-cisplatin (A), 5-FU-cisplatin (B) or Nutlin-cisplatin by values for vehicle or corresponding protective agent then multiplying by 100. Values plotted are therefore relative to the vehicle or protective agent treatment. Plotted here is the mean value and SEM of three independent experiments. P-values were calculated using Student's T-test.

Given the promising results of 5-FU as chemoprotective agent against cisplatin toxicity, an alternative assay was used to verify these results. Since cisplatin is a DNA damaging agent, immunofluorescence of γH2AX foci was used to quantify DNA damage following cisplatin. HCT116 cells were treated with vehicle or 5-FU (3μg/ml) followed by cisplatin (7.5μg/ml) treatment for 24 hours and after immunostaining levels of γH2AX and DAPI were measured and γH2AX signal per nuclei was calculated. 5-FU pre-treatment was also able to protect cells from genotoxic damage caused by subsequent cisplatin treatment since the 5-FU pre-treatment condition showed a smaller proportion of cells positive for γH2AX foci (Figure 5-24).

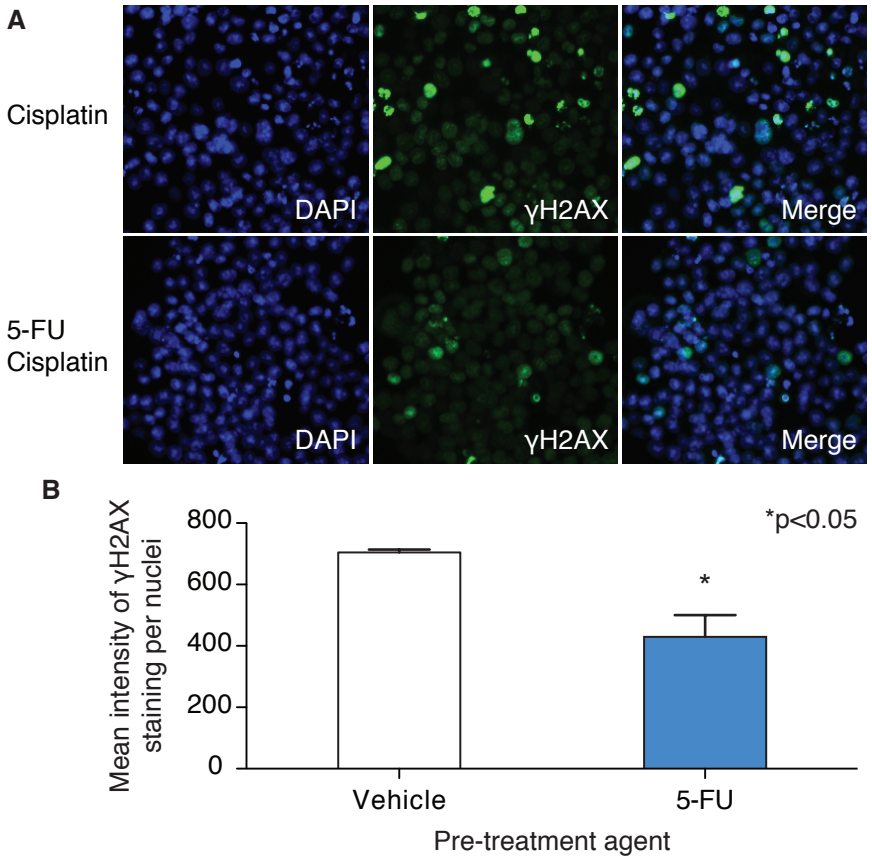

Figure 5-24: 5-FU pre-treatment protects wild-type p53 expressing cells from cisplatin treatment.
(A) HCT116 cells were treated with pre-treatment agent indicated then cisplatin. Cells were then fixed, permeabilised, and stained for γH2AX. (B) γH2AX intensity per nuclei was quantified using the Operetta system. Mean values are plotted and error bars represent SD. 10 000 cells were evaluated.

Taken together, these results indicate that 5-FU, but not Nutlin or act D, could be used in a chemoprotective strategy against cisplatin toxicity.

5.6 Are p53 deficient cells protected?

To test if act D treatment protects p53 null cells from paclitaxel or cisplatin, MTT assays were performed, this time with isogenic HCT116 cells null for p53 (Figure 5-25 A).

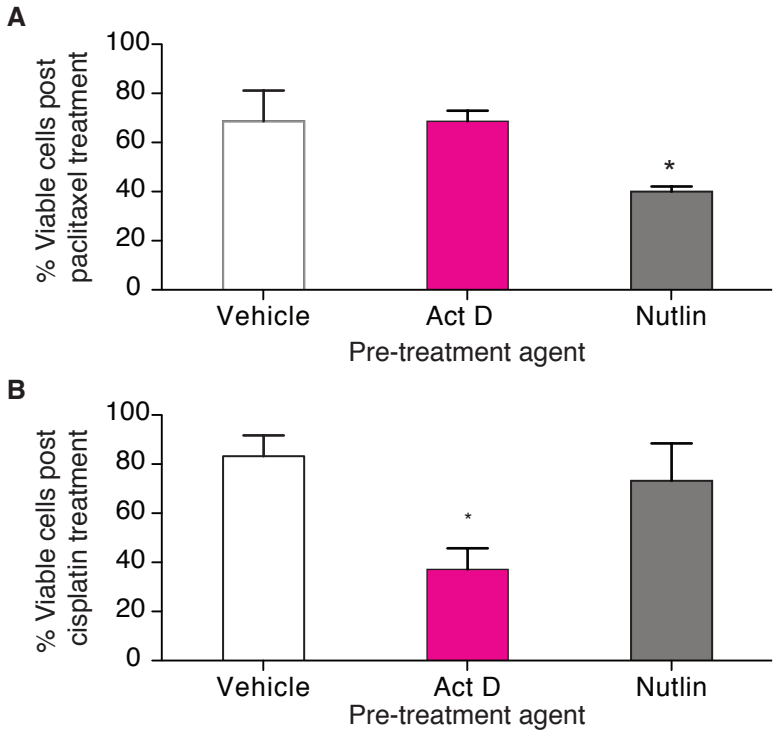

Figure 5-25: Act D does not protect p53 null cells from paclitaxel or cisplatin-mediated decreased cell viability.
p53 null HCT116 cells were plated in 96 well plates and treated with the indicated pre-treatment agent. Cells were subsequently treated with (A) paclitaxel or (B) cisplatin. An MTT assay was then performed. % Viable cells was calculated by dividing average absorbance values for each of vehicle-paclitaxel, act-D-paclitaxel or Nutlin-paclitaxel by values for respectively vehicle, act D or Nutlin treated cells without post-treatment and multiplied by 100. Plotted are the mean values of 4-8 replicates and SEM of three independent experiments. P-values were calculated using a Student's T-test.

Nutlin pre-treatment appears to enhance the cell death caused by paclitaxel treatment in p53 null cells while act D pre-treatment has no effect (Figure 5-25 A). Act D pre-treatment enhances cisplatin induced cell death while Nutlin appears to have no effect (Figure 5-25 B). Although the underlying mechanisms of the additive toxic effects of Nutlin on paclitaxel or act D on cisplatin treatment are unknown, these effects could be beneficial in killing tumour cells without p53, but will require further study.

Act D pre-treatment shows no evidence of protection of p53 null cells making it a suitable agent for further evaluation as a chemoprotective agent. These results

also demonstrate that the protective effect seen after act D pre-treatment, of wild-type p53 expressing cells prior to paclitaxel, observed in Figure 5-19, is p53 dependent.

To investigate the effects of 5-FU pre-treatment on the response to paclitaxel and cisplatin, p53 deficient HCT116 cells were pre-treated with vehicle, act D (4nM) or 5-FU (3μg/ml) for 24 hours then treated with paclitaxel (7nM) or cisplatin (7.5μg/ml) for a further 24 hours. Immunofluoresence for pHH3 and γH2AX were used to assess the effect of paclitaxel and cisplatin respectively (Figure 5-26).

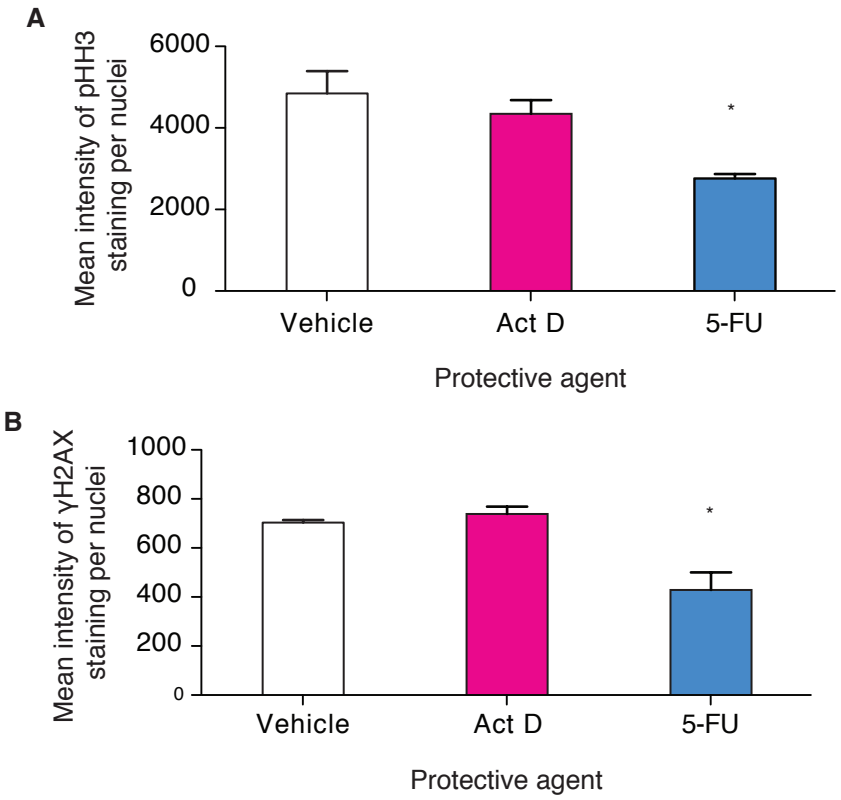

Figure 5-26: 5-FU protects p53 deficient cells from paclitaxel induced phosphorylation of histone H3 and cisplatin induced γH2AX foci formation.
(A) HCT116 p53 null cells treated with vehicle/ act D/5-FU then paclitaxel then stained for pHH3 and DAPI. Quantification of mean intensity per nuclei calculated on Operetta. At least 10 000 cells counted. Means and standard deviation plotted. (B) HCT116 p53 null cells treated with vehicle/ act D/5-FU then Cisplatin then stained for γH2AX and DAPI. Quantification of mean intensity per nuclei calculated on Operetta. At least 10 000 cells counted. Means and standard deviation plotted. *p<0.05, Student's T-test.

While act D had no effect on pHH3 or γH2AX levels, 5-FU treatment prior to both paclitaxel and cisplatin appeared to protect p53 null cells.

5.7 Summary and discussion

In an attempt to accelerate the journey to adoption of the chemoprotective strategy in clinical practice, the data presented here explores the usefulness of two traditional low-dose chemotherapeutics, with known MTD and DLTs, as chemoprotectants prior to treatment with other cytotoxics commonly used in clinical practice. While none of the therapeutic drugs used here may be ideal (for example it may be preferable to use Nutlin or another direct inhibitor of MDM2, rather than act D of 5-FU), this limitation would be outweighed by the potential to devise new therapeutic strategies based on existing clinically approved drugs.

The data presented here shows that low-dose act D and low-dose 5-FU are both capable of stabilising p53 without overt genotoxic damage. Importantly, the cell cycle arrest seen following treatment was reversible following removal of drug. Furthermore both act D and 5-FU were capable of protecting wild-type p53 expressing cells from subsequent paclitaxel treatment while only 5-FU appeared capable of protecting wild-type p53 expressing cells from cisplatin treatment (table 5-2 summarises the findings).

Table 5-2: Combinations examined in the present study.

Protective	Therapeutic agent	Protection	
		p53 wild-type	**p53 deficient**
LD act D	**Paclitaxel**	Yes	No
	Cisplatin	No	No
LD 5-FU	Paclitaxel	Yes	Yes
	Cisplatin	Yes	Yes

LD=Low-Dose, act D=Actinomycin D
Grey shaded boxes indicate combinations where wild-type p53 expressing cells are protected from cytotoxic effects while p53 deficient cells are not.

Kranz and Dobbelstein previously explored the combination of Nutlin pre-treatment prior to cisplatin treatment and found that Nutlin was not capable of protecting p53 wild-type cells from subsequent cisplatin treatment. It is therefore not surprising that low-dose act D is also not able to be chemoprotective in this setting[615]. Cisplatin can intercalate and cause DNA damage regardless of cell cycle phase so although act D pre-treatment will have arrested wild-type p53 expressing cells they remain sensitive to the cytotoxic effects of cisplatin.

It is therefore interesting to observe that low-dose 5-FU treatment appears to protect wild-type p53 expressing cells from cisplatin treatment as measured by a reduction in the formation of γH2AX foci following cisplatin and a smaller reduction in metabolic activity following cisplatin treatment in comparison with no pre-treatment. The mechanism of low-dose 5-FU protecting cells from cisplatin was not investigated further because of the p53 independent effects observed for 5-FU. Although this alone does not make 5-FU an entirely unsuitable chemoprotectant, the ability of low-dose 5-FU to protect p53 null cells from both paclitaxel and cisplatin does. The mechanism of protection would however be interesting to explore since the combination of cisplatin and 5-FU is frequently used in clinical practice. When given in combination usually platinum is followed by 5-FU although when the oral fluoropyrimidine capecitabine is used in combination with platinum the oral dosing starts prior to platinum. The reason for this sequence of the intravenous regimen is practical since cisplatin treatment requires hours of pre and post hydration and then the subsequent 5-FU is administered by a prolonged infusion. Certainly clinical data suggests that this combination of agents is more effective than either agent alone[663]. It would be interesting to explore the impact of the specific scheduling of the drugs. Clearly the data presented here used low doses of 5-FU while the clinical data examining the cisplatin and 5-FU combination used DNA damaging doses of 5-FU.

Interestingly in p53 null cells both low-dose act D and Nutlin pre-treatment were shown to increase the effects of cisplatin and paclitaxel respectively. This is obviously a desirable effect of a chemoprotective agent. It would be interesting to further explore the mechanism of this increased cellular toxicity. Previous studies have shown that in p53 deficient cells Nutlin is capable of increasing apoptosis by disrupting p73-MDM2 binding and therefore activating its pro-apoptotic activities[664, 665]. Additionally Nutlin can inhibit MDM2-E2F1 binding allowing it to contribute to the upregulation of pro-apoptotic activities via p73 and Noxa[666]. Why there should be a difference in act D and Nutlin pre-treatment in terms of contributing to apoptosis caused by a DNA damaging agent and a mitotic spinal poison is unclear however an obvious difference between these 2 agents is their mechanism of p53 activation. While act D induces stabilises p53 via the ribosomal pathway, Nutlin

activates p53 by inhibition of the MDM2-p53 interaction. It would be interesting to explore whether MDM2-L11 complex is capable of binding to E2F1 and p73.

Data presented here explored the chemoprotection strategy in p53 null cells only. Obviously it would be valuable to explore the strategy further in p53 mutant cells. Some preliminary cell line studies using isogenic HCT116 cells mutant for p53 suggest that low-dose act D does not protect cells from subsequent paclitaxel.

The combination of low-dose act D followed by paclitaxel is suitable for further evaluation. Data presented here confirmed that low-dose act D reversibly protected wild-type, but not null p53 cells from paclitaxel. In the treatment of cancer patients with cytotoxic drugs a key principal is to achieve a balance between therapeutic response and toxicity to normal tissues (the therapeutic index). Toxicity, tumour response and survival outcomes are related to systemic exposure[667-669]. In the first instance xenograft studies where wild-type p53 normal tissues and a p53 deficient xenograft can be assessed simultaneously would be useful. In addition the strategy should be examined in transgenic mouse models with conditional mutant p53 knock-in/p53 knock-out where a p53 deficient tumour can be examined within its wild-type p53 microenvironment. Study of the strategy *in vivo* is vital since the success of the strategy depends on the ability to escalate the dose of the chemotherapeutic agent significantly. Although act D's ability to protect wild-type expressing cells from paclitaxel has been shown here the ability to escalate paclitaxel dose has so far not been evaluated. Although pre-treatment would be expected to attenuate the myelosuppressive effects of paclitaxel it may not attenuate paclitaxel induced-neurotoxicity, non-haematological toxicities or toxicities related to the solvent required for delivery of paclitaxel. Consequently new dose limiting toxicities will emerge. Whether the therapeutic gain achieved by the increase in dose of paclitaxel is sufficient to compensate for the reduced cytotoxicity as compared with the combination of drugs used at their therapeutic/cytotoxic doses remains to be seen. *In vitro* testing of the strategy could give some clues of the likely emerging dose limiting toxicities, the potential dose escalation achievable and the therapeutic efficacy of the strategy.

For clinical studies to be able to evaluate the chemoprotective strategy using the low-dose act D/paclitaxel combination it is necessary to have a robust

pharmacodynamic marker of p53 activation since unlike conventional dose finding studies the aim is not to reach DLT with the pre-treatment but only to stabilise p53. The development of potential pharmacodynamic biomarkers of MDM2 inhibition (p53 activation) is discussed further in chapter 6.

6 Biomarkers of p53 activation

6.1 The clinical challenge

The ultimate aim of this work was to set up a clinical study to investigate the potential of MDM2 inhibitors as chemoprotective agents in patients with a p53 deficient tumour.

Clinical evaluation of the chemoprotective strategy would require the ability to demonstrate either the minimum dose required for MDM2 inhibition in a dose escalation study or, in an alternative de-escalation study design, evidence of MDM2 inhibition in the absence of genotoxic damage. Since MDM2 inhibition is designed to release p53 from MDM2 mediated degradation and therefore allow accumulation of p53 and restoration of anti-tumour activities, measurement of p53 accumulation could serve as a biomarker of MDM2 inhibition. Obviously any biomarker developed here would also be useful in studies developing MDM2 inhibitors in their role in the treatment of wild-type p53 tumours. In this therapeutic role evidence of p53 activation/absence of DNA damage would ideally be demonstrated in the tumour tissue. However, this is frequently not feasible because of the invasive procedures required for repeated tumour biopsy. The aim here was therefore to develop an assay using easily accessible material that could provide a robust biomarker of normal tissue p53 activation (for use in chemoprotection studies) and tumour p53 activation (for therapeutic studies).

The easy accessible normal tissues that would most likely demonstrate activation of p53 following chemotherapy treatment are the rapidly dividing cells of the hair follicles and haemopoietic system, as these are most sensitive to p53 dependent chemotherapy induced cell death.

Hair growth involves cycling through 4 stages; anagen, exogen (early anagen), catagen and telogen (Figure 6-1)[670]. Anagen phase encompasses migration of stem cells from the bulge, part of the upper outer root sheath, to the dermal papilla where the dividing matrix cells reside. A new hair is formed and the old hair shed (exogen) following which the lower hair follicle is destroyed but the dermal papilla remains associated with the regressing follicle in catagen phase. In telogen the follicle rests until a new growth cycle is initiated. At one time 90% of hair follicles are in anagen with rapidly dividing matrix cells susceptible to the effects of

chemotherapy. Furthermore the process of chemotherapy-induced alopecia is known to depend on p53 as demonstrated by the p53 knockout mouse, which does not develop chemotherapy-induced alopecia[671, 672].

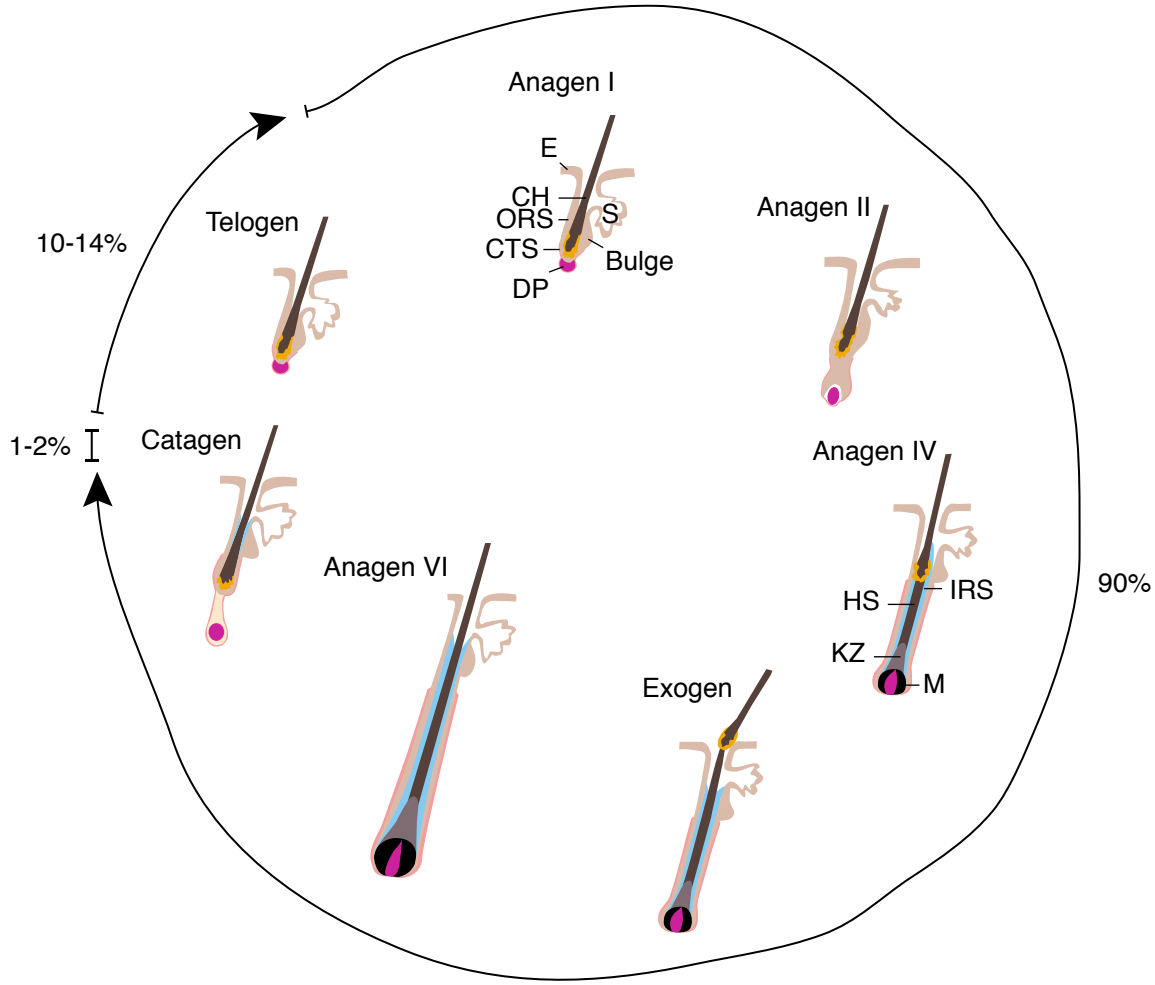

Figure 6-1: Hair growth cycle.
The dermal papilla signals to the stem cells in early anagen (anagen I). Matrix cells proliferate (anagen II) and a new hair shaft is produced and the old hair is released (anagen IV/exogen). During catagen the lower 2/3 of the follicle is destroyed but the dermal papilla remains associated with the regressing follicle. The hair develops a club structure at its base retaining the hair follicle. In telogen the follicle rests until a new growth cycle is initiated. The % given denotes the average % follicles in each phase of the cycle. (E=Epidermis, CH=Club Hair, ORS=Outer Root Sheath, CTS=Connective Tissue Sheath, DP=Dermal Papilla, S=Sebaceous Gland, HS=Hair Shaft, KZ=Keratogenous Zone, IRS=Inner Root Sheath, M=Matrix. Adapted from Cotsarelis and Millar, 2001.

Many groups have used immunofluorescence of hair follicles to study stem cells and a variety of signalling pathways in animal models[673, 674]. In animal studies the hair follicle is usually examined by taking dermal samples so that the follicle is always intact. To date there has been some limited success showing immunofluorescence/immunohistochemistry on plucked hair follicles as a potential pharmacodynamic marker of modulation of some signalling pathways for which

anti-cancer drugs are being developed[537, 538, 541, 543, 544, 675]. In examining plucked hair samples hairs need to have an intact bulb so that the outer root sheath ensures harvest of the chemotherapy sensitive matrix cells of the follicle. This approach has so far not been investigated as a pharmacodynamic marker of p53 activation.

Blood sampling is another easily accessible tissue source that can provide a substitute for tissues not easily accessible i.e. tumour tissues. Again due to their highly proliferative nature, blood cells are sensitive to biological alterations caused by systemic anticancer treatment.

Peripheral blood mononuclear cells (PBMCs) can be separated from whole blood by density gradient centrifugation using Ficoll, where red blood cells (RBCs) aggregate with Ficoll forming a lower plug and other blood constituents separate into layers based on their weight (Figure 6-2). Following Ficoll separation of whole blood, isolated PBMCs comprise of the lymphocytes (T cells, B cells and Natural Killer cells) (58-68%) and monocytes (32-40%). Collection of PBMCs is relatively easy and can be undertaken in multiple clinical sites, since it requires only basic equipment and expertise. In addition, PBMCs can be stored in liquid nitrogen for a significant length of time without affecting cell viability[676]. Importantly this allows time for cells to be shipped to the appropriate lab for processing.

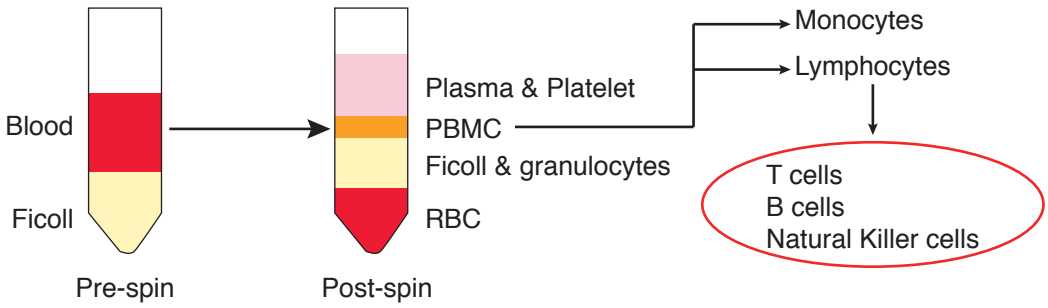

Figure 6-2: PBMC isolation using Ficoll.
Adapted from www.emdmillipore.com. RBC=Red Blood Cells

Serum or plasma may also provide markers for p53 activation, and both of these are easily accessible. Cell line and xenograft studies have shown that the secreted p53 target macrophage inhibitory cytokine -1 (MIC-1) is highly induced after genotoxic damage of p53 wild-type cells but not cells with a mutant or null p53 status[544, 571, 677, 678]. In addition, since MIC-1 is secreted it may provide a read out

of p53 activation from both normal cells and tumour (depending on the p53 mutation status of the tumour).

MIC-1 is a divergent member of the transforming growth factor beta family (TGF-β) and is also known as prostate-derived factor (PDF), placental TGF- β, placental bone morphogenetic protein, non-steroidal anti-inflammatory drug-activated gene-I or its murine ortholog growth differentiation factor-15. As a member of the TGF-β family, MIC-1 has diverse roles in cancer. In the early cancer stages MIC-1 has an anti-tumour role while in the late stages it promotes metastasis[679]. Interestingly it has been found to have a role in the pathogenesis of cancer associated weight loss and is produced in response to secretion of inflammatory cytokines[680].

Presently some early clinical studies of MDM2 inhibitors are using plasma or serum MIC-1 level as a potential biomarker for p53 activation[426].

As discussed in chapter 5 it was previously suggested that low-dose 5-fluorouracil (5-FU) may be useful as a non-genotoxic p53 activator, consistent with clinical data showing that mutant p53 expressing tumours are less likely to respond to 5-FU treatment, although in these studies high dose 5-FU was examined[681, 682]. Since the initial hypothesis was that low-dose 5-FU could be used as a chemoprotective agent, and since it is used in clinical practice in adults much more frequently than act D, patients receiving a 5-FU based regimen (using conventional cytotoxic 5-FU doses) were recruited to a sampling study to examine chemotherapy induced p53 activation in normal tissues.

6.2 The sampling study design

Originally a sampling study (MI45) was initiated in which serum and plasma samples were collected from patients with gastrointestinal cancers prior to and following 5-FU based chemotherapy treatment to explore 5-FU induced changes in the proteome. Patients recruited between 2004 and 2008 therefore had collection of serum and plasma only. In 2008 an amendment to the study was made to extend the study to allow examination of easily accessed normal tissues pre and post 5-FU for modulation of the p53 pathway with the aim of developing a

pharmacodynamic biomarker of p53 activation. Patients recruited post 2008 therefore had collection of serum, plasma, PBMCs and hair follicles.

6.3 Patient characteristics

The whole MI45 population consisted of 116 patients, 20 of whom had collection of serum, plasma, PBMCs and hair follicles. The patient population was highly heterogeneous as detailed in table 6-1.

Table 6-1: Study patient characteristics.

Characteristics		Number of patients
Age	Median	68
	Range	22-87
Gender	Male	72
	Female	44
Primary tumour site	Colorectal	55
	Oesophago-gastric	61
Disease extent	Unknown	1
	Adjuvant	16
	Locally advanced	21
	Metastatic	78
Chemotherapy	ECF	46
	Capecitabine	40
	Capecitabine (45Gy, 25)	9
	CF	5
	ECX	4
	Modified de Gramont	4
	CarboF	2
	EOX	1
	CAPOX	1
	ECarboF	1
	CAPOX/CETUX	1
	EOF	1
	ECX/Bev	1
Chemotherapy cycles	Median	4
	Range	1-12
Best clinical outcome	Non-evaluable	8
	Partial/complete response	28
	Stable disease	42
	Progressive disease	38

ECF=Epirubicin/Cisplatin/5-FU, CF=Cisplatin/5-FU, ECX=Epirubicin/Cisplatin/Xeloda, CarboF=Carboplatin/5-FU, EOX=Epirubicin/Oxaliplatin/Xeloda (Capecitabine), CAPOX=Capecitabine/Oxaliplatin, ECarboF=Epirubicin/Carboplatin/5-FU, CETUX=Cetuximab, EOF=Epirubicin/Oxaliplatin/5-FU, Bev=Bevacizumab.

The median patient age was 68 years old and the majority of patients were male. 55 patients had colorectal cancer and 61 oesophagogastric cancer. The vast majority of patients had metastatic disease (67% (78 patients)). In total 13 different chemotherapy schedules were used. The common backbone to all regimens was 5-FU either intravenously or as the oral fluoropyrimidine capecitabine. As explained in chapter 5, 5-FU is a p53 stabilising agent, which stabilises p53 at a low-dose via the ribosomal stress pathway and at a high dose via the DNA damage pathway. All patients would therefore be expected to have increased p53 levels following chemotherapy administration. The median number of chemotherapy cycles delivered was 4, which, depending on the regimen means a median of 8-12 weeks of treatment. Of 116 patients, 8 were not evaluable for response due to either no measurable disease or no scans being performed. All patients had blood sampling prior to administration of any treatment and at some time following chemotherapy. The timing of the post chemotherapy sample was variable depending on the patients' particular chemotherapy regimen. The vast majority of patients had their post treatment sample on cycle 2 day 1.

6.4 Hair follicle analysis

For a subset of patients hair follicles were collected for immunohistochemistry /immunofluorescence. Hair was plucked from the eyebrow of patients prior to receiving chemotherapy and then again prior to delivery of the subsequent chemotherapy cycle. The time from last chemotherapeutic administration was therefore dependent to the particular chemotherapy schedule. The eyebrow was the chosen site for hair plucking since eyebrow hairs are less frequently lost during chemotherapy treatment. In addition plucking an eyebrow hair is accepted as less uncomfortable than plucking a scalp hair.

For assay development, eyebrow hairs were plucked from healthy volunteers, formalin fixed and paraffin embedded. Sections were taken in longitudinal and in transverse section and Hematoxylin and Eosin (H&E) stained. In Figure 6-3 the nuclei of the hair follicle can be seen in both dimensions. Due to the structure of the hair follicle it was extremely difficult to determine its orientation and frequently the hair was lost from the block completely on sectioning. Limited published data has shown some success in immunohistochemistry of hair follicles using a more

viscous resin block; however this change in technique would require major investment and expertise that was beyond the scope of this study. An alternative option of immunofluorescence on intact hair follicles (rather than sections) with confocal imaging was explored[537, 538, 683].

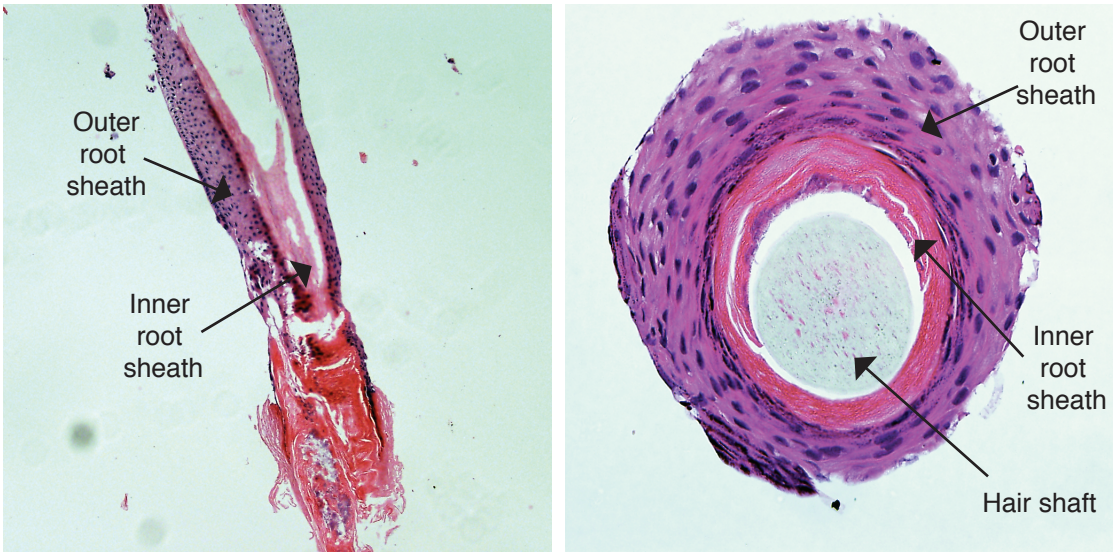

Figure 6-3: H&E staining of a hair follicle.
Hair follicles were formalin fixed and paraffin embedded then sectioned and H&E stained. Purple nuclei of the hair follicle can be seen in both dimensions. The inner root sheath and outer root sheath can also be identified in both orientations.

Hair follicles from healthy volunteers (n=9) were fixed with a selection of fixatives to establish the optimal agent. Considerations included the relative thickness of the hair follicle samples in comparison with tissue culture cells, minimising the risk of auto-fluorescence and antigen masking and maintaining cellular integrity required for confocal imaging. Cross-linking agent paraformaldehyde (PFA) was used since it has a small molecular weight that allows diffusion into thick samples. Precipitant methanol was used since it minimises auto-fluorescence and is less likely to mask antibody epitopes than paraformaldehyde. Lastly a 50:50 mix of methanol:acetone was used since acetone is less damaging than 100% methanol fixation. Following fixation with these 3 methods the hair follicles were washed, permeabilised (if required), incubated with anti-Ki67 antibody (a proliferation marker), washed, incubated with Alexa Fluoro 488 and DAPI then mounted on coverslips for confocal imaging. Figure 6-4 shows Ki67 staining in each hair follicle.

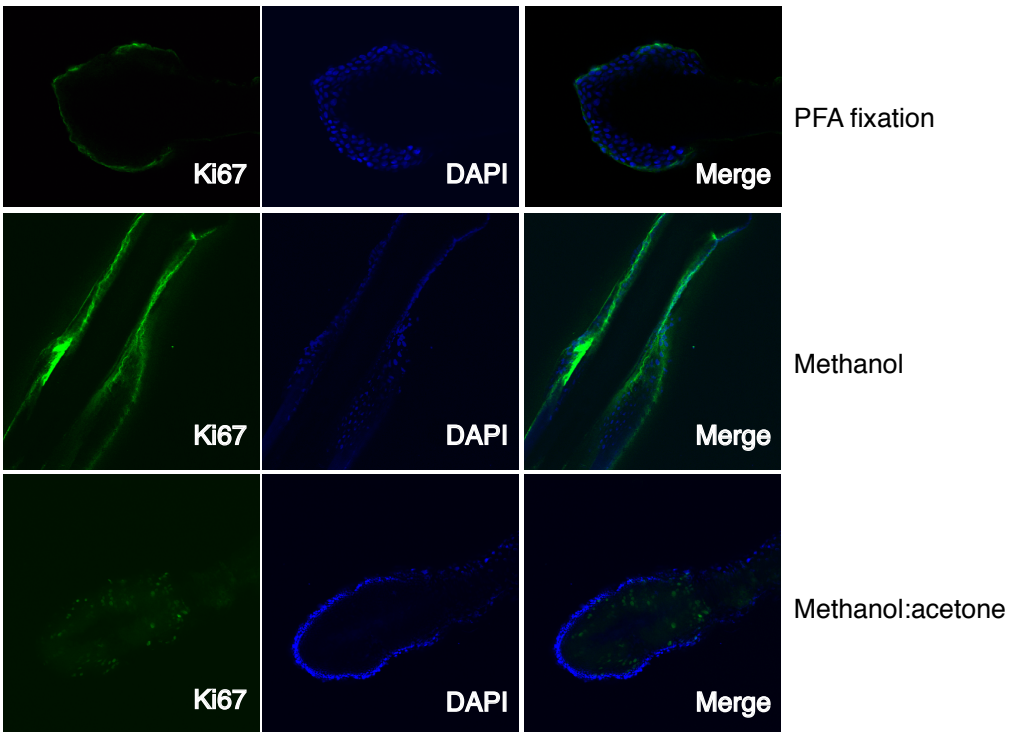

Figure 6-4: Ki67 staining of hair follicles using 3 different fixatives.
Hairs were fixed with the indicated fixative then stained with Ki67 antibody and DAPI and imaged on a confocal microscope. Shown here is a representative slice through each hair.

PFA fixation prior to Ki67 staining showed no Ki67 positive nuclei. Methanol fixation resulted in significant dehydration and shrinkage of the cells while after methanol:acetone fixation clear Ki67 nuclear staining was seen in the absence of cellular dehydration. Methanol:acetone fixation was therefore used for subsequent experiments. Ki67 antibody was chosen to assess the fixation method since it was expected that hair follicles should stain positive due to their high proliferative index. This is consistent with subsequent data presented in table 6-2.

49 eyebrow hairs were plucked from healthy volunteers and 45 from patients. Of the 45 patient samples there were 18 pairs of pre and post treatment hairs. Only 8/94 (9%) hairs were lost or damaged during processing. This is similar to studies using immunohistochemistry of whole plucked hair follicles[537].

Initially a selection of unpaired hairs (ie no pre and post treatment samples) was stained with a panel of antibodies for some proteins of interest. Since the primary objective of the study was to demonstrate p53 stabilisation and activation following chemotherapy, some hairs were stained for p53 and its transcriptional targets p21 and MDM2. Other cell cycle related proteins were also examined to assess

functional effects of p53 stabilisation (phosphohistone H3 (pHH3), retinoblastoma (Rb) and Ki67). Finally, some hairs were stained for γH2AX to establish whether the chemotherapy dose required for p53 stabilisation could be uncoupled from the presence of DNA damage. Two primary antibodies of differing species were used per hair as well as DAPI (to stain DNA). After initial testing it became clear that for several antibodies no cells of the hair follicle stained positive. Table 6-2 shows all hairs imaged. The number of hairs for each antibody that had no staining is shown (zero count). Ki67 and γH2AX were used for further analysis since they had relatively low zero counts (37% and 60%) and the therefore relatively high percentages of quantifiable hairs – that is hairs with positively stained nuclei to count (63% and 40%) (table 6-2). It is difficult to determine if the lack of staining was due to technical failure or truly a biological result. Most hairs were double stained and there was no correlation between zero counts for both antibodies staining the same hair suggesting the lack of a technical problem.

Table 6-2: Hair success rate.

Antibody	Number labelled	Expected cellular location	Zero count	High background	Quantified
Ki67	49	Yes	18 (37%)	0	31 (63%)
p53	12	NA	12 (100%)	0	0 (0%)
p21	32	Yes	27 (84%)	0	5 (16%)
γH2AX	25	Yes	15 (60%)	0	10 (40%)
pHH3	2	Yes	0 (0%)	0	2 (100%)
MDM2	4	N & C	2 (50%)	2	2 (50%)
Rb	2	No	1 (50%)	1	1 (50%)

N=nuclear, C=cytoplasmic. All hairs images are detailed here including paired patient samples, unpaired patient samples and healthy volunteer samples. The zero count is the percentage of hairs stained with a particular antibody that had no positive staining.

To establish the inter-subject variability of Ki67 staining, 1 hair from each of 7 healthy volunteers was fixed, stained, mounted on a coverslip then imaged by confocal microscopy. 10μM slices were taken then the percentage of positive nuclei in each slice was quantified using ImageJ. Figure 5 shows an example of a follicle with a low level of staining (0.4%), a medium level (3.6%) and a high level (9.8%). The mean percentage of Ki67 positive cells for the 7 volunteers was 4.5% (95% confidence intervals 1.7%-7.3%) (Figure 6-6).

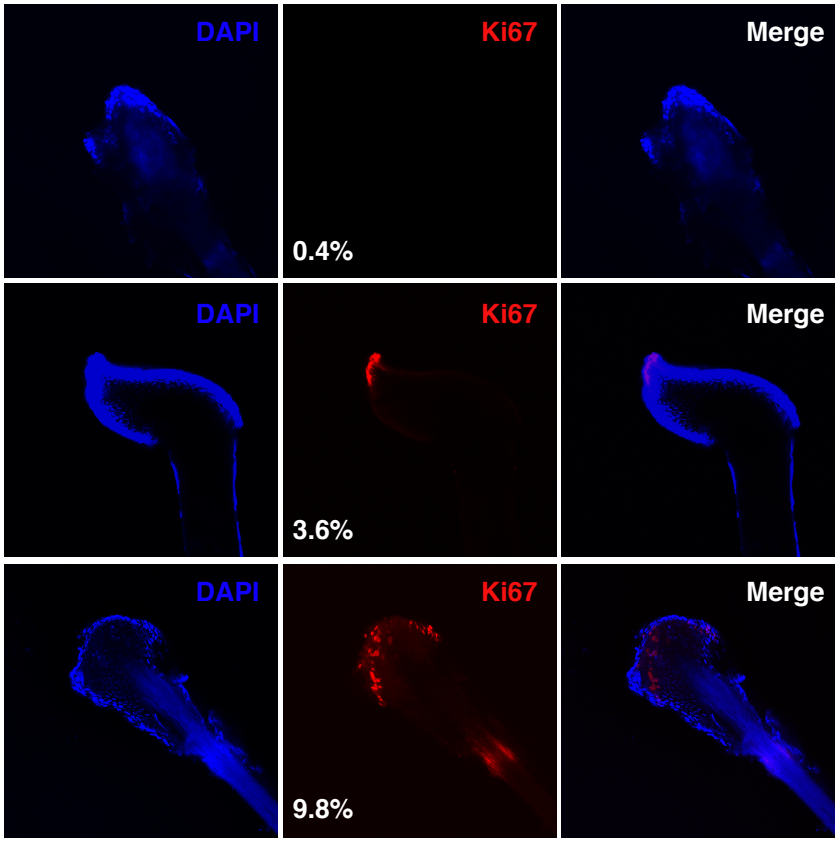

Figure 6-5: Immune fluorescent staining of Ki67 to test inter-subject variability for Ki67. Plucked hair follicles from 7 volunteers were fixed, washed, stained & mounted then imaged on Zeiss Confocal. 10µM slices of each hair were taken. DAPI positive & Ki67 positive nuclei were counted using ImageJ. The percentage positive Ki67 cells was calculated and shown in the middle panel.

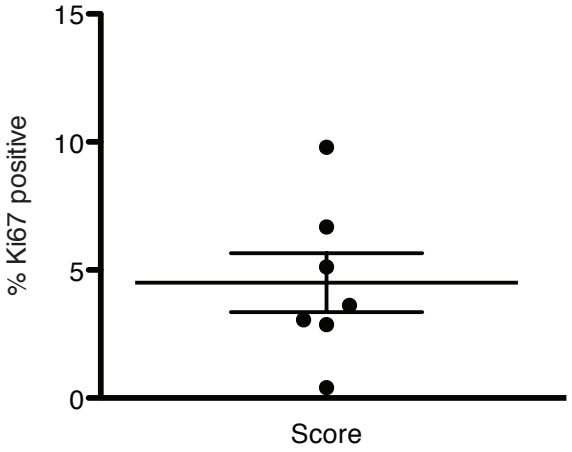

Figure 6-6: Quantification of inter-subject variability of % Ki67 positive hair follicles. Percentage Ki67 positive cells was plotted. Mean score & SEM (1.148) is shown.

The objective of the final assay was to determine when evidence of p53 activity occurs in one individual therefore it was vital to establish the intra-subject variability. Again 7 hair follicles were collected, this time from the same individual on different days. (Figure 6-7 & 6-8). Samples were analysed on the same day.

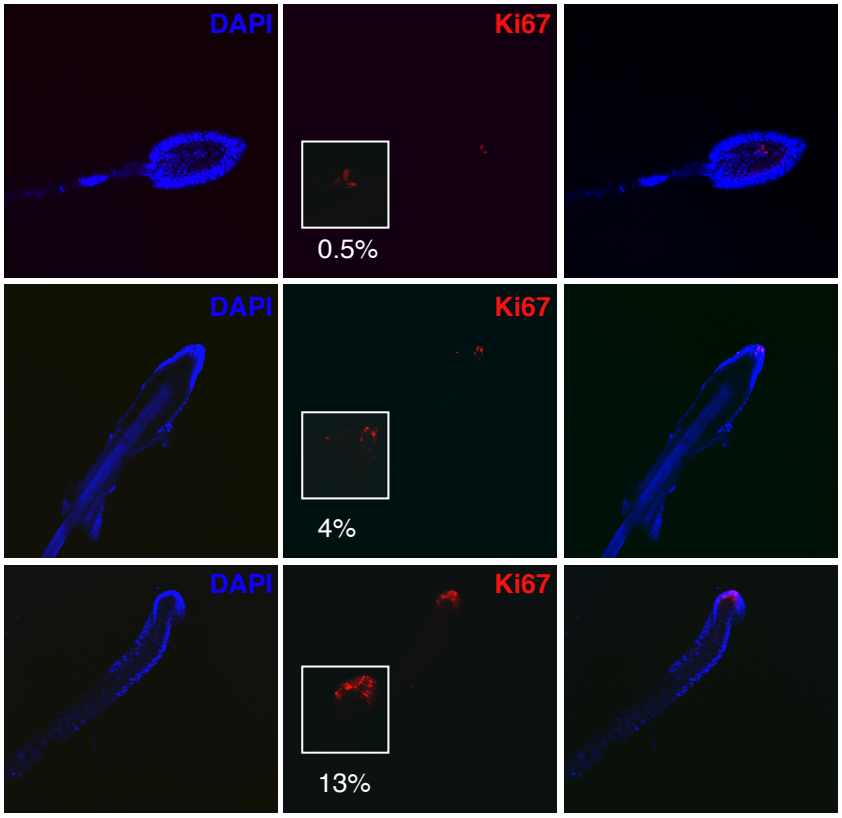

Figure 6-7: Immune fluorescent staining of Ki67 to test intra-subject variability. 7 plucked hair follicles from 1 individual were fixed, washed, stained & mounted then imaged on Zeiss Confocal. 10µM slices of each hair were taken. DAPI positive & Ki67 positive nuclei were counted using ImageJ. The percentage of positive cells was calculated and shown in the middle panel.

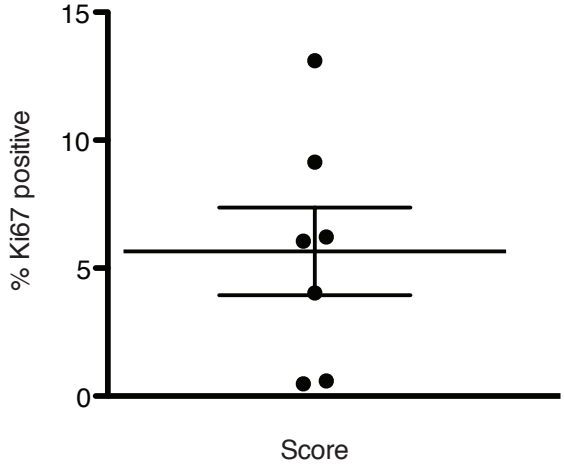

Figure 6-8: Quantification of intra-subject variability of Ki67 positive hair follicles. Percentage Ki67 positive cells was plotted. Mean score & SEM (1.713) is shown.

Again an example of a follicle with a low (0.5%), medium (4%) and a high (13%) percentage of Ki67 positive cells is shown (Figure 6-7). The mean percentage of Ki67 positive cells was 5.7% (95% confidence intervals 1.5%-9.9%) (Figure 6-8).

Both the inter-subject and intra-subject variability of Ki67 staining was wide with coefficients of variation of 67.43% and 80% respectively. In this case it is difficult

to measure the variability of the assay itself since this would require repeated analysis of the same sample. This was not possible since the whole intact hair follicle was stained.

Despite the wide intra-subject variability of the assay, plucked hair follicles pre and post chemotherapy treatment were examined for Ki67 staining.

Plucked hair follicles for 15 patients were fixed, washed, stained. 11 hairs were stained for Ki67, γH2AX and DAPI. 3 hairs were stained for Ki67 and DAPI only and 1 hair was stained for γH2AX and DAPI only. All hairs were then mounted and quantified.

7 patients had no Ki67 positive hair follicle cells pre-chemotherapy and post chemotherapy. These patients were excluded from further analysis.

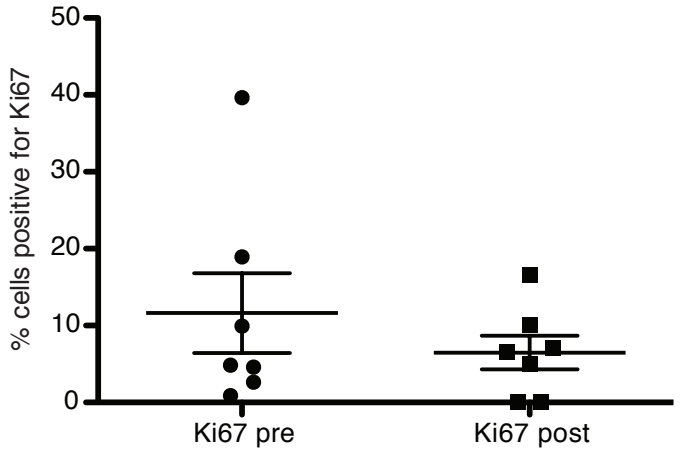

Figure 6-9: Ki67 positive nuclei pre and post chemotherapy.
Mean percentage and SEM are shown. Wilcoxon matched-pairs signed rank test showed no significant difference.

Of the remaining hairs the mean percentage of cells Ki67 positive was not significantly different at 11.6% in the pre-chemotherapy hairs (range 0.9%-39.6%, SEM 5.2) and 6.5% (range 0-16.6, SEM 2.2) in the post-chemotherapy hairs although the trend was in the expected direction (Figure 6-9). The lack of statistical significance could be due to the small sample size.

Of the 12 hairs stained for γH2AX, 6 hairs were negative post treatment. All of these patients also had a negative pre-treatment hair follicle. These 6 hairs were excluded from further analysis. Of the remaining 6 patients the mean percentage

of γH2AX positive nuclei was 0.6% (range 0-1.4%, SEM 0.3) pre-chemotherapy and 3.1% (range 0.7%-7.1%, SEM 1.1) post-chemotherapy (Figure 6-10). Despite a trend in the expected direction there was no significant difference as defined by a paired T-test although again a statistically significant difference would be difficult to detect due to the small sample size.

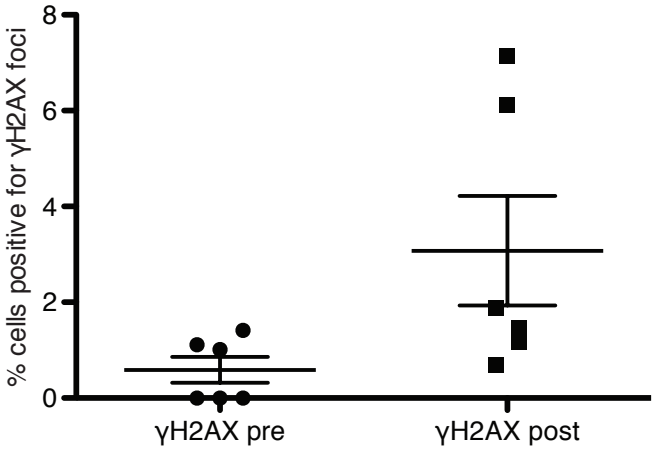

Figure 6-10: Percentage γH2AX positive cells pre and post chemotherapy. Mean and SEM are shown. Wilcoxon matched-pairs signed rank test showed no significant difference.

Unfortunately the high proportion of hairs with negative staining had a significant impact on the number of remaining cases for analysis and ultimately this presents a serious limitation of this technique.

6.5 Peripheral blood mononuclear cells

In an attempt to try to improve on and add to the information gained from the hair follicle immunofluorescence, blood was collected in cell preparation tubes (CPT) containing Ficoll for separation of red cells, granulocytes, platelets, plasma and PBMCs. For a number of patients a pre-treatment sample was obtained but no post treatment sample. These samples were therefore used for optimisation of the assay.

The lymphocyte population was identified by size criteria on forward scatter since monocytes are the largest cells present in the PBMC fraction (Figure 6-11).

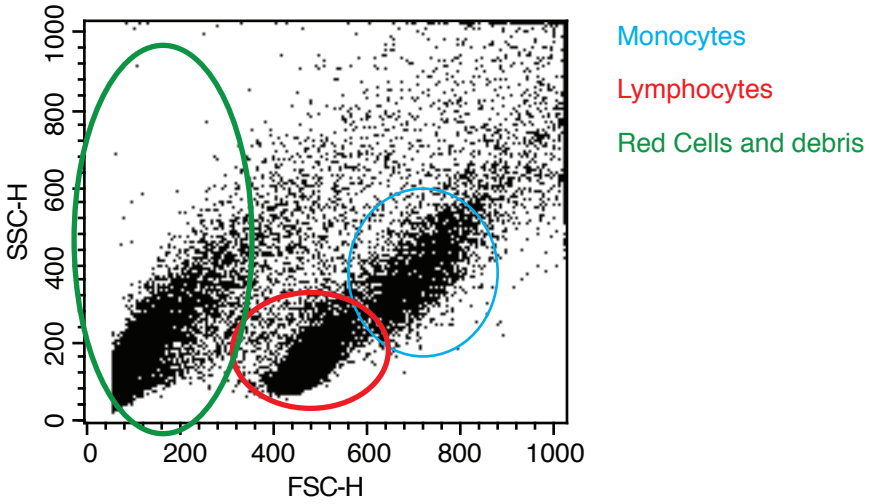

Figure 6-11: Isolation of lymphocytes.
PBMCs were washed, fixed & incubated with PBS/antibodies. Cells were run on FACS Calibur. Side scatter (SSC) versus forward scatter (FSC) was plotted.

PBMCs were stained for p53 and p21 and the mean fluorescence was measured on FACS Calibur. Each experiment included a sample with no primary antibody as a negative control. As can be seen in Figure 6-12 the mean p53 fluorescence and the mean p21 fluorescence was greater than the no primary antibody condition, indicating a fluorescence signal specific to each primary antibody.

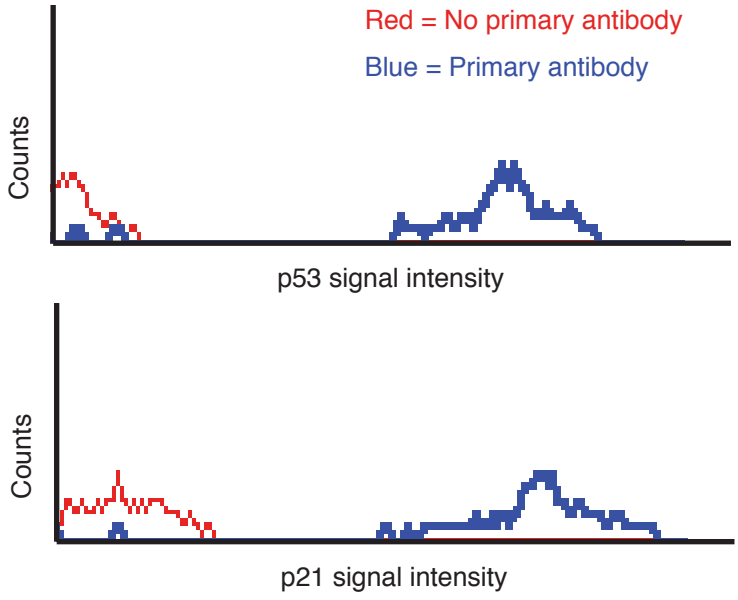

Figure 6-12: Signal intensity is specific for the primary antibody.
After gating of the lymphocyte population the mean fluorescence intensity (488 for p53 or 647 for p21) was plotted for each sample along side the no primary antibody control.

Samples from healthy volunteers were used to establish the variability of the assay. Firstly inter-assay variability was examined. Three samples were taken from the same volunteer and analysed on different days. The mean p53

fluorescence was 7.325 arbitrary units (range 2.38-14.53) and the mean p21 fluorescence was 22.88 arbitrary units (range 15.47-32.23) (Figure 6-13). The co-efficient of variation was 87% for p53 fluorescence and 37% for p21 staining.

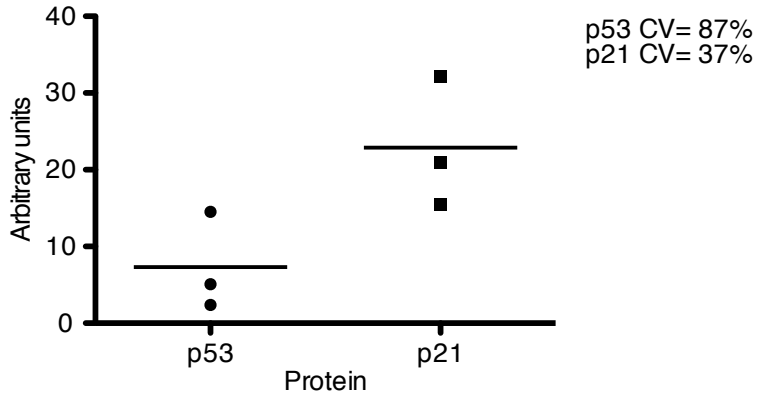

Figure 6-13: Inter-assay variability of PBMC staining for p53 and p21.
Samples taken from a healthy volunteer and analysed on different days. The mean fluorescence signal for p53 and p21 is shown as a horizontal line (arbitrary units). The co-efficient of variation was calculated.

Since the aim is to develop an assay where each patient will provide their own baseline p53 and p21 levels samples were again taken from a healthy volunteer on 5 different days and this time analysed on the same day to rule out deviations due to differences in sample processing (Figure 6-14).

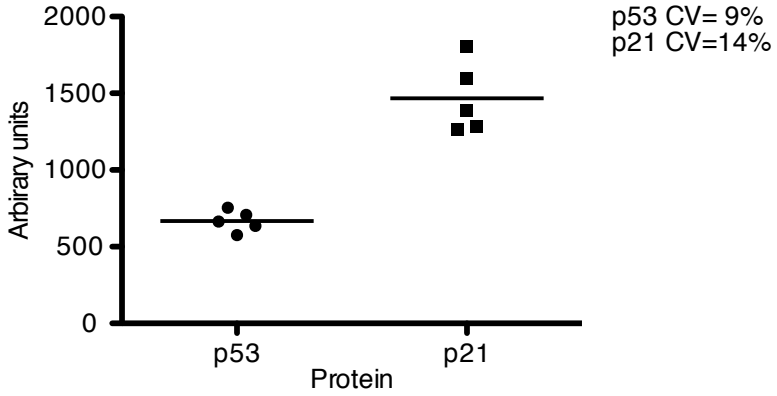

Figure 6-14: Intra-staining variability of PBMC staining for p53 and p21.
Samples taken from a healthy volunteer on 5 different days and analysed on same day. The mean fluorescence signal for p53 and p21 is shown as a horizontal line (arbitrary units). The co-efficient of variation was calculated.

As seen in Figure 6-14 this resulted in an improvement in the co-efficient of variation. The mean fluorescence for p53 was 667.6 arbitrary units (range 576.5-754.7) and for p21 was 1468 arbitrary units (range 1264-1805). The co-efficient of variation for p53 fluorescence was improved to 9% from 87% and for p21 to 14% from 37%.

Next pre and post treatment PBMCs for each patient were prepared and analysed to compare the pre and post treatment p53 and p21 levels as indicated by the mean fluorescence signal on FACS analysis. For 20 patients pre and post treatment samples were obtained for analysis of p53 fluorescence. There was no significant difference in mean fluorescence levels for p53 prior to treatment which was 222.3 (95% confidence intervals 120.8-323.8) and following treatment, which was 208.9 (95% confidence intervals 113.7-304) (Figure 6-15).

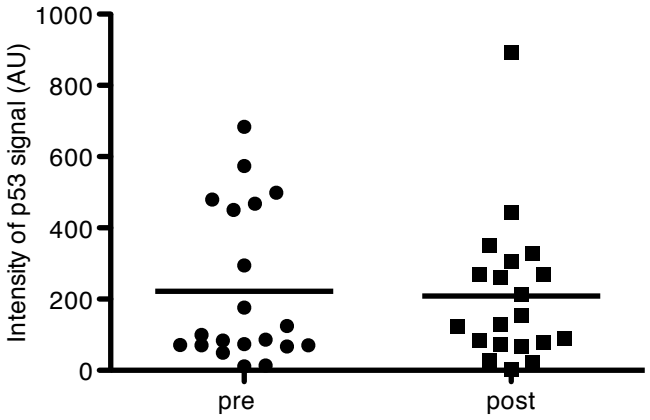

Figure 6-15: Mean PBMC p53 fluorescence following chemotherapy.
p53 fluorescence was measured by FACS analysis in PBMCs pre and post chemotherapy. Box plots show the mean fluorescence (horizontal line), AU=arbitrary units. No significant difference was detected (Wilcoxon matched-pairs signed rank test). n=20.

18 PBMC samples were analysed for p21 fluorescence following chemotherapy (Figure 6-16).

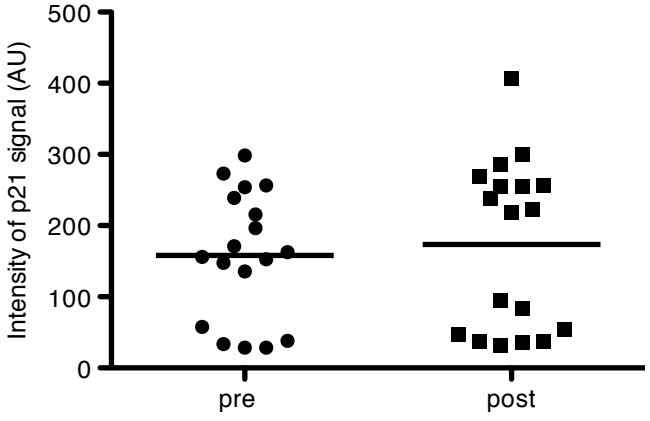

Figure 6-16: Mean PBMC p21 fluorescence following chemotherapy.
p21 fluorescence was measured by FACS analysis in PBMCs pre and post chemotherapy. Box plots show the mean fluorescence (horizontal line), AU=arbitrary units. No significant difference was detected (Wilcoxon matched-pairs signed rank test). n=18.

There was no significant difference in the mean p21 fluorescence of 158.1 (95% confidence intervals 113.3-202.8) pre-treatment and 173.7 (95% confidence intervals 114.5-233) post-treatment.

A small group of 4 patients appeared to have evidence of p53 induction following treatment (1.5 fold increase in mean fluorescence). Three of these patients also had a detectable induction of p21 (1.5 fold increase in fluorescence) (table 6-3). None of the patients where no p53 induction was detected induced p21. This represents a significant correlation between p53 and p21 mean fluorescence levels following chemotherapy.

Table 6-3: Correlation between p53 and p21 induction after chemotherapy.

	p21 not induced (<1.5x)	**p21 induced (>1.5x)**	**Total**
p53 not induced (<1.5x)	11	0	11
p53 induced (>1.5x)	4	3	7
Total	15	3	18

Fisher's exact p=0.04

Of the 3 patients who had a measurable induction of p53 and a measurable induction of p21 all 3 had a partial response to treatment. None of the patients who did not respond to treatment (radiological stable disease or progressive disease) had a measurable induction of p21 in their PBMCs. Overall there was no significant difference in the fold change in p21 fluorescence in responders (radiological complete or partial response) compared with non-responders (Figure 6-17).

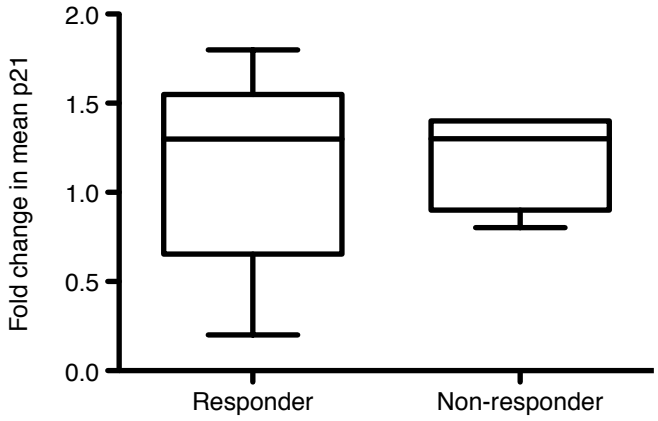

Figure 6-17: p21 induction in responders versus non-responders.
Median fold change in mean p21 fluorescence following chemotherapy. Whiskers represent minimum and maximum values. n=9 responders, 5 non-responders

The PBMC assay therefore appeared to be specific in terms of identifying non-responders since all 5 non-responders did not induce p21 (induction being defined as a 1.5 fold increase in mean fluorescence following treatment). It was however not sensitive since of 9 responders only 3 (33%) had a measurable induction in p21. The study population here was of mixed tumour p53 status. This would need to be established to make conclusions about the significance of normal cell p53 activation and tumour response.

Although there are some encouraging indications in these studies, the data do not establish whether the PBMC assay is sensitive or specific for detection of increased p53/p21 activity. To establish this, the results would need to be compared with quantification of p53/p21activity using another assay.

6.6 Macrophage inhibitory cytokine-1

In a further attempt to identify a biomarker for p53 activity, the expression of MIC-1 was examined. In contrast with p53 and p21, MIC-1 is secreted p53 target. In a wild-type p53 xenograft model treatment with chemotherapy led to increased serum MIC-1 expression[544]. In this model MIC-1 was analysed using an ELISA based protocol, which could measure human MIC-1 and therefore excluded the impact of secretion of MIC-1 from the normal mouse tissues. When measuring MIC-1 secretion solely from tumour cells a raised MIC-1 level following chemotherapy correlated with response in this xenograft model. However, in human studies measurement of MIC-1 represents MIC-1 secretion from both normal tissues and wild-type p53 expressing tumour tissues. Furthermore MIC-1 is expressed in the serum of cancer patients, prior to cancer treatment, at a higher level than in healthy volunteers and this correlates with tumour burden in prostate, breast, colorectal, pancreatic and gastric cancer (table 6-4)[543, 684-688]. While PBMCs and hair follicles provide an indication of the response of normal tissue to p53 activating therapy, analysis of MIC-1 expression provides a more complex picture of both tumour and normal cells response (depending on the tumour p53 status).

To confirm that a MIC-1 induction following p53 activation was p53 dependent, isogenic colorectal cancer cell line, HCT116, p53 wild-type or null were treated

with vehicle or Nutlin (the non-genotoxic p53 activating agent). Quantitative RT-PCR detection showed that Nutlin significantly induced transcription of MIC-1 mRNA in the p53 wild-type cells indicating that MIC-1 induction is p53 dependent (Figure 6-18).

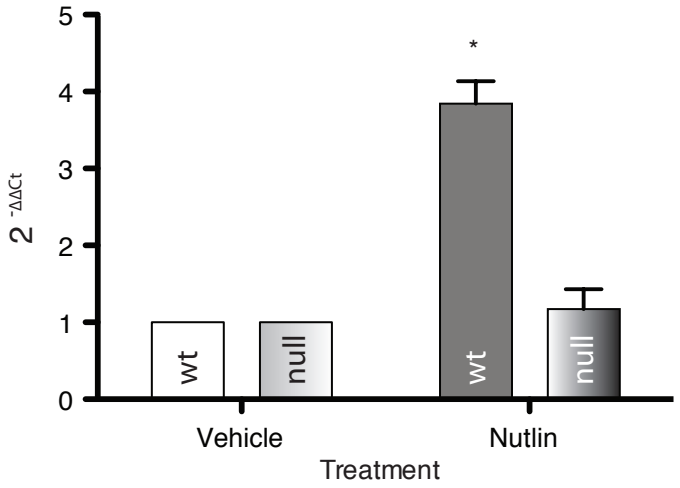

Figure 6-18: Nutlin induces MIC-1 expression in p53 wild-type cells.
HCT116 cells wild-type and null for p53 were treated with vehicle or Nutlin 10μM for 22h. MIC-1 mRNA levels were measured by qRT-PCR. Expression is quantified relative to control genes according to the comparative $\Delta\Delta C_t$ method. Values from three independent experiments are displayed as mean of $2^{-\Delta\Delta Ct}$. Student's two-tailed T-test indicates a significant change for Nutlin compared to vehicle treated wild-type cells. Error bars represent SEM.*p<0.05.

Serum MIC-1 levels were then measured in 116 gastrointestinal cancer patient samples taken prior to chemotherapy using a commercially available MIC-1 sandwich ELISA. For evaluation of MIC-1 correlation with survival, patients were divided into two groups of 54 patients with advanced oesophagogastric cancer and 44 patients with advanced colorectal cancer. This was necessary because the median survival for advanced oesophagogastric cancer was expected to be significantly shorter than for advanced colorectal cancer. Patients were excluded from this analysis; if their treatment was adjuvant (n=16); if their disease stage was unknown (n=1); and one patient was excluded from the upper gastrointestinal group since they were alive at 64 months follow-up. Mean MIC-1 level was 717.9pg/ml (range 116.6-2771, SEM 75.91) and 918.7pg/ml (range 177.6-2809, SEM 107.4) for oesophagogastric and colorectal cancer patients respectively. For the upper gastrointestinal patients the mean MIC-1 level was significantly higher for those who survived less than 12 months (mean 796.9pg/ml, range 137.7-2770.6) versus those who survived longer than 12 months (mean 470.9pg/ml, range 116.6-1364.2) as measured by Mann Whitney U test (p=0.018). For lower

gastrointestinal patients there was no significant difference (p=0.169 by Mann Whitney U test)) in MIC-1 level for those surviving less than 12 months (mean 1057.8pg/ml, range 177.6-2809.5) versus those surviving over 12 months (mean 801.3pg/ml, range 196.7-2585.4). Figure 6-19 displays a scatter plot of the baseline MIC-1 levels and survival for each patient group. Spearmann correlation analysis gave an r value of -0.4356 and -0.2276 for the upper gastrointestinal and the lower gastrointestinal groups respectively therefore no strong relationship was seen overall. This is in contrast with published data and may be in part a of the relatively small sample size in this study. Of note there are 2 patients with metastatic oesophagogastric cancer with survivals far longer than expected.

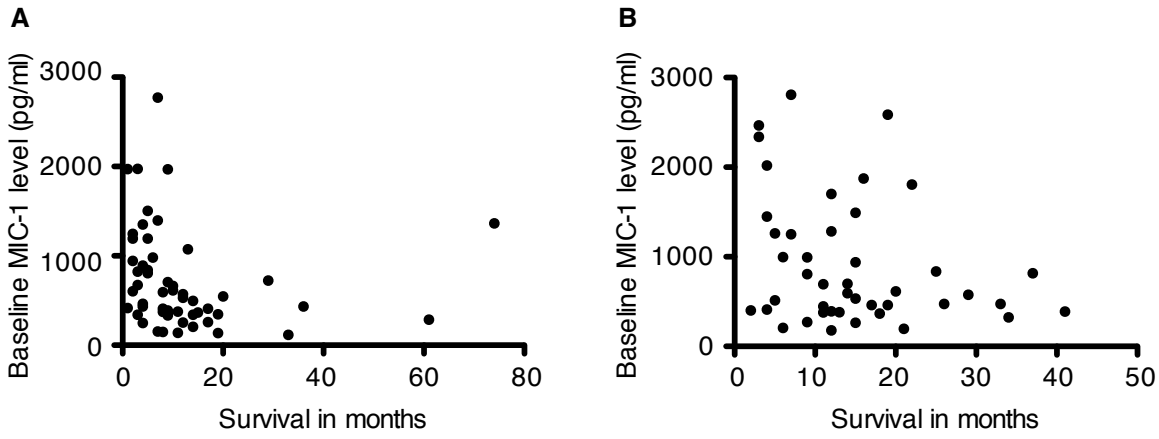

Figure 6-19: Correlation of baseline MIC-1 and survival.
(A) Patients with advanced oesophagogastric cancer, n=54, Spearman correlation r=-0.4356
(B) Patients with advanced colorectal cancer, n=44, Spearman correlation r=-0.2276.

In line with previously published data, in this study cohort baseline MIC-1 level was associated with more advanced cancer stage for both oesophagogastric and colorectal cancer (Figure 6-20). For oesophagogastric cancer the median MIC-1 level for patients who received adjuvant treatment (and are therefore of the lowest stage) was 262.6pg/ml (n=5), for those with locally advanced disease was 408pg/ml (n=18) and for those with metastatic disease was 599.3pg/ml (n=37). In patients with colorectal cancer median MIC-1 level was 380.8pg/ml for those who received adjuvant treatment (n=11) (the lowest stage), 698pg/ml for those with locally advanced disease (n=3) and 594.4pg/ml for those with metastatic disease (n=41).

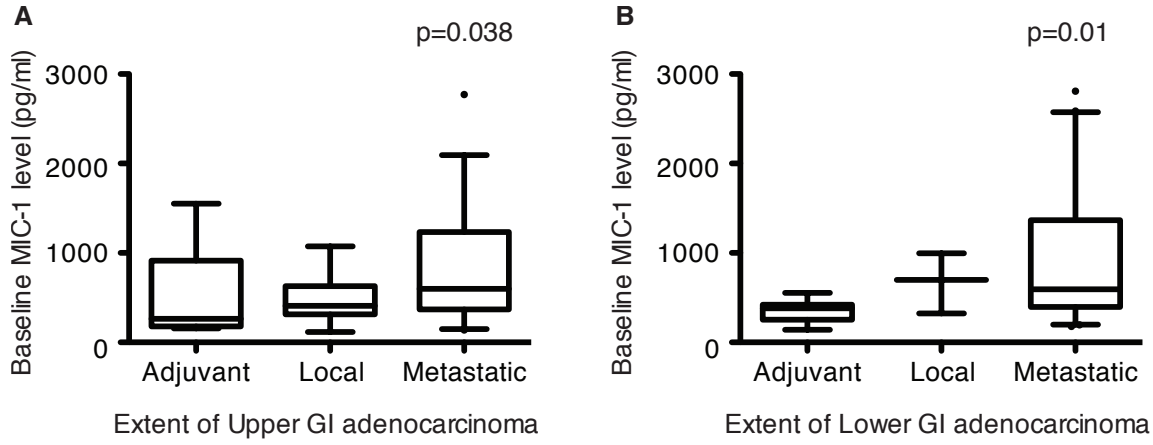

Figure 6-20: Association between baseline MIC-1 and cancer stage.
(A) Patients with oesophagogastric cancer, box and whiskers plot indicating the 5th-95th percentile, Kruskal-Wallis test p=0.038, n=60 (B) Patients with colorectal cancer, box and whiskers plot indicating the 5th-95th percentile, Kruskal-Wallis test p=0.01, n=55

The serum MIC-1 levels pre and post chemotherapy treatment were assessed for 101 patients. There was a significant difference between median MIC-1 level pre and post treatment as determined by a Wilcoxon matched-pairs signed rank test ($p<0.0001$) (Figure 6-21). Median MIC-1 level pre-chemotherapy was 552.9pg/ml (range 116.6-2809, SEM 60.88) and 901.9pg/ml (range 256.3-2815, SEM 64.78) post chemotherapy consistent with a chemotherapy-induced increase in transcriptional activity of p53. Whether this increase in p53 activity is only in normal tissues, as would be expected in patients with a p53 deficient tumour (mutant or null for p53) or whether it represents increased p53 activity in both normal tissues and a wild-type p53 tumour is unknown.

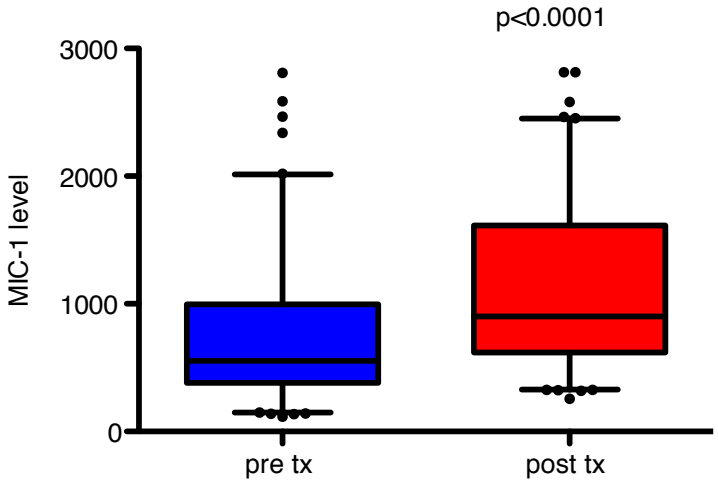

Figure 6-21: MIC-1 level pre and post chemotherapy
MIC-1 level (pg/ml) pre and post chemotherapy was plotted for all patients, Wilcoxon matched-pairs signed rank test p<0.0001, n=101

There is however clearly an easily quantifiable increase in MIC-1 following chemotherapy treatment and cell line data here and by others support that this is a p53 dependent response[677]. For those patients where serum, hair follicles and PBMCs were collected correlation between MIC-1 induction and reduced Ki67 and induction of γH2AX foci as detected by immunofluorescence of hair follicles and p53 and p21 induction in PBMCs was examined however no correlation was identified.

Patients with a wild-type p53 tumour who mount a p53 response after chemotherapy may be more likely to achieve a response to treatment (as assessed by reduced tumour size on imaging, a radiological response). The association between percentage fold change in MIC-1 level following treatment and radiological response to treatment was therefore explored (although a significant number of the patients here are likely to have tumours expressing a mutant p53, ≈50%). Patients for whom there was no post treatment sample were excluded from analysis. All patients who could be evaluated for response were included in this analysis. In total 36 patients had progressive disease following treatment as determined by RECIST (response evaluation criteria in solid tumours)[519] (≥20% increase in the sum of diameters of measurable lesions) and 2 patients had clinical progression (Figure 6-22).

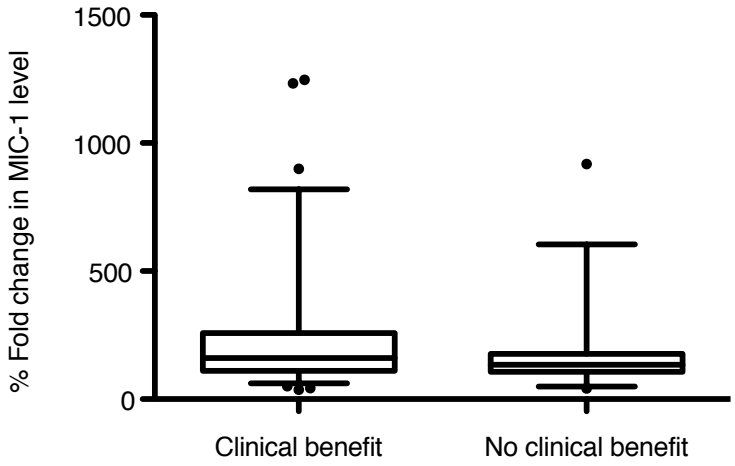

Figure 6-22: Association between MIC-1 change and clinical benefit.
Percentage change in MIC-1 following chemotherapy was plotted on a box and whiskers plot. 5-95 percentiles are indicated. Clinical benefit includes SD, PR & CR, no clinical benefit includes clinical or radiological progression. Significance was tested using Mann Whitney test for non-parametric data. No significant difference was detected.

For the 38 patients with no clinical benefit from chemotherapy the median percentage fold change in MIC-1 was 135% (range 41.9% -917.7%, SEM 25.94) (Figure 6-22). For the 69 patients with clinical benefit, as defined by RECIST stable disease, partial response or complete response, the median percentage change in MIC-1 was 160.4% (36.56%-1246%, SEM 27.56).

These results therefore show no significant difference in the median percentage fold change in MIC-1 after chemotherapy in those who had clinical benefit versus those who did not.

To examine if there is a relationship between chemotherapy induced change in MIC-1 and survival, correlation analysis was performed on all patients for whom pre and post treatment samples were available and patients treated in the adjuvant setting were excluded (Figure 6-23). There is no evidence of a strong relationship between change in MIC-1 level and survival.

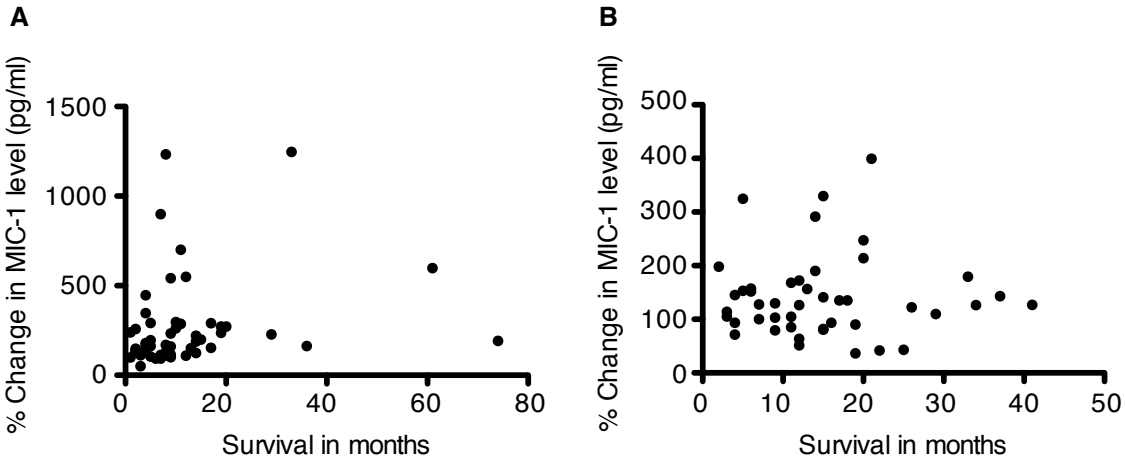

Figure 6-23: Correlation between change in MIC-1 and survival.
(A) Patients with advanced oesophagogastric cancer, Spearman correlation r=0.3622, n=53
(B) Patients with advanced colorectal cancer, Spearmann correlation r=-0.007915, n=45

Measurement of serum MIC-1 appears to provide a complex measure of normal cell and tumour cell biology.

6.7 Summary and discussion

The aim here was to examine a variety of easily accessible tissues for activation of p53 in response to chemotherapy, in order to identify biomarkers of p53 activity for use in clinical studies evaluating the chemoprotective strategy described in

chapter 5. A study of this kind is unconventional since in current clinical practice the endpoint in a dose finding study is MTD. In contrast, the aim here would be to establish the minimum dose required to activate p53 in normal tissues (as defined by pharmacodynamic biomarkers) whereby protecting them from the subsequent cytotoxic therapy. The normal tissues examined here included hair follicles, PBMCs and serum.

It was demonstrated that the usefulness of immunofluorescence of hair follicles as a pharmacodynamic marker of p53 activation is severely limited by the high number of hairs with a zero count. Additionally intra-subject Ki67 staining was found to be highly variable.

Ideally a pharmacodynamic marker of p53 activation would be more upstream (more upstream than Ki67) in the p53 pathway. A good marker would be p53 expression itself, but unfortunately no hair follicles could be successfully stained for p53. Since p53 is a tightly regulated protein, the study sampling times determined by the respective patient's chemotherapy schedule rather than the time of expected maximal p53 activation may well have been a methodological problem with the study design. In future studies, it would be useful to time hair follicle sampling with pharmacokinetic sampling to help determine the time of maximal pharmacodynamic response in relation to the Tmax of the p53-activating agent. Another consideration is that the success of staining hair follicles has been previously shown to be dependent on the site the follicle is plucked from[537]. All the hair follicles stained were plucked from the eyebrow area however for some particular proteins scalp follicles produce more quantifiable and thus reliable staining. As yet, it is unknown whether p53 staining of scalp follicles would be more successful.

The PBMC assay described here showed no significant difference in the p53 and p21 mean fluorescence following chemotherapy. Again this could be partly due to the inconsistent sampling times of the post treatment sample and timing sampling with pharmacokinetic sampling may be useful. Reassuringly there was some correlation between p53 induction and p21 induction, suggesting that p53 activation can potentially be detected.

To further optimise the PBMC assay, identification of the lymphocyte population could be improved by using antibodies against lymphocyte cell surface receptors. Defining the cell type studied more clearly could reduce assay variability allowing detection of smaller changes in p53 and p21. One other draw back of this assay was that sometimes lymphocyte numbers were fairly low due to chemotherapy-induced lymphopenia. This resulted in a prolonged sample running time which while not problematic here could become a problem when using the assay in a more heavily pre-treated patient population and also when using the assay across different sites. To minimise cell loss, conjugated antibodies could be used since this would limit assay handling steps. Ultimately the PBMC assay presented here has potential but would require further optimisation in a larger patient group before progression to biomarker qualification which in the UK would be according to the Cancer Research UK (CRUK) biomarker roadmap.

The study of p53 activation in hair follicles and PBMCs is ideal to study p53 activation in normal tissue exclusively. In contrast, the measurement of serum MIC-1 may be influenced by p53 activity in both tumour tissue (if the tumour has wild-type p53 status) and normal tissue providing a more complex output. However in a chemoprotection study patients would be required to have a p53 deficient tumour (mutant or null p53 status) therefore in this setting serum MIC-1 should also only measure p53 activity in normal tissues.

The results described here demonstrate that overall, in a population of mixed p53 tumour status, a high baseline level of, p53 target, MIC-1 is an indicator of poor prognosis in oesophagogastric cancer. Furthermore high baseline MIC-1 levels correlate with advancing disease stage in oesophagogastric and colorectal cancer. This is consistent with previously published data for cohorts of patients with oesophagogastric, colorectal and prostate cancer (table 6-4). Increased MIC-1 levels have also been correlated with more advanced cancer stage in breast, pancreatic and cholangio carcinoma and shorter survival in Glioblastoma.

Table 6-4: Previous studies associating serum MIC-1 with stage/survival.

Primary tumour site (reference)	p53** mutation	Cancer vs Healthy	Cancer Stage	Response to treatment		Overall survival
				Initial	***Post tx***	***Initial***
Prostate[543, 685,	10-30%	⇧ca	⇧ adv stage	⇧	⇧	⇧shorter

[686, 689 690 691]				docetaxel resistance	docetaxel resistance	
Breast[543]	25%	⇧ca	⇧ adv stage	NK	NK	NK
Colorectal[688, 692]	50%	⇧ca	⇧ adv stage	NK	NK	⇧shorter
Head & Neck[693]	45%	⇧ca ***	NK	NK	NK	NK
Pancreatic, cholangio[684]	35%	⇧ca	⇧ adv stage	NK	NK	NK
Glioblastoma[687] *	7-10%	⇧ca	NK	NK	NK	⇧shorter
Oesophago-gastric[694, 695]	40-45%	⇧ca	⇧ adv stage	NK	NK	⇧shorter

*csf MIC-1 for glioblastoma, plasma samples not consistent (csf=cerebrovascular fluid) ⇧ means increased expression or chemotherapy induced expression, **(IARC TP53 database), *** cell lines only, tx=treatment, adv=advanced, ca=cancer, NK=Not Known.

It is interesting to consider why an increased level of a wild-type p53 target would be associated with a poor prognosis. Since a high proportion of patients studied here are likely to have mutant p53 expressing tumours elevated MIC-1 appears to reflect a host (normal cell) response. Perhaps normal wild-type p53 tissues respond to a tumour by secreting MIC-1 and as a tumour becomes more invasive to the normal tissues more MIC-1 is secreted. This would fit with a strong body of data associating systemic inflammation in general with poor prognosis in cancer patients[696]. It would therefore be interesting to explore other markers of systemic inflammation in our patient cohort. Furthermore it would be interesting to measure the MIC-1 levels secreted from normal tissues in the presence of tumours of differing p53 genotypes and examine whether MIC-1 contributes to invasion in 3D models of invasion and animal models.

In this study MIC-1 was being examined as a measure of p53 activation in response to chemotherapy treatment. Indeed serum MIC-1 level was significantly induced after chemotherapy suggesting p53 activation in at least some tissues. MIC-1 induction after chemotherapy did not predict clinical benefit from treatment. Again this is consistent with previous clinical data, which suggested that an increase in MIC-1 following docetaxel chemotherapy predicted resistance to docetaxel[691].

In this study and the previous study, associating increased MIC-1 levels with resistance to docetaxel, p53 activation was via the DNA damage pathway therefore it could not be assumed that non-genotoxic p53 activation will also result in MIC-1 induction. However it is also shown here that in cell lines with wild-type

p53, MIC-1 is induced after Nutlin treatment and furthermore early phase studies evaluating Nutlin (RG7112) as a therapeutic for the treatment of wild-type p53 tumours are now investigating the role of MIC-1 as a pharmacodynamic biomarker of p53 activation. So far these studies have shown that serum MIC-1 levels correlated with increased drug exposure and haematological toxicity in a cohort of patients where 90% of tumours were wild-type for p53 suggesting that it may be a useful pharmacodynamic biomarker[426-428]. Ideally in these initial stages of biomarker development MIC-1 should be measured alongside another measure of p53 activation to validate it as a marker of p53 activation. The Nutlin clinical studies have not reported whether increased MIC-1 levels also correlated with response and survival in their study population (which is unsurprising since these early studies were not designed to assess response or survival).

The MIC-1 data from the present study allows only limited conclusions to be drawn due to the mixed p53 status population and the chemotherapy visit schedule determined sampling times. The results of the Nutlin clinical studies should help to resolve some of the complexities of the present data, in a population with mixed p53 status, since patients in these MDM2 inhibitor studies will mostly be of wild-type p53 status and more importantly will at least be of known p53 status. Additionally the early phase Nutlin studies have been able to correlate the MIC-1 level with pharmacokinetic information. This will allow determination of the ideal MIC-1 sampling time.

When looking for a therapeutic effect of p53 activation it is important to limit the analysis to wild-type p53 expressing cancers, which we have been unable to do. If it were possible to study only patients with a wild-type p53 tumour, MIC-1 induction following chemotherapy may show a stronger correlation with response to treatment. In contrast when looking for p53 activation in normal tissues the study population would need to be limited to only patients with tumours of mutant or null p53 status.

The primary aim here was to develop an assay capable of establishing the minimum p53 activating dose of some traditional cytotoxic agents to be used as chemoprotectants as discussed in chapter 5. An optimised version of the PBMC assay presented here and the MIC-1 ELISA assay (in the presence of a p53

deficient tumour) could both potentially be used in this role. Furthermore both assays may be useful in studies of MDM2 inhibitors as therapeutic agents for wild-type p53 tumours. In this setting the biological response of normal tissues would be used as a surrogate for events within the tumour in the PBMC assay and MIC-1 would provide a measure of p53 activity in both normal tissues and wild-type p53 tumour. Presently clinical studies are on-going using MIC-1 ELISA in combination with a panel of other assays to evaluate the pharmacodynamic effects of MDM2 inhibitors. At the outset of this work, information regarding these studies was not available in the public domain.

7 Summary and conclusions

The p53 pathway is the most commonly deregulated pathway in human cancer[372]. This may be because of mutation in the *p53* locus (leading to loss of p53 or expression of a mutant p53) or alternatively there may be a variety of other perturbations at other levels in the pathway. Ultimately most cancers have evaded p53 mediated tumour suppression in some way. Furthermore this loss of p53 appears to be required for maintenance of cancer, as demonstrated by mouse tumour models where in established mouse tumours reinstatement of p53 led to tumour regression. This was mediated via apoptosis in some models and senescence with associated immune mediated tumour clearance in others[134, 417, 418]. Together these data support the hypothesis that restoration of wild-type p53 activity could be a useful strategy for cancer treatment. Clearly the appropriate method of restoration of wild-type p53 activity depends on the specific means of p53 dysfunction in the tumour.

At the outset of this work the aims were (1) to evaluate 2 potential strategies designed to treat cancers where wild-type p53 has been inactivated by overexpression of p53's negative regulators MDM2 and MDMX, (2) to examine in cell lines a chemoprotection strategy for the treatment of p53 deficient cancers (p53 null or mutant) and (3) to develop a pharmacodynamic biomarker for p53 activation capable of providing proof of mechanism in clinical studies of MDM2/MDMX inhibitors.

One of the strategies tested as a means to treat cancers with wild-type p53 was the MPD class of compounds, described in chapter 3. These compounds are 5-deazaflavin compounds derived from a previously described group of compounds (HLI98)[447], which were shown to specifically inhibit MDM2's E3 ligase activity leading to stabilisation and activation of p53 in cells. The MPD compounds were derivatives designed to have improved chemical properties and potency in comparison with the parent HLI98 class.

Shown here, these new compounds inhibit ubiquitination of MDM2 and p53 *in vitro* and in cells via a mechanism that is specific to MDM2, since the MPD compounds are not capable of inhibiting autoubiquitination of a similar RING E3, Cbl. More specifically the MPD compounds' activity has been shown to depend on the MDM2

RING-tail and furthermore, using SPR, one of the MPD compounds has been shown to bind to the MDM2 RING-tail.

Despite some problems with MPD compound stability and solubility, a core set of compounds representing low, medium and high potency, as predicted by *in vitro* ubiquitination assays, could be tested in cell lines. Importantly treatment of cancer cell lines with the MPD compounds led to stabilisation of p53 and increased expression of p53 transcriptional targets. As a consequence, MPD compounds caused a cell cycle arrest, although some of the most active MPD compounds appeared to have some p53 independent pro-apoptotic effects.

As discussed at length in chapter 3, to fully elucidate the mechanism of action of the MPD compounds there are several interesting areas that remain to be explored. The outcome of p53 activation can be diverse and is determined by the particular p53 activating signal, the presence of p53's negative regulators, the binding partners of p53 and the modified state of p53[70]. To have a full understanding of the likely outcomes of p53 activation in response to MPD treatment, the influence of MPD on these regulatory levels should be investigated. For example since MPD compounds specifically inhibit E3 ligase activity of MDM2 without disrupting p53-MDM2 binding they may be expected to not fully activate p53 due to the absence of DNA damage signalling, continued p53-MDM2 binding, elevated MDM2 expression and the specific post-translation modification status.

Reassuringly mouse models where the acute DNA damage response to radiation is suppressed by temporarily switching off p53 signalling[482] and models where DNA damage activated phosphorylation sites are mutated[562-565] support a paradigm where DNA damage signalling is not necessary for p53-mediated tumour suppression. Furthermore treatment of xenograft models with Nutlin, the non-genotoxic p53 activator did lead to xenograft shrinkage[425]. There are also several examples of p53 activation in the presence of intact p53-MDM2 binding including activation of p53 via the ribosomal pathway[276-279] and in response to oncogene activity[274, 275] as well as in response to proteasome inhibitor bortezomib[697]. It would however be interesting to examine whether the anti-proliferation effects of the MPD compounds could be enhanced by additional

disruption of p53-MDM2 binding by the addition of Nutlin treatment as has been demonstrated in cell line studies with the combination of Nutlin and bortezomib[698].

In contrast with Nutlin the MPD compounds increase MDM2 levels by decreasing the proteasomal degradation of MDM2 in addition to the transcriptional upregulation of MDM2 due to p53 activation. The levels of MDM2 are therefore expected to be higher following MPD treatment than Nutlin treatment. Previous reports have suggested that the Nutlin induced elevation of MDM2 was of additive value in p53 activation since the Nutlin-bound MDM2 maintained the ability to cause proteasomal degradation of p53's other negative regulator MDMX[570]. Post MPD treatment however the elevated MDM2 levels may be expected to be E3 ligase dead and therefore incapable of reducing MDMX levels. A full examination of MPD compound-induced alterations in MDMX expression would be valuable. In contrast it is possible that the MPD compounds are capable of directly binding and inhibiting MDMX since there is a high level of similarity between MDM2 and MDMX. The ability of MPD compounds to bind to MDMX should therefore be examined. Regardless of whether the compounds bind MDMX, it is also possible that they can inhibit heterodimerisation of MDM2 and MDMX, causing MDM2 to become a less potent E3 ligase. Inhibition of heterodimerisation remains another possible mechanism of action of the MPD compounds that also warrants evaluation.

MPD compounds may result in activation of p53 with a specific post-translational modification profile that will have some effect on determining the specific p53 response. As well as the expected lack of DNA damage-induced phosphorylation it would be interesting to examine the acetylation status of MPD compound-induced p53 since acetylation is important for full p53 activation[300, 304]. Potentially MPD compound-induced p53 may present a pattern of post-translation modifications where there are high levels of Neddylation and SUMOylation since inhibition of MDM2's E3 ligase activity may drive alternative MDM2-dependent post-translation modifications with resultant effects of p53's transcriptional output.

Finally, structural analysis of the MPD compound-MDM2-RING-tail complex would be important to guide design of other more soluble MDM2 inhibiting compounds. This work would help to dissect the interaction between MDM2's E3 RING-tail and

E2. Such findings may shed light on the mechanistic details of MDM2's E3 ligase activity and could therefore have implications for the design of new compounds.

The work described here on the MPD compounds, presents the first evidence for a novel mechanism for E3 ligase inhibition, which has potential to have far reaching consequences for drug development and understanding the mechanism of MDM2's E3 ligase activity.

Testing of another potential MDM2 inhibiting drug – HLI373 - is described in chapter 4. This compound was originally discovered in a screen for soluble compounds structurally similar to the HLI98 class and shown to stabilise and activate p53 in cells[451]. However, in contrast to the published work, we were unable to see a direct effect of HLI373 on MDM2's E3 activity *in vitro*, suggesting that the activation of p53 (and inhibition of p53 ubiquitination in cells) was indirect. Since p53 can be activated via three distinct pathways (DNA damage-induced inhibition of p53-MDM2 binding[284], ARF-MDM2 binding in response to oncogene activity and L11-MDM2 binding in response to ribosomal stress), the effect of HLI373 on these pathways was explored in more detail. HLI373 was shown to stabilise p53 at doses that do not cause DNA damage and that did not affect p53-MDM2 binding. HLI373 was capable of stabilising p53 in cell lines deficient in tumour suppressor ARF, indicated that HLI373 did not function via interference in the ARF pathway. HLI373 inhibited ribosomal biogenesis via a mechanism dependent on intact p53-MDM2 binding and accordingly caused ribosomal stress as determined by translocation of nucleophosmin (B23) from the nucleolar compartment to the nucleoplasm. Furthermore ribosomal protein L11-MDM2 association was enhanced by HLI373 treatment, confirming HLI373 activates p53 via the ribosomal stress pathway. The present studies confirmed that HLI373 inhibited ubiquitination of p53 *in vivo*, but an inability to impair MDM2's E3 activity *in vitro* suggested that HLI373 had an indirect mechanism for inhibition of ubiquitination of p53. This observation is consistent with HLI373's ability to activate p53 via the ribosomal pathway.

Previous studies have shown that in response to ribosomal stress L11-MDM2 binding enhances degradation of MDMX, thereby enhancing p53 activation[280]. HLI373's influence on MDMX was therefore examined. Interestingly, HLI373

reduced the protein expression of MDMX and this was not rescued by inhibition of the proteasome. HLI373-induced loss of MDMX expression is therefore not due to enhanced proteasomal degradation of MDMX. To test whether HLI373's effect on MDMX was due to reduced transcription of MDMX, quantitative RT-PCR was used to examine MDMX mRNA levels. These studies showed that HLI373 inhibits MDMX mRNA expression via a p53 independent mechanism. Examination of MDMX pre-mRNA expression and MDMX promoter activity (shown by using an MDMX promoter luciferase) revealed that HLI373 inhibited MDMX transcription. Using Genomatix software the MDMX promoter was analysed for prediction of transcription factors that could be involved in regulating MDMX transcription and might therefore be the target of HLI373. Thirty-eight transcription factor binding sites were identified for 30 transcription factors, 2 of which have previously been shown to regulate expression of MDMX (Elk and ETS)[549]. Clearly further exploration is required to fully elucidate the mechanism of MDMX inhibition but one could speculate that HLI373 functions through one of the transcription factors predicted to bind to the MDMX promoter.

HLI373 has therefore been shown to function as a dual inhibitor of MDM2 and MDMX, which stabilises p53 and increases expression of p53 targets resulting in p53 dependent apoptosis in cancer cells. Further work to establish the contribution of the inhibition of MDMX to the p53 stabilising activity of HLI373 would be helpful, as well as confirmation that HLI373 inhibits MDMX *in vivo*. The dual inhibition strategy is attractive since one of the mechanisms of primary resistance to MDM2 inhibitors in cell line studies has been overexpression of MDMX[439]. Clearly normal tissues also express MDM2 and MDMX, which work together to control p53 levels, protecting normal cells from p53 mediated cell cycle arrest and apoptosis. Although the MDM2 null mouse is embryonic lethal due to p53 mediated apoptosis[245], early clinical studies have shown that pharmacological inhibition of MDM2 can be achieved by drug doses that are tolerable[426-428]. Likewise the MDMX null mouse is embryonic lethal[270], however the effect of specific pharmacological inhibition of MDMX in humans is as yet unknown. For HLI373, *in vivo* evidence of anti-tumour activity will be required in xenograft models or transgenic mouse models with tumour specific MDM2 or MDMX overexpression. Assuming that dual MDM2 and MDMX inhibition is not excessively toxic in longer

term experiments, these *in vivo* experiments would also be helpful in predicting likely secondary resistance mechanisms to the dual inhibition strategy.

The HLI373 compound presents one of the first dual inhibitors of MDM2 and MDMX and further exploration of the specific mechanism of MDMX inhibition and *in vivo* evaluation will prove valuable.

In an alternative strategy, described in chapter 5, MDM2 inhibitors may have a role in protecting wild-type p53 expressing normal tissues from treatment for a p53 deficient tumour. p53 deficient tumours have deregulated cell cycle control, with loss of the G1/S checkpoint and upregulation of genes controlling G(2)/M transition[515]. This presents a cancer specific feature that can be targeted. By treating patients with an MDM2 inhibitor normal, wild-type p53 expressing tissues can arrest while p53 deficient cells will continue to cycle. This then leaves them more susceptible to subsequent cytotoxic treatment. Furthermore this may allow escalation and therefore increase efficacy of the cytotoxic treatment. To date there have been several cell line studies examining this cyclotherapy strategy which have shown promise[510, 511, 514-517, 611-615]. However these studies have used drugs in the early stages of clinical development. Based on recent evidence showing that low-dose traditional anti-cancer drugs can be used at low dose as MDM2 inhibitors (non-genotoxic p53 stabilising agents)[469, 643] the aim in the present study was to test this theory in cell lines using drugs that are clinically approved. The motivation for this approach was an attempt to streamline clinical testing of the chemoprotection strategy to maximise timely patient benefit.

Data presented here shows that act D can stabilise p53 at low-dose without causing overt DNA damage by causing ribosomal stress and increased L11-MDM2 association, thereby inhibiting MDM2's E3 ligase activity. After low-dose act D treatment, normal cells can be reversibly arrested[469, 699].

Table 7-1 summarises the results of testing low-dose act D and low-dose 5-FU as chemoprotective agents prior to anti-mitotic paclitaxel and DNA damaging agent cisplatin.

Table 7-1: Combinations examined in the present study.

Protective	Therapeutic agent	Protection	
		p53 wild-type	p53 deficient
LD act D	**Paclitaxel**	Yes	No
	Cisplatin	No	No
LD 5-FU	Paclitaxel	Yes	Yes
	Cisplatin	Yes	Yes

LD=Low Dose, act D=Actinomycin D
Grey shaded boxes indicate combinations where wild-type p53 expressing cells are protected from cytotoxic effects while p53 deficient cells are not.

This low-dose treatment can protect wild-type p53 expressing cells from paclitaxel treatment (as measured by a increased cell viability). Importantly act D pre-treatment did not increase the viability of p53 deficient HCT116 cells. In contrast low-dose act D treatment was not capable of protecting wild-type p53 or p53 deficient cells from treatment with DNA crosslinker, cisplatin. This finding is likely to be explained by cisplatin's ability to crosslink DNA regardless of its cell cycle phase meaning that even if the cells are arrested in G1 phase after act D treatment they will still be susceptible to cisplatin-induced cell death. Pre-treatment of p53 deficient cells with act D prior to cisplatin reduced the cell viability in comparison with cisplatin treatment alone. This ability of low-dose act D to enhance the cytotoxic effect of cisplatin in p53 deficient cells warrants further exploration and strengthens the case for use of low-dose act D in a chemoprotective strategy. Previous studies have highlighted some p53 independent mechanisms through which Nutlin can enhance the effects of cytotoxics, including disruption of p73-MDM2 binding and E2F1-MDM2 binding with resultant activation of pro-apoptotic activities of p73 via Noxa[664-666]. These pathways should therefore be examined to elucidate the mechanism of act D's ability to enhance cisplatin induced cell death in p53 null or mutant cells.

Low-dose 5-FU treatment was also explored as a potential MDM2 inhibitor. It was capable of stabilising p53 via non-genotoxic means, but it also had some p53 independent effects on clonogenic survival. Interestingly low-dose 5-FU treatment was capable of protecting p53 wild-type cells and p53 null cells from both paclitaxel and cisplatin treatment. This suggests that 5-FU's ability to protect cells from paclitaxel and cisplatin is a p53 independent effect. Since the underlying mechanism for this protection is unknown, 5-FU is not suitable for use in a chemoprotection strategy that is dependent on p53. As a reason for the protection, one could hypothesize that since 5-FU slows cells' transit through the

cell cycle it reduces the cell fraction entering mitosis and consequently less cells are sensitive to paclitaxel. However, this is unlikely to explain 5-FU's ability to protect cells from cisplatin induced cell death, since cisplatin can have its effect regardless of cell cycle phase. An additional mechanism is likely to be required which could involve a 5-FU induced inhibition of cisplatin's access to guanine residues to crosslink due to 5-FU's incorporation of fluorodeoxyuridine triphosphate with DNA. It will be interesting to further explore these hypotheses.

In this study, p53 null HCT116 cells were used to represent p53 deficient tumours. Although it is likely that mutant p53 expressing tumour cells would respond in the same way, this remains to be confirmed in cell line studies.

Further cell line work is also required to examine the optimal duration of the chemoprotective treatment. It would be anticipated that chemoprotective cell cycle arrest of normal cells should be maintained for the duration of the paclitaxel treatment however confirmation of the continued reversibility of act D-induced cell cycle arrest with longer duration of arrest needs further exploration. Furthermore in current clinical practice it is not common to use a single agent cytotoxic and combinations are preferred to increase the death of cancer cells by differing mechanisms in an attempt to limit acquired resistance and to limit toxicity by using agents with different toxicity profiles. Application of the chemoprotective strategy prior to combination cytotoxic therapy would allow a broader application of the strategy so is worth pursuing.

Importantly the clinical success of the chemoprotective strategy relies on the ability to escalate the dose intensity of paclitaxel. Although low-dose act D has been shown to protect wild-type p53 cells from paclitaxel no assessment of the ability to dose escalate and effects of dose escalation following chemoprotection have been made so far. Although the dose limiting toxicity of paclitaxel is myelosuppression, in an attempt to maintain dose intensity patients can be supported by use of granulocyte colony-stimulating factor (G-CSF) however paclitaxel has other significant toxicities which are not easily abrogated by supportive measures. By adopting the chemoprotective strategy these other toxicities are likely to replace myelosuppression as the dose limiting toxicities. Currently the paclitaxel regimens in clinical use cause significant neurotoxicity leading to major patient morbidity[619].

This neurotoxicity is known to be dependent on dose, infusion duration, treatment schedule and drug delivery vehicle[700]. Conventional paclitaxel requires to be dissolved in a Cremophor El (polyoxyethylated castor oil) and ethanol solvent. This solvent has been implicated in contributing to the incidence of hypersensitivity reactions to paclitaxel and the incidence, severity and time to recovery from neurotoxicity. For this reason an albumin bound preparation of paclitaxel (nab-paclitaxel) has been designed to limit hypersensitivity reactions and neuropathy due to paclitaxel[701]. It may therefore be interesting to examine the chemoprotection strategy prior to nab-paclitaxel, which is approved for use in the treatment of breast cancer[702], since there may be more potential to escalate the dose.

To progress the chemoprotection strategy I would propose testing the strategy in xenografts formed from isogenic cell lines wild-type, null or mutant for p53 using low-dose act D and paclitaxel. The strategy could also be examined in conditional mutant p53 knock-in/p53 knock-out transgenic mouse models. Mouse models will allow simultaneous assessment of the therapeutic effect of escalation of cytotoxic therapy as measured by xenograft shrinkage or tumour shrinkage in a transgenic model, as well as the assessment of new emerging toxicities (by measuring white cell counts and assessing neurotoxicity using locomotor activity measures[703]).

Three different methods of modulation of the p53 pathway are described in this thesis. All of these strategies are in the pre-clinical development stages. In order to assist in the clinical development of such strategies there is a need for early investment in pharmacodynamic biomarker development. In a move from the tradition where drug dosage is dependent on reaching maximum tolerated dose, for molecularly targeted agents drug dosage should be a dose where proof of mechanism can be demonstrated. Furthermore the aim should be to establish a dose of maximal target blockade to allow for variability of drug delivery to tumour cells caused by differences in tumour structure and vascularisation[526]. Ideally if a drug shows no ability to hit its target at doses that are tolerable to patients then the drug should not be further developed. In practice this is difficult since it is desirable to prospectively validated biomarkers in cohorts of patients prior to use as a primary outcome measure in a clinical study. In reality a pragmatic approach

would be to develop biomarkers in phase I and then use the validated biomarker in from phase II. Biomarkers could then be used to indicate directly that the drug is affecting the expected target and could allow clinical decisions to be made using conventional measures of response as well as information regarding the biological effects of the treatment.

To test the chemoprotection strategy in a clinical study, a pharmacodynamic biomarker for p53 activation is needed to determine the MDM2 inhibiting dose of act D. With this in mind, chapter 6 describes 3 potential assays examining normal tissues for evidence of p53 activation.

Easily accessible tissues (hair follicles, PBMCs and serum) from patients prior to and following systemic traditional chemotherapy were examined for evidence of p53 activation.

The present study shows that it is possible to use immunofluorescence followed by confocal imaging of intact plucked hair follicles from the eyebrow. The assay was limited, however, by the high number of hairs where no nuclei stained positive. Disappointingly, no hairs stained positive for p53. Since p53 is tightly regulated with levels being kept low in normal tissues it is likely that the timing of hair follicle sampling in relation to chemotherapy dosing is critical. In addition, it has been suggested that protein expression varies significantly depending on whether the hair is plucked from the eyebrow or scalp[537]. In this study hairs were plucked from the eyebrow only since patients find this more acceptable and less uncomfortable.

p53 and p21 activation in peripheral blood mononuclear cells (PBMCs), as determined by antibody labelling and FACS analysis, appeared to be detected in a small proportion of patients following chemotherapy treatment. There were, however, a high number of patients for whom no induction of p53 or p21 was detected and there was no correlation between response to treatment and induction of p53 or p21. In the context of a study of patients with unknown tumour p53 mutation status this is difficult to interpret, since PBMCs are only a normal tissue surrogate for drug-induced changes in the tumour. While this is ideal for testing which dose of act D is suitable to use for chemoprotection, it is not ideal for assessing the tumour response to treatment. Ideally to assess response to

treatment repeat tumour biopsy could be undertaken however this is sometimes technically not feasible and in general patients would prefer to avoid an uncomfortable procedure that can potentially have complications. For this reason several non-invasive methods of assessing biological changes in tumours are in development including quantification of circulating tumour cells (CTCs)[704], assessment of circulating DNA[705] and functional positron emission tomography (PET[520]) imaging. Overall, although the PBMC assay has high variability in its present protocol, it has potential for further optimisation.

Finally serum was examined for detection of macrophage inhibitory cytokine 1 (MIC-1) levels using a sandwich ELISA. MIC-1 is a secreted p53 target[706]; this means that serum MIC-1 may reflect p53 activity in normal and tumour cells, if the tumour retains wild-type p53. In the cohort of patients studied (of unknown tumour p53 status), an elevated baseline MIC-1 level was significantly associated with a poorer survival in patients with upper gastrointestinal malignancies and with more advanced disease stage for both upper and lower gastrointestinal malignancies. It is counterintuitive that an elevated level of a p53 target gene should be associated with poorer survival and more advanced cancer stage. This is however a consistent finding across several previous publications in cohorts of patients with tumours from a variety of primary sites[688, 692, 694, 695]. It is likely that at least 50% of the patient population studied here have tumours with p53 mutations therefore since these p53 mutant tumours would not be expected to upregulate MIC-1 expression it seems plausible that the elevated MIC-1 levels detected reflect the host's (normal cell) response to tumour burden. This is an interesting area for further study. There is a breadth of data associating systemic inflammation, as assessed by measurement of non-specific marker of systemic inflammation C-reactive protein (CRP), with poor prognosis in cancer patients[696] and in a study of gastric cancer patients, elevated MIC-1 level was associated with poorer survival but not independently of systemic inflammation[695]. It would therefore be interesting to look for correlation between elevated MIC-1 levels and elevated CRP levels in our cohort.

In patients with a p53 deficient tumour a raised MIC-1 in response to chemotherapy suggests p53 induction in normal tissues. In this setting

assessment of MIC-1 may be a useful pharmacodynamic biomarker for p53 activation in studies testing the chemoprotective strategy since the aim is to activate p53 in normal cells. However MIC-1 is also regulated by transcription factor specificity protein 1 (Sp1)[707] as well as a host of other regulatory factors therefore further evaluation of MIC-1 induction in combination with another marker of p53 activation (perhaps using the optimised PBMC assay presented here) is necessary.

In patients with a wild-type p53 tumour, induction of MIC-1 may be both from normal tissues and also from tumour cells. In this context the interpretation of MIC-1-induction following treatment is even more complex since tumour cells may be making some contribution to the MIC-1 levels detected. In the Nutlin clinical studies serum MIC-1 (in a study cohort with wild-type p53 tumours) has been evaluated and has been shown to correlate with the level of drug exposure and thrombocytopenia suggesting that it is reflecting p53 activation in tissues[427, 428].

Of the 3 assays studied, the PBMC assay (although not in its current protocol) and measurement of serum MIC-1 appear to have potential as pharmacodynamic biomarkers for p53 activation. Further studies in larger cohorts of patients, of known tumour p53 status, are needed to validate the assays and establish threshold levels for p53 activation. Hopefully this can be achieved in the on-going clinical studies of p53-MDM2 inhibitor Nutlin.

Taken together data presented in this thesis highlight 3 potential strategies in which our knowledge of p53 pathway regulation could be used to develop promising new strategies to treat cancer patients. Furthermore, this study revealed some of the additional difficulties with using patient samples in biological assays due to high levels of variability.

Figure 7-1 suggests a scheme for applying knowledge of p53 pathway status to direct treatment decisions with the aim of achieving the most appropriate, most effective and least toxic treatment of cancers.

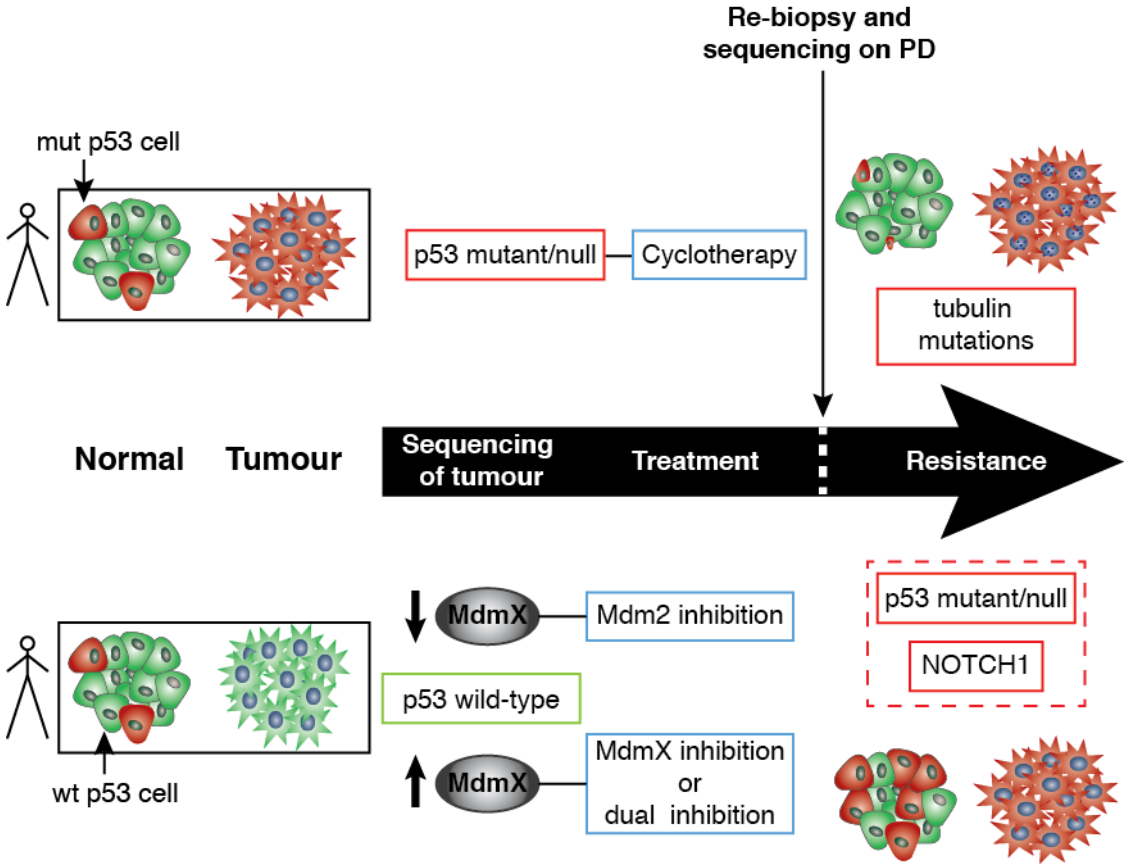

Figure 7-1: p53 directed anti-cancer treatment.
PD=progressive disease, NOTCH1=Notch homolog 1, translocation-associated, wt=wild-type, mut=mutant.

Firstly the application of the strategies presented here in clinical practice will require knowledge of tumour p53 status. At diagnosis patients will require sequencing of their tumour to establish the p53 status.

For those patients who have a p53 deficient tumour the cyclotherapy strategy could be adopted. On completion of treatment patients would be assessed until disease progression. Clearly if the progression free survival is substantial then re-challenge with the previously effective regimen would be the most sensible approach however in the event of a short disease free interval re-biopsy should be supported where possible to allow molecular testing for resistance pathways of interest (for example tubulin mutations may be acquired following paclitaxel treatment[708]). Understanding of the emergence of resistance mechanisms can then inform future treatment decisions. In the future hopefully non-invasive measures of tumour biology will be more informative however to achieve the required validation of these techniques a culture of re-biopsy on progression is required.

In the event of a wild-type p53 tumour, subsequent testing for MDMX overexpression is needed since MDMX overexpression would cause primary resistance to MDM2 inhibitors and indicate the need for MDMX inhibition or dual MDM2/MDMX inhibition[438]. Then on progression (depending on the duration of the progression free interval) tumour re-biopsy should be undertaken since the emergence of p53 mutations may be seen[709-711]. Furthermore in cell line work other resistance mechanisms have been seen including upregulation of NOTCH1 signalling, a finding that may suggest tumour sensitivity to mTOR inhibition therapy[712].

This aim of this simplistic scheme is to highlight the benefit that knowledge of p53 status could bring in terms of more rational treatment decisions and most importantly limiting patient exposure to systemic therapies (and their associated toxicities) which are likely to be ineffective. In the development of MDM2 inhibition therapy an issue of potential concern is that some normal (non-tumour) tissues have p53 mutations (fallopian tube[713] and UV damaged skin[476]). Potentially stabilising the mutant p53 in non-tumour tissues could promote tumour formation. The early phase studies of Nutlin so far have not indicated any concerns regarding the emergence of new primary tumours however these early phase studies have been in patient populations where patients have advanced, multi-resistant disease and the emergence of new primary tumours is therefore likely to be irrelevant. In future studies long term follow-up of patients for second malignancies will require close attention.

In the era of targeted therapy, knowledge of driving molecular forces of a particular tumour are required and the most robust way of determining this is by biopsy at diagnosis and on progression of disease. Even when this is technically feasible this is however not without limitations in that individual tumours themselves can be highly heterogeneous[526, 714]. The most sensible method of dealing with this is to take several biopsies at each timepoint, however, attention would need to be paid to the specific site of tumour biopsy since signalling pathways are likely to vary between the necrotic, hypoxic tumour centre and the leading edge.

As understanding of regulation of MDM2/MDMX and p53 is improved, multiple potential anti-cancer drug targets are likely to be identified. With the addition of

clinical studies, where pharmacodynamic biomarkers are utilised to demonstrate proof of mechanism below maximum tolerated dose, rational drug design and development should lead to improved cancer outcomes for patients.

Bibliography

1. Cheok CF, Verma CS, Baselga J, Lane DP. Translating P53 into the Clinic. Nature reviews Clinical oncology 2011; 8:25-37.
2. Ferlay J. Cancer Incidence, Mortality and Prevalence Worldwide. Globocan 2002. IARC CancerBase 2004; 5.
3. Cancer Incidence Data, 2008. Information and Statistics Division, NHS Scotland, 2011.
4. Cancer Statistics Registrations: Registrations of Cancer Diagnosed in 2008, England. MB1 no 38 London: Office of National Statistics, 2011.
5. Cancer Registrations in Wales 2008. Welsh Cancer Intelligence and Surveillance Unit, 2010.
6. Northern Ireland Incidence Data, 2008.: Northern Ireland Statistics and Research Agency.
7. Maddams J MHaDC. Cancer Prevalence in the Uk, 2008. Thames Cancer Registry and Macmillan Cancer Support 2008.
8. Register General Annual Report 2009. Northern Ireland Statistics and Research Agency.
9. Mortality Statistics: Deaths Registered in England & Wales, 2008. Office for National Statistics, 2010.
10. Deaths Time Series Data, 1997-2008. General Register Office for Scotland, 2010.
11. Iacobuzio-Donahue CA. Epigenetic Changes in Cancer. Annu Rev Pathol 2009; 4:229-49.
12. Yachida S, Jones S, Bozic I, Antal T, Leary R, Fu B, et al. Distant Metastasis Occurs Late During the Genetic Evolution of Pancreatic Cancer. Nature 2010; 467:1114-7.
13. Campbell PJ, Yachida S, Mudie LJ, Stephens PJ, Pleasance ED, Stebbings LA, et al. The Patterns and Dynamics of Genomic Instability in Metastatic Pancreatic Cancer. Nature 2010; 467:1109-13.
14. Bartkowiak K, Riethdorf S, Pantel K. The Interrelating Dynamics of Hypoxic Tumor Microenvironments and Cancer Cell Phenotypes in Cancer Metastasis. Cancer microenvironment : official journal of the International Cancer Microenvironment Society 2012; 5:59-72.
15. Houten L, Reilley AA. An Investigation of the Cause of Death from Cancer. J Surg Oncol 1980; 13:111-6.
16. Hanahan D, Weinberg RA. The Hallmarks of Cancer. Cell 2000; 100:57-70.
17. Hanahan D, Weinberg RA. Hallmarks of Cancer: The Next Generation. Cell 2011; 144:646-74.
18. McAllister SS, Weinberg RA. Tumor-Host Interactions: A Far-Reaching Relationship. J Clin Oncol 2010; 28:4022-8.
19. Stratton MR. Exploring the Genomes of Cancer Cells: Progress and Promise. Science 2011; 331:1553-8.
20. Garzon R, Marcucci G, Croce CM. Targeting Micrornas in Cancer: Rationale, Strategies and Challenges. Nat Rev Drug Discov 2010; 9:775-89.
21. McDermott U, Downing JR, Stratton MR. Genomics and the Continuum of Cancer Care. The New England journal of medicine 2011; 364:340-50.
22. Cairns RA, Harris IS, Mak TW. Regulation of Cancer Cell Metabolism. Nat Rev Cancer 2011; 11:85-95.

23. Deberardinis RJ, Sayed N, Ditsworth D, Thompson CB. Brick by Brick: Metabolism and Tumor Cell Growth. Curr Opin Genet Dev 2008; 18:54-61.
24. Weinstein IB. Cancer. Addiction to Oncogenes--the Achilles Heal of Cancer. Science 2002; 297:63-4.
25. Luo J, Solimini NL, Elledge SJ. Principles of Cancer Therapy: Oncogene and Non-Oncogene Addiction. Cell 2009; 136:823-37.
26. Ashworth A. A Synthetic Lethal Therapeutic Approach: Poly(Adp) Ribose Polymerase Inhibitors for the Treatment of Cancers Deficient in DNA Double-Strand Break Repair. J Clin Oncol 2008; 26:3785-90.
27. Kaelin WG, Jr. The Concept of Synthetic Lethality in the Context of Anticancer Therapy. Nat Rev Cancer 2005; 5:689-98.
28. Druker BJ, Talpaz M, Resta DJ, Peng B, Buchdunger E, Ford JM, et al. Efficacy and Safety of a Specific Inhibitor of the Bcr-Abl Tyrosine Kinase in Chronic Myeloid Leukemia. N Engl J Med 2001; 344:1031-7.
29. Tuveson DA, Willis NA, Jacks T, Griffin JD, Singer S, Fletcher CD, et al. Sti571 Inactivation of the Gastrointestinal Stromal Tumor C-Kit Oncoprotein: Biological and Clinical Implications. Oncogene 2001; 20:5054-8.
30. Slamon DJ, Leyland-Jones B, Shak S, Fuchs H, Paton V, Bajamonde A, et al. Use of Chemotherapy Plus a Monoclonal Antibody against Her2 for Metastatic Breast Cancer That Overexpresses Her2. N Engl J Med 2001; 344:783-92.
31. Hatzivassiliou G, Song K, Yen I, Brandhuber BJ, Anderson DJ, Alvarado R, et al. Raf Inhibitors Prime Wild-Type Raf to Activate the Mapk Pathway and Enhance Growth. Nature 2010; 464:431-5.
32. Heidorn SJ, Milagre C, Whittaker S, Nourry A, Niculescu-Duvas I, Dhomen N, et al. Kinase-Dead Braf and Oncogenic Ras Cooperate to Drive Tumor Progression through Craf. Cell 2010; 140:209-21.
33. Poulikakos PI, Zhang C, Bollag G, Shokat KM, Rosen N. Raf Inhibitors Transactivate Raf Dimers and Erk Signalling in Cells with Wild-Type Braf. Nature 2010; 464:427-30.
34. Vultur A, Villanueva J, Herlyn M. Targeting Braf in Advanced Melanoma: A First Step toward Manageable Disease. Clin Cancer Res 2011; 17:1658-63.
35. Poulikakos PI, Rosen N. Mutant Braf Melanomas--Dependence and Resistance. Cancer Cell 2011; 19:11-5.
36. Chapman PB, Hauschild A, Robert C, Haanen JB, Ascierto P, Larkin J, et al. Improved Survival with Vemurafenib in Melanoma with Braf V600e Mutation. N Engl J Med 2011; 364:2507-16.
37. Stommel JM, Kimmelman AC, Ying H, Nabioullin R, Ponugoti AH, Wiedemeyer R, et al. Coactivation of Receptor Tyrosine Kinases Affects the Response of Tumor Cells to Targeted Therapies. Science 2007; 318:287-90.
38. Toward Precision Medicine: Building a Knowledge Network for Biomedical Research and a New Taxonomy of Disease. Washington (DC): National Research Council (US), 2011.
39. Linzer DI, Levine AJ. Characterization of a 54k Dalton Cellular Sv40 Tumor Antigen Present in Sv40-Transformed Cells and Uninfected Embryonal Carcinoma Cells. Cell 1979; 17:43-52.
40. Lane DP, Crawford LV. T Antigen Is Bound to a Host Protein in Sv40-Transformed Cells. Nature 1979; 278:261-3.

41. Kress M, May E, Cassingena R, May P. Simian Virus 40-Transformed Cells Express New Species of Proteins Precipitable by Anti-Simian Virus 40 Tumor Serum. Journal of virology 1979; 31:472-83.
42. Melero JA, Stitt DT, Mangel WF, Carroll RB. Identification of New Polypeptide Species (48-55k) Immunoprecipitable by Antiserum to Purified Large T Antigen and Present in Sv40-Infected and -Transformed Cells. Virology 1979; 93:466-80.
43. Smith AE, Smith R, Paucha E. Characterization of Different Tumor Antigens Present in Cells Transformed by Simian Virus 40. Cell 1979; 18:335-46.
44. DeLeo AB, Jay G, Appella E, Dubois GC, Law LW, Old LJ. Detection of a Transformation-Related Antigen in Chemically Induced Sarcomas and Other Transformed Cells of the Mouse. Proceedings of the National Academy of Sciences of the United States of America 1979; 76:2420-4.
45. Chumakov PM, Iotsova VS, Georgiev GP. [Isolation of a Plasmid Clone Containing the Mrna Sequence for Mouse Nonviral T-Antigen]. Doklady Akademii nauk SSSR 1982; 267:1272-5.
46. Oren M, Levine AJ. Molecular Cloning of a Cdna Specific for the Murine P53 Cellular Tumor Antigen. Proceedings of the National Academy of Sciences of the United States of America 1983; 80:56-9.
47. Harlow E, Williamson NM, Ralston R, Helfman DM, Adams TE. Molecular Cloning and in Vitro Expression of a Cdna Clone for Human Cellular Tumor Antigen P53. Molecular and cellular biology 1985; 5:1601-10.
48. Pennica D, Goeddel DV, Hayflick JS, Reich NC, Anderson CW, Levine AJ. The Amino Acid Sequence of Murine P53 Determined from a C-DNA Clone. Virology 1984; 134:477-82.
49. Leppard K, Totty N, Waterfield M, Harlow E, Jenkins J, Crawford L. Purification and Partial Amino Acid Sequence Analysis of the Cellular Tumour Antigen, P53, from Mouse Sv40-Transformed Cells. The EMBO journal 1983; 2:1993-9.
50. Jenkins JR, Rudge K, Currie GA. Cellular Immortalization by a Cdna Clone Encoding the Transformation-Associated Phosphoprotein P53. Nature 1984; 312:651-4.
51. Eliyahu D, Raz A, Gruss P, Givol D, Oren M. Participation of P53 Cellular Tumour Antigen in Transformation of Normal Embryonic Cells. Nature 1984; 312:646-9.
52. Parada LF, Land H, Weinberg RA, Wolf D, Rotter V. Cooperation between Gene Encoding P53 Tumour Antigen and Ras in Cellular Transformation. Nature 1984; 312:649-51.
53. Eliyahu D, Michalovitz D, Oren M. Overproduction of P53 Antigen Makes Established Cells Highly Tumorigenic. Nature 1985; 316:158-60.
54. Wolf D, Harris N, Rotter V. Reconstitution of P53 Expression in a Nonproducer Ab-Mulv-Transformed Cell Line by Transfection of a Functional P53 Gene. Cell 1984; 38:119-26.
55. Wolf D, Rotter V. Inactivation of P53 Gene Expression by an Insertion of Moloney Murine Leukemia Virus-Like DNA Sequences. Molecular and cellular biology 1984; 4:1402-10.
56. Ben David Y, Prideaux VR, Chow V, Benchimol S, Bernstein A. Inactivation of the P53 Oncogene by Internal Deletion or Retroviral Integration in Erythroleukemic Cell Lines Induced by Friend Leukemia Virus. Oncogene 1988; 3:179-85.

57. Mowat M, Cheng A, Kimura N, Bernstein A, Benchimol S. Rearrangements of the Cellular P53 Gene in Erythroleukaemic Cells Transformed by Friend Virus. Nature 1985; 314:633-6.
58. Wolf D, Rotter V. Major Deletions in the Gene Encoding the P53 Tumor Antigen Cause Lack of P53 Expression in Hl-60 Cells. Proceedings of the National Academy of Sciences of the United States of America 1985; 82:790-4.
59. Eliyahu D, Goldfinger N, Pinhasi-Kimhi O, Shaulsky G, Skurnik Y, Arai N, et al. Meth a Fibrosarcoma Cells Express Two Transforming Mutant P53 Species. Oncogene 1988; 3:313-21.
60. Finlay CA, Hinds PW, Tan TH, Eliyahu D, Oren M, Levine AJ. Activating Mutations for Transformation by P53 Produce a Gene Product That Forms an Hsc70-P53 Complex with an Altered Half-Life. Molecular and cellular biology 1988; 8:531-9.
61. Finlay CA, Hinds PW, Levine AJ. The P53 Proto-Oncogene Can Act as a Suppressor of Transformation. Cell 1989; 57:1083-93.
62. Baker SJ, Fearon ER, Nigro JM, Hamilton SR, Preisinger AC, Jessup JM, et al. Chromosome 17 Deletions and P53 Gene Mutations in Colorectal Carcinomas. Science 1989; 244:217-21.
63. Eliyahu D, Michalovitz D, Eliyahu S, Pinhasi-Kimhi O, Oren M. Wild-Type P53 Can Inhibit Oncogene-Mediated Focus Formation. Proceedings of the National Academy of Sciences of the United States of America 1989; 86:8763-7.
64. Baker SJ, Preisinger AC, Jessup JM, Paraskeva C, Markowitz S, Willson JK, et al. P53 Gene Mutations Occur in Combination with 17p Allelic Deletions as Late Events in Colorectal Tumorigenesis. Cancer research 1990; 50:7717-22.
65. Malkin D, Li FP, Strong LC, Fraumeni JF, Jr., Nelson CE, Kim DH, et al. Germ Line P53 Mutations in a Familial Syndrome of Breast Cancer, Sarcomas, and Other Neoplasms. Science 1990; 250:1233-8.
66. Srivastava S, Zou ZQ, Pirollo K, Blattner W, Chang EH. Germ-Line Transmission of a Mutated P53 Gene in a Cancer-Prone Family with Li-Fraumeni Syndrome. Nature 1990; 348:747-9.
67. Donehower LA, Harvey M, Slagle BL, McArthur MJ, Montgomery CA, Jr., Butel JS, et al. Mice Deficient for P53 Are Developmentally Normal but Susceptible to Spontaneous Tumours. Nature 1992; 356:215-21.
68. Jacks T, Remington L, Williams BO, Schmitt EM, Halachmi S, Bronson RT, et al. Tumor Spectrum Analysis in P53-Mutant Mice. Curr Biol 1994; 4:1-7.
69. Levine AJ, Oren M. The First 30 Years of P53: Growing Ever More Complex. Nature reviews Cancer 2009; 9:749-58.
70. Vousden KH, Prives C. Blinded by the Light: The Growing Complexity of P53. Cell 2009; 137:413-31.
71. Feng Z, Zhang C, Wu R, Hu W. Tumor Suppressor P53 Meets Microrna s. Journal of molecular cell biology 2011; 3:44-50.
72. Wu WS, Heinrichs S, Xu D, Garrison SP, Zambetti GP, Adams JM, et al. Slug Antagonizes P53-Mediated Apoptosis of Hematopoietic Progenitors by Repressing Puma. Cell 2005; 123:641-53.
73. Wei X, Xu H, Kufe D. Human Muc1 Oncoprotein Regulates P53-Responsive Gene Transcription in the Genotoxic Stress Response. Cancer Cell 2005; 7:167-78.

74. Hudson CD, Morris PJ, Latchman DS, Budhram-Mahadeo VS. Brn-3a Transcription Factor Blocks P53-Mediated Activation of Proapoptotic Target Genes Noxa and Bax in Vitro and in Vivo to Determine Cell Fate. J Biol Chem 2005; 280:11851-8.
75. Budram-Mahadeo V, Morris PJ, Latchman DS. The Brn-3a Transcription Factor Inhibits the Pro-Apoptotic Effect of P53 and Enhances Cell Cycle Arrest by Differentially Regulating the Activity of the P53 Target Genes Encoding Bax and P21(Cip1/Waf1). Oncogene 2002; 21:6123-31.
76. Purvis JE, Karhohs KW, Mock C, Batchelor E, Loewer A, Lahav G. P53 Dynamics Control Cell Fate. Science 2012; 336:1440-4.
77. Vousden KH, Lane DP. P53 in Health and Disease. Nat Rev Mol Cell Biol 2007; 8:275-83.
78. Moll UM, Wolff S, Speidel D, Deppert W. Transcription-Independent Pro-Apoptotic Functions of P53. Curr Opin Cell Biol 2005; 17:631-6.
79. Laptenko O, Prives C. Transcriptional Regulation by P53: One Protein, Many Possibilities. Cell Death Differ 2006; 13:951-61.
80. Green DR, Kroemer G. Cytoplasmic Functions of the Tumour Suppressor P53. Nature 2009; 458:1127-30.
81. Maddocks OD, Vousden KH. Metabolic Regulation by P53. J Mol Med (Berl) 2011; 89:237-45.
82. Sablina AA, Budanov AV, Ilyinskaya GV, Agapova LS, Kravchenko JE, Chumakov PM. The Antioxidant Function of the P53 Tumor Suppressor. Nat Med 2005; 11:1306-13.
83. Weinberg RA. The Biology of Cancer. Garland Science 2007.
84. Vogelstein B, Lane D, Levine AJ. Surfing the P53 Network. Nature 2000; 408:307-10.
85. Harper JW, Adami GR, Wei N, Keyomarsi K, Elledge SJ. The P21 Cdk-Interacting Protein Cip1 Is a Potent Inhibitor of G1 Cyclin-Dependent Kinases. Cell 1993; 75:805-16.
86. el-Deiry WS, Tokino T, Velculescu VE, Levy DB, Parsons R, Trent JM, et al. Waf1, a Potential Mediator of P53 Tumor Suppression. Cell 1993; 75:817-25.
87. Waldman T, Kinzler KW, Vogelstein B. P21 Is Necessary for the P53-Mediated G1 Arrest in Human Cancer Cells. Cancer Res 1995; 55:5187-90.
88. Polyak K, Waldman T, He TC, Kinzler KW, Vogelstein B. Genetic Determinants of P53-Induced Apoptosis and Growth Arrest. Genes Dev 1996; 10:1945-52.
89. Harper JW, Elledge SJ, Keyomarsi K, Dynlacht B, Tsai LH, Zhang P, et al. Inhibition of Cyclin-Dependent Kinases by P21. Mol Biol Cell 1995; 6:387-400.
90. Zhan Q, Antinore MJ, Wang XW, Carrier F, Smith ML, Harris CC, et al. Association with Cdc2 and Inhibition of Cdc2/Cyclin B1 Kinase Activity by the P53-Regulated Protein Gadd45. Oncogene 1999; 18:2892-900.
91. Laronga C, Yang HY, Neal C, Lee MH. Association of the Cyclin-Dependent Kinases and 14-3-3 Sigma Negatively Regulates Cell Cycle Progression. J Biol Chem 2000; 275:23106-12.
92. Chan TA, Hermeking H, Lengauer C, Kinzler KW, Vogelstein B. 14-3-3sigma Is Required to Prevent Mitotic Catastrophe after DNA Damage. Nature 1999; 401:616-20.

93. Innocente SA, Lee JM. P53 Is a Nf-Y- and P21-Independent, Sp1-Dependent Repressor of Cyclin B1 Transcription. FEBS letters 2005; 579:1001-7.
94. Taylor WR, Stark GR. Regulation of the G2/M Transition by P53. Oncogene 2001; 20:1803-15.
95. Yun J, Chae HD, Choy HE, Chung J, Yoo HS, Han MH, et al. P53 Negatively Regulates Cdc2 Transcription Via the Ccaat-Binding Nf-Y Transcription Factor. J Biol Chem 1999; 274:29677-82.
96. Murphy M, Ahn J, Walker KK, Hoffman WH, Evans RM, Levine AJ, et al. Transcriptional Repression by Wild-Type P53 Utilizes Histone Deacetylases, Mediated by Interaction with Msin3a. Genes & development 1999; 13:2490-501.
97. Harms KL, Chen X. Histone Deacetylase 2 Modulates P53 Transcriptional Activities through Regulation of P53-DNA Binding Activity. Cancer research 2007; 67:3145-52.
98. Smith ML, Kontny HU, Zhan Q, Sreenath A, O'Connor PM, Fornace AJ, Jr. Antisense Gadd45 Expression Results in Decreased DNA Repair and Sensitizes Cells to U.V.-Irradiation or Cisplatin. Oncogene 1996; 13:2255-63.
99. Yamaguchi T, Matsuda K, Sagiya Y, Iwadate M, Fujino MA, Nakamura Y, et al. P53r2-Dependent Pathway for DNA Synthesis in a P53-Regulated Cell Cycle Checkpoint. Cancer Res 2001; 61:8256-62.
100. Tanaka H, Arakawa H, Yamaguchi T, Shiraishi K, Fukuda S, Matsui K, et al. A Ribonucleotide Reductase Gene Involved in a P53-Dependent Cell-Cycle Checkpoint for DNA Damage. Nature 2000; 404:42-9.
101. Tan M, Li S, Swaroop M, Guan K, Oberley LW, Sun Y. Transcriptional Activation of the Human Glutathione Peroxidase Promoter by P53. J Biol Chem 1999; 274:12061-6.
102. Hussain SP, Amstad P, He P, Robles A, Lupold S, Kaneko I, et al. P53-Induced up-Regulation of Mnsod and Gpx but Not Catalase Increases Oxidative Stress and Apoptosis. Cancer Res 2004; 64:2350-6.
103. Yoon KA, Nakamura Y, Arakawa H. Identification of Aldh4 as a P53-Inducible Gene and Its Protective Role in Cellular Stresses. J Hum Genet 2004; 49:134-40.
104. Budanov AV, Sablina AA, Feinstein E, Koonin EV, Chumakov PM. Regeneration of Peroxiredoxins by P53-Regulated Sestrins, Homologs of Bacterial Ahpd. Science 2004; 304:596-600.
105. Warburg O. On Respiratory Impairment in Cancer Cells. Science 1956; 124:269-70.
106. Matoba S, Kang JG, Patino WD, Wragg A, Boehm M, Gavrilova O, et al. P53 Regulates Mitochondrial Respiration. Science 2006; 312:1650-3.
107. Hu W, Zhang C, Wu R, Sun Y, Levine A, Feng Z. Glutaminase 2, a Novel P53 Target Gene Regulating Energy Metabolism and Antioxidant Function. Proc Natl Acad Sci U S A 2010; 107:7455-60.
108. Schwartzenberg-Bar-Yoseph F, Armoni M, Karnieli E. The Tumor Suppressor P53 Down-Regulates Glucose Transporters Glut1 and Glut4 Gene Expression. Cancer Res 2004; 64:2627-33.
109. Bensaad K, Tsuruta A, Selak MA, Vidal MN, Nakano K, Bartrons R, et al. Tigar, a P53-Inducible Regulator of Glycolysis and Apoptosis. Cell 2006; 126:107-20.

110. Jones RG, Plas DR, Kubek S, Buzzai M, Mu J, Xu Y, et al. Amp-Activated Protein Kinase Induces a P53-Dependent Metabolic Checkpoint. Molecular cell 2005; 18:283-93.
111. Feng Z, Hu W, de Stanchina E, Teresky AK, Jin S, Lowe S, et al. The Regulation of Ampk Beta1, Tsc2, and Pten Expression by P53: Stress, Cell and Tissue Specificity, and the Role of These Gene Products in Modulating the Igf-1-Akt-Mtor Pathways. Cancer research 2007; 67:3043-53.
112. Budanov AV, Karin M. P53 Target Genes Sestrin1 and Sestrin2 Connect Genotoxic Stress and Mtor Signaling. Cell 2008; 134:451-60.
113. Amaravadi RK, Yu D, Lum JJ, Bui T, Christophorou MA, Evan GI, et al. Autophagy Inhibition Enhances Therapy-Induced Apoptosis in a Myc-Induced Model of Lymphoma. The Journal of clinical investigation 2007; 117:326-36.
114. Crighton D, Wilkinson S, O'Prey J, Syed N, Smith P, Harrison PR, et al. Dram, a P53-Induced Modulator of Autophagy, Is Critical for Apoptosis. Cell 2006; 126:121-34.
115. Tasdemir E, Maiuri MC, Galluzzi L, Vitale I, Djavaheri-Mergny M, D'Amelio M, et al. Regulation of Autophagy by Cytoplasmic P53. Nat Cell Biol 2008; 10:676-87.
116. Komarova EA, Diatchenko L, Rokhlin OW, Hill JE, Wang ZJ, Krivokrysenko VI, et al. Stress-Induced Secretion of Growth Inhibitors: A Novel Tumor Suppressor Function of P53. Oncogene 1998; 17:1089-96.
117. Yu X, Harris SL, Levine AJ. The Regulation of Exosome Secretion: A Novel Function of the P53 Protein. Cancer research 2006; 66:4795-801.
118. Lespagnol A, Duflaut D, Beekman C, Blanc L, Fiucci G, Marine JC, et al. Exosome Secretion, Including the DNA Damage-Induced P53-Dependent Secretory Pathway, Is Severely Compromised in Tsap6/Steap3-Null Mice. Cell Death Differ 2008; 15:1723-33.
119. Ravi R, Mookerjee B, Bhujwalla ZM, Sutter CH, Artemov D, Zeng Q, et al. Regulation of Tumor Angiogenesis by P53-Induced Degradation of Hypoxia-Inducible Factor 1alpha. Genes Dev 2000; 14:34-44.
120. Pal S, Datta K, Mukhopadhyay D. Central Role of P53 on Regulation of Vascular Permeability Factor/Vascular Endothelial Growth Factor (Vpf/Vegf) Expression in Mammary Carcinoma. Cancer Res 2001; 61:6952-7.
121. Teodoro JG, Evans SK, Green MR. Inhibition of Tumor Angiogenesis by P53: A New Role for the Guardian of the Genome. J Mol Med 2007; 85:1175-86.
122. Jesenberger V, Jentsch S. Deadly Encounter: Ubiquitin Meets Apoptosis. Nat Rev Mol Cell Biol 2002; 3:112-21.
123. Miyashita T, Reed JC. Tumor Suppressor P53 Is a Direct Transcriptional Activator of the Human Bax Gene. Cell 1995; 80:293-9.
124. Nakano K, Vousden KH. Puma, a Novel Proapoptotic Gene, Is Induced by P53. Mol Cell 2001; 7:683-94.
125. Yu J, Zhang L, Hwang PM, Kinzler KW, Vogelstein B. Puma Induces the Rapid Apoptosis of Colorectal Cancer Cells. Molecular cell 2001; 7:673-82.
126. Oda E, Ohki R, Murasawa H, Nemoto J, Shibue T, Yamashita T, et al. Noxa, a Bh3-Only Member of the Bcl-2 Family and Candidate Mediator of P53-Induced Apoptosis. Science 2000; 288:1053-8.
127. Chipuk JE, Kuwana T, Bouchier-Hayes L, Droin NM, Newmeyer DD, Schuler M, et al. Direct Activation of Bax by P53 Mediates Mitochondrial Membrane Permeabilization and Apoptosis. Science 2004; 303:1010-4.

128. Budhram-Mahadeo V, Morris PJ, Smith MD, Midgley CA, Boxer LM, Latchman DS. P53 Suppresses the Activation of the Bcl-2 Promoter by the Brn-3a Pou Family Transcription Factor. J Biol Chem 1999; 274:15237-44.
129. Munsch D, Watanabe-Fukunaga R, Bourdon JC, Nagata S, May E, Yonish-Rouach E, et al. Human and Mouse Fas (Apo-1/Cd95) Death Receptor Genes Each Contain a P53-Responsive Element That Is Activated by P53 Mutants Unable to Induce Apoptosis. J Biol Chem 2000; 275:3867-72.
130. Wu GS, Burns TF, McDonald ER, 3rd, Jiang W, Meng R, Krantz ID, et al. Killer/Dr5 Is a DNA Damage-Inducible P53-Regulated Death Receptor Gene. Nat Genet 1997; 17:141-3.
131. Lin Y, Ma W, Benchimol S. Pidd, a New Death-Domain-Containing Protein, Is Induced by P53 and Promotes Apoptosis. Nat Genet 2000; 26:122-7.
132. Rufini A, Tucci P, Celardo I, Melino G. Senescence and Aging: The Critical Roles of P53. Oncogene 2013.
133. Kortlever RM, Higgins PJ, Bernards R. Plasminogen Activator Inhibitor-1 Is a Critical Downstream Target of P53 in the Induction of Replicative Senescence. Nat Cell Biol 2006; 8:877-84.
134. Xue W, Zender L, Miething C, Dickins RA, Hernando E, Krizhanovsky V, et al. Senescence and Tumour Clearance Is Triggered by P53 Restoration in Murine Liver Carcinomas. Nature 2007; 445:656-60.
135. Van Nguyen T, Puebla-Osorio N, Pang H, Dujka ME, Zhu C. DNA Damage-Induced Cellular Senescence Is Sufficient to Suppress Tumorigenesis: A Mouse Model. J Exp Med 2007; 204:1453-61.
136. Barboza JA, Liu G, Ju Z, El-Naggar AK, Lozano G. P21 Delays Tumor Onset by Preservation of Chromosomal Stability. Proc Natl Acad Sci U S A 2006; 103:19842-7.
137. Joerger AC, Fersht AR. Structural Biology of the Tumor Suppressor P53. Annual review of biochemistry 2008; 77:557-82.
138. Venot C, Maratrat M, Sierra V, Conseiller E, Debussche L. Definition of a P53 Transactivation Function-Deficient Mutant and Characterization of Two Independent P53 Transactivation Subdomains. Oncogene 1999; 18:2405-10.
139. Brady CA, Jiang D, Mello SS, Johnson TM, Jarvis LA, Kozak MM, et al. Distinct P53 Transcriptional Programs Dictate Acute DNA-Damage Responses and Tumor Suppression. Cell 2011; 145:571-83.
140. Johnson TM, Hammond EM, Giaccia A, Attardi LD. The P53qs Transactivation-Deficient Mutant Shows Stress-Specific Apoptotic Activity and Induces Embryonic Lethality. Nature genetics 2005; 37:145-52.
141. Chen J, Marechal V, Levine AJ. Mapping of the P53 and Mdm-2 Interaction Domains. Mol Cell Biol 1993; 13:4107-14.
142. Bottger V, Bottger A, Garcia-Echeverria C, Ramos YF, van der Eb AJ, Jochemsen AG, et al. Comparative Study of the P53-Mdm2 and P53-Mdmx Interfaces. Oncogene 1999; 18:189-99.
143. Toledo F, Lee CJ, Krummel KA, Rodewald LW, Liu CW, Wahl GM. Mouse Mutants Reveal That Putative Protein Interaction Sites in the P53 Proline-Rich Domain Are Dispensable for Tumor Suppression. Molecular and cellular biology 2007; 27:1425-32.
144. Cho Y, Gorina S, Jeffrey PD, Pavletich NP. Crystal Structure of a P53 Tumor Suppressor-DNA Complex: Understanding Tumorigenic Mutations. Science 1994; 265:346-55.

145. Kitayner M, Rozenberg H, Kessler N, Rabinovich D, Shaulov L, Haran TE, et al. Structural Basis of DNA Recognition by P53 Tetramers. Molecular cell 2006; 22:741-53.
146. Gorina S, Pavletich NP. Structure of the P53 Tumor Suppressor Bound to the Ankyrin and Sh3 Domains of 53bp2. Science 1996; 274:1001-5.
147. Derbyshire DJ, Basu BP, Serpell LC, Joo WS, Date T, Iwabuchi K, et al. Crystal Structure of Human 53bp1 Brct Domains Bound to P53 Tumour Suppressor. The EMBO journal 2002; 21:3863-72.
148. Joo WS, Jeffrey PD, Cantor SB, Finnin MS, Livingston DM, Pavletich NP. Structure of the 53bp1 Brct Region Bound to P53 and Its Comparison to the Brca1 Brct Structure. Genes & development 2002; 16:583-93.
149. Lilyestrom W, Klein MG, Zhang R, Joachimiak A, Chen XS. Crystal Structure of Sv40 Large T-Antigen Bound to P53: Interplay between a Viral Oncoprotein and a Cellular Tumor Suppressor. Genes & development 2006; 20:2373-82.
150. Bullock AN, Henckel J, DeDecker BS, Johnson CM, Nikolova PV, Proctor MR, et al. Thermodynamic Stability of Wild-Type and Mutant P53 Core Domain. Proceedings of the National Academy of Sciences of the United States of America 1997; 94:14338-42.
151. Jeffrey PD, Gorina S, Pavletich NP. Crystal Structure of the Tetramerization Domain of the P53 Tumor Suppressor at 1.7 Angstroms. Science 1995; 267:1498-502.
152. Shaulsky G, Goldfinger N, Ben-Ze'ev A, Rotter V. Nuclear Accumulation of P53 Protein Is Mediated by Several Nuclear Localization Signals and Plays a Role in Tumorigenesis. Molecular and cellular biology 1990; 10:6565-77.
153. Liang SH, Clarke MF. A Bipartite Nuclear Localization Signal Is Required for P53 Nuclear Import Regulated by a Carboxyl-Terminal Domain. The Journal of biological chemistry 1999; 274:32699-703.
154. Stommel JM, Marchenko ND, Jimenez GS, Moll UM, Hope TJ, Wahl GM. A Leucine-Rich Nuclear Export Signal in the P53 Tetramerization Domain: Regulation of Subcellular Localization and P53 Activity by Nes Masking. The EMBO journal 1999; 18:1660-72.
155. Zhang Y, Xiong Y. A P53 Amino-Terminal Nuclear Export Signal Inhibited by DNA Damage-Induced Phosphorylation. Science 2001; 292:1910-5.
156. Espinosa JM, Emerson BM. Transcriptional Regulation by P53 through Intrinsic DNA/Chromatin Binding and Site-Directed Cofactor Recruitment. Molecular cell 2001; 8:57-69.
157. McKinney K, Mattia M, Gottifredi V, Prives C. P53 Linear Diffusion Along DNA Requires Its C Terminus. Molecular cell 2004; 16:413-24.
158. Bourdon JC, Fernandes K, Murray-Zmijewski F, Liu G, Diot A, Xirodimas DP, et al. P53 Isoforms Can Regulate P53 Transcriptional Activity. Genes Dev 2005; 19:2122-37.
159. Marcel V, Perrier S, Aoubala M, Ageorges S, Groves MJ, Diot A, et al. Delta160p53 Is a Novel N-Terminal P53 Isoform Encoded by Delta133p53 Transcript. FEBS letters 2010; 584:4463-8.
160. Reisman D, Greenberg M, Rotter V. Human P53 Oncogene Contains One Promoter Upstream of Exon 1 and a Second, Stronger Promoter within Intron 1. Proceedings of the National Academy of Sciences of the United States of America 1988; 85:5146-50.
161. Courtois S, Verhaegh G, North S, Luciani MG, Lassus P, Hibner U, et al. Deltan-P53, a Natural Isoform of P53 Lacking the First Transactivation

Domain, Counteracts Growth Suppression by Wild-Type P53. Oncogene 2002; 21:6722-8.
162. Yin Y, Stephen CW, Luciani MG, Fahraeus R. P53 Stability and Activity Is Regulated by Mdm2-Mediated Induction of Alternative P53 Translation Products. Nature cell biology 2002; 4:462-7.
163. Ghosh A, Stewart D, Matlashewski G. Regulation of Human P53 Activity and Cell Localization by Alternative Splicing. Molecular and cellular biology 2004; 24:7987-97.
164. Dichtel-Danjoy ML, Ma D, Dourlen P, Chatelain G, Napoletano F, Robin M, et al. Drosophila P53 Isoforms Differentially Regulate Apoptosis and Apoptosis-Induced Proliferation. Cell Death Differ 2013; 20:108-16.
165. Hofstetter G, Berger A, Berger R, Zoric A, Braicu EI, Reimer D, et al. The N-Terminally Truncated P53 Isoform Delta40p53 Influences Prognosis in Mucinous Ovarian Cancer. Int J Gynecol Cancer 2012; 22:372-9.
166. Fujita K, Mondal AM, Horikawa I, Nguyen GH, Kumamoto K, Sohn JJ, et al. P53 Isoforms Delta133p53 and P53beta Are Endogenous Regulators of Replicative Cellular Senescence. Nat Cell Biol 2009; 11:1135-42.
167. Bernard H, Garmy-Susini B, Ainaoui N, Van Den Berghe L, Peurichard A, Javerzat S, et al. The P53 Isoform, Delta133p53alpha, Stimulates Angiogenesis and Tumour Progression. Oncogene 2012.
168. Ahmed AA, Etemadmoghadam D, Temple J, Lynch AG, Riad M, Sharma R, et al. Driver Mutations in Tp53 Are Ubiquitous in High Grade Serous Carcinoma of the Ovary. The Journal of pathology 2010; 221:49-56.
169. Hofstetter G, Berger A, Schuster E, Wolf A, Hager G, Vergote I, et al. Delta133p53 Is an Independent Prognostic Marker in P53 Mutant Advanced Serous Ovarian Cancer. Br J Cancer 2011; 105:1593-9.
170. Camus S, Menendez S, Fernandes K, Kua N, Liu G, Xirodimas DP, et al. The P53 Isoforms Are Differentially Modified by Mdm2. Cell Cycle 2012; 11:1646-55.
171. Flaman JM, Waridel F, Estreicher A, Vannier A, Limacher JM, Gilbert D, et al. The Human Tumour Suppressor Gene P53 Is Alternatively Spliced in Normal Cells. Oncogene 1996; 12:813-8.
172. Murray-Zmijewski F, Lane DP, Bourdon JC. P53/P63/P73 Isoforms: An Orchestra of Isoforms to Harmonise Cell Differentiation and Response to Stress. Cell death and differentiation 2006; 13:962-72.
173. Machado-Silva A, Perrier S, Bourdon JC. P53 Family Members in Cancer Diagnosis and Treatment. Seminars in Cancer Biology 2010; 20:57-62.
174. Chen J, Ng SM, Chang C, Zhang Z, Bourdon JC, Lane DP, et al. P53 Isoform Delta113p53 Is a P53 Target Gene That Antagonizes P53 Apoptotic Activity Via Bclxl Activation in Zebrafish. Genes Dev 2009; 23:278-90.
175. Marcel V, Tran PL, Sagne C, Martel-Planche G, Vaslin L, Teulade-Fichou MP, et al. G-Quadruplex Structures in Tp53 Intron 3: Role in Alternative Splicing and in Production of P53 Mrna Isoforms. Carcinogenesis 2011; 32:271-8.
176. Lazar V, Hazard F, Bertin F, Janin N, Bellet D, Bressac B. Simple Sequence Repeat Polymorphism within the P53 Gene. Oncogene 1993; 8:1703-5.
177. Cattelani S, Ferrari-Amorotti G, Galavotti S, Defferrari R, Tanno B, Cialfi S, et al. The P53 Codon 72 Pro/Pro Genotype Identifies Poor-Prognosis Neuroblastoma Patients: Correlation with Reduced Apoptosis and

Enhanced Senescence by the P53-72p Isoform. Neoplasia 2012; 14:634-43.
178. Dumont P, Leu JI, Della Pietra AC, 3rd, George DL, Murphy M. The Codon 72 Polymorphic Variants of P53 Have Markedly Different Apoptotic Potential. Nat Genet 2003; 33:357-65.
179. Bergamaschi D, Samuels Y, Sullivan A, Zvelebil M, Breyssens H, Bisso A, et al. Iaspp Preferentially Binds P53 Proline-Rich Region and Modulates Apoptotic Function of Codon 72-Polymorphic P53. Nat Genet 2006; 38:1133-41.
180. Schmidt MK, Reincke S, Broeks A, Braaf LM, Hogervorst FB, Tollenaar RA, et al. Do Mdm2 Snp309 and Tp53 R72p Interact in Breast Cancer Susceptibility? A Large Pooled Series from the Breast Cancer Association Consortium. Cancer Res 2007; 67:9584-90.
181. Matakidou A, Eisen T, Houlston RS. Tp53 Polymorphisms and Lung Cancer Risk: A Systematic Review and Meta-Analysis. Mutagenesis 2003; 18:377-85.
182. Olivier M, Hollstein M, Hainaut P. Tp53 Mutations in Human Cancers: Origins, Consequences, and Clinical Use. Cold Spring Harbor perspectives in biology 2010; 2:a001008.
183. Whibley C, Pharoah PD, Hollstein M. P53 Polymorphisms: Cancer Implications. Nat Rev Cancer 2009; 9:95-107.
184. Roy B, Beamon J, Balint E, Reisman D. Transactivation of the Human P53 Tumor Suppressor Gene by C-Myc/Max Contributes to Elevated Mutant P53 Expression in Some Tumors. Mol Cell Biol 1994; 14:7805-15.
185. Reisman D, Elkind NB, Roy B, Beamon J, Rotter V. C-Myc Trans-Activates the P53 Promoter through a Required Downstream Cacgtg Motif. Cell Growth Differ 1993; 4:57-65.
186. Furlong EE, Rein T, Martin F. Yy1 and Nf1 Both Activate the Human P53 Promoter by Alternatively Binding to a Composite Element, and Yy1 and E1a Cooperate to Amplify P53 Promoter Activity. Mol Cell Biol 1996; 16:5933-45.
187. Reisman D, Takahashi P, Polson A, Boggs K. Transcriptional Regulation of the P53 Tumor Suppressor Gene in S-Phase of the Cell-Cycle and the Cellular Response to DNA Damage. Biochem Res Int 2012; 2012:808934.
188. Stuart ET, Haffner R, Oren M, Gruss P. Loss of P53 Function through Pax-Mediated Transcriptional Repression. EMBO J 1995; 14:5638-45.
189. Zhao X, Wu N, Ding L, Liu M, Liu H, Lin X. Zebrafish P53 Protein Enhances the Translation of Its Own Mrna in Response to Uv Irradiation and Cpt Treatment. FEBS Lett 2012; 586:1220-5.
190. Mazan-Mamczarz K, Galban S, Lopez de Silanes I, Martindale JL, Atasoy U, Keene JD, et al. Rna-Binding Protein Hur Enhances P53 Translation in Response to Ultraviolet Light Irradiation. Proc Natl Acad Sci U S A 2003; 100:8354-9.
191. Takagi M, Absalon MJ, McLure KG, Kastan MB. Regulation of P53 Translation and Induction after DNA Damage by Ribosomal Protein L26 and Nucleolin. Cell 2005; 123:49-63.
192. Kim DY, Kim W, Lee KH, Kim SH, Lee HR, Kim HJ, et al. Hnrnp Q Regulates Translation of P53 in Normal and Stress Conditions. Cell Death Differ 2013; 20:226-34.

193. Rosenstierne MW, Vinther J, Mittler G, Larsen L, Mann M, Norrild B. Conserved Cpes in the P53 3' Untranslated Region Influence Mrna Stability and Protein Synthesis. Anticancer Res 2008; 28:2553-9.
194. Gajjar M, Candeias MM, Malbert-Colas L, Mazars A, Fujita J, Olivares-Illana V, et al. The P53 Mrna-Mdm2 Interaction Controls Mdm2 Nuclear Trafficking and Is Required for P53 Activation Following DNA Damage. Cancer Cell 2012; 21:25-35.
195. Welchman RL, Gordon C, Mayer RJ. Ubiquitin and Ubiquitin-Like Proteins as Multifunctional Signals. Nat Rev Mol Cell Biol 2005; 6:599-609.
196. Schwartz AL, Ciechanover A. The Ubiquitin-Proteasome Pathway and Pathogenesis of Human Diseases. Annual review of medicine 1999; 50:57-74.
197. Chau V, Tobias JW, Bachmair A, Marriott D, Ecker DJ, Gonda DK, et al. A Multiubiquitin Chain Is Confined to Specific Lysine in a Targeted Short-Lived Protein. Science 1989; 243:1576-83.
198. Thrower JS, Hoffman L, Rechsteiner M, Pickart CM. Recognition of the Polyubiquitin Proteolytic Signal. The EMBO journal 2000; 19:94-102.
199. Ye Y, Rape M. Building Ubiquitin Chains: E2 Enzymes at Work. Nature reviews Molecular cell biology 2009; 10:755-64.
200. Shih SC, Sloper-Mould KE, Hicke L. Monoubiquitin Carries a Novel Internalization Signal That Is Appended to Activated Receptors. The EMBO journal 2000; 19:187-98.
201. Hicke L. Protein Regulation by Monoubiquitin. Nature reviews Molecular cell biology 2001; 2:195-201.
202. Groettrup M, Pelzer C, Schmidtke G, Hofmann K. Activating the Ubiquitin Family: Uba6 Challenges the Field. Trends Biochem Sci 2008; 33:230-7.
203. Ardley HC, Robinson PA. E3 Ubiquitin Ligases. Essays in biochemistry 2005; 41:15-30.
204. Fang S, Weissman AM. A Field Guide to Ubiquitylation. Cell Mol Life Sci 2004; 61:1546-61.
205. Glickman MH, Ciechanover A. The Ubiquitin-Proteasome Proteolytic Pathway: Destruction for the Sake of Construction. Physiological reviews 2002; 82:373-428.
206. David Y, Ternette N, Edelmann MJ, Ziv T, Gayer B, Sertchook R, et al. E3 Ligases Determine Ubiquitination Site and Conjugate Type by Enforcing Specificity on E2 Enzymes. The Journal of biological chemistry 2011; 286:44104-15.
207. Markson G, Kiel C, Hyde R, Brown S, Charalabous P, Bremm A, et al. Analysis of the Human E2 Ubiquitin Conjugating Enzyme Protein Interaction Network. Genome research 2009; 19:1905-11.
208. van Wijk SJ, de Vries SJ, Kemmeren P, Huang A, Boelens R, Bonvin AM, et al. A Comprehensive Framework of E2-Ring E3 Interactions of the Human Ubiquitin-Proteasome System. Molecular systems biology 2009; 5:295.
209. Carter S, Vousden KH. Modifications of P53: Competing for the Lysines. Curr Opin Genet Dev 2009.
210. Pichler A, Melchior F. Ubiquitin-Related Modifier Sumo1 and Nucleocytoplasmic Transport. Traffic 2002; 3:381-7.
211. Melchior F, Hengst L. Sumo-1 and P53. Cell Cycle 2002; 1:245-9.

212. Stindt MH, Carter S, Vigneron AM, Ryan KM, Vousden KH. Mdm2 Promotes Sumo-2/3 Modification of P53 to Modulate Transcriptional Activity. Cell Cycle 2011; 10:3176-88.
213. Weger S, Hammer E, Heilbronn R. Topors Acts as a Sumo-1 E3 Ligase for P53 in Vitro and in Vivo. FEBS Lett 2005; 579:5007-12.
214. Chu Y, Yang X. Sumo E3 Ligase Activity of Trim Proteins. Oncogene 2011; 30:1108-16.
215. Chen L, Chen J. Mdm2-Arf Complex Regulates P53 Sumoylation. Oncogene 2003; 22:5348-57.
216. Bischof O, Schwamborn K, Martin N, Werner A, Sustmann C, Grosschedl R, et al. The E3 Sumo Ligase Piasy Is a Regulator of Cellular Senescence and Apoptosis. Mol Cell 2006; 22:783-94.
217. Xirodimas DP, Saville MK, Bourdon JC, Hay RT, Lane DP. Mdm2-Mediated Nedd8 Conjugation of P53 Inhibits Its Transcriptional Activity. Cell 2004; 118:83-97.
218. Abida WM, Nikolaev A, Zhao W, Zhang W, Gu W. Fbxo11 Promotes the Neddylation of P53 and Inhibits Its Transcriptional Activity. J Biol Chem 2007; 282:1797-804.
219. Carter S, Vousden KH. P53-Ubl Fusions as Models of Ubiquitination, Sumoylation and Neddylation of P53. Cell Cycle 2008; 7:2519-28.
220. Scheffner M, Staub O. Hect E3s and Human Disease. BMC biochemistry 2007; 8 Suppl 1:S6.
221. Huibregtse JM, Scheffner M, Beaudenon S, Howley PM. A Family of Proteins Structurally and Functionally Related to the E6-Ap Ubiquitin-Protein Ligase. Proceedings of the National Academy of Sciences of the United States of America 1995; 92:2563-7.
222. Scheffner M, Huibregtse JM, Vierstra RD, Howley PM. The Hpv-16 E6 and E6-Ap Complex Functions as a Ubiquitin-Protein Ligase in the Ubiquitination of P53. Cell 1993; 75:495-505.
223. Sun Y. E3 Ubiquitin Ligases as Cancer Targets and Biomarkers. Neoplasia 2006; 8:645-54.
224. Joazeiro CA, Weissman AM. Ring Finger Proteins: Mediators of Ubiquitin Ligase Activity. Cell 2000; 102:549-52.
225. Aravind L, Koonin EV. The U Box Is a Modified Ring Finger - a Common Domain in Ubiquitination. Current biology : CB 2000; 10:R132-4.
226. Ohi MD, Vander Kooi CW, Rosenberg JA, Chazin WJ, Gould KL. Structural Insights into the U-Box, a Domain Associated with Multi-Ubiquitination. Nature structural biology 2003; 10:250-5.
227. Rechsteiner M, Hoffman L, Dubiel W. The Multicatalytic and 26 S Proteases. The Journal of biological chemistry 1993; 268:6065-8.
228. Burger AM, Seth AK. The Ubiquitin-Mediated Protein Degradation Pathway in Cancer: Therapeutic Implications. European journal of cancer 2004; 40:2217-29.
229. Krummel KA, Lee CJ, Toledo F, Wahl GM. The C-Terminal Lysines Fine-Tune P53 Stress Responses in a Mouse Model but Are Not Required for Stability Control or Transactivation. Proc Natl Acad Sci U S A 2005; 102:10188-93.
230. Feng L, Lin T, Uranishi H, Gu W, Xu Y. Functional Analysis of the Roles of Posttranslational Modifications at the P53 C Terminus in Regulating P53 Stability and Activity. Mol Cell Biol 2005; 25:5389-95.

231. Leng RP, Lin Y, Ma W, Wu H, Lemmers B, Chung S, et al. Pirh2, a P53-Induced Ubiquitin-Protein Ligase, Promotes P53 Degradation. Cell 2003; 112:779-91.
232. Esser C, Scheffner M, Hohfeld J. The Chaperone-Associated Ubiquitin Ligase Chip Is Able to Target P53 for Proteasomal Degradation. The Journal of biological chemistry 2005; 280:27443-8.
233. Chen D, Kon N, Li M, Zhang W, Qin J, Gu W. Arf-Bp1/Mule Is a Critical Mediator of the Arf Tumor Suppressor. Cell 2005; 121:1071-83.
234. Sun L, Shi L, Li W, Yu W, Liang J, Zhang H, et al. Jfk, a Kelch Domain-Containing F-Box Protein, Links the Scf Complex to P53 Regulation. Proc Natl Acad Sci U S A 2009; 106:10195-200.
235. Nag A, Bagchi S, Raychaudhuri P. Cul4a Physically Associates with Mdm2 and Participates in the Proteolysis of P53. Cancer Res 2004; 64:8152-5.
236. Sato Y, Kamura T, Shirata N, Murata T, Kudoh A, Iwahori S, et al. Degradation of Phosphorylated P53 by Viral Protein-Ecs E3 Ligase Complex. PLoS Pathog 2009; 5:e1000530.
237. Jung JH, Bae S, Lee JY, Woo SR, Cha HJ, Yoon Y, et al. E3 Ubiquitin Ligase Hades Negatively Regulates the Exonuclear Function of P53. Cell Death Differ 2011; 18:1865-75.
238. Kruse JP, Gu W. Msl2 Promotes Mdm2-Independent Cytoplasmic Localization of P53. J Biol Chem 2009; 284:3250-63.
239. Muscolini M, Montagni E, Palermo V, Di Agostino S, Gu W, Abdelmoula-Souissi S, et al. The Cancer-Associated K351n Mutation Affects the Ubiquitination and the Translocation to Mitochondria of P53 Protein. J Biol Chem 2011; 286:39693-702.
240. Yamasaki S, Yagishita N, Sasaki T, Nakazawa M, Kato Y, Yamadera T, et al. Cytoplasmic Destruction of P53 by the Endoplasmic Reticulum-Resident Ubiquitin Ligase 'Synoviolin'. EMBO J 2007; 26:113-22.
241. Allton K, Jain AK, Herz HM, Tsai WW, Jung SY, Qin J, et al. Trim24 Targets Endogenous P53 for Degradation. Proc Natl Acad Sci U S A 2009; 106:11612-6.
242. Doyle JM, Gao J, Wang J, Yang M, Potts PR. Mage-Ring Protein Complexes Comprise a Family of E3 Ubiquitin Ligases. Mol Cell 2010; 39:963-74.
243. Zhang L, Huang NJ, Chen C, Tang W, Kornbluth S. Ubiquitylation of P53 by the Apc/C Inhibitor Trim39. Proc Natl Acad Sci U S A 2012; 109:20931-6.
244. Love IM, Grossman SR. It Takes 15 to Tango: Making Sense of the Many Ubiquitin Ligases of P53. Genes Cancer 2012; 3:249-63.
245. Jones SN, Roe AE, Donehower LA, Bradley A. Rescue of Embryonic Lethality in Mdm2-Deficient Mice by Absence of P53. Nature 1995; 378:206-8.
246. Montes de Oca Luna R, Wagner DS, Lozano G. Rescue of Early Embryonic Lethality in Mdm2-Deficient Mice by Deletion of P53. Nature 1995; 378:203-6.
247. Li M, Brooks CL, Wu-Baer F, Chen D, Baer R, Gu W. Mono- Versus Polyubiquitination: Differential Control of P53 Fate by Mdm2. Science 2003; 302:1972-5.
248. Kubbutat MH, Jones SN, Vousden KH. Regulation of P53 Stability by Mdm2. Nature 1997; 387:299-303.
249. Haupt Y, Maya R, Kazaz A, Oren M. Mdm2 Promotes the Rapid Degradation of P53. Nature 1997; 387:296-9.

250. Tao W, Levine AJ. Nucleocytoplasmic Shuttling of Oncoprotein Hdm2 Is Required for Hdm2-Mediated Degradation of P53. Proceedings of the National Academy of Sciences of the United States of America 1999; 96:3077-80.
251. Barak Y, Juven T, Haffner R, Oren M. Mdm2 Expression Is Induced by Wild Type P53 Activity. EMBO J 1993; 12:461-8.
252. Saville MK, Sparks A, Xirodimas DP, Wardrop J, Stevenson LF, Bourdon JC, et al. Regulation of P53 by the Ubiquitin-Conjugating Enzymes Ubch5b/C in Vivo. J Biol Chem 2004; 279:42169-81.
253. Kostic M, Matt T, Martinez-Yamout MA, Dyson HJ, Wright PE. Solution Structure of the Hdm2 C2h2c4 Ring, a Domain Critical for Ubiquitination of P53. J Mol Biol 2006; 363:433-50.
254. Shi D, Pop MS, Kulikov R, Love IM, Kung AL, Grossman SR. Cbp and P300 Are Cytoplasmic E4 Polyubiquitin Ligases for P53. Proc Natl Acad Sci U S A 2009; 106:16275-80.
255. Wu H, Pomeroy SL, Ferreira M, Teider N, Mariani J, Nakayama KI, et al. Ube4b Promotes Hdm2-Mediated Degradation of the Tumor Suppressor P53. Nat Med 2011; 17:347-55.
256. Higashitsuji H, Higashitsuji H, Itoh K, Sakurai T, Nagao T, Sumitomo Y, et al. The Oncoprotein Gankyrin Binds to Mdm2/Hdm2, Enhancing Ubiquitylation and Degradation of P53. Cancer Cell 2005; 8:75-87.
257. Lee JS, Galvin KM, See RH, Eckner R, Livingston D, Moran E, et al. Relief of Yy1 Transcriptional Repression by Adenovirus E1a Is Mediated by E1a-Associated Protein P300. Genes Dev 1995; 9:1188-98.
258. Yuan J, Luo K, Zhang L, Cheville JC, Lou Z. Usp10 Regulates P53 Localization and Stability by Deubiquitinating P53. Cell 2010; 140:384-96.
259. Liu J, Chung HJ, Vogt M, Jin Y, Malide D, He L, et al. Jtv1 Co-Activates Fbp to Induce Usp29 Transcription and Stabilize P53 in Response to Oxidative Stress. EMBO J 2011; 30:846-58.
260. Hock AK, Vigneron AM, Carter S, Ludwig RL, Vousden KH. Regulation of P53 Stability and Function by the Deubiquitinating Enzyme Usp42. EMBO J 2011; 30:4921-30.
261. Cummins JM, Rago C, Kohli M, Kinzler KW, Lengauer C, Vogelstein B. Tumour Suppression: Disruption of Hausp Gene Stabilizes P53. Nature 2004; 428:1 p following 486.
262. Meulmeester E, Maurice MM, Boutell C, Teunisse AF, Ovaa H, Abraham TE, et al. Loss of Hausp-Mediated Deubiquitination Contributes to DNA Damage-Induced Destabilization of Hdmx and Hdm2. Mol Cell 2005; 18:565-76.
263. Marine JC, Francoz S, Maetens M, Wahl G, Toledo F, Lozano G. Keeping P53 in Check: Essential and Synergistic Functions of Mdm2 and Mdm4. Cell Death Differ 2006; 13:927-34.
264. Wade M, Wahl GM. Targeting Mdm2 and Mdmx in Cancer Therapy: Better Living through Medicinal Chemistry? Mol Cancer Res 2009; 7:1-11.
265. Uldrijan S, Pannekoek WJ, Vousden KH. An Essential Function of the Extreme C-Terminus of Mdm2 Can Be Provided by Mdmx. EMBO J 2007; 26:102-12.
266. Poyurovsky MV, Priest C, Kentsis A, Borden KL, Pan ZQ, Pavletich N, et al. The Mdm2 Ring Domain C-Terminus Is Required for Supramolecular Assembly and Ubiquitin Ligase Activity. EMBO J 2007; 26:90-101.

267. Kawai H, Lopez-Pajares V, Kim MM, Wiederschain D, Yuan ZM. Ring Domain-Mediated Interaction Is a Requirement for Mdm2's E3 Ligase Activity. Cancer Res 2007; 67:6026-30.
268. Linares LK, Hengstermann A, Ciechanover A, Muller S, Scheffner M. Hdmx Stimulates Hdm2-Mediated Ubiquitination and Degradation of P53. Proc Natl Acad Sci U S A 2003; 100:12009-14.
269. Gu J, Kawai H, Nie L, Kitao H, Wiederschain D, Jochemsen AG, et al. Mutual Dependence of Mdm2 and Mdmx in Their Functional Inactivation of P53. J Biol Chem 2002; 277:19251-4.
270. Parant J, Chavez-Reyes A, Little NA, Yan W, Reinke V, Jochemsen AG, et al. Rescue of Embryonic Lethality in Mdm4-Null Mice by Loss of Trp53 Suggests a Nonoverlapping Pathway with Mdm2 to Regulate P53. Nat Genet 2001; 29:92-5.
271. Migliorini D, Lazzerini Denchi E, Danovi D, Jochemsen A, Capillo M, Gobbi A, et al. Mdm4 (Mdmx) Regulates P53-Induced Growth Arrest and Neuronal Cell Death During Early Embryonic Mouse Development. Mol Cell Biol 2002; 22:5527-38.
272. Quelle DE, Zindy F, Ashmun RA, Sherr CJ. Alternative Reading Frames of the Ink4a Tumor Suppressor Gene Encode Two Unrelated Proteins Capable of Inducing Cell Cycle Arrest. Cell 1995; 83:993-1000.
273. Kamijo T, Zindy F, Roussel MF, Quelle DE, Downing JR, Ashmun RA, et al. Tumor Suppression at the Mouse Ink4a Locus Mediated by the Alternative Reading Frame Product P19arf. Cell 1997; 91:649-59.
274. Honda R, Yasuda H. Association of P19(Arf) with Mdm2 Inhibits Ubiquitin Ligase Activity of Mdm2 for Tumor Suppressor P53. EMBO J 1999; 18:22-7.
275. Weber JD, Taylor LJ, Roussel MF, Sherr CJ, Bar-Sagi D. Nucleolar Arf Sequesters Mdm2 and Activates P53. Nat Cell Biol 1999; 1:20-6.
276. Lohrum MA, Ludwig RL, Kubbutat MH, Hanlon M, Vousden KH. Regulation of Hdm2 Activity by the Ribosomal Protein L11. Cancer Cell 2003; 3:577-87.
277. Zhou X, Hao Q, Liao J, Zhang Q, Lu H. Ribosomal Protein S14 Unties the Mdm2-P53 Loop Upon Ribosomal Stress. Oncogene 2012.
278. Dai MS, Lu H. Inhibition of Mdm2-Mediated P53 Ubiquitination and Degradation by Ribosomal Protein L5. The Journal of biological chemistry 2004; 279:44475-82.
279. Jin A, Itahana K, O'Keefe K, Zhang Y. Inhibition of Hdm2 and Activation of P53 by Ribosomal Protein L23. Mol Cell Biol 2004; 24:7669-80.
280. Gilkes DM, Chen L, Chen J. Mdmx Regulation of P53 Response to Ribosomal Stress. EMBO J 2006; 25:5614-25.
281. Appella E, Anderson CW. Post-Translational Modifications and Activation of P53 by Genotoxic Stresses. European journal of biochemistry / FEBS 2001; 268:2764-72.
282. Canman CE, Lim DS, Cimprich KA, Taya Y, Tamai K, Sakaguchi K, et al. Activation of the Atm Kinase by Ionizing Radiation and Phosphorylation of P53. Science 1998; 281:1677-9.
283. Hirao A, Kong YY, Matsuoka S, Wakeham A, Ruland J, Yoshida H, et al. DNA Damage-Induced Activation of P53 by the Checkpoint Kinase Chk2. Science 2000; 287:1824-7.

284. Shieh SY, Ikeda M, Taya Y, Prives C. DNA Damage-Induced Phosphorylation of P53 Alleviates Inhibition by Mdm2. Cell 1997; 91:325-34.
285. Shieh SY, Taya Y, Prives C. DNA Damage-Inducible Phosphorylation of P53 at N-Terminal Sites Including a Novel Site, Ser20, Requires Tetramerization. The EMBO journal 1999; 18:1815-23.
286. Matsuoka S, Rotman G, Ogawa A, Shiloh Y, Tamai K, Elledge SJ. Ataxia Telangiectasia-Mutated Phosphorylates Chk2 in Vivo and in Vitro. Proceedings of the National Academy of Sciences of the United States of America 2000; 97:10389-94.
287. Saito S, Goodarzi AA, Higashimoto Y, Noda Y, Lees-Miller SP, Appella E, et al. Atm Mediates Phosphorylation at Multiple P53 Sites, Including Ser(46), in Response to Ionizing Radiation. J Biol Chem 2002; 277:12491-4.
288. Oda K, Arakawa H, Tanaka T, Matsuda K, Tanikawa C, Mori T, et al. P53aip1, a Potential Mediator of P53-Dependent Apoptosis, and Its Regulation by Ser-46-Phosphorylated P53. Cell 2000; 102:849-62.
289. Fang S, Jensen JP, Ludwig RL, Vousden KH, Weissman AM. Mdm2 Is a Ring Finger-Dependent Ubiquitin Protein Ligase for Itself and P53. J Biol Chem 2000; 275:8945-51.
290. Tibbetts RS, Brumbaugh KM, Williams JM, Sarkaria JN, Cliby WA, Shieh SY, et al. A Role for Atr in the DNA Damage-Induced Phosphorylation of P53. Genes & development 1999; 13:152-7.
291. Hao M, Lowy AM, Kapoor M, Deffie A, Liu G, Lozano G. Mutation of Phosphoserine 389 Affects P53 Function in Vivo. The Journal of biological chemistry 1996; 271:29380-5.
292. Lu H, Fisher RP, Bailey P, Levine AJ. The Cdk7-Cych-P36 Complex of Transcription Factor Iih Phosphorylates P53, Enhancing Its Sequence-Specific DNA Binding Activity in Vitro. Molecular and cellular biology 1997; 17:5923-34.
293. Keller DM, Zeng X, Wang Y, Zhang QH, Kapoor M, Shu H, et al. A DNA Damage-Induced P53 Serine 392 Kinase Complex Contains Ck2, Hspt16, and Ssrp1. Molecular cell 2001; 7:283-92.
294. Huang C, Ma WY, Maxiner A, Sun Y, Dong Z. P38 Kinase Mediates Uv-Induced Phosphorylation of P53 Protein at Serine 389. The Journal of biological chemistry 1999; 274:12229-35.
295. Cuddihy AR, Wong AH, Tam NW, Li S, Koromilas AE. The Double-Stranded Rna Activated Protein Kinase Pkr Physically Associates with the Tumor Suppressor P53 Protein and Phosphorylates Human P53 on Serine 392 in Vitro. Oncogene 1999; 18:2690-702.
296. Lohrum M, Scheidtmann KH. Differential Effects of Phosphorylation of Rat P53 on Transactivation of Promoters Derived from Different P53 Responsive Genes. Oncogene 1996; 13:2527-39.
297. Knippschild U, Milne DM, Campbell LE, DeMaggio AJ, Christenson E, Hoekstra MF, et al. P53 Is Phosphorylated in Vitro and in Vivo by the Delta and Epsilon Isoforms of Casein Kinase 1 and Enhances the Level of Casein Kinase 1 Delta in Response to Topoisomerase-Directed Drugs. Oncogene 1997; 15:1727-36.
298. Murray-Zmijewski F, Slee EA, Lu X. A Complex Barcode Underlies the Heterogeneous Response of P53 to Stress. Nature reviews Molecular cell biology 2008; 9:702-12.

299. Grossman SR. P300/Cbp/P53 Interaction and Regulation of the P53 Response. European journal of biochemistry / FEBS 2001; 268:2773-8.
300. Tang Y, Zhao W, Chen Y, Zhao Y, Gu W. Acetylation Is Indispensable for P53 Activation. Cell 2008; 133:612-26.
301. Knights CD, Catania J, Di Giovanni S, Muratoglu S, Perez R, Swartzbeck A, et al. Distinct P53 Acetylation Cassettes Differentially Influence Gene-Expression Patterns and Cell Fate. The Journal of cell biology 2006; 173:533-44.
302. Tang Y, Luo J, Zhang W, Gu W. Tip60-Dependent Acetylation of P53 Modulates the Decision between Cell-Cycle Arrest and Apoptosis. Molecular cell 2006; 24:827-39.
303. Sykes SM, Mellert HS, Holbert MA, Li K, Marmorstein R, Lane WS, et al. Acetylation of the P53 DNA-Binding Domain Regulates Apoptosis Induction. Molecular cell 2006; 24:841-51.
304. Li T, Kon N, Jiang L, Tan M, Ludwig T, Zhao Y, et al. Tumor Suppression in the Absence of P53-Mediated Cell-Cycle Arrest, Apoptosis, and Senescence. Cell 2012; 149:1269-83.
305. Chuikov S, Kurash JK, Wilson JR, Xiao B, Justin N, Ivanov GS, et al. Regulation of P53 Activity through Lysine Methylation. Nature 2004; 432:353-60.
306. Huang J, Perez-Burgos L, Placek BJ, Sengupta R, Richter M, Dorsey JA, et al. Repression of P53 Activity by Smyd2-Mediated Methylation. Nature 2006; 444:629-32.
307. Shi X, Kachirskaia I, Yamaguchi H, West LE, Wen H, Wang EW, et al. Modulation of P53 Function by Set8-Mediated Methylation at Lysine 382. Molecular cell 2007; 27:636-46.
308. Wade M, Wang YV, Wahl GM. The P53 Orchestra: Mdm2 and Mdmx Set the Tone. Trends Cell Biol 2010; 20:299-309.
309. Kussie PH, Gorina S, Marechal V, Elenbaas B, Moreau J, Levine AJ, et al. Structure of the Mdm2 Oncoprotein Bound to the P53 Tumor Suppressor Transactivation Domain. Science 1996; 274:948-53.
310. Momand J, Zambetti GP, Olson DC, George D, Levine AJ. The Mdm-2 Oncogene Product Forms a Complex with the P53 Protein and Inhibits P53-Mediated Transactivation. Cell 1992; 69:1237-45.
311. Roth J, Dobbelstein M, Freedman DA, Shenk T, Levine AJ. Nucleo-Cytoplasmic Shuttling of the Hdm2 Oncoprotein Regulates the Levels of the P53 Protein Via a Pathway Used by the Human Immunodeficiency Virus Rev Protein. The EMBO journal 1998; 17:554-64.
312. Freedman DA, Levine AJ. Nuclear Export Is Required for Degradation of Endogenous P53 by Mdm2 and Human Papillomavirus E6. Molecular and cellular biology 1998; 18:7288-93.
313. Xirodimas DP, Stephen CW, Lane DP. Cocompartmentalization of P53 and Mdm2 Is a Major Determinant for Mdm2-Mediated Degradation of P53. Exp Cell Res 2001; 270:66-77.
314. Lohrum MA, Ashcroft M, Kubbutat MH, Vousden KH. Identification of a Cryptic Nucleolar-Localization Signal in Mdm2. Nature cell biology 2000; 2:179-81.
315. Marechal V, Elenbaas B, Piette J, Nicolas JC, Levine AJ. The Ribosomal L5 Protein Is Associated with Mdm-2 and Mdm-2-P53 Complexes. Mol Cell Biol 1994; 14:7414-20.

316. Argentini M, Barboule N, Wasylyk B. The Contribution of the Acidic Domain of Mdm2 to P53 and Mdm2 Stability. Oncogene 2001; 20:1267-75.
317. Zhu Q, Yao J, Wani G, Wani MA, Wani AA. Mdm2 Mutant Defective in Binding P300 Promotes Ubiquitination but Not Degradation of P53: Evidence for the Role of P300 in Integrating Ubiquitination and Proteolysis. The Journal of biological chemistry 2001; 276:29695-701.
318. Wallace M, Worrall E, Pettersson S, Hupp TR, Ball KL. Dual-Site Regulation of Mdm2 E3-Ubiquitin Ligase Activity. Mol Cell 2006; 23:251-63.
319. Ma J, Martin JD, Zhang H, Auger KR, Ho TF, Kirkpatrick RB, et al. A Second P53 Binding Site in the Central Domain of Mdm2 Is Essential for P53 Ubiquitination. Biochemistry 2006; 45:9238-45.
320. Grossman SR, Perez M, Kung AL, Joseph M, Mansur C, Xiao ZX, et al. P300/Mdm2 Complexes Participate in Mdm2-Mediated P53 Degradation. Molecular cell 1998; 2:405-15.
321. Kawai H, Nie L, Wiederschain D, Yuan ZM. Dual Role of P300 in the Regulation of P53 Stability. The Journal of biological chemistry 2001; 276:45928-32.
322. Lindstrom MS, Jin A, Deisenroth C, White Wolf G, Zhang Y. Cancer-Associated Mutations in the Mdm2 Zinc Finger Domain Disrupt Ribosomal Protein Interaction and Attenuate Mdm2-Induced P53 Degradation. Mol Cell Biol 2007; 27:1056-68.
323. Lai Z, Ferry KV, Diamond MA, Wee KE, Kim YB, Ma J, et al. Human Mdm2 Mediates Multiple Mono-Ubiquitination of P53 by a Mechanism Requiring Enzyme Isomerization. J Biol Chem 2001; 276:31357-67.
324. Itahana K, Mao H, Jin A, Itahana Y, Clegg HV, Lindstrom MS, et al. Targeted Inactivation of Mdm2 Ring Finger E3 Ubiquitin Ligase Activity in the Mouse Reveals Mechanistic Insights into P53 Regulation. Cancer Cell 2007; 12:355-66.
325. Sharp DA, Kratowicz SA, Sank MJ, George DL. Stabilization of the Mdm2 Oncoprotein by Interaction with the Structurally Related Mdmx Protein. The Journal of biological chemistry 1999; 274:38189-96.
326. Cahilly-Snyder L, Yang-Feng T, Francke U, George DL. Molecular Analysis and Chromosomal Mapping of Amplified Genes Isolated from a Transformed Mouse 3t3 Cell Line. Somatic cell and molecular genetics 1987; 13:235-44.
327. Fakharzadeh SS, Trusko SP, George DL. Tumorigenic Potential Associated with Enhanced Expression of a Gene That Is Amplified in a Mouse Tumor Cell Line. The EMBO journal 1991; 10:1565-9.
328. Oliner JD, Kinzler KW, Meltzer PS, George DL, Vogelstein B. Amplification of a Gene Encoding a P53-Associated Protein in Human Sarcomas. Nature 1992; 358:80-3.
329. Iwakuma T, Lozano G. Mdm2, an Introduction. Mol Cancer Res 2003; 1:993-1000.
330. Zauberman A, Flusberg D, Haupt Y, Barak Y, Oren M. A Functional P53-Responsive Intronic Promoter Is Contained within the Human Mdm2 Gene. Nucleic acids research 1995; 23:2584-92.
331. Pinkas J, Naber SP, Butel JS, Medina D, Jerry DJ. Expression of Mdm2 During Mammary Tumorigenesis. International journal of cancer Journal international du cancer 1999; 81:292-8.
332. Sigalas I, Calvert AH, Anderson JJ, Neal DE, Lunec J. Alternatively Spliced Mdm2 Transcripts with Loss of P53 Binding Domain Sequences:

Transforming Ability and Frequent Detection in Human Cancer. Nature medicine 1996; 2:912-7.
333. Matsumoto R, Tada M, Nozaki M, Zhang CL, Sawamura Y, Abe H. Short Alternative Splice Transcripts of the Mdm2 Oncogene Correlate to Malignancy in Human Astrocytic Neoplasms. Cancer research 1998; 58:609-13.
334. Evans SC, Viswanathan M, Grier JD, Narayana M, El-Naggar AK, Lozano G. An Alternatively Spliced Hdm2 Product Increases P53 Activity by Inhibiting Hdm2. Oncogene 2001; 20:4041-9.
335. Meek DW, Knippschild U. Posttranslational Modification of Mdm2. Mol Cancer Res 2003; 1:1017-26.
336. Stommel JM, Wahl GM. A New Twist in the Feedback Loop: Stress-Activated Mdm2 Destabilization Is Required for P53 Activation. Cell Cycle 2005; 4:411-7.
337. Mayo LD, Turchi JJ, Berberich SJ. Mdm-2 Phosphorylation by DNA-Dependent Protein Kinase Prevents Interaction with P53. Cancer research 1997; 57:5013-6.
338. Goldberg Z, Vogt Sionov R, Berger M, Zwang Y, Perets R, Van Etten RA, et al. Tyrosine Phosphorylation of Mdm2 by C-Abl: Implications for P53 Regulation. The EMBO journal 2002; 21:3715-27.
339. Lu X, Ma O, Nguyen TA, Jones SN, Oren M, Donehower LA. The Wip1 Phosphatase Acts as a Gatekeeper in the P53-Mdm2 Autoregulatory Loop. Cancer Cell 2007; 12:342-54.
340. Lu X, Nguyen TA, Zhang X, Donehower LA. The Wip1 Phosphatase and Mdm2: Cracking the "Wip" on P53 Stability. Cell Cycle 2008; 7:164-8.
341. Lu X, Nannenga B, Donehower LA. Ppm1d Dephosphorylates Chk1 and P53 and Abrogates Cell Cycle Checkpoints. Genes & development 2005; 19:1162-74.
342. Wang X, Taplick J, Geva N, Oren M. Inhibition of P53 Degradation by Mdm2 Acetylation. FEBS Lett 2004; 561:195-201.
343. Xirodimas DP, Chisholm J, Desterro JM, Lane DP, Hay RT. P14arf Promotes Accumulation of Sumo-1 Conjugated (H)Mdm2. FEBS letters 2002; 528:207-11.
344. Ding B, Sun Y, Huang J. Overexpression of Ski Oncoprotein Leads to P53 Degradation through Regulation of Mdm2 Protein Sumoylation. J Biol Chem 2012; 287:14621-30.
345. Zhao R, Yeung SC, Chen J, Iwakuma T, Su CH, Chen B, et al. Subunit 6 of the Cop9 Signalosome Promotes Tumorigenesis in Mice through Stabilization of Mdm2 and Is Upregulated in Human Cancers. The Journal of clinical investigation 2011; 121:851-65.
346. Shvarts A, Steegenga WT, Riteco N, van Laar T, Dekker P, Bazuine M, et al. Mdmx: A Novel P53-Binding Protein with Some Functional Properties of Mdm2. EMBO J 1996; 15:5349-57.
347. Sabbatini P, McCormick F. Mdmx Inhibits the P300/Cbp-Mediated Acetylation of P53. DNA and cell biology 2002; 21:519-25.
348. Zdzalik M, Pustelny K, Kedracka-Krok S, Huben K, Pecak A, Wladyka B, et al. Interaction of Regulators Mdm2 and Mdmx with Transcription Factors P53, P63 and P73. Cell Cycle 2010; 9:4584-91.
349. Chen L, Li C, Pan Y, Chen J. Regulation of P53-Mdmx Interaction by Casein Kinase 1 Alpha. Molecular and cellular biology 2005; 25:6509-20.

350. Tanimura S, Ohtsuka S, Mitsui K, Shirouzu K, Yoshimura A, Ohtsubo M. Mdm2 Interacts with Mdmx through Their Ring Finger Domains. FEBS Lett 1999; 447:5-9.
351. Linke K, Mace PD, Smith CA, Vaux DL, Silke J, Day CL. Structure of the Mdm2/Mdmx Ring Domain Heterodimer Reveals Dimerization Is Required for Their Ubiquitylation in Trans. Cell Death Differ 2008; 15:841-8.
352. Huang L, Yan Z, Liao X, Li Y, Yang J, Wang ZG, et al. The P53 Inhibitors Mdm2/Mdmx Complex Is Required for Control of P53 Activity in Vivo. Proceedings of the National Academy of Sciences of the United States of America 2011; 108:12001-6.
353. Pant V, Xiong S, Iwakuma T, Quintas-Cardama A, Lozano G. Heterodimerization of Mdm2 and Mdm4 Is Critical for Regulating P53 Activity During Embryogenesis but Dispensable for P53 and Mdm2 Stability. Proceedings of the National Academy of Sciences of the United States of America 2011; 108:11995-2000.
354. Phillips A, Teunisse A, Lam S, Lodder K, Darley M, Emaduddin M, et al. Hdmx-L Is Expressed from a Functional P53-Responsive Promoter in the First Intron of the Hdmx Gene and Participates in an Autoregulatory Feedback Loop to Control P53 Activity. J Biol Chem 2010; 285:29111-27.
355. Markey M, Berberich SJ. Full-Length Hdmx Transcripts Decrease Following Genotoxic Stress. Oncogene 2008; 27:6657-66.
356. Perry ME. The Regulation of the P53-Mediated Stress Response by Mdm2 and Mdm4. Cold Spring Harbor perspectives in biology 2010; 2:a000968.
357. Chandler DS, Singh RK, Caldwell LC, Bitler JL, Lozano G. Genotoxic Stress Induces Coordinately Regulated Alternative Splicing of the P53 Modulators Mdm2 and Mdm4. Cancer Res 2006; 66:9502-8.
358. Bartel F, Schulz J, Bohnke A, Blumke K, Kappler M, Bache M, et al. Significance of Hdmx-S (or Mdm4) Mrna Splice Variant Overexpression and Hdmx Gene Amplification on Primary Soft Tissue Sarcoma Prognosis. Int J Cancer 2005; 117:469-75.
359. Lenos K, Grawenda AM, Lodder K, Kuijjer ML, Teunisse AF, Repapi E, et al. Alternate Splicing of the P53 Inhibitor Hdmx Offers a Superior Prognostic Biomarker Than P53 Mutation in Human Cancer. Cancer Res 2012; 72:4074-84.
360. Chen L, Gilkes DM, Pan Y, Lane WS, Chen J. Atm and Chk2-Dependent Phosphorylation of Mdmx Contribute to P53 Activation after DNA Damage. The EMBO journal 2005; 24:3411-22.
361. Okamoto K, Kashima K, Pereg Y, Ishida M, Yamazaki S, Nota A, et al. DNA Damage-Induced Phosphorylation of Mdmx at Serine 367 Activates P53 by Targeting Mdmx for Mdm2-Dependent Degradation. Molecular and cellular biology 2005; 25:9608-20.
362. LeBron C, Chen L, Gilkes DM, Chen J. Regulation of Mdmx Nuclear Import and Degradation by Chk2 and 14-3-3. The EMBO journal 2006; 25:1196-206.
363. Pereg Y, Lam S, Teunisse A, Biton S, Meulmeester E, Mittelman L, et al. Differential Roles of Atm- and Chk2-Mediated Phosphorylations of Hdmx in Response to DNA Damage. Molecular and cellular biology 2006; 26:6819-31.
364. Zuckerman V, Lenos K, Popowicz GM, Silberman I, Grossman T, Marine JC, et al. C-Abl Phosphorylates Hdmx and Regulates Its Interaction with P53. The Journal of biological chemistry 2009; 284:4031-9.

365. Lopez-Pajares V, Kim MM, Yuan ZM. Phosphorylation of Mdmx Mediated by Akt Leads to Stabilization and Induces 14-3-3 Binding. The Journal of biological chemistry 2008; 283:13707-13.
366. Wang YV, Leblanc M, Wade M, Jochemsen AG, Wahl GM. Increased Radioresistance and Accelerated B Cell Lymphomas in Mice with Mdmx Mutations That Prevent Modifications by DNA-Damage-Activated Kinases. Cancer Cell 2009; 16:33-43.
367. Zhang X, Lin L, Guo H, Yang J, Jones SN, Jochemsen A, et al. Phosphorylation and Degradation of Mdmx Is Inhibited by Wip1 Phosphatase in the DNA Damage Response. Cancer research 2009; 69:7960-8.
368. Pan Y, Chen J. Mdm2 Promotes Ubiquitination and Degradation of Mdmx. Mol Cell Biol 2003; 23:5113-21.
369. Pan Y, Chen J. Modification of Mdmx by Sumoylation. Biochemical and biophysical research communications 2005; 332:702-9.
370. Hollstein M, Sidransky D, Vogelstein B, Harris CC. P53 Mutations in Human Cancers. Science 1991; 253:49-53.
371. Hainaut P, Hollstein M. P53 and Human Cancer: The First Ten Thousand Mutations. Adv Cancer Res 2000; 77:81-137.
372. Wood LD, Parsons DW, Jones S, Lin J, Sjoblom T, Leary RJ, et al. The Genomic Landscapes of Human Breast and Colorectal Cancers. Science 2007; 318:1108-13.
373. Petitjean A, Achatz MI, Borresen-Dale AL, Hainaut P, Olivier M. Tp53 Mutations in Human Cancers: Functional Selection and Impact on Cancer Prognosis and Outcomes. Oncogene 2007; 26:2157-65.
374. Liu Y, Wu F. Global Burden of Aflatoxin-Induced Hepatocellular Carcinoma: A Risk Assessment. Environ Health Perspect 2010; 118:818-24.
375. Bressac B, Kew M, Wands J, Ozturk M. Selective G to T Mutations of P53 Gene in Hepatocellular Carcinoma from Southern Africa. Nature 1991; 350:429-31.
376. Patterson M. The Trouble with Smoking. Nat Rev Genet 2000; 1:168.
377. Rodin SN, Rodin AS. Human Lung Cancer and P53: The Interplay between Mutagenesis and Selection. Proc Natl Acad Sci U S A 2000; 97:12244-9.
378. Brash DE, Rudolph JA, Simon JA, Lin A, McKenna GJ, Baden HP, et al. A Role for Sunlight in Skin Cancer: Uv-Induced P53 Mutations in Squamous Cell Carcinoma. Proc Natl Acad Sci U S A 1991; 88:10124-8.
379. Audrey Petitjean EMSKCISVTPHMO. Impact of Mutant P53 Functional Properties on <I>Tp53</I> Mutation Patterns and Tumor Phenotype: Lessons from Recent Developments in the Iarc Tp53 Database. Human Mutation 2007; 28:622-9.
380. Sigal A, Rotter V. Oncogenic Mutations of the P53 Tumor Suppressor: The Demons of the Guardian of the Genome. Cancer Res 2000; 60:6788-93.
381. Lang GA, Iwakuma T, Suh YA, Liu G, Rao VA, Parant JM, et al. Gain of Function of a P53 Hot Spot Mutation in a Mouse Model of Li-Fraumeni Syndrome. Cell 2004; 119:861-72.
382. Olive KP, Tuveson DA, Ruhe ZC, Yin B, Willis NA, Bronson RT, et al. Mutant P53 Gain of Function in Two Mouse Models of Li-Fraumeni Syndrome. Cell 2004; 119:847-60.
383. Liu DP, Song H, Xu Y. A Common Gain of Function of P53 Cancer Mutants in Inducing Genetic Instability. Oncogene 2010; 29:949-56.

384. Muller PA, Vousden KH. P53 Mutations in Cancer. Nat Cell Biol 2013; 15:2-8.
385. Muller PA, Caswell PT, Doyle B, Iwanicki MP, Tan EH, Karim S, et al. Mutant P53 Drives Invasion by Promoting Integrin Recycling. Cell 2009; 139:1327-41.
386. Schilling T, Kairat A, Melino G, Krammer PH, Stremmel W, Oren M, et al. Interference with the P53 Family Network Contributes to the Gain of Oncogenic Function of Mutant P53 in Hepatocellular Carcinoma. Biochem Biophys Res Commun 2010; 394:817-23.
387. Liu K, Ling S, Lin WC. Topbp1 Mediates Mutant P53 Gain of Function through Nf-Y and P63/P73. Mol Cell Biol 2011; 31:4464-81.
388. Adorno M, Cordenonsi M, Montagner M, Dupont S, Wong C, Hann B, et al. A Mutant-P53/Smad Complex Opposes P63 to Empower Tgfbeta-Induced Metastasis. Cell 2009; 137:87-98.
389. Freed-Pastor WA, Mizuno H, Zhao X, Langerod A, Moon SH, Rodriguez-Barrueco R, et al. Mutant P53 Disrupts Mammary Tissue Architecture Via the Mevalonate Pathway. Cell 2012; 148:244-58.
390. Muller PA, Trinidad AG, Timpson P, Morton JP, Zanivan S, van den Berghe PV, et al. Mutant P53 Enhances Met Trafficking and Signalling to Drive Cell Scattering and Invasion. Oncogene 2012.
391. Bonnefoi H, Piccart M, Bogaerts J, Mauriac L, Fumoleau P, Brain E, et al. Tp53 Status for Prediction of Sensitivity to Taxane Versus Non-Taxane Neoadjuvant Chemotherapy in Breast Cancer (Eortc 10994/Big 1-00): A Randomised Phase 3 Trial. The lancet oncology 2011; 12:527-39.
392. Varna M, Bousquet G, Plassa LF, Bertheau P, Janin A. Tp53 Status and Response to Treatment in Breast Cancers. Journal of biomedicine & biotechnology 2011; 2011:284584.
393. Jackson JG, Pant V, Li Q, Chang LL, Quintas-Cardama A, Garza D, et al. P53-Mediated Senescence Impairs the Apoptotic Response to Chemotherapy and Clinical Outcome in Breast Cancer. Cancer Cell 2012; 21:793-806.
394. Russo A, Bazan V, Iacopetta B, Kerr D, Soussi T, Gebbia N. The Tp53 Colorectal Cancer International Collaborative Study on the Prognostic and Predictive Significance of P53 Mutation: Influence of Tumor Site, Type of Mutation, and Adjuvant Treatment. Journal of clinical oncology : official journal of the American Society of Clinical Oncology 2005; 23:7518-28.
395. Vahteristo P, Tamminen A, Karvinen P, Eerola H, Eklund C, Aaltonen LA, et al. P53, Chk2, and Chk1 Genes in Finnish Families with Li-Fraumeni Syndrome: Further Evidence of Chk2 in Inherited Cancer Predisposition. Cancer Res 2001; 61:5718-22.
396. Lee SB, Kim SH, Bell DW, Wahrer DC, Schiripo TA, Jorczak MM, et al. Destabilization of Chk2 by a Missense Mutation Associated with Li-Fraumeni Syndrome. Cancer Res 2001; 61:8062-7.
397. Kang JH, Kim SJ, Noh DY, Park IA, Choe KJ, Yoo OJ, et al. Methylation in the P53 Promoter Is a Supplementary Route to Breast Carcinogenesis: Correlation between Cpg Methylation in the P53 Promoter and the Mutation of the P53 Gene in the Progression from Ductal Carcinoma in Situ to Invasive Ductal Carcinoma. Laboratory investigation; a journal of technical methods and pathology 2001; 81:573-9.

398. Khan D, Sharathchandra A, Ponnuswamy A, Grover R, Das S. Effect of a Natural Mutation in the 5' Untranslated Region on the Translational Control of P53 Mrna. Oncogene 2012.
399. Nyiraneza C, Sempoux C, Detry R, Kartheuser A, Dahan K. Hypermethylation of the 5' Cpg Island of the P14arf Flanking Exon 1beta in Human Colorectal Cancer Displaying a Restricted Pattern of P53 Overexpression Concomitant with Increased Mdm2 Expression. Clin Epigenetics 2012; 4:9.
400. Mayo LD, Donner DB. A Phosphatidylinositol 3-Kinase/Akt Pathway Promotes Translocation of Mdm2 from the Cytoplasm to the Nucleus. Proceedings of the National Academy of Sciences of the United States of America 2001; 98:11598-603.
401. Myers MP, Pass I, Batty IH, Van der Kaay J, Stolarov JP, Hemmings BA, et al. The Lipid Phosphatase Activity of Pten Is Critical for Its Tumor Supressor Function. Proc Natl Acad Sci U S A 1998; 95:13513-8.
402. Toledo F, Wahl GM. Regulating the P53 Pathway: In Vitro Hypotheses, in Vivo Veritas. Nat Rev Cancer 2006; 6:909-23.
403. Ladanyi M, Cha C, Lewis R, Jhanwar SC, Huvos AG, Healey JH. Mdm2 Gene Amplification in Metastatic Osteosarcoma. Cancer Res 1993; 53:16-8.
404. Riemenschneider MJ, Buschges R, Wolter M, Reifenberger J, Bostrom J, Kraus JA, et al. Amplification and Overexpression of the Mdm4 (Mdmx) Gene from 1q32 in a Subset of Malignant Gliomas without Tp53 Mutation or Mdm2 Amplification. Cancer research 1999; 59:6091-6.
405. Danovi D, Meulmeester E, Pasini D, Migliorini D, Capra M, Frenk R, et al. Amplification of Mdmx (or Mdm4) Directly Contributes to Tumor Formation by Inhibiting P53 Tumor Suppressor Activity. Mol Cell Biol 2004; 24:5835-43.
406. Laurie NA, Donovan SL, Shih CS, Zhang J, Mills N, Fuller C, et al. Inactivation of the P53 Pathway in Retinoblastoma. Nature 2006; 444:61-6.
407. Gembarska A, Luciani F, Fedele C, Russell EA, Dewaele M, Villar S, et al. Mdm4 Is a Key Therapeutic Target in Cutaneous Melanoma. Nature medicine 2012.
408. Bond GL, Hu W, Bond EE, Robins H, Lutzker SG, Arva NC, et al. A Single Nucleotide Polymorphism in the Mdm2 Promoter Attenuates the P53 Tumor Suppressor Pathway and Accelerates Tumor Formation in Humans. Cell 2004; 119:591-602.
409. Schlaeger C, Longerich T, Schiller C, Bewerunge P, Mehrabi A, Toedt G, et al. Etiology-Dependent Molecular Mechanisms in Human Hepatocarcinogenesis. Hepatology 2008; 47:511-20.
410. Valentin-Vega YA, Barboza JA, Chau GP, El-Naggar AK, Lozano G. High Levels of the P53 Inhibitor Mdm4 in Head and Neck Squamous Carcinomas. Hum Pathol 2007; 38:1553-62.
411. Scheffner M, Werness BA, Huibregtse JM, Levine AJ, Howley PM. The E6 Oncoprotein Encoded by Human Papillomavirus Types 16 and 18 Promotes the Degradation of P53. Cell 1990; 63:1129-36.
412. Parkin DM. The Global Health Burden of Infection-Associated Cancers in the Year 2002. Int J Cancer 2006; 118:3030-44.
413. Villa LL. Hpv Prophylactic Vaccination: The First Years and What to Expect from Now. Cancer Lett 2011; 305:106-12.

414. Moll UM, Ostermeyer AG, Haladay R, Winkfield B, Frazier M, Zambetti G. Cytoplasmic Sequestration of Wild-Type P53 Protein Impairs the G1 Checkpoint after DNA Damage. Molecular and cellular biology 1996; 16:1126-37.
415. Moll UM, LaQuaglia M, Benard J, Riou G. Wild-Type P53 Protein Undergoes Cytoplasmic Sequestration in Undifferentiated Neuroblastomas but Not in Differentiated Tumors. Proceedings of the National Academy of Sciences of the United States of America 1995; 92:4407-11.
416. Moll UM, Riou G, Levine AJ. Two Distinct Mechanisms Alter P53 in Breast Cancer: Mutation and Nuclear Exclusion. Proceedings of the National Academy of Sciences of the United States of America 1992; 89:7262-6.
417. Martins CP, Brown-Swigart L, Evan GI. Modeling the Therapeutic Efficacy of P53 Restoration in Tumors. Cell 2006; 127:1323-34.
418. Ventura A, Kirsch DG, McLaughlin ME, Tuveson DA, Grimm J, Lintault L, et al. Restoration of P53 Function Leads to Tumour Regression in Vivo. Nature 2007; 445:661-5.
419. Wang Y, Suh YA, Fuller MY, Jackson JG, Xiong S, Terzian T, et al. Restoring Expression of Wild-Type P53 Suppresses Tumor Growth but Does Not Cause Tumor Regression in Mice with a P53 Missense Mutation. The Journal of clinical investigation 2011; 121:893-904.
420. Terzian T, Suh YA, Iwakuma T, Post SM, Neumann M, Lang GA, et al. The Inherent Instability of Mutant P53 Is Alleviated by Mdm2 or P16ink4a Loss. Genes Dev 2008; 22:1337-44.
421. Mendrysa SM, O'Leary KA, McElwee MK, Michalowski J, Eisenman RN, Powell DA, et al. Tumor Suppression and Normal Aging in Mice with Constitutively High P53 Activity. Genes Dev 2006; 20:16-21.
422. Mendrysa SM, McElwee MK, Michalowski J, O'Leary KA, Young KM, Perry ME. Mdm2 Is Critical for Inhibition of P53 During Lymphopoiesis and the Response to Ionizing Irradiation. Molecular and cellular biology 2003; 23:462-72.
423. Terzian T, Wang Y, Van Pelt CS, Box NF, Travis EL, Lozano G. Haploinsufficiency of Mdm2 and Mdm4 in Tumorigenesis and Development. Molecular and cellular biology 2007; 27:5479-85.
424. Ringshausen I, O'Shea CC, Finch AJ, Swigart LB, Evan GI. Mdm2 Is Critically and Continuously Required to Suppress Lethal P53 Activity in Vivo. Cancer Cell 2006; 10:501-14.
425. Vassilev LT, Vu BT, Graves B, Carvajal D, Podlaski F, Filipovic Z, et al. In Vivo Activation of the P53 Pathway by Small-Molecule Antagonists of Mdm2. Science 2004; 303:844-8.
426. Andreeff M, Kojima K, Padmanabhan S, Strair R, Kirschbaum M, Maslak P, et al. A Multi-Center, Open-Label, Phase I Study of Single Agent Rg7112, a First in Class P53-Mdm2 Antagonist, in Patients with Relapsed/Refractory Acute Myeloid and Lymphoid Leukemias (Aml/All) and Refractory Chronic Lymphocytic Leukemia/Small Cell Lymphocytic Lymphomas (Cll/Scll). ASH annual meeting 2010.
427. Kurzrock R, Blay JY, Nguyen B, Wagner A, Maki R, Schwartz G, et al. A Phase I Study of Mdm2 Antagonist Rg7112 in Patients (Pts) with Relapsed/Refractory Solid Tumors. J Clin Oncol 2012; 30, (suppl):abstr e13600^.
428. Ray-Coquard I, Blay JY, Italiano A, Le Cesne A, Penel N, Zhi J, et al. Effect of the Mdm2 Antagonist Rg7112 on the P53 Pathway in Patients with

Mdm2-Amplified, Well-Differentiated or Dedifferentiated Liposarcoma: An Exploratory Proof-of-Mechanism Study. The lancet oncology 2012; 13:1133-40.
429. Sato N, Mizumoto K, Maehara N, Kusumoto M, Nishio S, Urashima T, et al. Enhancement of Drug-Induced Apoptosis by Antisense Oligodeoxynucleotides Targeted against Mdm2 and P21waf1/Cip1. Anticancer Res 2000; 20:837-42.
430. Zhang R, Wang H, Agrawal S. Novel Antisense Anti-Mdm2 Mixed-Backbone Oligonucleotides: Proof of Principle, in Vitro and in Vivo Activities, and Mechanisms. Current cancer drug targets 2005; 5:43-9.
431. Ding K, Lu Y, Nikolovska-Coleska Z, Qiu S, Ding Y, Gao W, et al. Structure-Based Design of Potent Non-Peptide Mdm2 Inhibitors. J Am Chem Soc 2005; 127:10130-1.
432. Shangary S, Qin D, McEachern D, Liu M, Miller RS, Qiu S, et al. Temporal Activation of P53 by a Specific Mdm2 Inhibitor Is Selectively Toxic to Tumors and Leads to Complete Tumor Growth Inhibition. Proc Natl Acad Sci U S A 2008; 105:3933-8.
433. Grasberger BL, Lu T, Schubert C, Parks DJ, Carver TE, Koblish HK, et al. Discovery and Cocrystal Structure of Benzodiazepinedione Hdm2 Antagonists That Activate P53 in Cells. J Med Chem 2005; 48:909-12.
434. Koblish HK, Zhao S, Franks CF, Donatelli RR, Tominovich RM, LaFrance LV, et al. Benzodiazepinedione Inhibitors of the Hdm2:P53 Complex Suppress Human Tumor Cell Proliferation in Vitro and Sensitize Tumors to Doxorubicin in Vivo. Mol Cancer Ther 2006; 5:160-9.
435. Parks DJ, LaFrance LV, Calvo RR, Milkiewicz KL, Marugan JJ, Raboisson P, et al. Enhanced Pharmacokinetic Properties of 1,4-Benzodiazepine-2,5-Dione Antagonists of the Hdm2-P53 Protein-Protein Interaction through Structure-Based Drug Design. Bioorg Med Chem Lett 2006; 16:3310-4.
436. Issaeva N, Bozko P, Enge M, Protopopova M, Verhoef LG, Masucci M, et al. Small Molecule Rita Binds to P53, Blocks P53-Hdm-2 Interaction and Activates P53 Function in Tumors. Nat Med 2004; 10:1321-8.
437. Krajewski M, Ozdowy P, D'Silva L, Rothweiler U, Holak TA. Nmr Indicates That the Small Molecule Rita Does Not Block P53-Mdm2 Binding in Vitro. Nat Med 2005; 11:1135-6; author reply 6-7.
438. Hu B, Gilkes DM, Farooqi B, Sebti SM, Chen J. Mdmx Overexpression Prevents P53 Activation by the Mdm2 Inhibitor Nutlin. J Biol Chem 2006; 281:33030-5.
439. Patton JT, Mayo LD, Singhi AD, Gudkov AV, Stark GR, Jackson MW. Levels of Hdmx Expression Dictate the Sensitivity of Normal and Transformed Cells to Nutlin-3. Cancer Res 2006; 66:3169-76.
440. Wade M, Wong ET, Tang M, Stommel JM, Wahl GM. Hdmx Modulates the Outcome of P53 Activation in Human Tumor Cells. The Journal of biological chemistry 2006; 281:33036-44.
441. Bernal F, Tyler AF, Korsmeyer SJ, Walensky LD, Verdine GL. Reactivation of the P53 Tumor Suppressor Pathway by a Stapled P53 Peptide. J Am Chem Soc 2007; 129:2456-7.
442. Baek S, Kutchukian PS, Verdine GL, Huber R, Holak TA, Lee KW, et al. Structure of the Stapled P53 Peptide Bound to Mdm2. J Am Chem Soc 2012; 134:103-6.
443. Lehmann S, Bykov VJ, Ali D, Andren O, Cherif H, Tidefelt U, et al. Targeting P53 in Vivo: A First-in-Human Study with P53-Targeting Compound Apr-

246 in Refractory Hematologic Malignancies and Prostate Cancer. Journal of clinical oncology : official journal of the American Society of Clinical Oncology 2012; 30:3633-9.
444. Yuan Y, Liao YM, Hsueh CT, Mirshahidi HR. Novel Targeted Therapeutics: Inhibitors of Mdm2, Alk and Parp. J Hematol Oncol 2011; 4:16.
445. Lai Z, Yang T, Kim YB, Sielecki TM, Diamond MA, Strack P, et al. Differentiation of Hdm2-Mediated P53 Ubiquitination and Hdm2 Autoubiquitination Activity by Small Molecular Weight Inhibitors. Proc Natl Acad Sci U S A 2002; 99:14734-9.
446. Davydov IV, Woods D, Safiran YJ, Oberoi P, Fearnhead HO, Fang S, et al. Assay for Ubiquitin Ligase Activity: High-Throughput Screen for Inhibitors of Hdm2. J Biomol Screen 2004; 9:695-703.
447. Yang Y, Ludwig RL, Jensen JP, Pierre SA, Medaglia MV, Davydov IV, et al. Small Molecule Inhibitors of Hdm2 Ubiquitin Ligase Activity Stabilize and Activate P53 in Cells. Cancer Cell 2005; 7:547-59.
448. Wilson JM, Henderson G, Black F, Sutherland A, Ludwig RL, Vousden KH, et al. Synthesis of 5-Deazaflavin Derivatives and Their Activation of P53 in Cells. Bioorg Med Chem 2007; 15:77-86.
449. Murray MF, Jurewicz AJ, Martin JD, Ho TF, Zhang H, Johanson KO, et al. A High-Throughput Screen Measuring Ubiquitination of P53 by Human Mdm2. J Biomol Screen 2007; 12:1050-8.
450. Sasiela CA, Stewart DH, Kitagaki J, Safiran YJ, Yang Y, Weissman AM, et al. Identification of Inhibitors for Mdm2 Ubiquitin Ligase Activity from Natural Product Extracts by a Novel High-Throughput Electrochemiluminescent Screen. J Biomol Screen 2008; 13:229-37.
451. Kitagaki J, Agama KK, Pommier Y, Yang Y, Weissman AM. Targeting Tumor Cells Expressing P53 with a Water-Soluble Inhibitor of Hdm2. Mol Cancer Ther 2008; 7:2445-54.
452. Yang Y, Kitagaki J, Dai RM, Tsai YC, Lorick KL, Ludwig RL, et al. Inhibitors of Ubiquitin-Activating Enzyme (E1), a New Class of Potential Cancer Therapeutics. Cancer Res 2007; 67:9472-81.
453. Richardson PG, Sonneveld P, Schuster MW, Irwin D, Stadtmauer EA, Facon T, et al. Bortezomib or High-Dose Dexamethasone for Relapsed Multiple Myeloma. N Engl J Med 2005; 352:2487-98.
454. Reverdy C, Conrath S, Lopez R, Planquette C, Atmanene C, Collura V, et al. Discovery of Specific Inhibitors of Human Usp7/Hausp Deubiquitinating Enzyme. Chem Biol 2012; 19:467-77.
455. Toledo F, Krummel KA, Lee CJ, Liu CW, Rodewald LW, Tang M, et al. A Mouse P53 Mutant Lacking the Proline-Rich Domain Rescues Mdm4 Deficiency and Provides Insight into the Mdm2-Mdm4-P53 Regulatory Network. Cancer Cell 2006; 9:273-85.
456. Reed D, Shen Y, Shelat A, Arnold A, Ferreira A, Zhu F, et al. Identification and Characterization of the First Small-Molecule Inhibitor of Mdmx. Journal of Biological Chemistry 2010:-.
457. Wang H, Ma X, Ren S, Buolamwini JK, Yan C. A Small-Molecule Inhibitor of Mdmx Activates P53 and Induces Apoptosis in Cancer Cells. Mol Cancer Ther 2010.
458. Popowicz GM, Czarna A, Wolf S, Wang K, Wang W, Domling A, et al. Structures of Low Molecular Weight Inhibitors Bound to Mdmx and Mdm2 Reveal New Approaches for P53-Mdmx/Mdm2 Antagonist Drug Discovery. Cell Cycle 2010; 9.

459. Hu B, Gilkes DM, Chen J. Efficient P53 Activation and Apoptosis by Simultaneous Disruption of Binding to Mdm2 and Mdmx. Cancer Res 2007; 67:8810-7.
460. Czarna A, Popowicz GM, Pecak A, Wolf S, Dubin G, Holak TA. High Affinity Interaction of the P53 Peptide-Analogue with Human Mdm2 and Mdmx. Cell Cycle 2009; 8.
461. Kallen J, Goepfert A, Blechschmidt A, Izaac A, Geiser M, Tavares G, et al. Crystal Structures of Human Mdmx (Hdmx) in Complex with P53 Peptide Analogues Reveal Surprising Conformational Changes. J Biol Chem 2009; 284:8812-21.
462. Pazgier M, Liu M, Zou G, Yuan W, Li C, Li C, et al. Structural Basis for High-Affinity Peptide Inhibition of P53 Interactions with Mdm2 and Mdmx. Proc Natl Acad Sci U S A 2009; 106:4665-70.
463. Li C, Pazgier M, Li C, Yuan W, Liu M, Wei G, et al. Systematic Mutational Analysis of Peptide Inhibition of the P53-Mdm2/Mdmx Interactions. J Mol Biol 2010; 398:200-13.
464. Schoentjes B, Lacrampe J, Meyer C, Valckx A, Ligny Y, Lardeau D, et al. Identification of a Novel Orally Active Hdm2 Antagonist with Potent Antitumour Activity. Natl Med Chem Symp 2008:Abstract 146.
465. Arts J, Page M, Valckx A, Blattner C, Kulikov R, Floren W, et al. Jnj-26854165 - a Novel Hdm2 Antagonist in Clinical Development Showing Broad-Spectrum Preclinical Antitumor Activity against Solid Malignancies. AACR Meeting Abstracts 2008; 2008:1592.
466. Stuhmer T, Arts J, King P, Page M, Bommert K, Leo E, et al. A First-in-Class Hdm2-Inhibitor (Jnj-26854165) in Phase I Development Shows Potent Activity against Multiple Myeloma (Mm) Cells in Vitro and Ex Vivo. J Clin Oncol (Meeting Abstracts) 2008; 26:14694-.
467. Tabernero J, Schoffski P, Dirix L, Capdevila J, Dumez H, Kraljevic S, et al. First-in-Human Study of the First-in-Class Hdm2 Inhibitor Jnj-26854165. European Journal of Cancer 2008; 6:81.
468. Lain S, Hollick JJ, Campbell J, Staples OD, Higgins M, Aoubala M, et al. Discovery, in Vivo Activity, and Mechanism of Action of a Small-Molecule P53 Activator. Cancer Cell 2008; 13:454-63.
469. Choong ML, Yang H, Lee MA, Lane DP. Specific Activation of the P53 Pathway by Low Dose Actinomycin D: A New Route to P53 Based Cyclotherapy. Cell Cycle 2009; 8.
470. Berkson RG, Hollick JJ, Westwood NJ, Woods JA, Lane DP, Lain S. Pilot Screening Programme for Small Molecule Activators of P53. Int J Cancer 2005; 115:701-10.
471. Patten N, Truong S, Tripathy D, Gluck S, Dugan U, Wu L. Distribution of P53 Mutations by Amplichip Assay in Patients Receiving Neoadjuvant Capecitabine (C) Plus Docetaxel (D) with or without Trastuzumab (T) for Newly Diagnosed Breast Cancer (Bc). 2007 Breast Cancer Symposium 2007; Abstract No: 100.
472. Chavez-Reyes A, Parant JM, Amelse LL, de Oca Luna RM, Korsmeyer SJ, Lozano G. Switching Mechanisms of Cell Death in Mdm2- and Mdm4-Null Mice by Deletion of P53 Downstream Targets. Cancer research 2003; 63:8664-9.
473. Steinman HA, Sluss HK, Sands AT, Pihan G, Jones SN. Absence of P21 Partially Rescues Mdm4 Loss and Uncovers an Antiproliferative Effect of Mdm4 on Cell Growth. Oncogene 2004; 23:303-6.

474. Grier JD, Xiong S, Elizondo-Fraire AC, Parant JM, Lozano G. Tissue-Specific Differences of P53 Inhibition by Mdm2 and Mdm4. Molecular and cellular biology 2006; 26:192-8.
475. Francoz S, Froment P, Bogaerts S, De Clercq S, Maetens M, Doumont G, et al. Mdm4 and Mdm2 Cooperate to Inhibit P53 Activity in Proliferating and Quiescent Cells in Vivo. Proc Natl Acad Sci U S A 2006; 103:3232-7.
476. Brash DE, Ponten J. Skin Precancer. Cancer Surv 1998; 32:69-113.
477. Prives C, White E. Does Control of Mutant P53 by Mdm2 Complicate Cancer Therapy? Genes Dev 2008; 22:1259-64.
478. Lukashchuk N, Vousden KH. Ubiquitination and Degradation of Mutant P53. Mol Cell Biol 2007; 27:8284-95.
479. Guo L, Liew HP, Camus S, Goh AM, Chee LL, Lunny DP, et al. Ionizing Radiation Induces a Dramatic Persistence of P53 Protein Accumulation and DNA Damage Signaling in Mutant P53 Zebrafish. Oncogene 2012.
480. Liu X, Chua CC, Gao J, Chen Z, Landy CL, Hamdy R, et al. Pifithrin-Alpha Protects against Doxorubicin-Induced Apoptosis and Acute Cardiotoxicity in Mice. Am J Physiol Heart Circ Physiol 2004; 286:H933-9.
481. Komarov PG, Komarova EA, Kondratov RV, Christov-Tselkov K, Coon JS, Chernov MV, et al. A Chemical Inhibitor of P53 That Protects Mice from the Side Effects of Cancer Therapy. Science 1999; 285:1733-7.
482. Christophorou MA, Ringshausen I, Finch AJ, Swigart LB, Evan GI. The Pathological Response to DNA Damage Does Not Contribute to P53-Mediated Tumour Suppression. Nature 2006; 443:214-7.
483. Senzer N, Nemunaitis J. A Review of Contusugene Ladenovec (Advexin) P53 Therapy. Curr Opin Mol Ther 2009; 11:54-61.
484. Peng Z. Current Status of Gendicine in China: Recombinant Human Ad-P53 Agent for Treatment of Cancers. Hum Gene Ther 2005; 16:1016-27.
485. O'Shea CC, Johnson L, Bagus B, Choi S, Nicholas C, Shen A, et al. Late Viral Rna Export, Rather Than P53 Inactivation, Determines Onyx-015 Tumor Selectivity. Cancer Cell 2004; 6:611-23.
486. Bischoff JR, Kirn DH, Williams A, Heise C, Horn S, Muna M, et al. An Adenovirus Mutant That Replicates Selectively in P53-Deficient Human Tumor Cells. Science 1996; 274:373-6.
487. Nemunaitis J, Ganly I, Khuri F, Arseneau J, Kuhn J, McCarty T, et al. Selective Replication and Oncolysis in P53 Mutant Tumors with Onyx-015, an E1b-55kd Gene-Deleted Adenovirus, in Patients with Advanced Head and Neck Cancer: A Phase Ii Trial. Cancer Res 2000; 60:6359-66.
488. Khuri FR, Nemunaitis J, Ganly I, Arseneau J, Tannock IF, Romel L, et al. A Controlled Trial of Intratumoral Onyx-015, a Selectively-Replicating Adenovirus, in Combination with Cisplatin and 5-Fluorouracil in Patients with Recurrent Head and Neck Cancer. Nat Med 2000; 6:879-85.
489. Galanis E, Okuno SH, Nascimento AG, Lewis BD, Lee RA, Oliveira AM, et al. Phase I-Ii Trial of Onyx-015 in Combination with Map Chemotherapy in Patients with Advanced Sarcomas. Gene Ther 2005; 12:437-45.
490. Reid TR, Freeman S, Post L, McCormick F, Sze DY. Effects of Onyx-015 among Metastatic Colorectal Cancer Patients That Have Failed Prior Treatment with 5-Fu/Leucovorin. Cancer Gene Ther 2005; 12:673-81.
491. Sangrajrang S, Sornprom A, Chernrungroj G, Soussi T. Serum P53 Antibodies in Patients with Lung Cancer: Correlation with Clinicopathologic Features and Smoking. Lung Cancer 2003; 39:297-301.

492. Met O, Balslev E, Flyger H, Svane IM. High Immunogenic Potential of P53 Mrna-Transfected Dendritic Cells in Patients with Primary Breast Cancer. Breast Cancer Res Treat 2011; 125:395-406.
493. Chiappori AA, Soliman H, Janssen WE, Antonia SJ, Gabrilovich DI. Ingn-225: A Dendritic Cell-Based P53 Vaccine (Ad.P53-Dc) in Small Cell Lung Cancer: Observed Association between Immune Response and Enhanced Chemotherapy Effect. Expert Opin Biol Ther 2010; 10:983-91.
494. Zache N, Lambert JM, Rokaeus N, Shen J, Hainaut P, Bergman J, et al. Mutant P53 Targeting by the Low Molecular Weight Compound Stima-1. Molecular oncology 2008; 2:70-80.
495. Bykov VJ, Issaeva N, Zache N, Shilov A, Hultcrantz M, Bergman J, et al. Reactivation of Mutant P53 and Induction of Apoptosis in Human Tumor Cells by Maleimide Analogs. J Biol Chem 2005; 280:30384-91.
496. Boeckler FM, Joerger AC, Jaggi G, Rutherford TJ, Veprintsev DB, Fersht AR. Targeted Rescue of a Destabilized Mutant of P53 by an in Silico Screened Drug. Proceedings of the National Academy of Sciences of the United States of America 2008; 105:10360-5.
497. Yu X, Vazquez A, Levine AJ, Carpizo DR. Allele-Specific P53 Mutant Reactivation. Cancer Cell 2012; 21:614-25.
498. Rippin TM, Bykov VJ, Freund SM, Selivanova G, Wiman KG, Fersht AR. Characterization of the P53-Rescue Drug Cp-31398 in Vitro and in Living Cells. Oncogene 2002; 21:2119-29.
499. Demma M, Maxwell E, Ramos R, Liang L, Li C, Hesk D, et al. Sch529074, a Small Molecule Activator of Mutant P53, Which Binds P53 DNA Binding Domain (Dbd), Restores Growth-Suppressive Function to Mutant P53 and Interrupts Hdm2-Mediated Ubiquitination of Wild Type P53. The Journal of biological chemistry 2010; 285:10198-212.
500. Bykov VJ, Issaeva N, Shilov A, Hultcrantz M, Pugacheva E, Chumakov P, et al. Restoration of the Tumor Suppressor Function to Mutant P53 by a Low-Molecular-Weight Compound. Nat Med 2002; 8:282-8.
501. Lambert JM, Gorzov P, Veprintsev DB, Soderqvist M, Segerback D, Bergman J, et al. Prima-1 Reactivates Mutant P53 by Covalent Binding to the Core Domain. Cancer Cell 2009; 15:376-88.
502. Foster BA, Coffey HA, Morin MJ, Rastinejad F. Pharmacological Rescue of Mutant P53 Conformation and Function. Science 1999; 286:2507-10.
503. Wang W, Ho WC, Dicker DT, MacKinnon C, Winkler JD, Marmorstein R, et al. Acridine Derivatives Activate P53 and Induce Tumor Cell Death through Bax. Cancer Biol Ther 2005; 4:893-8.
504. Selivanova G, Iotsova V, Okan I, Fritsche M, Strom M, Groner B, et al. Restoration of the Growth Suppression Function of Mutant P53 by a Synthetic Peptide Derived from the P53 C-Terminal Domain. Nat Med 1997; 3:632-8.
505. Selivanova G, Ryabchenko L, Jansson E, Iotsova V, Wiman KG. Reactivation of Mutant P53 through Interaction of a C-Terminal Peptide with the Core Domain. Mol Cell Biol 1999; 19:3395-402.
506. Kim AL, Raffo AJ, Brandt-Rauf PW, Pincus MR, Monaco R, Abarzua P, et al. Conformational and Molecular Basis for Induction of Apoptosis by a P53 C-Terminal Peptide in Human Cancer Cells. J Biol Chem 1999; 274:34924-31.

507. Li D, Marchenko ND, Moll UM. Saha Shows Preferential Cytotoxicity in Mutant P53 Cancer Cells by Destabilizing Mutant P53 through Inhibition of the Hdac6-Hsp90 Chaperone Axis. Cell Death Differ 2011; 18:1904-13.
508. Yan W, Liu S, Xu E, Zhang J, Zhang Y, Chen X, et al. Histone Deacetylase Inhibitors Suppress Mutant P53 Transcription Via Histone Deacetylase 8. Oncogene 2013; 32:599-609.
509. Kravchenko JE, Ilyinskaya GV, Komarov PG, Agapova LS, Kochetkov DV, Strom E, et al. Small-Molecule Retra Suppresses Mutant P53-Bearing Cancer Cells through a P73-Dependent Salvage Pathway. Proc Natl Acad Sci U S A 2008; 105:6302-7.
510. Blagosklonny MV, Pardee AB. Exploiting Cancer Cell Cycling for Selective Protection of Normal Cells. Cancer Res 2001; 61:4301-5.
511. Blagosklonny MV, Darzynkiewicz Z. Cyclotherapy: Protection of Normal Cells and Unshielding of Cancer Cells. Cell Cycle 2002; 1:375-82.
512. Keyomarsi K, Pardee AB. Selective Protection of Normal Proliferating Cells against the Toxic Effects of Chemotherapeutic Agents. Prog Cell Cycle Res 2003; 5:527-32.
513. Kranz D, Dobbelstein M. Nongenotoxic P53 Activation Protects Cells against S-Phase-Specific Chemotherapy. Cancer Res 2006; 66:10274-80.
514. Carvajal D, Tovar C, Yang H, Vu BT, Heimbrook DC, Vassilev LT. Activation of P53 by Mdm2 Antagonists Can Protect Proliferating Cells from Mitotic Inhibitors. Cancer Res 2005; 65:1918-24.
515. Sur S, Pagliarini R, Bunz F, Rago C, Diaz LA, Jr., Kinzler KW, et al. A Panel of Isogenic Human Cancer Cells Suggests a Therapeutic Approach for Cancers with Inactivated P53. Proc Natl Acad Sci U S A 2009; 106:3964-9.
516. Tokalov SV, Abolmaali ND. Protection of P53 Wild Type Cells from Taxol by Nutlin-3 in the Combined Lung Cancer Treatment. BMC Cancer 2010; 10:57.
517. Cheok CF, Kua N, Kaldis P, Lane DP. Combination of Nutlin-3 and Vx-680 Selectively Targets P53 Mutant Cells with Reversible Effects on Cells Expressing Wild-Type P53. Cell Death Differ 2010.
518. Sawyers CL. The Cancer Biomarker Problem. Nature 2008; 452:548-52.
519. Eisenhauer EA, Therasse P, Bogaerts J, Schwartz LH, Sargent D, Ford R, et al. New Response Evaluation Criteria in Solid Tumours: Revised Recist Guideline (Version 1.1). European journal of cancer 2009; 45:228-47.
520. Weissleder R, Pittet MJ. Imaging in the Era of Molecular Oncology. Nature 2008; 452:580-9.
521. Jordan VC. Is Tamoxifen the Rosetta Stone for Breast Cancer? J Natl Cancer Inst 2003; 95:338-40.
522. Sharma SV, Bell DW, Settleman J, Haber DA. Epidermal Growth Factor Receptor Mutations in Lung Cancer. Nat Rev Cancer 2007; 7:169-81.
523. Pao W, Wang TY, Riely GJ, Miller VA, Pan Q, Ladanyi M, et al. Kras Mutations and Primary Resistance of Lung Adenocarcinomas to Gefitinib or Erlotinib. PLoS Med 2005; 2:e17.
524. Khambata-Ford S, Garrett CR, Meropol NJ, Basik M, Harbison CT, Wu S, et al. Expression of Epiregulin and Amphiregulin and K-Ras Mutation Status Predict Disease Control in Metastatic Colorectal Cancer Patients Treated with Cetuximab. J Clin Oncol 2007; 25:3230-7.
525. Siehl J, Thiel E. C-Kit, Gist, and Imatinib. Recent Results Cancer Res 2007; 176:145-51.

526. Saunders NA, Simpson F, Thompson EW, Hill MM, Endo-Munoz L, Leggatt G, et al. Role of Intratumoural Heterogeneity in Cancer Drug Resistance: Molecular and Clinical Perspectives. EMBO Mol Med 2012; 4:675-84.
527. Phillips KA. Closing the Evidence Gap in the Use of Emerging Testing Technologies in Clinical Practice. JAMA 2008; 300:2542-4.
528. Cressey D. Britain to Launch Personalized Medicine Project. Nature 2011.
529. Olmos D, Baird RD, Yap TA, Massard C, Pope L, Sandhu SK, et al. Baseline Circulating Tumor Cell Counts Significantly Enhance a Prognostic Score for Patients Participating in Phase I Oncology Trials. Clin Cancer Res 2011; 17:5188-96.
530. Shaffer DR, Leversha MA, Danila DC, Lin O, Gonzalez-Espinoza R, Gu B, et al. Circulating Tumor Cell Analysis in Patients with Progressive Castration-Resistant Prostate Cancer. Clin Cancer Res 2007; 13:2023-9.
531. de Bono JS, Attard G, Adjei A, Pollak MN, Fong PC, Haluska P, et al. Potential Applications for Circulating Tumor Cells Expressing the Insulin-Like Growth Factor-I Receptor. Clin Cancer Res 2007; 13:3611-6.
532. Attard G, Swennenhuis JF, Olmos D, Reid AH, Vickers E, A'Hern R, et al. Characterization of Erg, Ar and Pten Gene Status in Circulating Tumor Cells from Patients with Castration-Resistant Prostate Cancer. Cancer Res 2009; 69:2912-8.
533. Attard G, de Bono JS. Utilizing Circulating Tumor Cells: Challenges and Pitfalls. Curr Opin Genet Dev 2011; 21:50-8.
534. Diehl F, Schmidt K, Choti MA, Romans K, Goodman S, Li M, et al. Circulating Mutant DNA to Assess Tumor Dynamics. Nat Med 2008; 14:985-90.
535. Perkins G, Yap TA, Pope L, Cassidy AM, Dukes JP, Riisnaes R, et al. Multi-Purpose Utility of Circulating Plasma DNA Testing in Patients with Advanced Cancers. PLoS ONE 2012; 7:e47020.
536. Diehl F, Li M, Dressman D, He Y, Shen D, Szabo S, et al. Detection and Quantification of Mutations in the Plasma of Patients with Colorectal Tumors. Proceedings of the National Academy of Sciences of the United States of America 2005; 102:16368-73.
537. Camidge DR, Randall KR, Foster JR, Sadler CJ, Wright JA, Soames AR, et al. Plucked Human Hair as a Tissue in Which to Assess Pharmacodynamic End Points During Drug Development Studies. Br J Cancer 2005; 92:1837-41.
538. Randall KJ, Foster JR. The Demonstration of Immunohistochemical Biomarkers in Methyl Methacrylate-Embedded Plucked Human Hair Follicles. Toxicol Pathol 2007; 35:952-7.
539. Hanash SM, Pitteri SJ, Faca VM. Mining the Plasma Proteome for Cancer Biomarkers. Nature 2008; 452:571-9.
540. Wang X, Yu J, Sreekumar A, Varambally S, Shen R, Giacherio D, et al. Autoantibody Signatures in Prostate Cancer. N Engl J Med 2005; 353:1224-35.
541. Camidge DR, Pemberton M, Growcott J, Amakye D, Wilson D, Swaisland H, et al. A Phase I Pharmacodynamic Study of the Effects of the Cyclin-Dependent Kinase-Inhibitor Azd5438 on Cell Cycle Markers within the Buccal Mucosa, Plucked Scalp Hairs and Peripheral Blood Mononucleocytes of Healthy Male Volunteers. Cancer Chemother Pharmacol 2007; 60:479-88.

542. Bergh J, Norberg T, Sjogren S, Lindgren A, Holmberg L. Complete Sequencing of the P53 Gene Provides Prognostic Information in Breast Cancer Patients, Particularly in Relation to Adjuvant Systemic Therapy and Radiotherapy. Nat Med 1995; 1:1029-34.
543. Welsh JB, Sapinoso LM, Kern SG, Brown DA, Liu T, Bauskin AR, et al. Large-Scale Delineation of Secreted Protein Biomarkers Overexpressed in Cancer Tissue and Serum. Proc Natl Acad Sci U S A 2003; 100:3410-5.
544. Yang H, Filipovic Z, Brown D, Breit SN, Vassilev LT. Macrophage Inhibitory Cytokine-1: A Novel Biomarker for P53 Pathway Activation. Mol Cancer Ther 2003; 2:1023-9.
545. Maniatis T, Fritsch E, Sambrook J. Molecular Cloning: A Laboratory Manual. Cold Spring Harbor: Cold Spring Harbor Laboratory, 1982.
546. Carter S, Bischof O, Dejean A, Vousden KH. C-Terminal Modifications Regulate Mdm2 Dissociation and Nuclear Export of P53. Nat Cell Biol 2007; 9:428-35.
547. Kubbutat MH, Ludwig RL, Levine AJ, Vousden KH. Analysis of the Degradation Function of Mdm2. Cell Growth Differ 1999; 10:87-92.
548. Kern SE, Pietenpol JA, Thiagalingam S, Seymour A, Kinzler KW, Vogelstein B. Oncogenic Forms of P53 Inhibit P53-Regulated Gene Expression. Science 1992; 256:827-30.
549. Gilkes DM, Pan Y, Coppola D, Yeatman T, Reuther GW, Chen J. Regulation of Mdmx Expression by Mitogenic Signaling. Mol Cell Biol 2008; 28:1999-2010.
550. Laemmli UK. Cleavage of Structural Proteins During the Assembly of the Head of Bacteriophage T4. Nature 1970; 227:680-5.
551. Burnette WN. "Western Blotting": Electrophoretic Transfer of Proteins from Sodium Dodecyl Sulfate--Polyacrylamide Gels to Unmodified Nitrocellulose and Radiographic Detection with Antibody and Radioiodinated Protein A. Anal Biochem 1981; 112:195-203.
552. Towbin H, Staehelin T, Gordon J. Electrophoretic Transfer of Proteins from Polyacrylamide Gels to Nitrocellulose Sheets: Procedure and Some Applications. Proc Natl Acad Sci U S A 1979; 76:4350-4.
553. Vojtesek B, Bartek J, Midgley CA, Lane DP. An Immunochemical Analysis of the Human Nuclear Phosphoprotein P53. New Monoclonal Antibodies and Epitope Mapping Using Recombinant P53. J Immunol Methods 1992; 151:237-44.
554. Rowan S, Ludwig RL, Haupt Y, Bates S, Lu X, Oren M, et al. Specific Loss of Apoptotic but Not Cell-Cycle Arrest Function in a Human Tumor Derived P53 Mutant. EMBO J 1996; 15:827-38.
555. Vassilev LT. Small-Molecule Antagonists of P53-Mdm2 Binding: Research Tools and Potential Therapeutics. Cell Cycle 2004; 3:419-21.
556. Dou H, Buetow L, Hock A, Sibbet GJ, Vousden KH, Huang DT. Structural Basis for Autoinhibition and Phosphorylation-Dependent Activation of C-Cbl. Nat Struct Mol Biol 2012; 19:184-92.
557. Yang Y, Li CC, Weissman AM. Regulating the P53 System through Ubiquitination. Oncogene 2004; 23:2096-106.
558. Saucedo LJ, Myers CD, Perry ME. Multiple Murine Double Minute Gene 2 (Mdm2) Proteins Are Induced by Ultraviolet Light. The Journal of biological chemistry 1999; 274:8161-8.
559. Dai MS, Zeng SX, Jin Y, Sun XX, David L, Lu H. Ribosomal Protein L23 Activates P53 by Inhibiting Mdm2 Function in Response to Ribosomal

Perturbation but Not to Translation Inhibition. Molecular and cellular biology 2004; 24:7654-68.
560. Sherr CJ, Weber JD. The Arf/P53 Pathway. Curr Opin Genet Dev 2000; 10:94-9.
561. Zhang Y, Wolf GW, Bhat K, Jin A, Allio T, Burkhart WA, et al. Ribosomal Protein L11 Negatively Regulates Oncoprotein Mdm2 and Mediates a P53-Dependent Ribosomal-Stress Checkpoint Pathway. Mol Cell Biol 2003; 23:8902-12.
562. Chao C, Hergenhahn M, Kaeser MD, Wu Z, Saito S, Iggo R, et al. Cell Type- and Promoter-Specific Roles of Ser18 Phosphorylation in Regulating P53 Responses. J Biol Chem 2003; 278:41028-33.
563. Sluss HK, Armata H, Gallant J, Jones SN. Phosphorylation of Serine 18 Regulates Distinct P53 Functions in Mice. Mol Cell Biol 2004; 24:976-84.
564. Wu Z, Earle J, Saito S, Anderson CW, Appella E, Xu Y. Mutation of Mouse P53 Ser23 and the Response to DNA Damage. Mol Cell Biol 2002; 22:2441-9.
565. MacPherson D, Kim J, Kim T, Rhee BK, Van Oostrom CT, DiTullio RA, et al. Defective Apoptosis and B-Cell Lymphomas in Mice with P53 Point Mutation at Ser 23. EMBO J 2004; 23:3689-99.
566. Ito A, Lai CH, Zhao X, Saito S, Hamilton MH, Appella E, et al. P300/Cbp-Mediated P53 Acetylation Is Commonly Induced by P53-Activating Agents and Inhibited by Mdm2. EMBO J 2001; 20:1331-40.
567. Mellert H, Sykes SM, Murphy ME, McMahon SB. The Arf/Oncogene Pathway Activates P53 Acetylation within the DNA Binding Domain. Cell Cycle 2007; 6:1304-6.
568. Shloush J, Vlassov JE, Engson I, Duan S, Saridakis V, Dhe-Paganon S, et al. Structural and Functional Comparison of the Ring Domains of Two P53 E3 Ligases, Mdm2 and Pirh2. The Journal of biological chemistry 2011; 286:4796-808.
569. Wade M, Li YC, Matani AS, Braun SM, Milanesi F, Rodewald LW, et al. Functional Analysis and Consequences of Mdm2 E3 Ligase Inhibition in Human Tumor Cells. Oncogene 2012.
570. Xia M, Knezevic D, Tovar C, Huang B, Heimbrook DC, Vassilev LT. Elevated Mdm2 Boosts the Apoptotic Activity of P53-Mdm2 Binding Inhibitors by Facilitating Mdmx Degradation. Cell Cycle 2008; 7:1604-12.
571. Kannan K, Amariglio N, Rechavi G, Givol D. Profile of Gene Expression Regulated by Induced P53: Connection to the Tgf-Beta Family. FEBS Lett 2000; 470:77-82.
572. Kitagawa M, Aonuma M, Lee SH, Fukutake S, McCormick F. E2f-1 Transcriptional Activity Is a Critical Determinant of Mdm2 Antagonist-Induced Apoptosis in Human Tumor Cell Lines. Oncogene 2008; 27:5303-14.
573. Brummelkamp TR, Fabius AW, Mullenders J, Madiredjo M, Velds A, Kerkhoven RM, et al. An Shrna Barcode Screen Provides Insight into Cancer Cell Vulnerability to Mdm2 Inhibitors. Nat Chem Biol 2006; 2:202-6.
574. Sherr CJ, McCormick F. The Rb and P53 Pathways in Cancer. Cancer Cell 2002; 2:103-12.
575. Yang Y, Fang S, Jensen JP, Weissman AM, Ashwell JD. Ubiquitin Protein Ligase Activity of Iaps and Their Degradation in Proteasomes in Response to Apoptotic Stimuli. Science 2000; 288:874-7.

576. Zaaroor-Regev D, de Bie P, Scheffner M, Noy T, Shemer R, Heled M, et al. Regulation of the Polycomb Protein Ring1b by Self-Ubiquitination or by E6-Ap May Have Implications to the Pathogenesis of Angelman Syndrome. Proceedings of the National Academy of Sciences of the United States of America 2010; 107:6788-93.
577. Ward IM, Chen J. Histone H2ax Is Phosphorylated in an Atr-Dependent Manner in Response to Replicational Stress. The Journal of biological chemistry 2001; 276:47759-62.
578. Furuta T, Takemura H, Liao ZY, Aune GJ, Redon C, Sedelnikova OA, et al. Phosphorylation of Histone H2ax and Activation of Mre11, Rad50, and Nbs1 in Response to Replication-Dependent DNA Double-Strand Breaks Induced by Mammalian DNA Topoisomerase I Cleavage Complexes. The Journal of biological chemistry 2003; 278:20303-12.
579. Rogakou EP, Pilch DR, Orr AH, Ivanova VS, Bonner WM. DNA Double-Stranded Breaks Induce Histone H2ax Phosphorylation on Serine 139. The Journal of biological chemistry 1998; 273:5858-68.
580. Meek DW. Tumour Suppression by P53: A Role for the DNA Damage Response? Nature reviews Cancer 2009; 9:714-23.
581. Banin S, Moyal L, Shieh S, Taya Y, Anderson CW, Chessa L, et al. Enhanced Phosphorylation of P53 by Atm in Response to DNA Damage. Science 1998; 281:1674-7.
582. Koumenis C, Alarcon R, Hammond E, Sutphin P, Hoffman W, Murphy M, et al. Regulation of P53 by Hypoxia: Dissociation of Transcriptional Repression and Apoptosis from P53-Dependent Transactivation. Molecular and cellular biology 2001; 21:1297-310.
583. Lees-Miller SP, Sakaguchi K, Ullrich SJ, Appella E, Anderson CW. Human DNA-Activated Protein Kinase Phosphorylates Serines 15 and 37 in the Amino-Terminal Transactivation Domain of Human P53. Molecular and cellular biology 1992; 12:5041-9.
584. Pestov DG, Strezoska Z, Lau LF. Evidence of P53-Dependent Cross-Talk between Ribosome Biogenesis and the Cell Cycle: Effects of Nucleolar Protein Bop1 on G(1)/S Transition. Molecular and cellular biology 2001; 21:4246-55.
585. Zhu Y, Poyurovsky MV, Li Y, Biderman L, Stahl J, Jacq X, et al. Ribosomal Protein S7 Is Both a Regulator and a Substrate of Mdm2. Molecular Cell 2009; 35:316-26.
586. Horn HF, Vousden KH. Cooperation between the Ribosomal Proteins L5 and L11 in the P53 Pathway. Oncogene 2008; 27:5774-84.
587. Chen D, Zhang Z, Li M, Wang W, Li Y, Rayburn ER, et al. Ribosomal Protein S7 as a Novel Modulator of P53-Mdm2 Interaction: Binding to Mdm2, Stabilization of P53 Protein, and Activation of P53 Function. Oncogene 2007; 26:5029-37.
588. Stott FJ, Bates S, James MC, McConnell BB, Starborg M, Brookes S, et al. The Alternative Product from the Human Cdkn2a Locus, P14(Arf), Participates in a Regulatory Feedback Loop with P53 and Mdm2. The EMBO journal 1998; 17:5001-14.
589. Ashcroft M, Taya Y, Vousden KH. Stress Signals Utilize Multiple Pathways to Stabilize P53. Mol Cell Biol 2000; 20:3224-33.
590. Ljungman M, Zhang F, Chen F, Rainbow AJ, McKay BC. Inhibition of Rna Polymerase Ii as a Trigger for the P53 Response. Oncogene 1999; 18:583-92.

591. Perry RP, Kelley DE. Inhibition of Rna Synthesis by Actinomycin D: Characteristic Dose-Response of Different Rna Species. Journal of cellular physiology 1970; 76:127-39.
592. Yokoyama Y, Niwa K, Tamaya T. Scattering of the Silver-Stained Proteins of Nucleolar Organizer Regions in Ishikawa Cells by Actinomycin D. Exp Cell Res 1992; 202:77-86.
593. Ramos YF, Stad R, Attema J, Peltenburg LT, van der Eb AJ, Jochemsen AG. Aberrant Expression of Hdmx Proteins in Tumor Cells Correlates with Wild-Type P53. Cancer Res 2001; 61:1839-42.
594. He L, He X, Lowe SW, Hannon GJ. Microrna Join the P53 Network--Another Piece in the Tumour-Suppression Puzzle. Nat Rev Cancer 2007; 7:819-22.
595. He L, He X, Lim LP, de Stanchina E, Xuan Z, Liang Y, et al. A Microrna Component of the P53 Tumour Suppressor Network. Nature 2007; 447:1130-4.
596. Chang TC, Wentzel EA, Kent OA, Ramachandran K, Mullendore M, Lee KH, et al. Transactivation of Mir-34a by P53 Broadly Influences Gene Expression and Promotes Apoptosis. Mol Cell 2007; 26:745-52.
597. Betel D, Wilson M, Gabow A, Marks DS, Sander C. The Microrna.Org Resource: Targets and Expression. Nucleic Acids Res 2008; 36:D149-53.
598. Alt JR, Greiner TC, Cleveland JL, Eischen CM. Mdm2 Haplo-Insufficiency Profoundly Inhibits Myc-Induced Lymphomagenesis. EMBO J 2003; 22:1442-50.
599. Brown CJ, Lain S, Verma CS, Fersht AR, Lane DP. Awakening Guardian Angels: Drugging the P53 Pathway. Nat Rev Cancer 2009; 9:862-73.
600. Kawai H, Wiederschain D, Kitao H, Stuart J, Tsai KK, Yuan ZM. DNA Damage-Induced Mdmx Degradation Is Mediated by Mdm2. J Biol Chem 2003; 278:45946-53.
601. Stommel JM, Wahl GM. Accelerated Mdm2 Auto-Degradation Induced by DNA-Damage Kinases Is Required for P53 Activation. EMBO J 2004; 23:1547-56.
602. Pereg Y, Shkedy D, de Graaf P, Meulmeester E, Edelson-Averbukh M, Salek M, et al. Phosphorylation of Hdmx Mediates Its Hdm2- and Atm-Dependent Degradation in Response to DNA Damage. Proceedings of the National Academy of Sciences of the United States of America 2005; 102:5056-61.
603. Stuhmer T, Chatterjee M, Hildebrandt M, Herrmann P, Gollasch H, Gerecke C, et al. Nongenotoxic Activation of the P53 Pathway as a Therapeutic Strategy for Multiple Myeloma. Blood 2005; 106:3609-17.
604. Drakos E, Thomaides A, Medeiros LJ, Li J, Leventaki V, Konopleva M, et al. Inhibition of P53-Murine Double Minute 2 Interaction by Nutlin-3a Stabilizes P53 and Induces Cell Cycle Arrest and Apoptosis in Hodgkin Lymphoma. Clin Cancer Res 2007; 13:3380-7.
605. Riedinger C, McDonnell JM. Inhibitors of Mdm2 and Mdmx: A Structural Perspective. Future Med Chem 2009; 1:1075-94.
606. Popowicz GM, Czarna A, Rothweiler U, Szwagierczak A, Krajewski M, Weber L, et al. Molecular Basis for the Inhibition of P53 by Mdmx. Cell Cycle 2007; 6:2386-92.
607. Popowicz GM, Czarna A, Holak TA. Structure of the Human Mdmx Protein Bound to the P53 Tumor Suppressor Transactivation Domain. Cell Cycle 2008; 7:2441-3.

608. Bernal F, Wade M, Godes M, Davis TN, Whitehead DG, Kung AL, et al. A Stapled P53 Helix Overcomes Hdmx-Mediated Suppression of P53. Cancer Cell 2010; 18:411-22.
609. Graves B, Thompson T, Xia M, Janson C, Lukacs C, Deo D, et al. Activation of the P53 Pathway by Small-Molecule-Induced Mdm2 and Mdmx Dimerization. Proceedings of the National Academy of Sciences of the United States of America 2012; 109:11788-93.
610. Tovar C, Rosinski J, Filipovic Z, Higgins B, Kolinsky K, Hilton H, et al. Small-Molecule Mdm2 Antagonists Reveal Aberrant P53 Signaling in Cancer: Implications for Therapy. Proc Natl Acad Sci U S A 2006; 103:1888-93.
611. Blagosklonny MV. The Power of Chemotherapeutic Engineering: Arresting Cell Cycle and Suppressing Senescence to Protect from Mitotic Inhibitors. Cell Cycle 2011; 10:2295-8.
612. Blagosklonny MV, Robey R, Bates S, Fojo T. Pretreatment with DNA-Damaging Agents Permits Selective Killing of Checkpoint-Deficient Cells by Microtubule-Active Drugs. The Journal of clinical investigation 2000; 105:533-9.
613. Rao B, van Leeuwen IM, Higgins M, Campbel J, Thompson AM, Lane DP, et al. Evaluation of an Actinomycin D/Vx-680 Aurora Kinase Inhibitor Combination in P53-Based Cyclotherapy. Oncotarget 2010; 1:639-50.
614. Apontes P, Leontieva OV, Demidenko ZN, Li F, Blagosklonny MV. Exploring Long-Term Protection of Normal Human Fibroblasts and Epithelial Cells from Chemotherapy in Cell Culture. Oncotarget 2011; 2:222-33.
615. Kranz D, Dobbelstein M. Nongenotoxic P53 Activation Protects Cells against S-Phase-Specific Chemotherapy. Cancer research 2006; 66:10274-80.
616. van Leeuwen IM, Rao B, Sachweh MC, Lain S. An Evaluation of Small-Molecule P53 Activators as Chemoprotectants Ameliorating Adverse Effects of Anticancer Drugs in Normal Cells. Cell Cycle 2012; 11:1851-61.
617. Mini E, Nobili S, Caciagli B, Landini I, Mazzei T. Cellular Pharmacology of Gemcitabine. Ann Oncol 2006; 17 Suppl 5:v7-12.
618. Wattel E, Preudhomme C, Hecquet B, Vanrumbeke M, Quesnel B, Dervite I, et al. P53 Mutations Are Associated with Resistance to Chemotherapy and Short Survival in Hematologic Malignancies. Blood 1994; 84:3148-57.
619. UK-Medicines-and-Healthcare-products-Regulatory-Agency, European-Medicines-Agency. Summary of Product Characteristics: Paclitaxel. electronic Medicines Compendium, 2012.
620. Tibaldi C, Ricci S, Russo F, Bernardini I, Galli L, Chioni A, et al. Increased Dose-Intensity of Gemcitabine in Advanced Non Small Cell Lung Cancer (Nsclc): A Multicenter Phase Ii Study in Elderly Patients from the "Polmone Toscano Group" (Polto). Lung Cancer 2005; 48:121-7.
621. Keen N, Taylor S. Aurora-Kinase Inhibitors as Anticancer Agents. Nat Rev Cancer 2004; 4:927-36.
622. Schoffski P, Jones SF, Dumez H, Infante JR, Van Mieghem E, Fowst C, et al. Phase I, Open-Label, Multicentre, Dose-Escalation, Pharmacokinetic and Pharmacodynamic Trial of the Oral Aurora Kinase Inhibitor Pf-03814735 in Advanced Solid Tumours. Eur J Cancer 2011; 47:2256-64.

623. Gautschi O, Heighway J, Mack PC, Purnell PR, Lara PN, Jr., Gandara DR. Aurora Kinases as Anticancer Drug Targets. Clin Cancer Res 2008; 14:1639-48.
624. Strebhardt K, Ullrich A. Targeting Polo-Like Kinase 1 for Cancer Therapy. Nat Rev Cancer 2006; 6:321-30.
625. Mross K, Frost A, Steinbild S, Hedbom S, Rentschler J, Kaiser R, et al. Phase I Dose Escalation and Pharmacokinetic Study of Bi 2536, a Novel Polo-Like Kinase 1 Inhibitor, in Patients with Advanced Solid Tumors. J Clin Oncol 2008; 26:5511-7.
626. Lain S, Midgley C, Sparks A, Lane EB, Lane DP. An Inhibitor of Nuclear Export Activates the P53 Response and Induces the Localization of Hdm2 and P53 to U1a-Positive Nuclear Bodies Associated with the Pods. Experimental cell research 1999; 248:457-72.
627. Hietanen S, Lain S, Krausz E, Blattner C, Lane DP. Activation of P53 in Cervical Carcinoma Cells by Small Molecules. Proceedings of the National Academy of Sciences of the United States of America 2000; 97:8501-6.
628. UK-Medicines-and-Healthcare-products-Regulatory-Agency, European-Medicines-Agency. Summary of Product Characteristics: Actinomycin D. electronic Medicines Compendium, 2012.
629. Luck HJ, Thomssen C, duBois A, Lisboa BW, Untch M, Kuhnle H, et al. Interim Analysis of a Phase Ii Study of Epirubicin and Paclitaxel as First-Line Therapy in Patients with Metastatic Breast Cancer. Semin Oncol 1996; 23:33-6.
630. Goldberg IH, Rabinowitz M, Reich E. Basis of Actinomycin Action. I. DNA Binding and Inhibition of Rna-Polymerase Synthetic Reactions by Actinomycin. Proc Natl Acad Sci U S A 1962; 48:2094-101.
631. Perry RP, Kelley DE. Persistent Synthesis of 5s Rna When Production of 28s and 18s Ribosomal Rna Is Inhibited by Low Doses of Actinomycin D. Journal of cellular physiology 1968; 72:235-46.
632. Jain SC, Sobell HM. Stereochemistry of Actinomycin Binding to DNA. I. Refinement and Further Structural Details of the Actinomycin-Deoxyguanosine Crystalline Complex. Journal of molecular biology 1972; 68:1-20.
633. Sobell HM, Jain SC. Stereochemistry of Actinomycin Binding to DNA. Ii. Detailed Molecular Model of Actinomycin-DNA Complex and Its Implications. Journal of molecular biology 1972; 68:21-34.
634. Sobell HM, Jain SC, Sakore TD, Nordman CE. Stereochemistry of Actinomycin--DNA Binding. Nature: New biology 1971; 231:200-5.
635. UK-Medicines-and-Healthcare-products-Regulatory-Agency, European-Medicines-Agency. Summary of Product Characteristics: 5-Fu. electronic Medicines Compendium, 2007.
636. Longley DB, Harkin DP, Johnston PG. 5-Fluorouracil: Mechanisms of Action and Clinical Strategies. Nat Rev Cancer 2003; 3:330-8.
637. Houghton JA, Tillman DM, Harwood FG. Ratio of 2'-Deoxyadenosine-5'-Triphosphate/Thymidine-5'-Triphosphate Influences the Commitment of Human Colon Carcinoma Cells to Thymineless Death. Clinical cancer research : an official journal of the American Association for Cancer Research 1995; 1:723-30.
638. Yoshioka A, Tanaka S, Hiraoka O, Koyama Y, Hirota Y, Ayusawa D, et al. Deoxyribonucleoside Triphosphate Imbalance. 5-Fluorodeoxyuridine-Induced DNA Double Strand Breaks in Mouse Fm3a Cells and the

Mechanism of Cell Death. The Journal of biological chemistry 1987; 262:8235-41.
639. Kunz C, Focke F, Saito Y, Schuermann D, Lettieri T, Selfridge J, et al. Base Excision by Thymine DNA Glycosylase Mediates DNA-Directed Cytotoxicity of 5-Fluorouracil. PLoS Biol 2009; 7:e91.
640. Ghoshal K, Jacob ST. Specific Inhibition of Pre-Ribosomal Rna Processing in Extracts from the Lymphosarcoma Cells Treated with 5-Fluorouracil. Cancer Res 1994; 54:632-6.
641. Modulation of Fluorouracil by Leucovorin in Patients with Advanced Colorectal Cancer: Evidence in Terms of Response Rate. Advanced Colorectal Cancer Meta-Analysis Project. Journal of clinical oncology : official journal of the American Society of Clinical Oncology 1992; 10:896-903.
642. Meta-Analysis of Randomized Trials Testing the Biochemical Modulation of Fluorouracil by Methotrexate in Metastatic Colorectal Cancer. Advanced Colorectal Cancer Meta-Analysis Project. Journal of clinical oncology : official journal of the American Society of Clinical Oncology 1994; 12:960-9.
643. Sun X-X, Dai M-S, Lu H. 5-Fluorouracil Activation of P53 Involves an Mdm2-Ribosomal Protein Interaction. Journal of Biological Chemistry 2007; 282:8052-9.
644. Scherf U, Ross DT, Waltham M, Smith LH, Lee JK, Tanabe L, et al. A Gene Expression Database for the Molecular Pharmacology of Cancer. Nature genetics 2000; 24:236-44.
645. Fragkos M, Jurvansuu J, Beard P. H2ax Is Required for Cell Cycle Arrest Via the P53/P21 Pathway. Molecular and cellular biology 2009; 29:2828-40.
646. Benjamin RS, Hall SW, Burgess MA, Wheeler WL, Murphy WK, Blumenschein GR, et al. A Pharmacokinetically Based Phase I-Ii Study of Single-Dose Actinomycin D (Nsc-3053). Cancer Treat Rep 1976; 60:289-91.
647. Green DM. Evaluation of Single-Dose Vincristine, Actinomycin D, and Cyclophosphamide in Childhood Solid Tumors. Cancer Treat Rep 1978; 62:1517-20.
648. Verma R, Rigatti MJ, Belinsky GS, Godman CA, Giardina C. DNA Damage Response to the Mdm2 Inhibitor Nutlin-3. Biochem Pharmacol 2010; 79:565-74.
649. Ploylearmsaeng SA, Fuhr U, Jetter A. How May Anticancer Chemotherapy with Fluorouracil Be Individualised? Clinical pharmacokinetics 2006; 45:567-92.
650. Saif MW, Choma A, Salamone SJ, Chu E. Pharmacokinetically Guided Dose Adjustment of 5-Fluorouracil: A Rational Approach to Improving Therapeutic Outcomes. Journal of the National Cancer Institute 2009; 101:1543-52.
651. Gamelin E, Delva R, Jacob J, Merrouche Y, Raoul JL, Pezet D, et al. Individual Fluorouracil Dose Adjustment Based on Pharmacokinetic Follow-up Compared with Conventional Dosage: Results of a Multicenter Randomized Trial of Patients with Metastatic Colorectal Cancer. Journal of clinical oncology : official journal of the American Society of Clinical Oncology 2008; 26:2099-105.
652. Capitain O, Asevoaia A, Boisdron-Celle M, Poirier AL, Morel A, Gamelin E. Individual Fluorouracil Dose Adjustment in Folfox Based on Pharmacokinetic Follow-up Compared with Conventional Body-Area-

Surface Dosing: A Phase Ii, Proof-of-Concept Study. Clinical colorectal cancer 2012; 11:263-7.
653. Bhat KP, Itahana K, Jin A, Zhang Y. Essential Role of Ribosomal Protein L11 in Mediating Growth Inhibition-Induced P53 Activation. The EMBO journal 2004; 23:2402-12.
654. Yung BY, Bor AM, Chan PK. Short Exposure to Actinomycin D Induces "Reversible" Translocation of Protein B23 as Well as "Reversible" Inhibition of Cell Growth and Rna Synthesis in Hela Cells. Cancer Res 1990; 50:5987-91.
655. Fumagalli S, Di Cara A, Neb-Gulati A, Natt F, Schwemberger S, Hall J, et al. Absence of Nucleolar Disruption after Impairment of 40s Ribosome Biogenesis Reveals an Rpl11-Translation-Dependent Mechanism of P53 Induction. Nat Cell Biol 2009; 11:501-8.
656. Untch M, Fasching PA, Konecny GE, von Koch F, Conrad U, Fett W, et al. Prepare Trial: A Randomized Phase Iii Trial Comparing Preoperative, Dose-Dense, Dose-Intensified Chemotherapy with Epirubicin, Paclitaxel and Cmf Versus a Standard-Dosed Epirubicin/Cyclophosphamide Followed by Paclitaxel {+/-} Darbepoetin Alfa in Primary Breast Cancer--Results at the Time of Surgery. Ann Oncol 2011; 22:1988-98.
657. Moebus V, Jackisch C, Lueck HJ, du Bois A, Thomssen C, Kurbacher C, et al. Intense Dose-Dense Sequential Chemotherapy with Epirubicin, Paclitaxel, and Cyclophosphamide Compared with Conventionally Scheduled Chemotherapy in High-Risk Primary Breast Cancer: Mature Results of an Ago Phase Iii Study. J Clin Oncol 2010; 28:2874-80.
658. UK-Medicines-and-Healthcare-products-Regulatory-Agency, European-Medicines-Agency. Summary of Product Characteristics: Cisplatin. electronic Medicines Compendium, 2009.
659. Teicher BA. Newer Cytotoxic Agents: Attacking Cancer Broadly. Clin Cancer Res 2008; 14:1610-7.
660. Siddik ZH. Cisplatin: Mode of Cytotoxic Action and Molecular Basis of Resistance. Oncogene 2003; 22:7265-79.
661. Inoue T, Obara T, Saito M, Kumazawa T, Yuasa T, Matuura S, et al. Possible Survival Benefit of High-Dose-Intensity Methotrexate, Vinblastine, Doxorubicin, and Cisplatin Combination Therapy (Hd-Mvac) over Conventional Mvac in Metastatic Urothelial Carcinoma Patients. Hinyokika Kiyo 2007; 53:613-8.
662. Nemet D, Piura B, Cohen Y, Glezerman M. Dose Intensity of Cisplatin-Based Chemotherapy in Epithelial Ovarian Carcinoma. An Important Factor Affecting Survival. Eur J Gynaecol Oncol 1995; 16:107-14.
663. Peters GJ, van der Wilt CL, van Moorsel CJ, Kroep JR, Bergman AM, Ackland SP. Basis for Effective Combination Cancer Chemotherapy with Antimetabolites. Pharmacol Ther 2000; 87:227-53.
664. Lau LM, Nugent JK, Zhao X, Irwin MS. Hdm2 Antagonist Nutlin-3 Disrupts P73-Hdm2 Binding and Enhances P73 Function. Oncogene 2008; 27:997-1003.
665. Ray RM, Bhattacharya S, Johnson LR. Mdm2 Inhibition Induces Apoptosis in P53 Deficient Human Colon Cancer Cells by Activating P73- and E2f1-Mediated Expression of Puma and Siva-1. Apoptosis 2011; 16:35-44.
666. Ambrosini G, Sambol EB, Carvajal D, Vassilev LT, Singer S, Schwartz GK. Mouse Double Minute Antagonist Nutlin-3a Enhances Chemotherapy-

Induced Apoptosis in Cancer Cells with Mutant P53 by Activating E2f1. Oncogene 2007; 26:3473-81.
667. Masson E, Zamboni WC. Pharmacokinetic Optimisation of Cancer Chemotherapy. Effect on Outcomes. Clinical pharmacokinetics 1997; 32:324-43.
668. Jodrell DI, Stewart M, Aird R, Knowles G, Bowman A, Wall L, et al. 5-Fluorouracil Steady State Pharmacokinetics and Outcome in Patients Receiving Protracted Venous Infusion for Advanced Colorectal Cancer. British journal of cancer 2001; 84:600-3.
669. Gamelin E, Boisdron-Celle M, Delva R, Regimbeau C, Cailleux PE, Alleaume C, et al. Long-Term Weekly Treatment of Colorectal Metastatic Cancer with Fluorouracil and Leucovorin: Results of a Multicentric Prospective Trial of Fluorouracil Dosage Optimization by Pharmacokinetic Monitoring in 152 Patients. Journal of clinical oncology : official journal of the American Society of Clinical Oncology 1998; 16:1470-8.
670. Cotsarelis G, Millar SE. Towards a Molecular Understanding of Hair Loss and Its Treatment. Trends in molecular medicine 2001; 7:293-301.
671. Chon SY, Champion RW, Geddes ER, Rashid RM. Chemotherapy-Induced Alopecia. Journal of the American Academy of Dermatology 2012; 67:e37-47.
672. Botchkarev VA, Komarova EA, Siebenhaar F, Botchkareva NV, Komarov PG, Maurer M, et al. P53 Is Essential for Chemotherapy-Induced Hair Loss. Cancer Res 2000; 60:5002-6.
673. Hebert JM, Rosenquist T, Gotz J, Martin GR. Fgf5 as a Regulator of the Hair Growth Cycle: Evidence from Targeted and Spontaneous Mutations. Cell 1994; 78:1017-25.
674. Hsu YC, Pasolli HA, Fuchs E. Dynamics between Stem Cells, Niche, and Progeny in the Hair Follicle. Cell 2011; 144:92-105.
675. Gho CG, Braun JE, Tilli CM, Neumann HA, Ramaekers FC. Human Follicular Stem Cells: Their Presence in Plucked Hair and Follicular Cell Culture. Br J Dermatol 2004; 150:860-8.
676. Weinberg A, Song LY, Wilkening C, Sevin A, Blais B, Louzao R, et al. Optimization and Limitations of Use of Cryopreserved Peripheral Blood Mononuclear Cells for Functional and Phenotypic T-Cell Characterization. Clinical and vaccine immunology : CVI 2009; 16:1176-86.
677. Tan M, Wang Y, Guan K, Sun Y. Ptgf-Beta, a Type Beta Transforming Growth Factor (Tgf-Beta) Superfamily Member, Is a P53 Target Gene That Inhibits Tumor Cell Growth Via Tgf-Beta Signaling Pathway. Proc Natl Acad Sci U S A 2000; 97:109-14.
678. Li PX, Wong J, Ayed A, Ngo D, Brade AM, Arrowsmith C, et al. Placental Transforming Growth Factor-Beta Is a Downstream Mediator of the Growth Arrest and Apoptotic Response of Tumor Cells to DNA Damage and P53 Overexpression. J Biol Chem 2000; 275:20127-35.
679. Khaled YS, Elkord E, Ammori BJ. Macrophage Inhibitory Cytokine-1: A Review of Its Pleiotropic Actions in Cancer. Cancer biomarkers : section A of Disease markers 2012; 11:183-90.
680. Johnen H, Lin S, Kuffner T, Brown DA, Tsai VW, Bauskin AR, et al. Tumor-Induced Anorexia and Weight Loss Are Mediated by the Tgf-Beta Superfamily Cytokine Mic-1. Nat Med 2007; 13:1333-40.
681. Ahnen DJ, Feigl P, Quan G, Fenoglio-Preiser C, Lovato LC, Bunn PA, Jr., et al. Ki-Ras Mutation and P53 Overexpression Predict the Clinical

Behavior of Colorectal Cancer: A Southwest Oncology Group Study. Cancer research 1998; 58:1149-58.
682. Salonga D, Danenberg KD, Johnson M, Metzger R, Groshen S, Tsao-Wei DD, et al. Colorectal Tumors Responding to 5-Fluorouracil Have Low Gene Expression Levels of Dihydropyrimidine Dehydrogenase, Thymidylate Synthase, and Thymidine Phosphorylase. Clinical cancer research : an official journal of the American Association for Cancer Research 2000; 6:1322-7.
683. Randall VA. Hormonal Regulation of Hair Follicles Exhibits a Biological Paradox. Semin Cell Dev Biol 2007; 18:274-85.
684. Koopmann J, Buckhaults P, Brown DA, Zahurak ML, Sato N, Fukushima N, et al. Serum Macrophage Inhibitory Cytokine 1 as a Marker of Pancreatic and Other Periampullary Cancers. Clin Cancer Res 2004; 10:2386-92.
685. Nakamura T, Scorilas A, Stephan C, Yousef GM, Kristiansen G, Jung K, et al. Quantitative Analysis of Macrophage Inhibitory Cytokine-1 (Mic-1) Gene Expression in Human Prostatic Tissues. British journal of cancer 2003; 88:1101-4.
686. Karan D, Chen SJ, Johansson SL, Singh AP, Paralkar VM, Lin MF, et al. Dysregulated Expression of Mic-1/Pdf in Human Prostate Tumor Cells. Biochemical and biophysical research communications 2003; 305:598-604.
687. Shnaper S, Desbaillets I, Brown DA, Murat A, Migliavacca E, Schluep M, et al. Elevated Levels of Mic-1/Gdf15 in the Cerebrospinal Fluid of Patients Are Associated with Glioblastoma and Worse Outcome. International journal of cancer Journal international du cancer 2009; 125:2624-30.
688. Brown DA, Ward RL, Buckhaults P, Liu T, Romans KE, Hawkins NJ, et al. Mic-1 Serum Level and Genotype: Associations with Progress and Prognosis of Colorectal Carcinoma. Clinical cancer research : an official journal of the American Association for Cancer Research 2003; 9:2642-50.
689. Brown DA, Lindmark F, Stattin P, Balter K, Adami HO, Zheng SL, et al. Macrophage Inhibitory Cytokine 1: A New Prognostic Marker in Prostate Cancer. Clinical cancer research : an official journal of the American Association for Cancer Research 2009; 15:6658-64.
690. Cheung PK, Woolcock B, Adomat H, Sutcliffe M, Bainbridge TC, Jones EC, et al. Protein Profiling of Microdissected Prostate Tissue Links Growth Differentiation Factor 15 to Prostate Carcinogenesis. Cancer research 2004; 64:5929-33.
691. Zhao L, Lee BY, Brown DA, Molloy MP, Marx GM, Pavlakis N, et al. Identification of Candidate Biomarkers of Therapeutic Response to Docetaxel by Proteomic Profiling. Cancer research 2009; 69:7696-703.
692. Xue H, Lu B, Zhang J, Wu M, Huang Q, Wu Q, et al. Identification of Serum Biomarkers for Colorectal Cancer Metastasis Using a Differential Secretome Approach. Journal of proteome research 2010; 9:545-55.
693. Zhang L, Yang X, Pan HY, Zhou XJ, Li J, Chen WT, et al. Expression of Growth Differentiation Factor 15 Is Positively Correlated with Histopathological Malignant Grade and in Vitro Cell Proliferation in Oral Squamous Cell Carcinoma. Oral oncology 2009; 45:627-32.
694. Baek KE, Yoon SR, Kim JT, Kim KS, Kang SH, Yang Y, et al. Upregulation and Secretion of Macrophage Inhibitory Cytokine-1 (Mic-1) in Gastric Cancers. Clinica chimica acta; international journal of clinical chemistry 2009; 401:128-33.

695. Skipworth RJ, Deans DA, Tan BH, Sangster K, Paterson-Brown S, Brown DA, et al. Plasma Mic-1 Correlates with Systemic Inflammation but Is Not an Independent Determinant of Nutritional Status or Survival in Oesophago-Gastric Cancer. British journal of cancer 2010; 102:665-72.
696. Roxburgh CS, McMillan DC. Role of Systemic Inflammatory Response in Predicting Survival in Patients with Primary Operable Cancer. Future Oncol 2010; 6:149-63.
697. Richardson PG, Mitsiades C. Bortezomib: Proteasome Inhibition as an Effective Anticancer Therapy. Future Oncol 2005; 1:161-71.
698. Ooi MG, Hayden PJ, Kotoula V, McMillin DW, Charalambous E, Daskalaki E, et al. Interactions of the Hdm2/P53 and Proteasome Pathways May Enhance the Antitumor Activity of Bortezomib. Clinical Cancer Research 2009; 15:7153-60.
699. Bates S, Hickman ES, Vousden KH. Reversal of P53-Induced Cell-Cycle Arrest. Mol Carcinog 1999; 24:7-14.
700. Scripture CD, Figg WD, Sparreboom A. Peripheral Neuropathy Induced by Paclitaxel: Recent Insights and Future Perspectives. Curr Neuropharmacol 2006; 4:165-72.
701. Yared JA, Tkaczuk KH. Update on Taxane Development: New Analogs and New Formulations. Drug Des Devel Ther 2012; 6:371-84.
702. Gradishar WJ, Tjulandin S, Davidson N, Shaw H, Desai N, Bhar P, et al. Phase Iii Trial of Nanoparticle Albumin-Bound Paclitaxel Compared with Polyethylated Castor Oil-Based Paclitaxel in Women with Breast Cancer. J Clin Oncol 2005; 23:7794-803.
703. Ray MA, Trammell RA, Verhulst S, Ran S, Toth LA. Development of a Mouse Model for Assessing Fatigue During Chemotherapy. Comp Med 2011; 61:119-30.
704. van de Stolpe A, Pantel K, Sleijfer S, Terstappen LW, den Toonder JM. Circulating Tumor Cell Isolation and Diagnostics: Toward Routine Clinical Use. Cancer research 2011; 71:5955-60.
705. Forshew T, Murtaza M, Parkinson C, Gale D, Tsui DW, Kaper F, et al. Noninvasive Identification and Monitoring of Cancer Mutations by Targeted Deep Sequencing of Plasma DNA. Science translational medicine 2012; 4:136ra68.
706. Bootcov MR, Bauskin AR, Valenzuela SM, Moore AG, Bansal M, He XY, et al. Mic-1, a Novel Macrophage Inhibitory Cytokine, Is a Divergent Member of the Tgf-Beta Superfamily. Proc Natl Acad Sci U S A 1997; 94:11514-9.
707. Baek SJ, Horowitz JM, Eling TE. Molecular Cloning and Characterization of Human Nonsteroidal Anti-Inflammatory Drug-Activated Gene Promoter. Basal Transcription Is Mediated by Sp1 and Sp3. J Biol Chem 2001; 276:33384-92.
708. Seve P, Dumontet C. Is Class Iii Beta-Tubulin a Predictive Factor in Patients Receiving Tubulin-Binding Agents? The lancet oncology 2008; 9:168-75.
709. Jones RJ, Bjorklund CC, Baladandayuthapani V, Kuhn DJ, Orlowski RZ. Drug Resistance to Inhibitors of the Human Double Minute-2 E3 Ligase Is Mediated by Point Mutations of P53, but Can Be Overcome with the P53 Targeting Agent Rita. Mol Cancer Ther 2012; 11:2243-53.
710. Michaelis M, Rothweiler F, Barth S, Cinatl J, van Rikxoort M, Loschmann N, et al. Adaptation of Cancer Cells from Different Entities to the Mdm2

Inhibitor Nutlin-3 Results in the Emergence of P53-Mutated Multi-Drug-Resistant Cancer Cells. Cell Death Dis 2011; 2:e243.
711. Michaelis M, Rothweiler F, Agha B, Barth S, Voges Y, Loschmann N, et al. Human Neuroblastoma Cells with Acquired Resistance to the P53 Activator Rita Retain Functional P53 and Sensitivity to Other P53 Activating Agents. Cell Death Dis 2012; 3:e294.
712. Secchiero P, Melloni E, di Iasio MG, Tiribelli M, Rimondi E, Corallini F, et al. Nutlin-3 Upregulates the Expression of Notch1 in Both Myeloid and Lymphoid Leukemic Cells, as Part of a Negative Feed-Back Anti-Apoptotic Mechanism. Blood 2009:blood-2008-11-187708.
713. Lee Y, Miron A, Drapkin R, Nucci MR, Medeiros F, Saleemuddin A, et al. A Candidate Precursor to Serous Carcinoma That Originates in the Distal Fallopian Tube. J Pathol 2007; 211:26-35.
714. Fisher R, Larkin J, Swanton C. Inter and Intratumour Heterogeneity: A Barrier to Individualized Medical Therapy in Renal Cell Carcinoma? Front Oncol 2012; 2:49.